Full Scale Test SSP 34m blade, Combined load. Data report

Nielsen, Per Hørlyk; Nielsen, Magda; Jensen, Find Mølholt; Berring, Peter; Roczek-Sieradzan, Agnieszka; Roudnitski, Vatslav; Bitsche, Robert; Andrlová, Zuzana; Branner, Kim; Bak, Christian

Total number of authors:
17

Publication date:
2011

Document Version
Publisher's PDF, also known as Version of record

Full Scale Test SSP 34m blade, Combined load. Data report

Risø-R-Report

Risø DTU:
Per H. Nielsen Magda Nielsen, Find M. Jensen, Peter Berring, Agnieszka Roczek-Sieradzan, Vatslav Roudnitski, Robert Bitsche, Zuzana Andrlová, Kim Branner, Christian Bak, Bjarne Kallesøe, Malcolm McGugan, Mikkel Lagerbon

Vestas: Jakob Wedel-Heinen
LM-Glasfiber A/S: Torben Lindby
SSP-Technology A/S: Hans Jørgen Riber
ECC: Christian Jensen

Risø-R-1749(EN)
December 2010
Funded by Energiteknologisk Udviklings-og demonstrationsprogram, EUDP-2008

Risø DTU
National Laboratory for Sustainable Energy

Author: Per H. Nielsen Magda Nielsen, Find M. Jensen, Peter Berring, Agnieszka Roczek-Sieradzan, Vatslav Roudnitski, Robert Bitsche, Zuzana Andrlová, Kim Branner, Christian Bak, Bjarne Kallesøe, Malcolm McGugan, Mikkel Lagerbon, Jakob Wedel-Heinen, Torben Lindby, Hans Jørgen Riber, Christian Jensen
Title: Full Scale Test SSP 34m blade, Combined load. Data report
Division: Wind Energy Division

Risø-R-1749(EN)
November 2010

Abstract (max. 2000 char.):

This report is part of the research project entitled "Eksperimentel vingeforskning: Strukturelle mekanismer i nutidens og fremtidens store vinger under kombineret last" where a 34m wind turbine blade from SSP-Technology A/S was tested in combined flap and edgewise load. The applied load is 55% of an imaginary extreme event based on the certification load of the blade.
This report describes the reason for choosing the loads and the load direction and the method of applying the loads to the blade. A novel load introduction allows the blade to deform in a more realistic manner, allowing the observation of e.g. transverse shear distortion.
The global and local deformation of the blade as well as the blades' respond to repeated tests has been studied and the result from these investigations are presented, including the measurements performed.

ISSN 0106-2840
ISBN 978-87-550-3847-9

Contract no.:

Group's own reg. no.:
(psp1120180-01)

Sponsorship: Energitek - nologisk Udviklings - og demonstrationsprogram, EUDP-2008

Cover :

Pages: 184
Tables:
References:

Wind Energy Division
Risø National Laboratory for Sustainable Energy
Technical University of Denmark
P.O.Box 49
DK-4000 Roskilde
Denmark

Contents

Terms and Definitions

The blade cross section with the main structural features is presented in Figure 0.1.

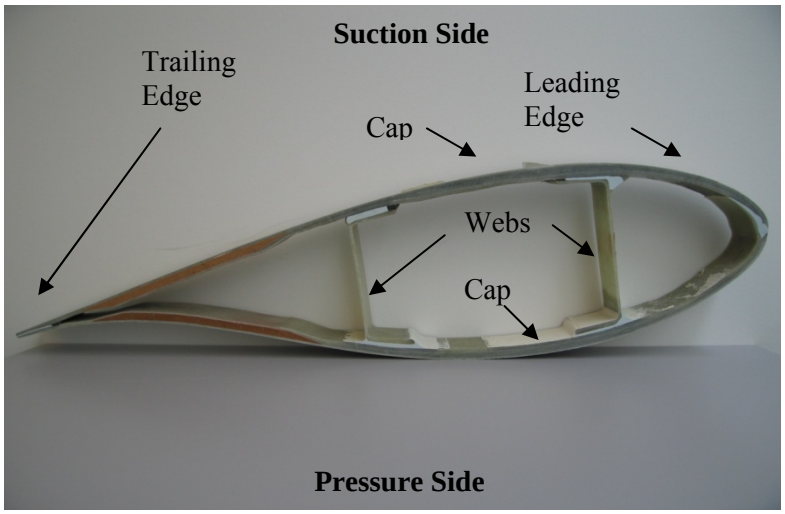

Figure 0.1. Picture of a blade cross-section indicating construction elements

Definitions

Blade root:	Part of the wind turbine blade that is closest to the rig
Box girder:	Primary lengthwise structural member of a wind turbine blade
Edgewise:	Direction that is parallel to the local chord of the blade
Flapwise:	Direction that is perpendicular to the surface swept by the non-deformed rotor blade axis
Trailing edge (TE):	Edge of blade pointing opposite travelling direction
Leading edge (LE):	Smooth edge of blade pointing the travelling direction
FEM:	Finite Element Method

Table 0.1. Loading directions with respect to the blade

Load case
PTS - pressure side towards suction side
STP - suction side towards pressure side
TTL - trailing edge towards leading edge
LTT - leading edge towards trailing edge

The coordinate system

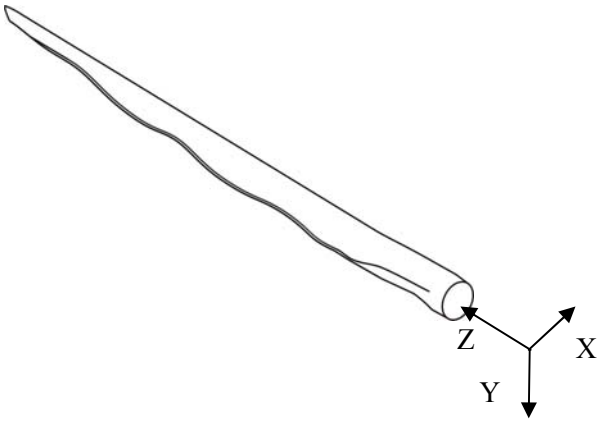

Figure 0.2. Coordinate system.

The x-axis is directed in edgewise (wind) direction, positive towards leading edge. The y-axis is in flapwise direction, positive in direction from pressure to suction side. The z-axis is along the blade, pointed from the root of the blade, as indicated in Figure 0.2.

Measurement equipment

Strain gauges (SG)

UD	Unidirectional (0° in longitudinal direction)
Bx	Biax (0°/90°)
Tx	Triax-Rosette (0°/45°/90°)
Back to back	One strain gauge on each (inner and outer) side of the blade

Linear transducers (LT)

LT-ASM	Length Transducer from ASM – Cable actuated position sensors
LT-NT	Length Transducer from NovoTechnik

Optical measurement

DIC:	Digital Image Correlation
Aramis:	3D-DIC-system from GOM (www.gom.com)

1. Introduction

For decades, wind turbine blade design and test methods have been based on flapwise and edgewise loading. This seems reasonable because these are the main directions of the blade profile. The assumption might be appropriate for small blades, but for larger blades the edgewise loads become more important. Recent results have shown that the loads in other directions than pure flap- or edgewise appear to have major importance.

The majority of blades in use today are designed on this basis, but in spite of the structural analyses and full scale tests performed on wind turbine blades, damages still occur. Therefore it could be questioned if the foundations of the design rules are sufficient and a topic subject to critical questions is the loads and their direction used for full scale tests.

This report describes the tests performed with the blade exposed to a combined flap- and edgewise loads. It is the third and last data report included in the EUDP project "Eksperimentel vingeforskning: Strukturelle mekanismer i nutidens og fremtidens store vinger under kombineret last". The report is divided into two parts. In the first part (chapter 2 and 3), the test setup, loads, measurement equipment etc. are described and in the second part (chapter 4) the result are presented.

In the first data report, ref. [1], a general and more detailed description of the measurements, the measurement equipment and basic conditions for the test is presented, and therefore it will be referred to this report concerning these matters.

2. Background for and choosing the load and load direction

The loads the wind turbine blades are designed to carry are derived from aeroelastic analyses. These analyses are carried out for a large number of load cases, but it is not feasible to perform structural analyse for each of these load cases. Instead the biggest loads are sorted out and found for both edgewise and flapwise direction at each section of the blade, and the design loads are composed from these.

Experience has shown that if the loads are extracted by this method, it is not certain the blade is designed according to the numerically biggest load or the most critical loads for the structure.

The traditional structural analysis of wind turbine blade has been based on calculation of stress or strain in the material and elastic instability of cap and web. New research (ref.[3]) revealed that there occur failure mechanisms which have not been accounted for.

FEM calculations indicated that those failure mechanisms may be sensitive to direction of the critical load. Failure is difficult to predict by FEM studies alone,

therefore it is important to perform experimental test as well in order to make sure that the analytical and/or numerical studies are interpreted correctly.

The consideration made for this test were to choose loads of the similar size as the flapwise loads and apply the load at an angle to the flapwise direction, which according to the FEM calculation seems to be critical. Unfortunately, there is no available examination of the loads variation as function of the load direction and no full scale test results is available exploring the impact on the blade deformation caused by the load direction.

A part of this project has therefore been to explore which loads were appropriate to use in the examination of the blade in the combined load case. For the SSP 34m blade the only loads released are the extreme loads in flap and edgewise direction. The calculation of the loads has not been disclosed.

The ideal case would be to perform load calculations for the blade and from these calculations choose suitable load direction where the load is an angle with respect to the main direction on the blade. Such studies demand bigger resources than this project allows for.

As the overall purpose was to clarify how the blade reacts to different load directions, and not to examine its ability to withstand critical loads, it is sufficient to apply the loads are that similar the real situation. The determination of the loading on the blade was performed in a simplified way. It was done by summing vectorily the extreme loads in flap and edgewise direction.

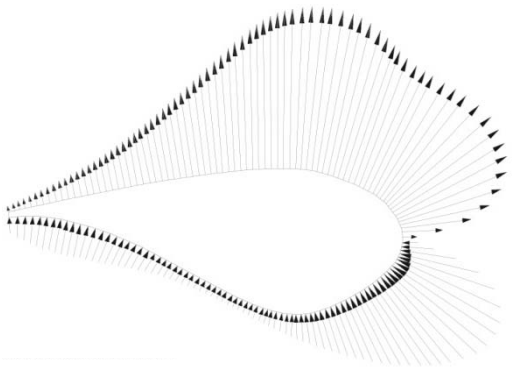

Figure 2.1. Pressure distribution on an aerodynamic profile generating the aerodynamic loads.

The typical load in the flapwise direction is the aero dynamical load as shown in Figure 2.1. As the profile is moving towards the wind at an angle, the resulting aerodynamic force is mainly directed flapwise with a small angle towards the leading edge.

In the edgewise case the typical loads are gravity load and dynamic loads which e.g. arise by an emergency stop of the turbine. During operation the gravity load changes sign and the direction depends on the pitched of the blade ..The dynamic

load from the emergency stop is often towards the leading edge. Therefore, edgewise loads on blade will usually be the largest towards the leading edge.

A combination of the highest flapwise load towards suction side and the highest edgewise load towards trailing edge results in load at an angle of aprox. 30° with respect to the cord of the blade and directed towards the leading edge.

Moreover, at this angle the performed numerical structural analyses predict that new failure mechanism may be prevailing. Therefore, it was decided to carry out the test with the load applied in this direction. The size and distribution of the load is calculated from the edgewise and flapwise loads, see Section 3.1.

Further calculation based on the loads can reveal how well these loads resemble a real load situation. As previous mentioned it was not feasible to perform these calculations within the frame of this project. Therefore it is suggested, as a follow up, to carry out the analysis on the basis of the loads for the SSP 34m blade forming a general view of critical loads and load direction and comparing these with the load and the load direction in the performed test.

3. Experimental Procedure

As mentioned in the introduction, the experiment presented in this report is a part of a series of experiments within the project, and in this chapter a presentation of the test conditions which are distinct for the combined test are made. A description of the basic conditions and measuring methods as well as the test setup and preparation of the test can be found in the "Data report 1", ref [1]. It covers, among others:

- Description of the test rig and winches
- Compensation for blade mass
- Measuring system for strain gauges
- Measuring of deflection with linear censors.
- Digital image correlation (DIC) measurements of surface deformations on the blade.
- Data acquisition.

3.1 Loads

In the test the blade is loaded with a combined flap- and edgewise load. The applied forces are presented in Table 3.1. These values are defined in relation to the Risø load, which is considered the extreme load, and for this project is defined as the design load multiplied by a factor of 1.23. The background for this factor is experience of a similar blade, which has carried such amount of load (in flapwise direction) before it failed, see ref. [3] The experiment consists of two separate test series where the load was increased to 35 % and 55 % of the Risø load

respectively. Original is was only planned to test at the 35 % load due to the capability of the test rig, but as the test rig was reinforced during the project it was decided to carry out at second experiment with 55 % load.

Table 3.1. The forces incl. mass of blade applied in the investigated combined load case.

Section of application [m from the root]	Applied force [N] 35 %	Applied force [N] 55 %
13.21	30300	47700
18.61	28200	44300
24.91	50000	78600

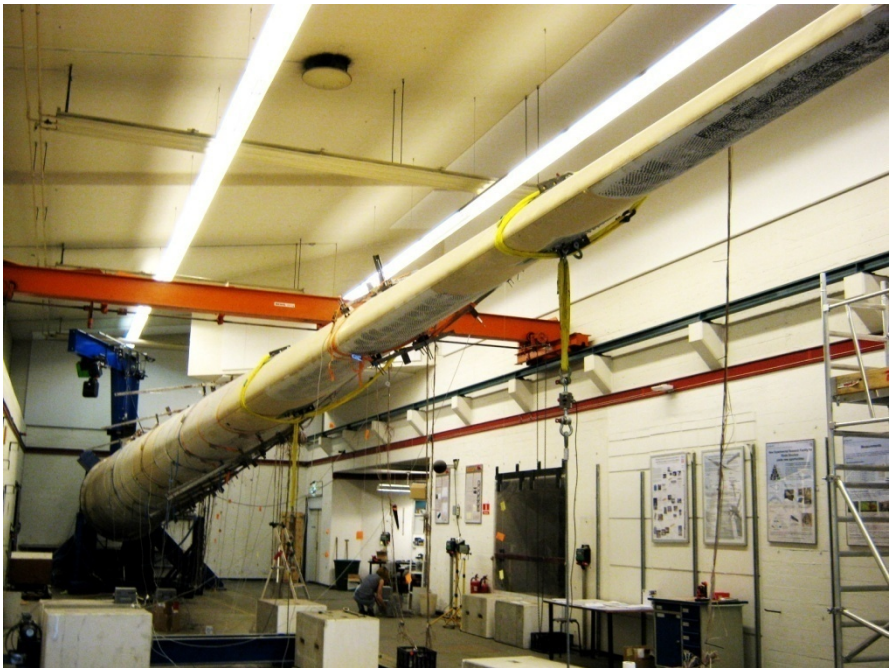

Figure 3.1. Photo of the blade bolted to the test rig. The tip has been cut off, so only 25m is tested. The blade is loaded at an angle of 30^{o} to the flapwise direction, simulating a combined flap- and edgewise loads.

For the combined load test, the blade is mounted on the test rig as shown in Figure 3.1. This is different from the previous tests, and required some efforts as the setup and handling of blade are a rather elaborate process. In this position the force can be applied to the suction side of the blade in a plane that is 30^{o} from the flapwise plane, in the direction towards the leading edge.

In order to allow comparison with the previous tests, the load caused by the gravity force needed to be considered while establishing the applied load. The gravity load was accounted for by reducing the values of the applied load. The gravity load was represented by forces acting on the blade in the same three sections at which the test load is applied. Moreover, the truncated tip needed to be compensated for, and therefore, a preloading was applied at the tip in order to account for the forces from the missing part. The calculations and adjustments made are presented in ref. [1]. After applying the preloading and the adjustment forces, all the measuring equipment excluding the measurement of the applied forces was set to zero. Due to

the gravity load (including the tip preloading) and adjustment, the measurements were started at 12.5% of the Risø load.

3.2 Measurements

The experimental methods used in the tests include a large number of strain gauges and displacement sensors. Moreover, an advanced 3D optical measuring system (DIC) and acoustic emission equipment has been used. A description of the data acquisition system and measurement equipment as well as how the tests were performed can be found in ref.[1]. At the pull to 55% Risø load, the blade was also monitored by acoustic emission.

In the first pull at 35% load all the measurement equipment were included, but in the second pull at 55% load only some of the strain gauges where included.

The results from these measurements presented by Graph Tool can be found in Appendix B. Appendix A gives an overview of the placement of all the measurement equipment.

The direction of the strain with respect to the blade are 1 - longitudinal direction, 2 - transversal direction, as indicated in Figure 3.2.

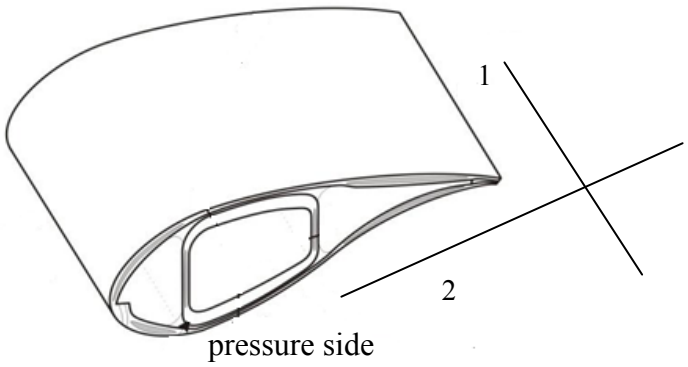

Figure 3.2. Directions of the strain measurements with respect to the blade.

For further, detailed explanation of the measurement equipment positioning see ref. [1] and [2].

3.3 Considerations regarding the winch

Due to the new position of the blade in the test rig and the higher loads, that are applied in the combined load case, the global deflection of the blade will be much higher compared to the edgewise testing. This must be considered in the preparation of the experiment.

The deformation of the blade was analyzed using FEM. The results of the global deformation were used to plan the new setup for the winches and wires to ensure there was enough space for the planned deformation of the blade. It was necessary to investigate if there is enough span for the blade to be able to be deflected to approx. 80 % percent of the capacity leaving space for measuring equipment. Due

to the higher loads, it was necessary to change the wire loop of the third winch, and a part of the wire loop consists of 0.8 meters of force transducers and connections between elements, which needs to be taken into consideration.

In Figure 3.3, the global deflections the blade profile calculated by FEM is plotted together with the winch in the three positions: undeformed, 40% load and 80% load. It is apparent that, due to the characteristics of the blade stiffness, the blade will not only deflect in the direction the force is applied, but also deflect horizontally. However, this will to a certain extend be prevented during the test, because the wire from the winch will pull it back against the neutral position.

The deflection towards the root end is about 0.18 m, and even if this seems to be a small deflection, the winch is not designed for high loads at an angle in the longitudinal direction of the blade. Therefore the foundation for the winch is adjusted so that wire is vertical in transverse direction at maximum load.

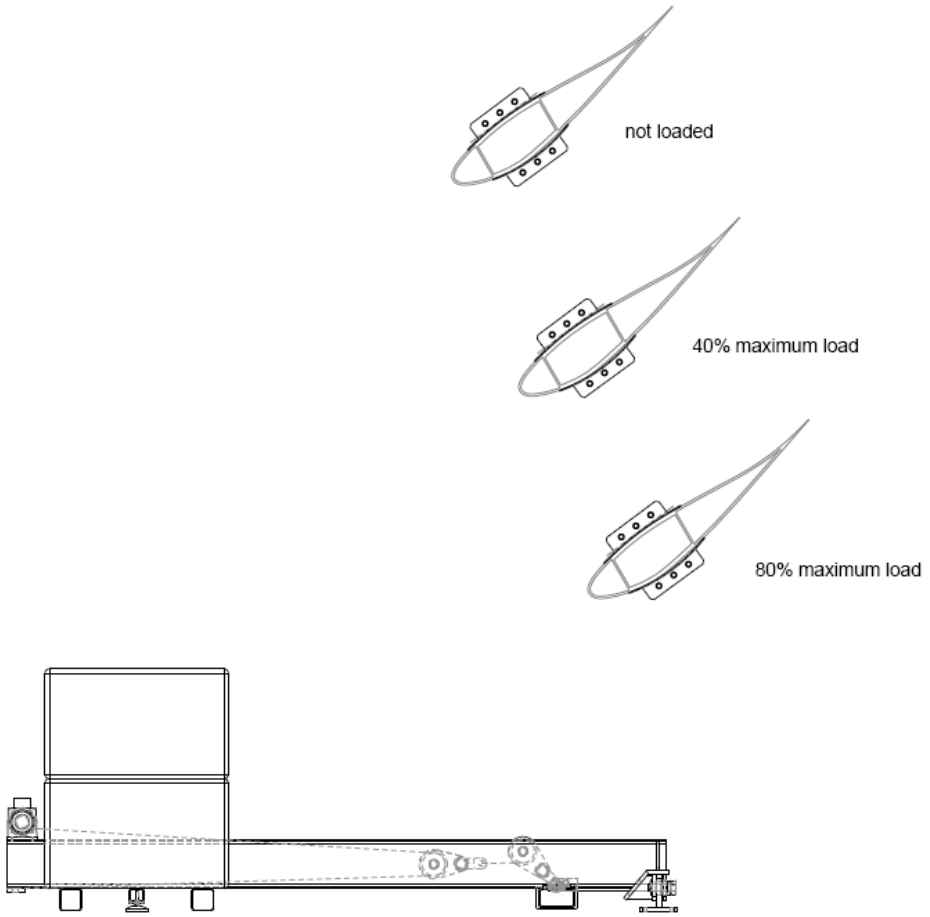

Figure 3.3. Global deformation of the blade at the 25 m section. The position of the deflected wing is plotted together with the winch. Since the tip deflects the most we are interested in how it behaves compared to the winch.

3.4 Load application

In the edgewise test, ref. [1], a novel method for the load application was used. The new method allows the blade to deform without limitation and makes it possible to

test the blade in relation to new failure mechanisms. In the test combined loading, these failure mechanisms are also significant, and therefore it is important to use a load introduction which exhibits similar properties.

The method for load application used in the edgewise test is presented in Figure 3.4. This is a specially shaped steel fitting which is bonded to the blade with epoxy adhesive.

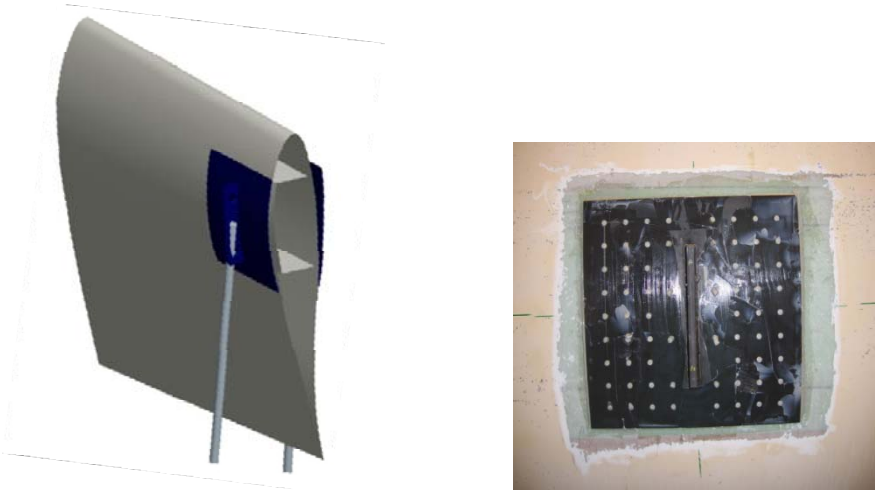

Figure 3.4. Load introduction used in edgewise test. The loads are transferred to blade using a bonded steel fitting.

This type of connection is suited for transferring the load as shear forces in the bond line, but in the combined load case, the bond is also exposed to peel forces. In the present test, the fitting is not loaded centrally. This is because the fitting is bonded to the blade in the position of the main reinforcement, but if the load is acting through the center of this field, the load will not act through the shear center of the blade profile, and by this introduces torsion in the blade. This must be avoided, and it implies that load cannot be applied centrally to the steel fitting. This is reflected in an uneven distribution of peel stress across the steel fitting, which will cause a stress concentration in the edge of steel fitting. The disadvantage of a bond connection is, that is does not exhibit any particular plastic deformation before failure. Therefore it will not present any warning if the bond is overloaded, and in the case the stress concentration causes a crack at the edge of the steel fitting, there is a risk for the crack to propagate very fast, and a unexpected failure of the load introduction can occur.

Several possibilities for load introduction have been investigated, which provides the need freedom of deformation for the blade, but does not depend on the strength of bond line. One suggestion is shown in Figure 3.5a, which consist of an anchor plates on each side of the profile. The load is transferred between the anchor plates using steel rods. Unfortunately the arrangement does not allow the determination of distribution of the load between two side of the profile, and this is important the results from the full scale test are going to be compared to a FEM analysis.

Another method is shown in Figure 3.5b. This utilizes one anchor plate only, but this is connected to steel plates inside the blade. With this solution however one has to perforate the main reinforcement, which is not considered an issue for the SSP 34 m blade since the stresses in the main reinforcement are relative low.

Another thing to consider when transferring the load to only one side of the profile, is the webs, which may be overloaded, because they distribute the load between the suction and pressure side of the blade. However this has been investigated by FEM analysis, and no risk of failure was indicated.

Considering all aspects it was decided to only use one anchor plate, and transfer the load to one side of the blade. Foremost in order to avoid the uncertainty regarding the distribution of the loads, and thereby the uncertainty of the blade behaviour caused by the load introduction. It was also considered too complicated and time consuming to establish the solution with two connected anchor plates within the project.

As mentioned, when the loads are introduced to a single side of the blade, there is a risk of failure in the bond line between the anchor plate and the blade. This was solved with a revised version of the load introduction shown in Figure 3.5b. With this solution it has been selected to reinforce the bond line between the blade and the anchor plate in the part where the largest peel stresses were expected to occur. In the tip it was solved by placing a steel bar inside the blade and fastening this to the anchor plates with bolts through the main reinforcement. The other sections of the blade, the load introduction were reinforced with special screws fastened to the main laminate though holes in the anchor plate. The connection has been tested with a similar type of glassfiber laminate and it showed adequate strength.

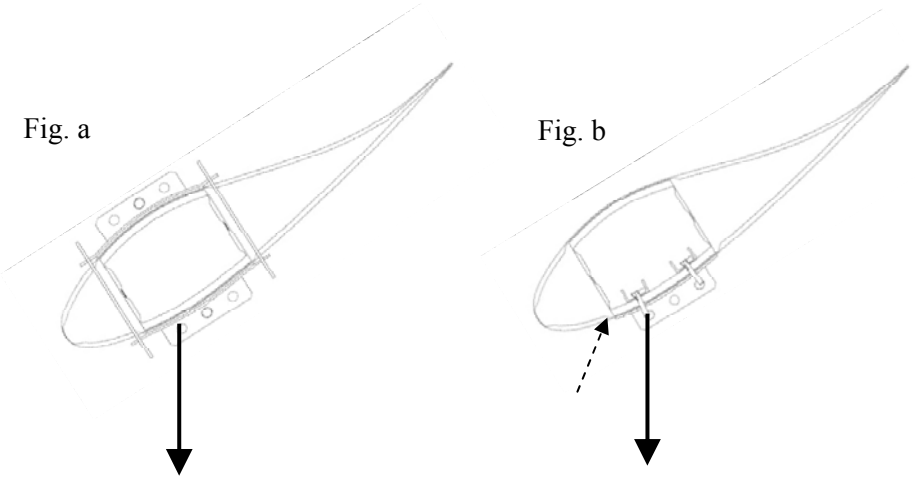

Figure 3.5. Fig. a: Load introduction with steel plates on both suction and pressure side of the blade and steel rods on each side of the web connecting the steel plates. Fig. b: Bonded steel plate with internal steel bars bolted through the cap to the steel plate. The dotted arrow indicates possible stress concentration in the bonding line.

4. Results

This chapter presents findings from pulls performed in the combined load case. The first pulls were performed at 35% Risø load. Such value was selected as this would not cause any risk of failure to the blade and more pulls were expected in order to give measurements from all the strain gauges. After the 35% Risø load pulls were performed, the load was increased to 55% Risø load, where the risk for failure was much higher. presents the individual pulls and their order.

Table 4.1. List of tests carried out in combined load case and presented in this data report

Name of pull	Load in %	Date	Center of DIC-measurements	Acoustic emission
Ecombined_300810	35%	300810		
Ecombined_010910	35%	010910		
Ecombined_020910	35%	020910		
Ecombined_070910	55%	070910	4m -6m S	4.5m and 10.5m S

Combined load test have not been carried out at Risø before and therefore precaution was taken in case the blade might fail. The blade was monitored with DIC and AE during the pull reaching 55% Risø load. This pull was performed without any indication of damage in the blade. The acoustic emission measurement was performed because it would detect if the blade was damaged during test.
The results from the AE measurements can be found in Appendix C and the main conclusions from these were:

- More activity at 10.5m than 4m
- Only one significant event detected (at 55% load at 10.5m)
- Only limited activity during the long load hold/unload sequence (therefore no progressive damage developed at the two sensor zones)

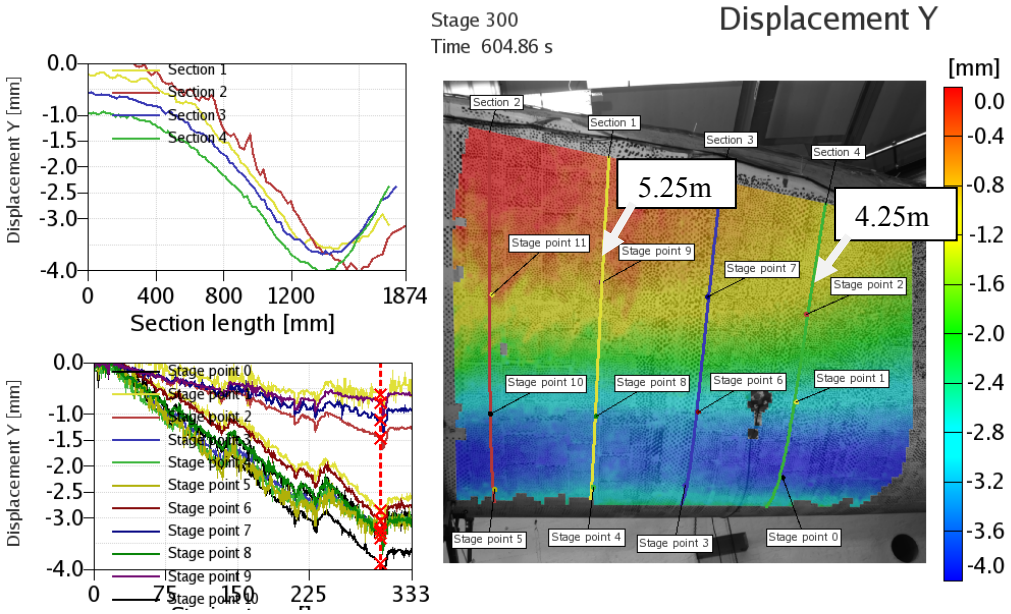

Figure 4.1. Snapshot of DIC measurement between 4m and 6m suction side section in the combined load case at 55% Risø load

The DIC measurement (The DIC measurement method is described in data report ref. [1]), was performed between 4m and 6m sections on the suction side. This was motivated by the previous measurements, which indicated that something might happen in this region. is a snapshot from the DIC measurements at 55% Risø load presenting the horizontal displacement. This snapshot includes both the global and local deformation in the horizontal direction and further treatment is required to extract more relevant information.

Before testing the combined load case, finite element analysis (FEA) was performed in order to predict possible failure of the blade. It indicated buckling of the cap at approximately 3.5m and 9m for load reaching 90% to 100% Risø load. The deformation of the cap centre with respect to the box corners between cap and panels, are extracted from the FE calculation and presented in Appendix G. These results are the same deformation as measured by the length transducers (LT-NT) placed on the outside of the cap. The method for placing the LT-NT frames is illustrated in .

Figure 4.2. Photo presenting the method for placing the LT-NT frames

The FEM and experimental results at 55% Risø loads are compared in 9m section only since no LT-NT measurements were performed in the 3.5m section. The values in are read from the diagrams.

Table 4.2. FEM results of cap deformation at 55% Risø load in 3.5 and 9m section. In 9m section the calculated deformations is compared to LT-NT measurements.

Section (m from the root)	3.5m	9m
FEM calculation	2.5 mm	3.5mm
LT-NT measurement		1 mm

The measured suction side cap deformation at 9m is smaller than the predicted by FEM and does not indicate buckling at this stage, i.e. 55% of Risø load. This difference should be investigated in future work.
Accompanied by DIC and acoustic emission measurements, numerous other measurements were performed. The findings from these are described in this chapter. The investigations considered:

- Load adjustments findings
- Repeated tests
- Cap deformation
- Global flapwise deformation
- Global trailing edge deformation
- Transverse shear distortion
- Deformation in 4m, 7m and 10m sections. (main sections)
- Strain measurement

4.1 Load adjustment findings

As described in 'Data report 1', ref. [1], the loads are applied continuously by three winches. The frequency regulation of the winch motors was preset in such a way that the three loading wires should induce the same % of the Risø load at the three load application system. This frequency adjusting is not without drawbacks as the regulation is affected by the load on the winches. To perform the test properly, the loads were adjusted during testing. Such method proved to be working well during the edgewise (LTT) load case tests.
For the combined load case it is different because the blade is more flexible than in the LTT case. The frequency regulation controlling the speed of the wire loading *FT-3*, the load application nearest to the root, could not be reduced sufficiently, which caused the adjustment of the loads to be inaccurate. presents the load at the three load application in percentage of the Risø load during the test. It appears clearly that the load measured by *FT-3* (green) is increasing significantly faster than the other two. This is adjusted by reducing this load at *FT-3*.
Decreasing load *FT-3* increases load at *FT-2*, i.e. the middle load application point (at 18.61m).

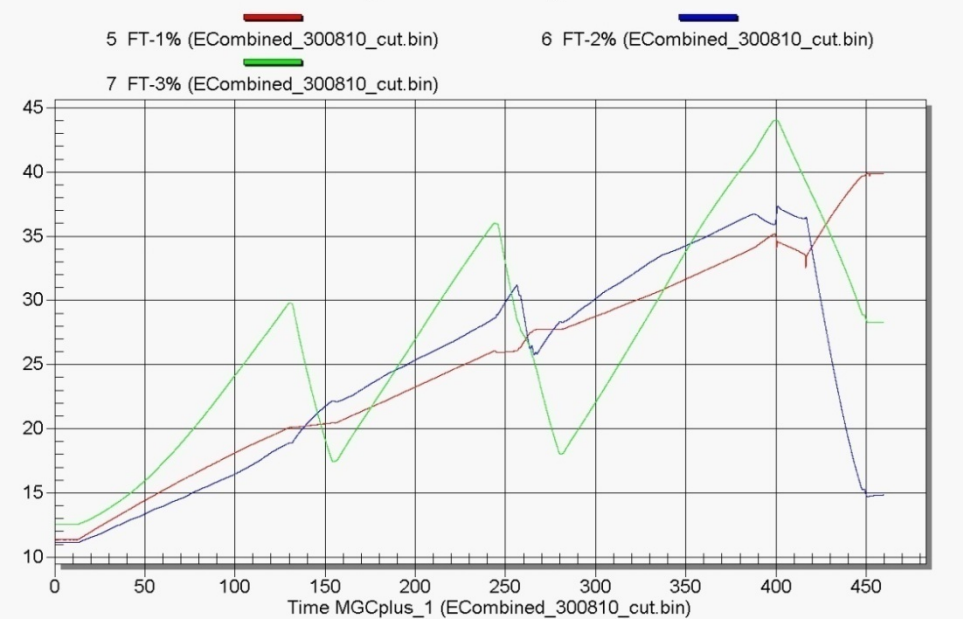

Figure 4.3. Loads in % of Risø load as a function of time for pull Ecombined_300810. FT-3% is the load application nearest to the root.

The overall reduction of the load during adjusting the forces causes the root bending moment to decrease as well. illustrates this behaviour in the *Ecombined_300810* test. The graphs show the forces at three load application sections in % of Risø load as a function of the root bending moment.

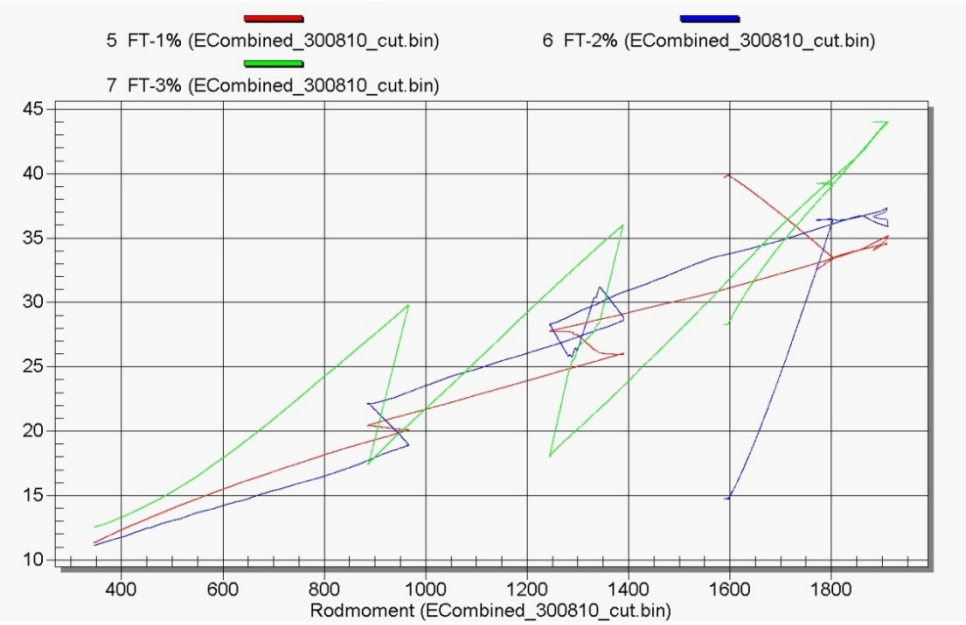

Figure 4.4. Loads in % of Risø load as a function of root moment for *Ecombined_300810* test.

When the loads are not perfectly adjusted it provides the opportunity to examine the blade behaviour when the loads are changed and the bending moment is reduced in a short period. When the root moment is reduced, the local bending moment is reduced as well.

Presenting the data from the pulls, deformation and strain measurements are presented as a function of the local bending moment. The force adjustment is not

very pronounced in the strain results, see Appendix B, but in the deflection it is noticeable.

As an example, the deformation of the panels in 4m is presented in a. It shows measurement of the distance between the two panels and here the force adjustments are clearly visible, e.g. at the local bending moment 1050kNm and 1350kNm. The pattern is that while the local bending moment is reduced the panels' relative deformation remains constant until the local bending moment reaches is previously attained value, and then the deformation starts to increase again. This behaviour is seen in more ASM measurement of panel's and web's deflections see Appendix B.

Results from two different type of measurement equipment are compared to make probable that this behaviour is not caused by the measurement equipment. At 4m section, the deformation of the pressure side panel was measured with *LT-NT-50-4*. If this measurement reveals the same behaviour it should confirmed such blade behaviour as reliable.

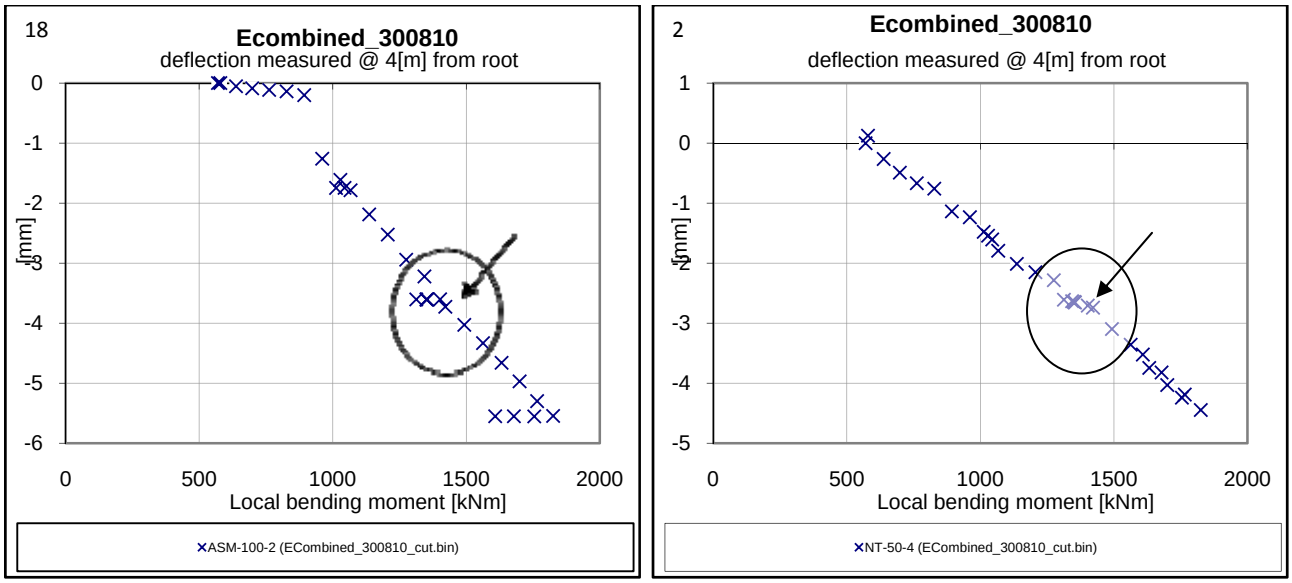

Fig. a Fig. b

Figure 4.5. Fig. a Displacement of the panels in 4m section measured with ASM-*100-2*, Fig. b. displacement of the pressure side panel in 4m section measured by LT-NT. See position on the blade

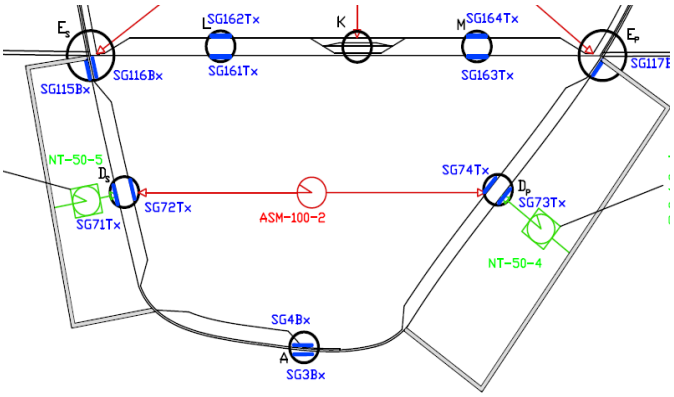

Figure 4.6. Position of the displacement measurements

As visible in , the same behaviour is seen for both ASM and LT-NT measurements, what supports the assumption that this is the behaviour of the panels. However, it cannot be surely discarded that it is a problem with the measurement equipment.

4.2 Repeated tests

For the combined load case until 35% Risø load all deflection measurements were repeated three times. The three pulls were performed in order to collect all strain measurements data and nothing was rearranged apart from the strain gauge connections. There was no change to the blade or deflection measurement equipment and these three pulls were performed at three days in a row. All the tests were performed in the same manner.

Repeating measurements allowed examining the reproducibility of the measurements and to estimate the effect of the load adjustment. The deflection measurement data from the three pulls were plotted together. These results can be found in Appendix F.

It appears that the load adjustment, for most of the measurements, does not influence the behaviour of the deformations, even if the deflection clearly does not decrease when the bending moment is reduced.

However, it was noticed that the behaviour of the blade in fact differs when the test is repeated. Two kinds of deviation are found.

The first one occurs mainly in the flexible parts of the blade (panels and web). This behaviour is presented in showing the deformation of the panels in 4m section. It can be seen that pull *Ecombined_020910* is separated from the two other pulls: *Ecombined_300810* and *Ecombined_01091*. It shows the same trend, so it would fit together with the two pulls if it was moved parallel 1mm downwards. Such parallel behaviour can be seen for more measurements. In this behaviour is recognized for the web and panel, even if it is not as pronounced for the panels in 4m section .

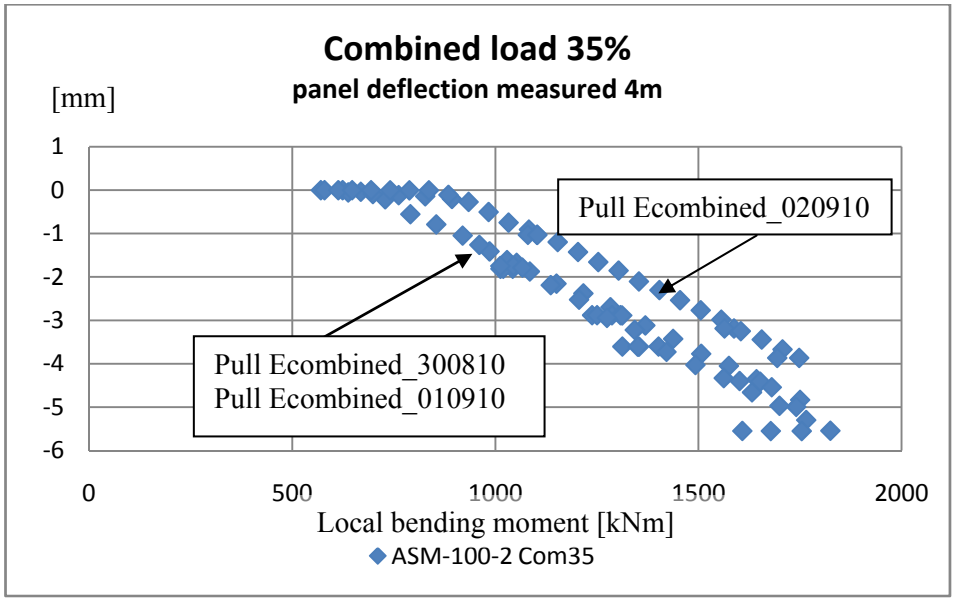

Figure 4.7. Data from 3 repeated pulls showing the deformation of the panels in 4m section. Pull *Ecombined_ 020910* differs from *Ecombined_300810* and *Ecombined_010910*

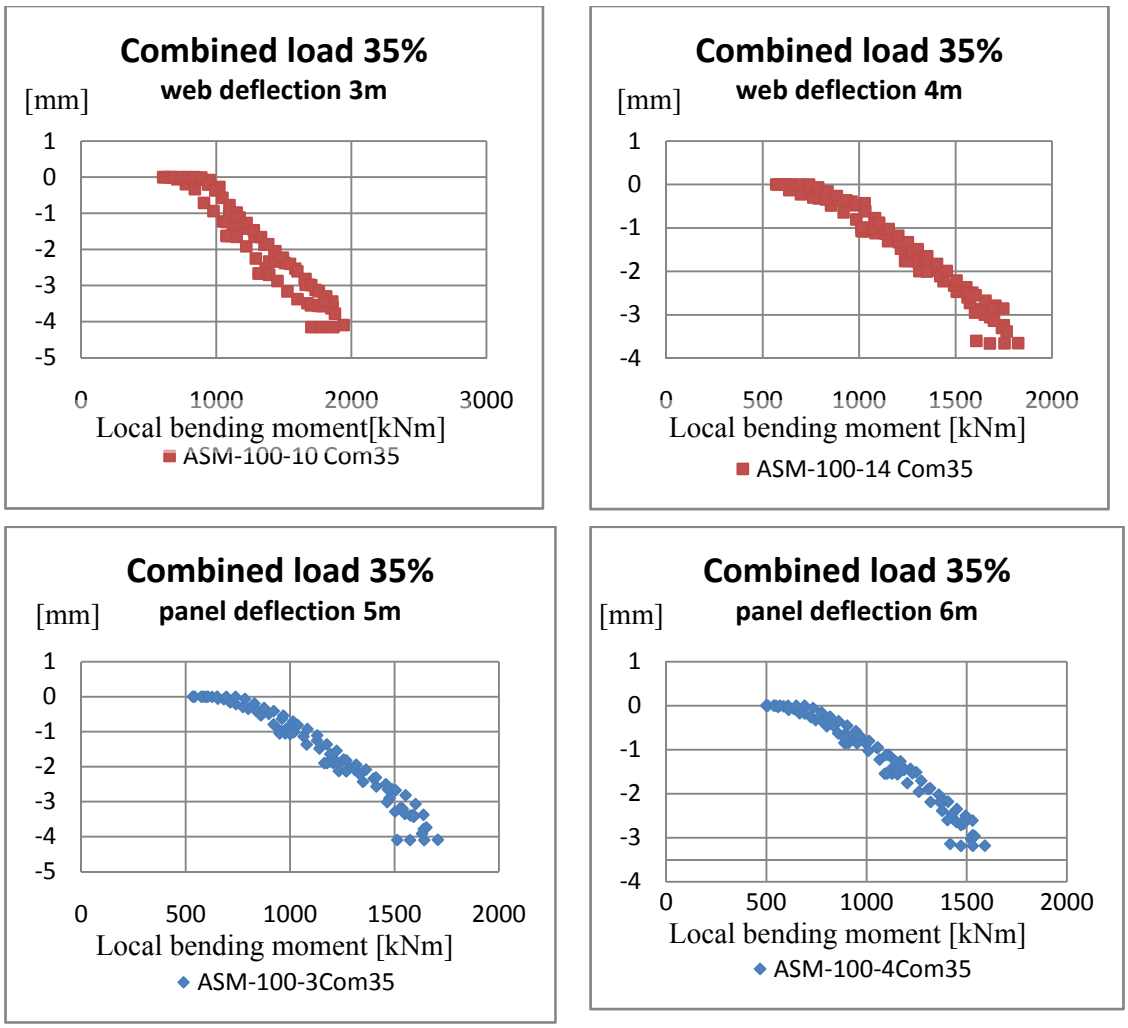

Figure 4.8 More measurements at 35% Risø load, showing deviation in repeated pulls, where one pull is differencing itself from the others and can be parallel displaced into the measurements from the others.

The second type of change is when the results are not parallel to each other. This behaviour can be seen for:

- Shear distortion in 10m section,
- Panel deformation in 3m section,
- Trailing edge web deformation in 7m,

Examination of the above mentioned graphs revealed that the pull *Ecombined_300810* deviated from the others. The only thing that differed was that it was the first one performed after the blade was rotated from testing it in LTT case to combined load case.

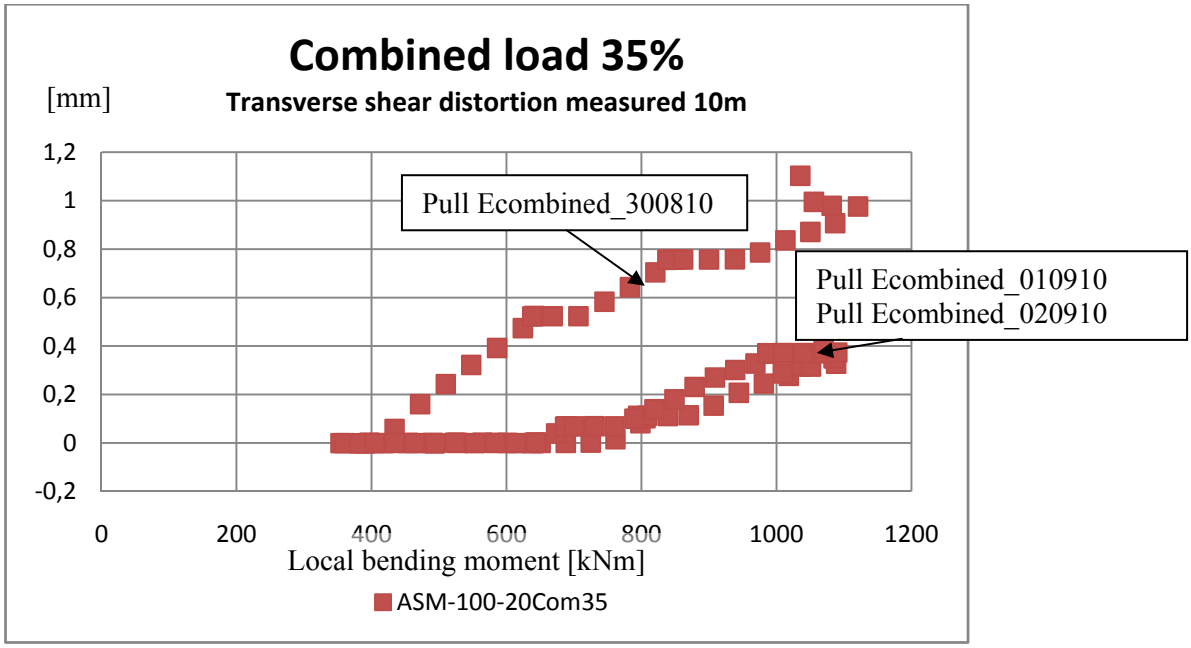

Figure 4.9. Data from 3 repeated pulls showing transverse shear deformation. The data from *Ecombined_300810* differs from the results from the remaining pulls.

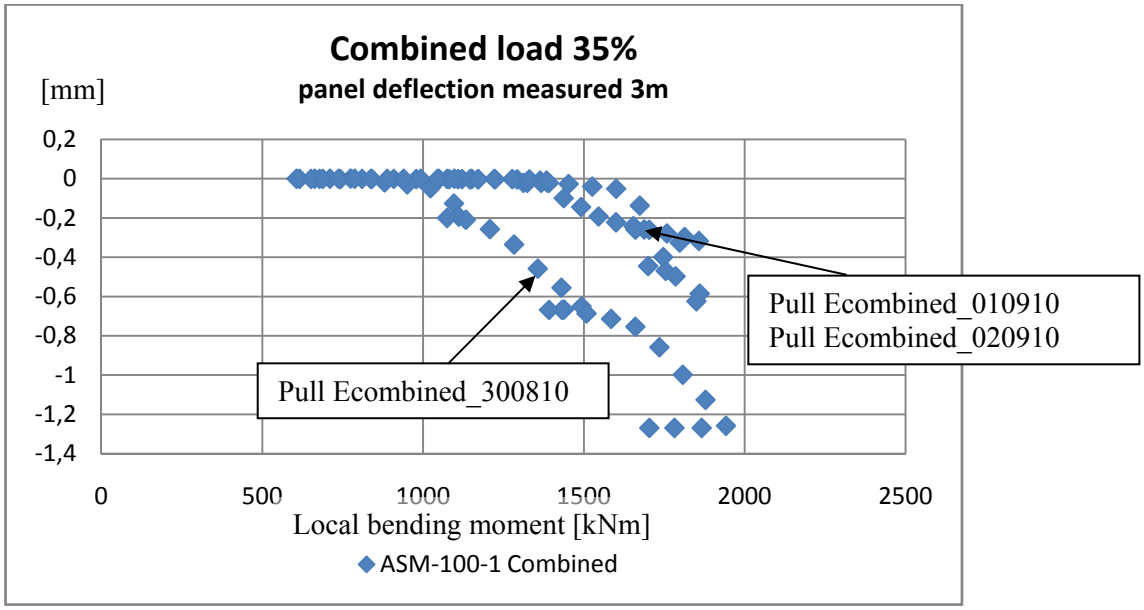

Figure 4.10. Data from 3 repeated pulls showing the deformation of the panel in 3m section. The data from *Ecombined_300810* differs from the results from the remaining pulls.

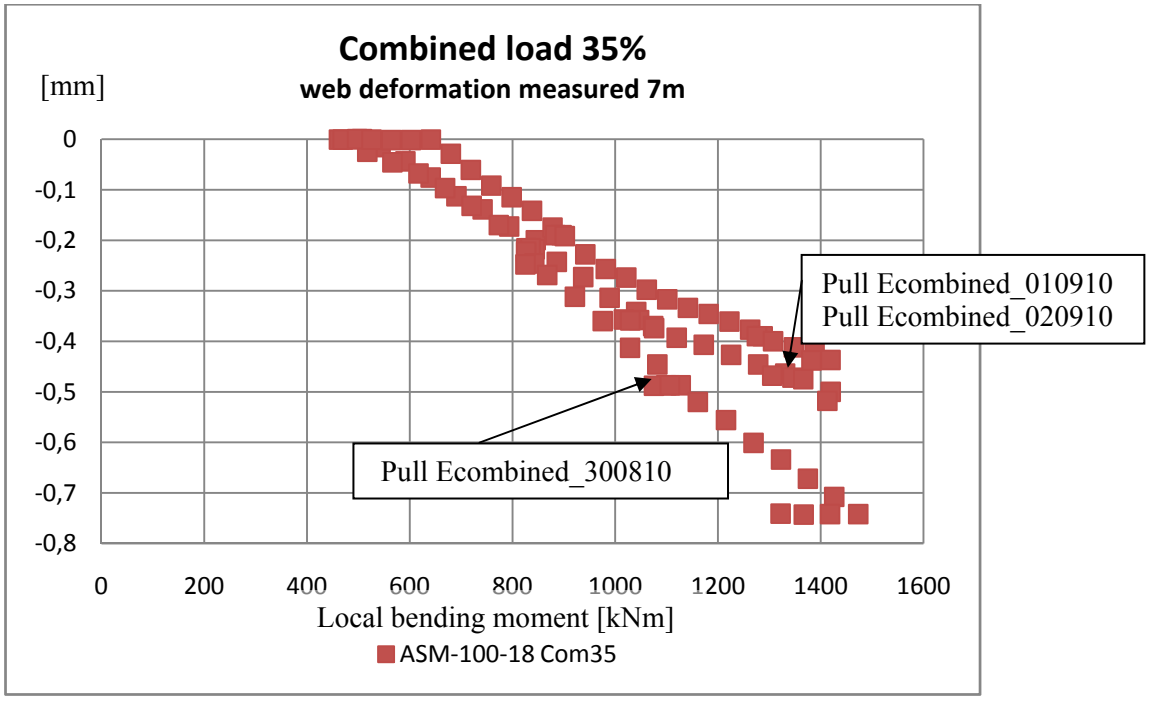

Figure 4.11. Data from 3 repeated pulls showing the trailing edge cap deformation in 7m section. Again, the data from *Ecombined_300810* deviate.

In section 0 it was revealed that while the local bending moment was reduced due to force adjustment the blade was reluctant to change shape. This indicates that the previously tested load case may influence the results of the following one. When testing a new load case, the blade might have been pre-deformed slightly from the loading direction it has been exposed to, and the adjustment of the shape to the existing load case is included in the measurements from following two tests.

4.3 Cap deformation

LT-NT displacement measurements were used to measure cap deformation, where the displacement transducers were fastened to frames which were supported at the box corners, see . These measurements are the displacement of the cap centre with respect to the box corners. The box corners are considered fairly stiff, but there may come some disturbance from the frame and its support, as it is possible that, when bending the blade, the frames may slightly move or bend.

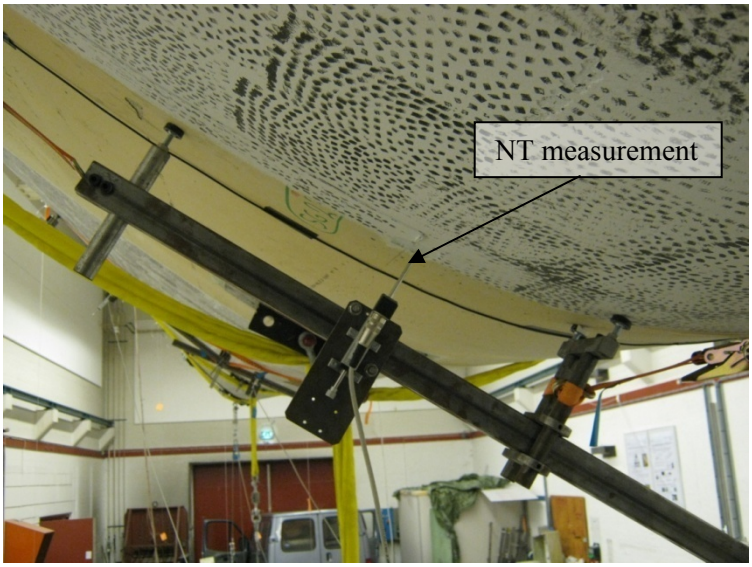

Figure 4.12 Photo presenting LT-NT measurement

The measurements of the cap deformation are presented in and . The results presented in are from pressure side cap deformation at 10m and 16m section. The graphs include measurements from the three repeated pulls put together.

It is outstanding that the cap deformation behaves in the same way in all three pulls with very small variations in the measurements (at the level of 0.1, 0.2mm). Here, it cannot be undoubtedly concluded if this variation comes from the cap behaviour or the frames. As it is the same in all three performed pulls it suggests that it is the cap behaviour or some other behaviour induced by the blade.

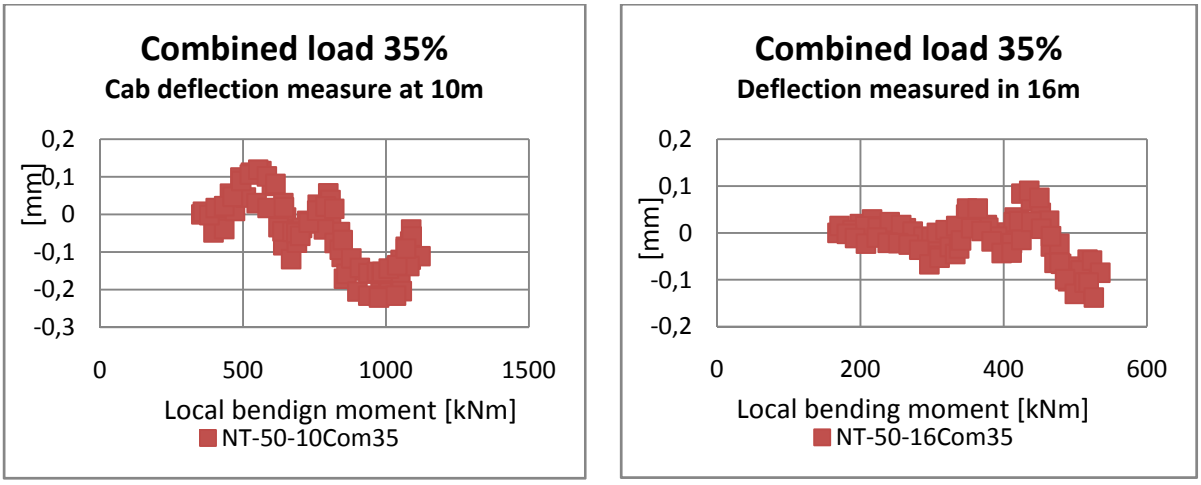

Figure 4.13. Pressure side cap deformation in 10 and 16m sections.

 presents the suction side cap deformations at 8m, 9m, 10m, 11m and 12m sections, and here as well, some interesting cap deformations are indicated. Further study of this phenomenon may be considered.

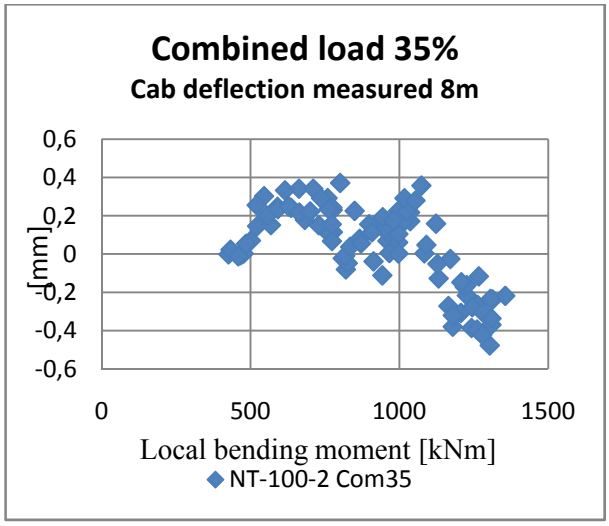

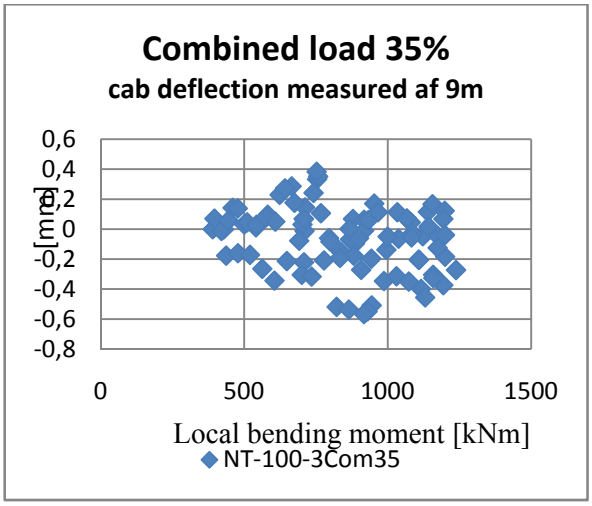

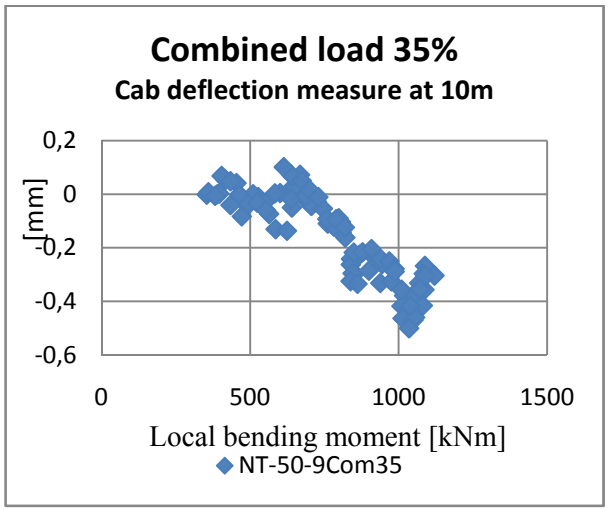

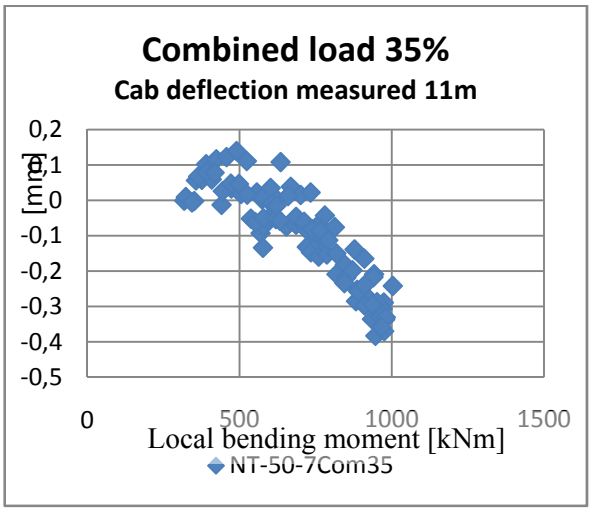

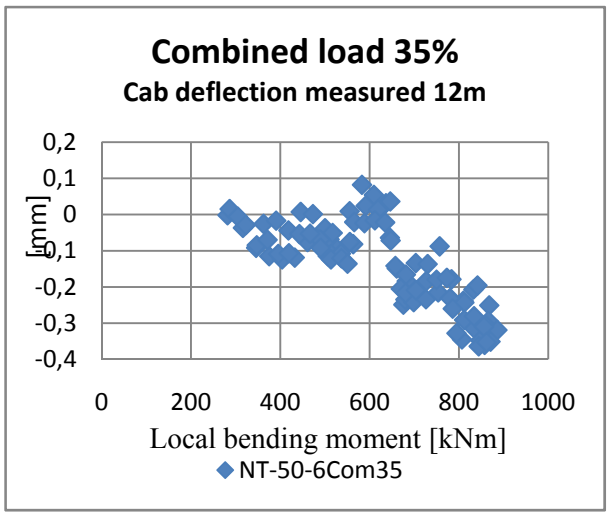

Figure 4.14 Local deformations measured on the suction side cap.

4.4 Global vertical and horizontal deflection

The global behaviour of the blade in both vertical and horizontal direction is presented in and . The results presented here are from pull *Ecombined_070910* at 55% Risø load.

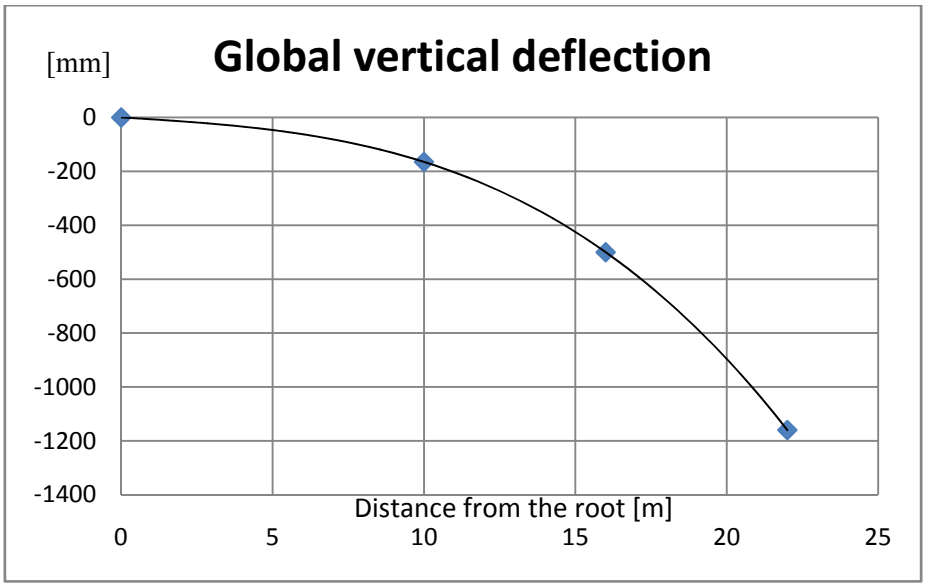

Figure 4.15. Global vertical deflection measured at 55% Risø combined load.

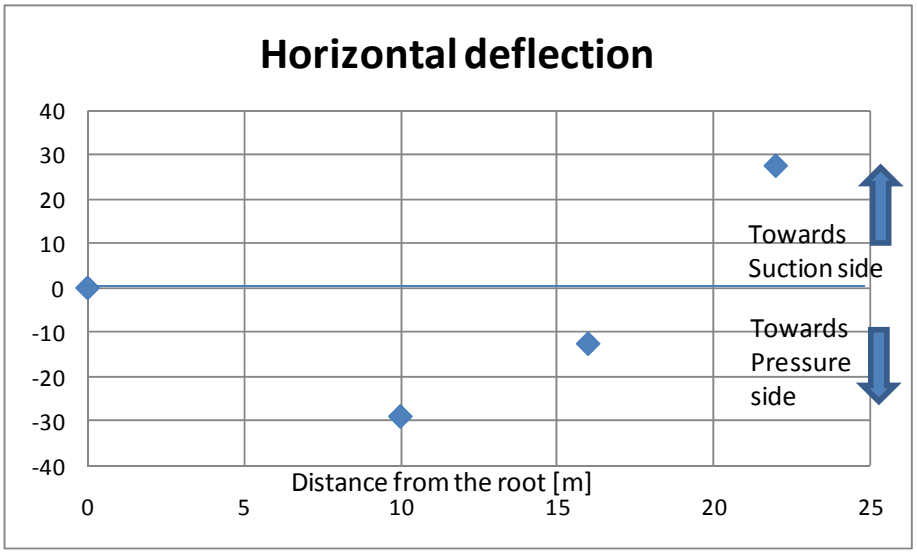

Figure 4.16. Horizontal deflection measured at 55% Risø combined load. The (–) sign indicates when the blade is moving towards left seen from the tip (pressure side mostly)

The horizontal displacement is extracted from the measurements, as the measured quantity is angled, see the calculation in Appendix E.

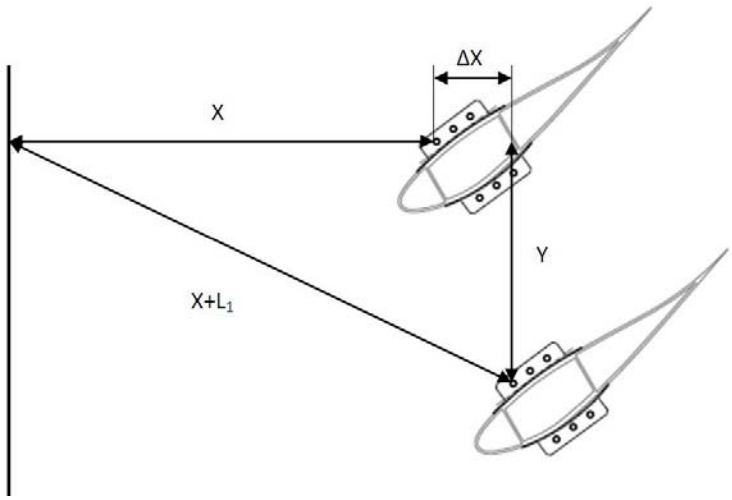

Figure 4.17. Scheme showing the horizontal displacement. ΔX is the horizontal displacement needed and the measured angled displacement is L_1

The horizontal global deflection moves to pressure side starting at the root and around 10m turns and moves towards the suction side. The trend line for this horizontal deflection was not added, as the measurement does not reveal how the horizontal deflection acts in the root region.

The horizontal displacement at 25m was found via FEM study. The horizontal deflection at 25m was not measured in the test so a direct comparison is impossible. However, it appears that the result given by FEM is significantly larger than experimentally measured displacement.

Table 4.3. Comparison of horizontal displacement

	Load	Distance from root	Horizontal movement
FEM analyses	40% Risø load	25m	365mm
Measurements	55% Risø load	22m	28mm

This difference should be investigated in future work.

4.5 Global deformation of trailing edge

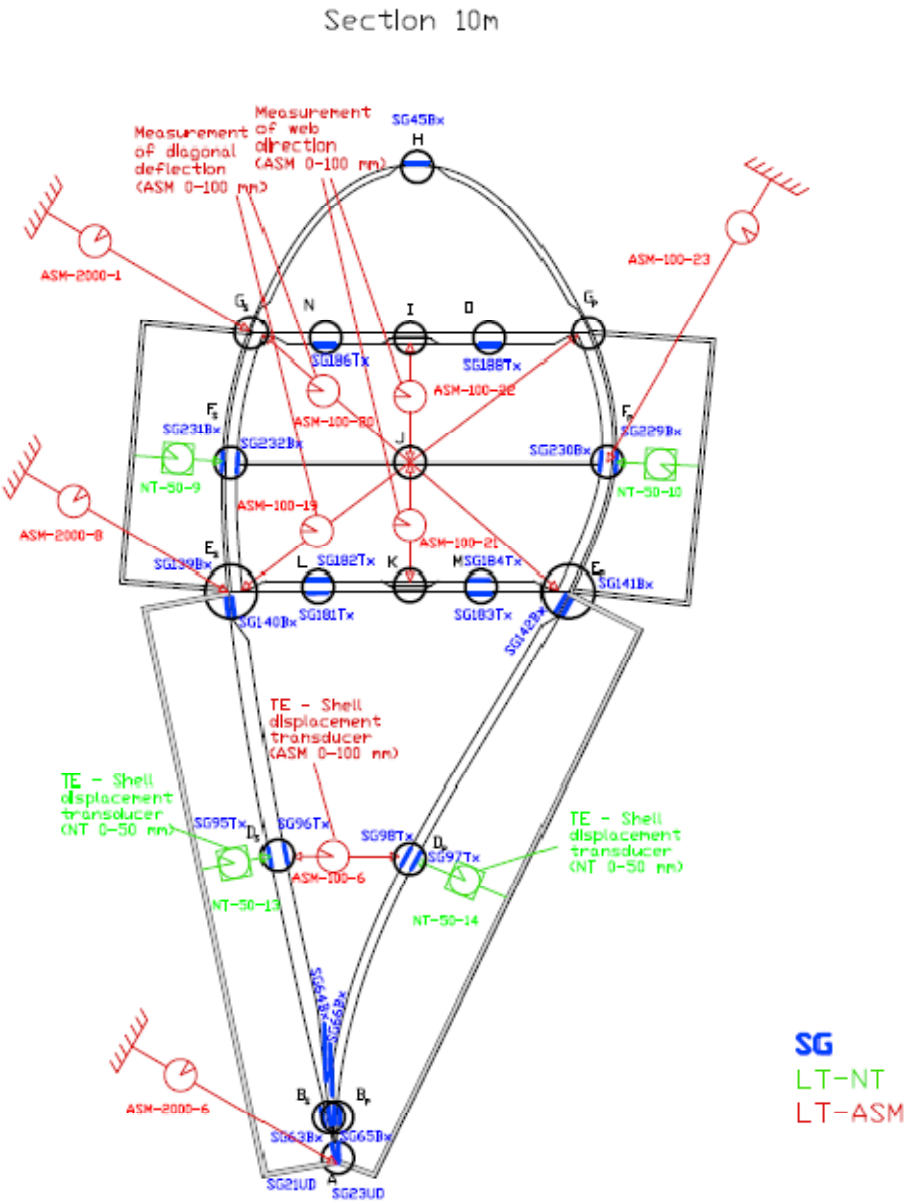

Figure 4.18. Scheme presenting the measurement equipment mounted at 10m section.

The global deflection of the blade in 10m, 16m and 22m sections was measured with the measurement equipment placed as demonstrated in . ASM-*2000-1*, *2000-8* and *2000-6* measure the movement of the blade towards the floor.

These measurements do not show the local behaviour of the trailing edge of the blade unless we look at the difference between them. The difference between these measurements shows how the box and the panels twist horizontally during the test. Such results from pull *Ecombined_070910* 55% Risø load are presented in , and . Three relative deformations are presented:

- plot **g-e** shows the box twisting with respect to point G_s
- plot **e-a** shows the twisting of the panels with respect to point E_s
- plot **g-a** shows the twisting of the blade centreline with respect to G_s

The displacements are found with respect to the points on the suction side. The blade section behaviour is presented in , and .

In , showing the global behaviour in 10m section, it can be seen that for local bending moment below 1000kNm the blade twists counter-clockwise. Then it starts turning in the opposite direction and at 1600kNm it is already twisted clockwise (seen from the root). This behaviour is presented in .

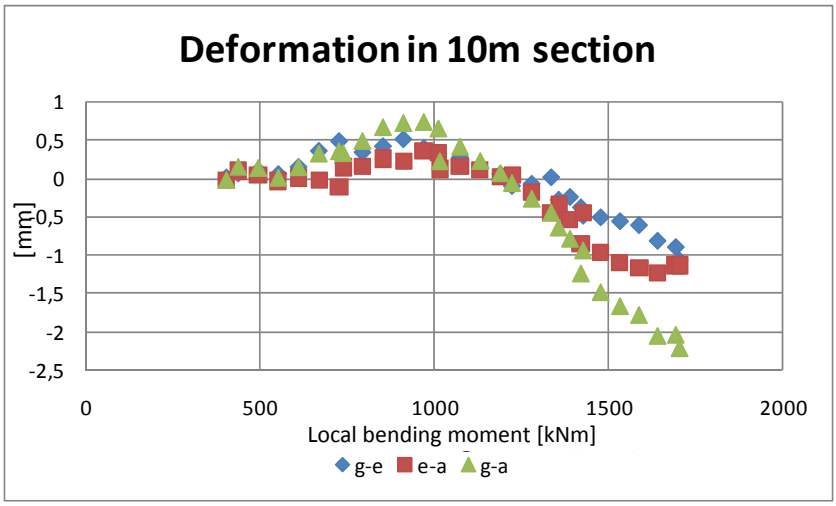

Figure 4.19. Global deflection of the 10m section.

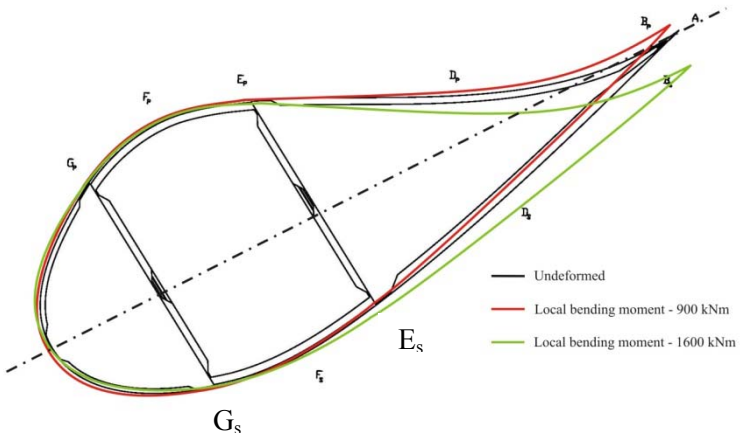

Figure 4.20 Sketch of the 10m section showing the blade behaviour during loading

In 16m section, see , the box twists counter-clockwise (seen from the root) at low local bending moment and clockwise when approaching the maximum bending moment, whereas the panels move clockwise during the entire loading path.

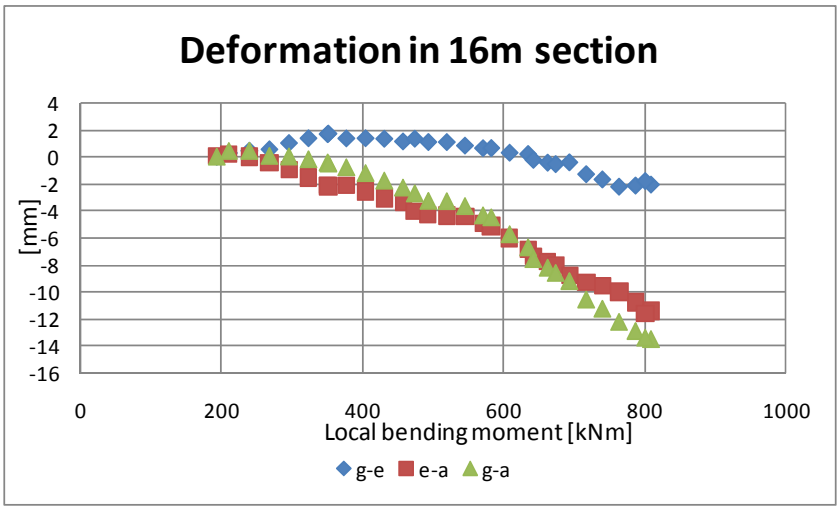

Figure 4.21. Global deformation in 16m section

This deformation of 16m section at 55% Risø load is presented .

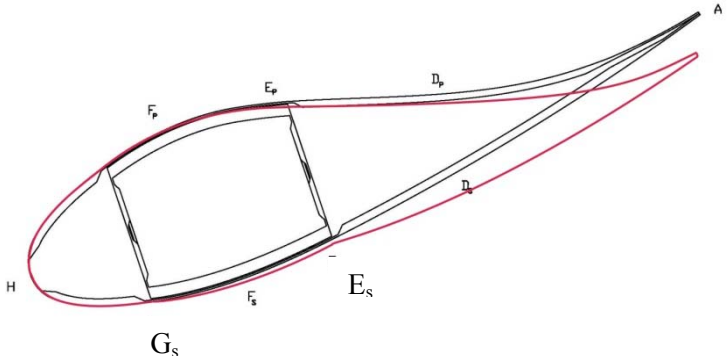

Figure 4.22 Sketch of the 16m section showing the blade deformation at 55% Risø load.

In 22m section, the box and the panels twist in opposite directions, the box counter-clockwise and the panels - clockwise (seen from the tip), see .

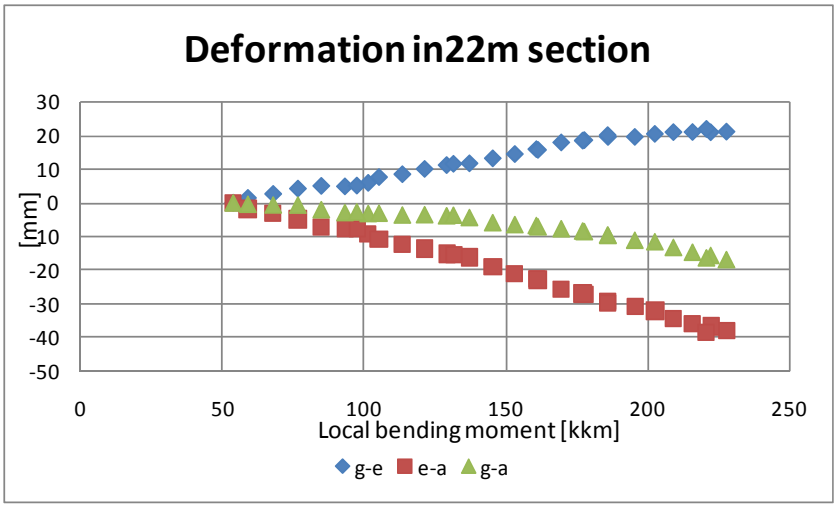

Figure 4.23. Global deformation in 22m section.

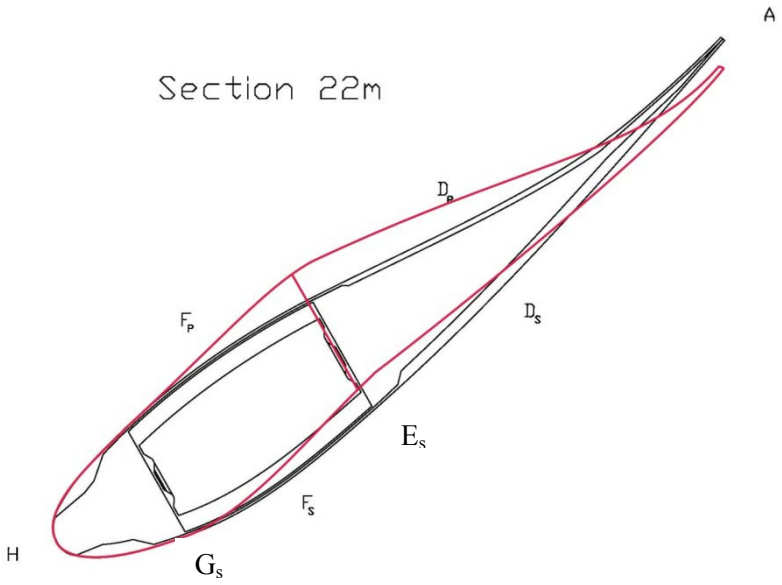

Figure 4.24 Sketch of the 22m section showing the blade deformation at 55% Risø load.

This behaviour of the blade, i.e. changing the tilting direction in 10m section as the load is increased and the special way the blade deforms in 22m section, may be related to the horizontal forces induced by the load application system when the blade moves sideward. demonstrates the source of the horizontal forces.

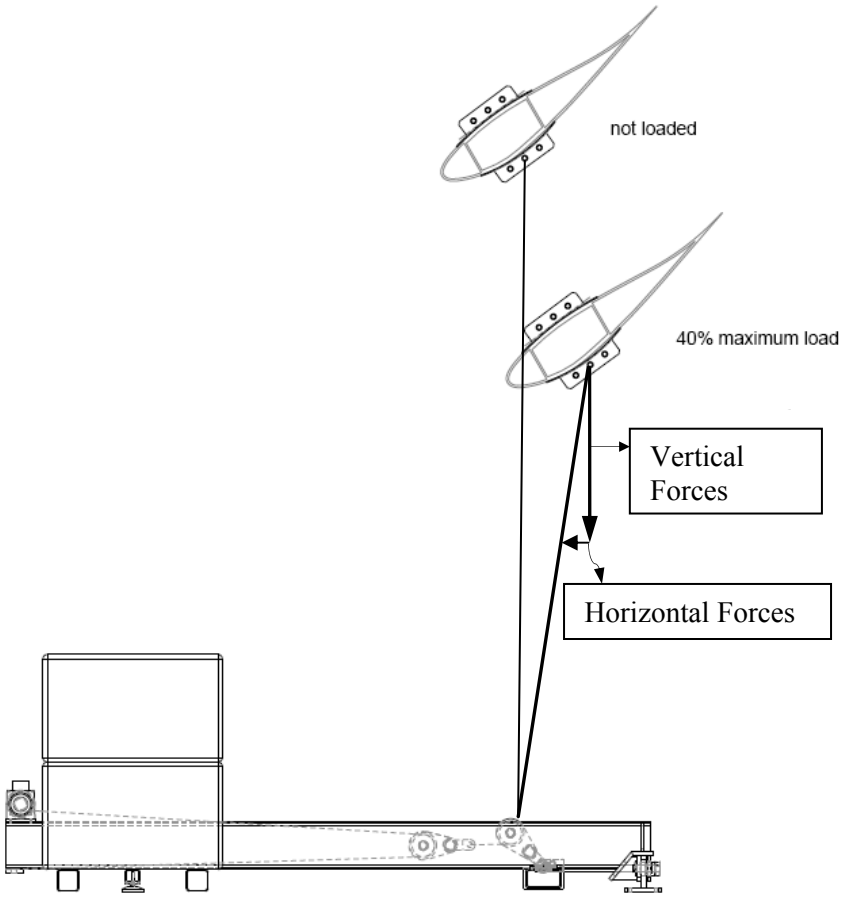

Figure 4.25 The direction of the forces during loading.

4.6 Transverse shear distortion

The transverse shear distortion was considered an important failure mode, which could cause collapse of the blade. This failure mode was therefore followed on real time graphs during the pull to 55% Risø load. Transverse shear distortion phenomenon is shown schematically in .

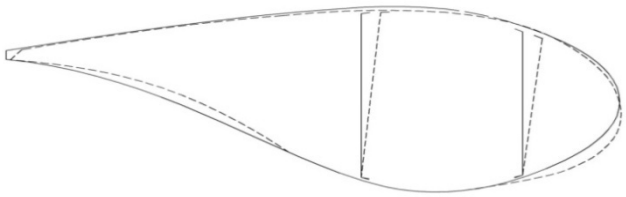

Figure 4.26. Drawing presenting the transverse shears distortion.

The transverse shear distortion can be measured in the box diagonals. Therefore, displacement transducers (*ASM*) are placed inside the blade measuring the change in diagonals. See

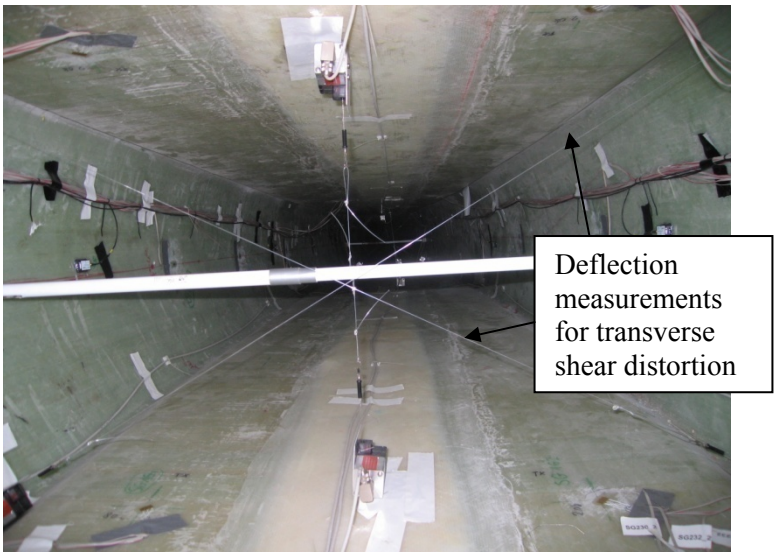

Figure 4.27. Photo showing the deflection measurements of the transverse shear distortion

The results from these measurements at 55% Risø load are presented in , where the transverse shear distortion is measured in 3m, 4m, 7m and 10m section.

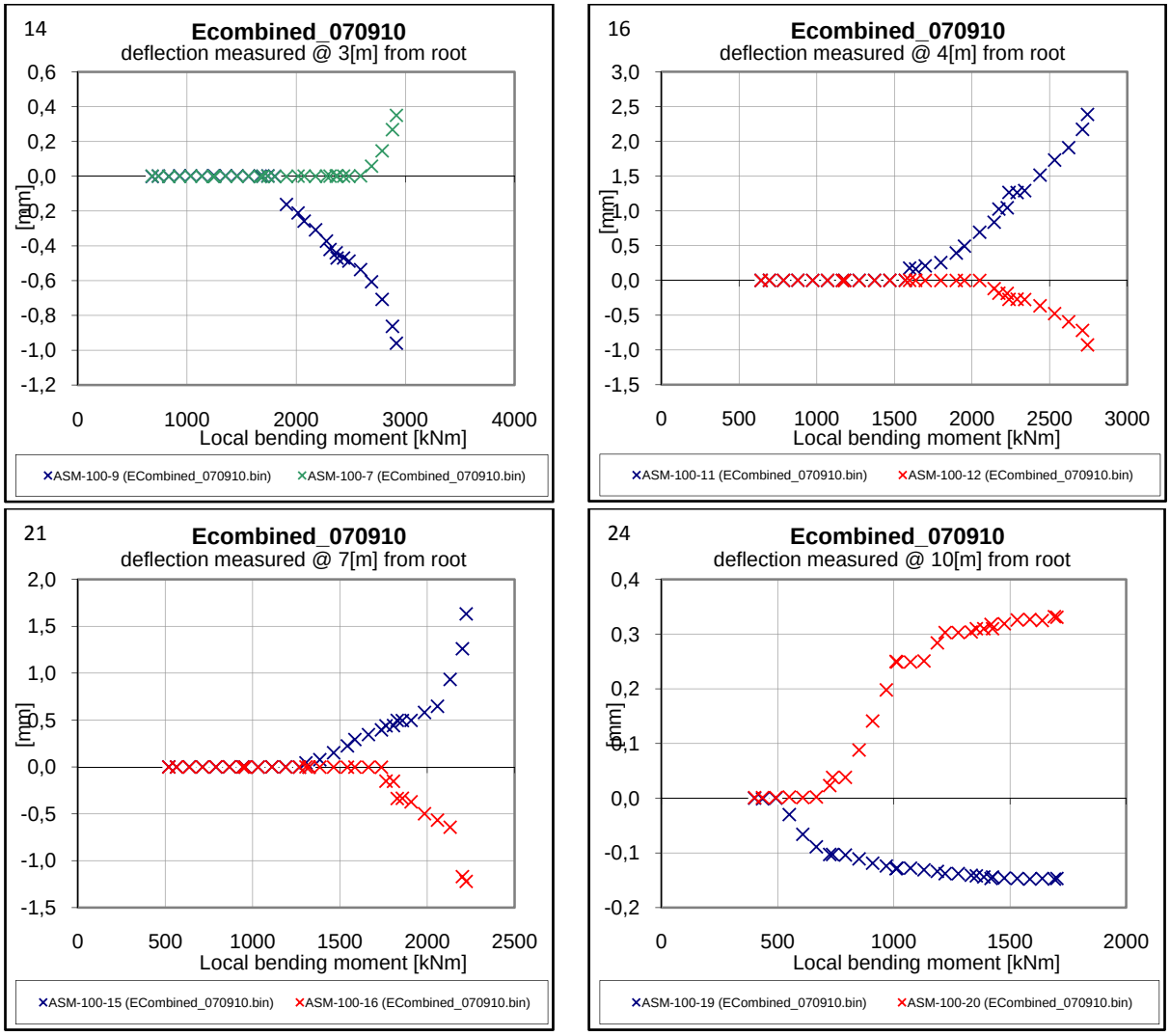

Figure 4.28 Results presenting the transverse shear distortion in 3m, 4m,7m and 10m sections.

The transverse shear distortion causes the box to twist. The twist shifts from clockwise to counter-clockwise at approx.10m section, see sketches of the direction of transverse shear deformation in . The sketches are seen from the root and the deformations are exaggerated for better illustration. The red shapes resembling parallelograms of the distorted box. The webs (vertical lines) are not parallel (see also results in).

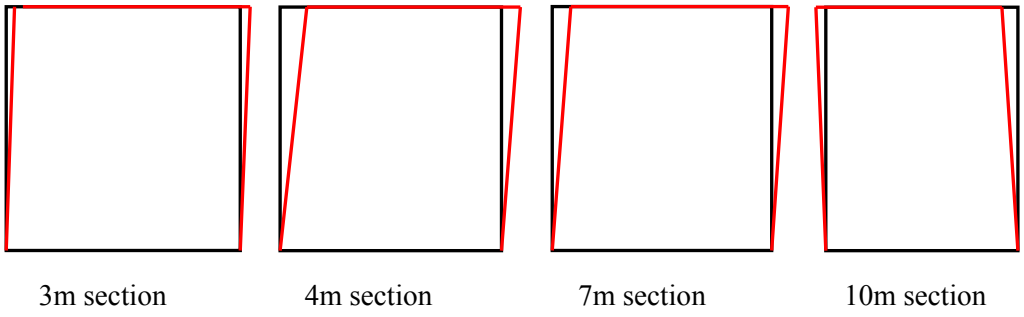

Figure 4.29. Sketch showing direction of the twisting of the box caused by the transverse shear distortion at different sections of the blade. The deformation is seen from the root.

The measured transverse shear distortion in the different sections is not significant, below 3mm change of diagonal lengths in 4m section, where it is pronounced the most, and the measured shear deformations are asymmetric, see also .
The asymmetry of the transverse shear distortion could be due to the deformation of the webs. The leading and trailing edge webs do not deform in the same way see , , and .
The transverse shear distortion measurements at 3m, 4m and 7m section up to only 55% of the Risø load are very steep indicating that there is some instability here. The steep region is of the size of 1mm so at this stage it is not possible to conclude that the transverse shear distortion can become a serious problem, size the unstable behaviour could change to a stable phase. This will be tested in a coming test reaching higher load.

4.7 Deformations in the main sections

When preparing the measurements, four sections were chosen as the main sections and were heavily instrumented. The four sections are: 3m, 4m, 7m and 10m, where the deformations of caps, webs and panels were measured. These deformations are illustrated for three of the four sections, see , and . The web deformation was not measured in 3m section because a maintenance hole in the trailing edge web was placed there, as explained in the second data report, ref.[2]
The deformations are exaggerated for better visualization. The web behaviour, illustrated in these sketches, indicates that both webs in 4m as well as 7m sections deform inwards, whereas the webs in 10m section deform outwards. Data showing this deformation is presented in Appendix D. At the pressure side, the cap deformation changes from moving inwards (slightly at 4m) to outwards (7m) and then inwards again (10m), whereas the suction side cap deforms outwards in 4m, decreased outwards in 7m section and inwards in 10m section.

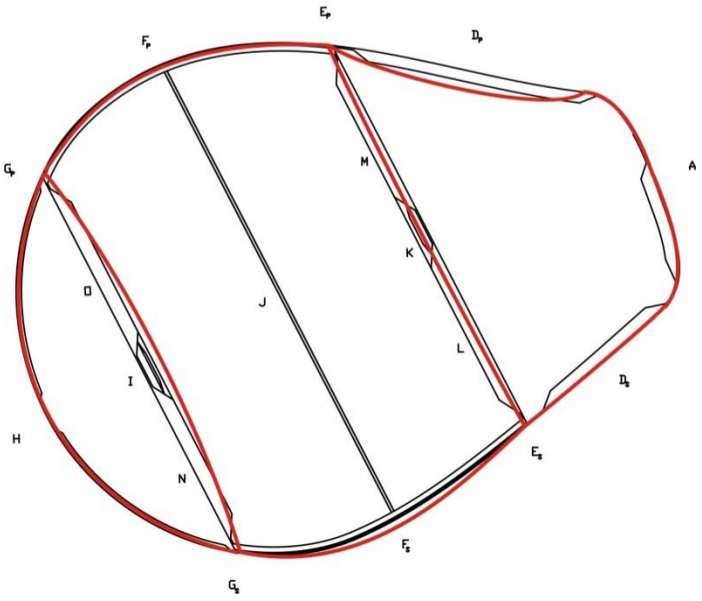

Figure 4.30. Illustration of the profile deformations in 4m, the deformation pattern is illustrated by the red line and is exaggerated to better illustrate the behaviour.

The panel deformations are illustrated as well. The pressure side panel is deforms inwards in 4m and 7m sections and outwards in 10m section.

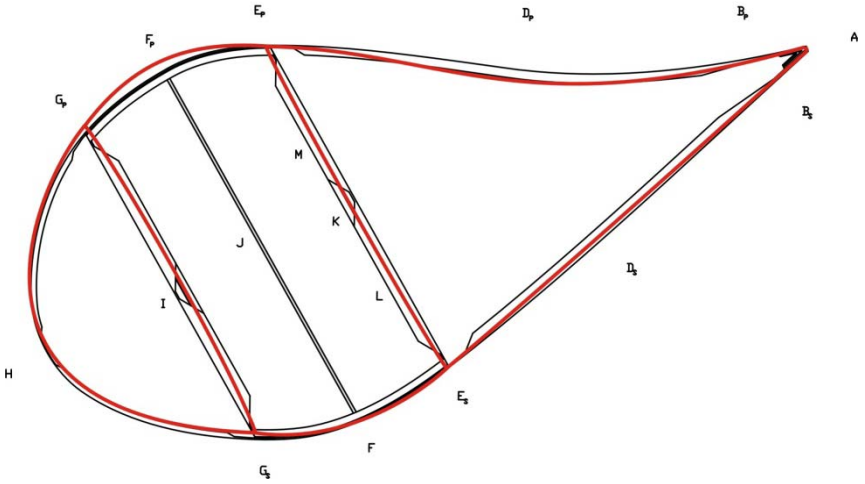

Figure 4.31. Illustration of deformations in 7m section

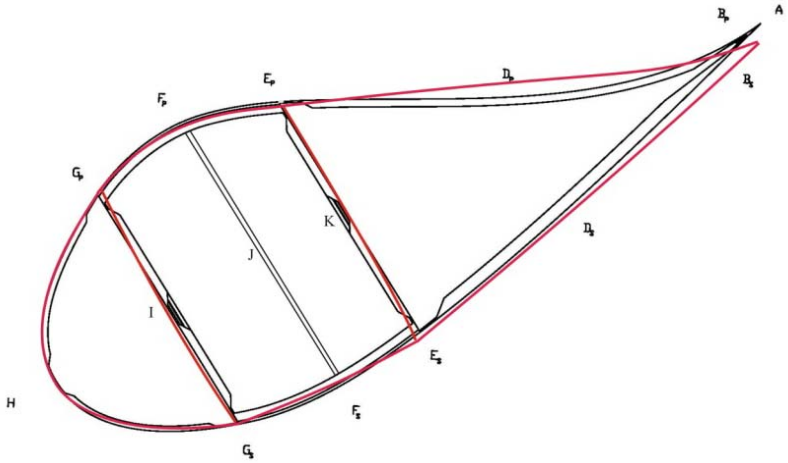

Figure 4.32. Illustration of deformations in 10m section

The horizontal displacement of the blade and the positions of the load applications have some influence on the profile deformation. To illustrate this, the horizontal movement of the blade at the load application positions is presented together with the local and global deformations of several sections, see . The local deformations are exaggerated for better visualization. In each section they are scaled with the same factor giving comparable illustration of the deformations.

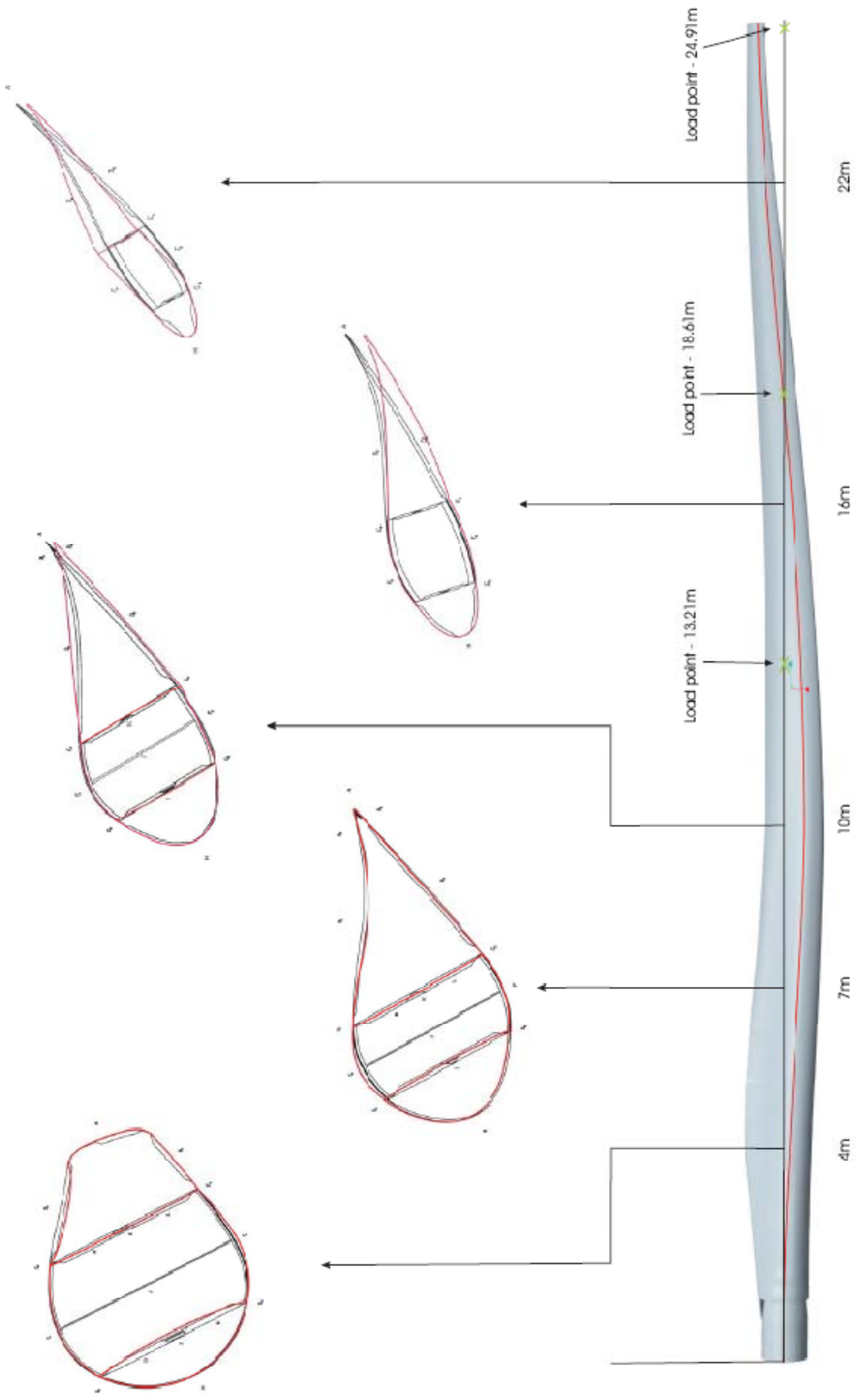

Figure 4.33. Overview of local and global deformations as selected sections.

4.8 Strain measurements

At 35% Risø load all strain gauges mounted on the blade were used. As mentioned earlier, three pulls were needed to record them all. Therefore, 35% Risø load level for these measurements was chosen in order to prevent damage of the blade. Under the studied combined load case, 55% Risø load was expected to be able to damage the blade. Thus, this load level was reached once with the strain measurements called 'other group' were performed.
In this section, the strain results are presented, both for 35% and 55% Risø load. The results 35% for Risø loads are presented where they contain more measurements for the studied area or where the 55% Risø loads was not measured. The results can be found in Appendix B.
The strain measurements are presented at the maximum load from the studied pull. They are presented as a function of the distance from the root. It needs to be underlined that the strain measurements present the change of strain between 13% Risø load and the maximum load attained, see chapter 3.

In the strain measurements in position E are presented at 35% Risø load. The same position is presented in for fewer measurements at 55% load.
 presents the strain measurements in position F at 35% Risø load. The same position is given in for fewer measurements at 55% Risø load.
The results measured on the web (points L,M,N,O) at 35% Risø load are presented in .
The strain measurements in the middle of the trailing edge panels are given in .
Measurements on the panels just above the trailing edge (position B) are presented in .
 and present the measurement at the trailing edge (A), at 35% Risø load. presents the measurements close to the root.
 gives the results at the leading edge panels (point H) at 35% Risø load.
The notation for measurement positions is presented in .

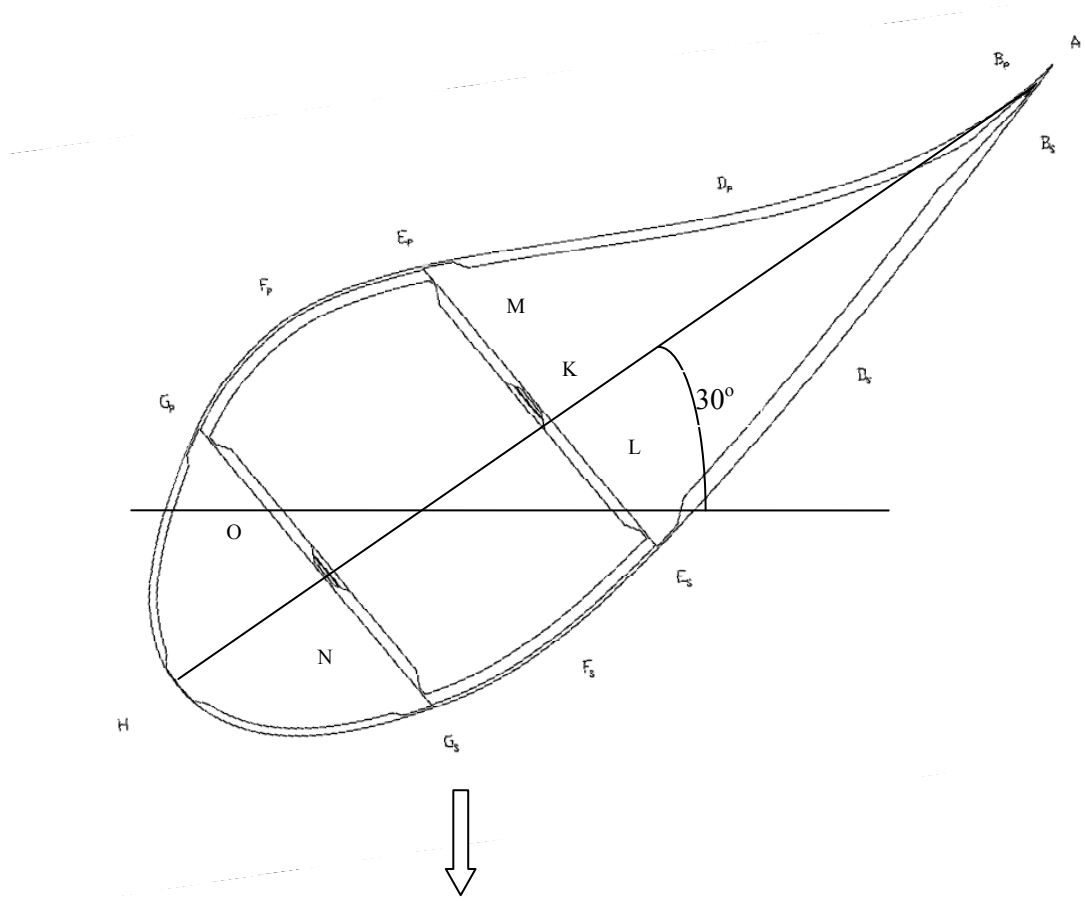

Figure 4.34. Sketch of a blade section presenting the notation of the position and the orientation of the blade according to the load direction.

For the strain measurements presented for the combined load case it is distinct that the strain near to the horizontal line passing through the shear centre are small compared to the other side of the blade, that is measurement from position O, L $E_{s,}$ and D_s are small compared to M,N, E_p and D_p.

The results in , , and indicate that two sets of measurements, marked with yellow, distinguish from the rest. The first one is the strain measurements placed at 5m on the transition area between the box and the trailing edge panels E_s, and the second one is at the cap centre at 10m section F_S. Both measurements are placed on the suction side and reveal similar behaviour.
The strain gauges at 10m, position F_s and 5m, point E_s, were examined in order to explore if the longitudinal and transversal strains were interchanged. The investigation was performed by placing a finger on the actual strain gauge and checking which signal responded to the finger temperature. The strain gauges appear to be interchanged and the corrected values are marked with blue colour in

the tables. The original results are not presented here, as they are gathered in Appendix B.

Table 4.4. Strain measured at the transition between the box and the panels (E) at 35% Risø load.

	Suction side Strain gauge E_s [μS]				Pressure side strain gauge E_p [μS]			
	Outer L	Inner L	Outer T	Inner T	Outer L	Inner L	Outer T	Inner T
3 m	-290	-290	70	210	1000			
4 m	-450	-450	20	290	1100		-490	
4.5m					900		-350	-900
5 m	50	-550	-550	100		900	-250	-750
5m	-550	-550	50	100	5m suction side corrected values			
6 m	-600	-600	220	230	1000			-650
7 m	-790	-700	200	320		1050	-500	-710
8 m	-800	-800	550	50	900	800	-430	-320
9 m	-800	-950	700	150	1000	950	-450	-490
10 m	-790	-800	260	440	1100	1100	-400	-550

Table 4.5. Strain measurements from pull *Ecombined_070910* at 55% Risø load at the transition between the cap and the trailing edge panels (position E).

	Suction side Strain gauge E_s [μS]				Pressure side strain gauge E_p [μS]			
	Outer L	Inner L	Outer T	Inner T	Outer L	Inner L	Outer T	Inner T
3 m	-500	-500	330	170	1800			
4,5 m					1800		-600	-1700
5 m	300	-1000	-1000	App. 0		1700	-500	-1400
5m	-1000	-1000	300	App. 0	5m Suction side corrected values			
6 m	-1150	-1100	400	250	1800			-1250
7 m								
8 m		-1500		-100		1550		-600
9 m		-1800		100		1800		-900
10 m								
11 m								
12 m								

Table 4.6. Strain measurements from pull *Ecombined_020110* and *010910* at point F (cap mid-point) at 35% of the Risø load.

	Suction side Strain gauge F_s [μS]				Pressure side strain gauge F_p [μS]			
	Outer L	Inner L	Outer T	Inner T	Outer L	Inner L	Outer T	Inner T
3 m	-700	-800			700	690		
4 m	-820	-880			750	750		
5 m	-1050	-1000			800	750		
6 m	-1100	-1000			800	800		
7 m	-1100	-880	600	30	900	750	-300	-300
8 m	-1150				1000	900		
9 m	-1300	-1050			950	950		
10 m	100	-1000	-1100	600	950	950	-520	-180
10m	-1100	-1000	100	600	10m Suction side corrected values			
11 m	-1150	-1100			1000	900		
12 m	-1200	-1100			1050	700		

Table 4.7. Strain measurements at the cap midpoint. (position F) from pull *Ecombined_070910* at 55% Risø load.

	Suction side Strain gauge F_s [μS]				Pressure side strain gauge F_p [μS]			
	Outer L	Inner L	Outer T	Inner T	Outer L	Inner L	Outer T	Inner T
3 m	-1390	-1590			1200	1250		
4 m	-1600	-1650			1400	1400		
5 m	-1900	-1800			1450	1450		
6 m	-2100	-1800			1500	1500		
7 m	-2100	-1750	1100	50	1600	1400	-600	-500
8 m	-2100				1800	1600		
9 m	-2250	-1950			1750	1750		
10 m	50	-1800	-2000	1200	1750	1750	-250	-1050
10m	-2000	-1800	50	1200	10m suction side corrected values			
11 m	-2100	-2000			1800	1750		
12 m	-2100	-2000			1200	1900		

Two strain measurements both at position E_s, the first in 8m and the next in 9m section, are marked with yellow. The measurement results from these are presented in as they change from positive to negative (tension into compression) during the tests.

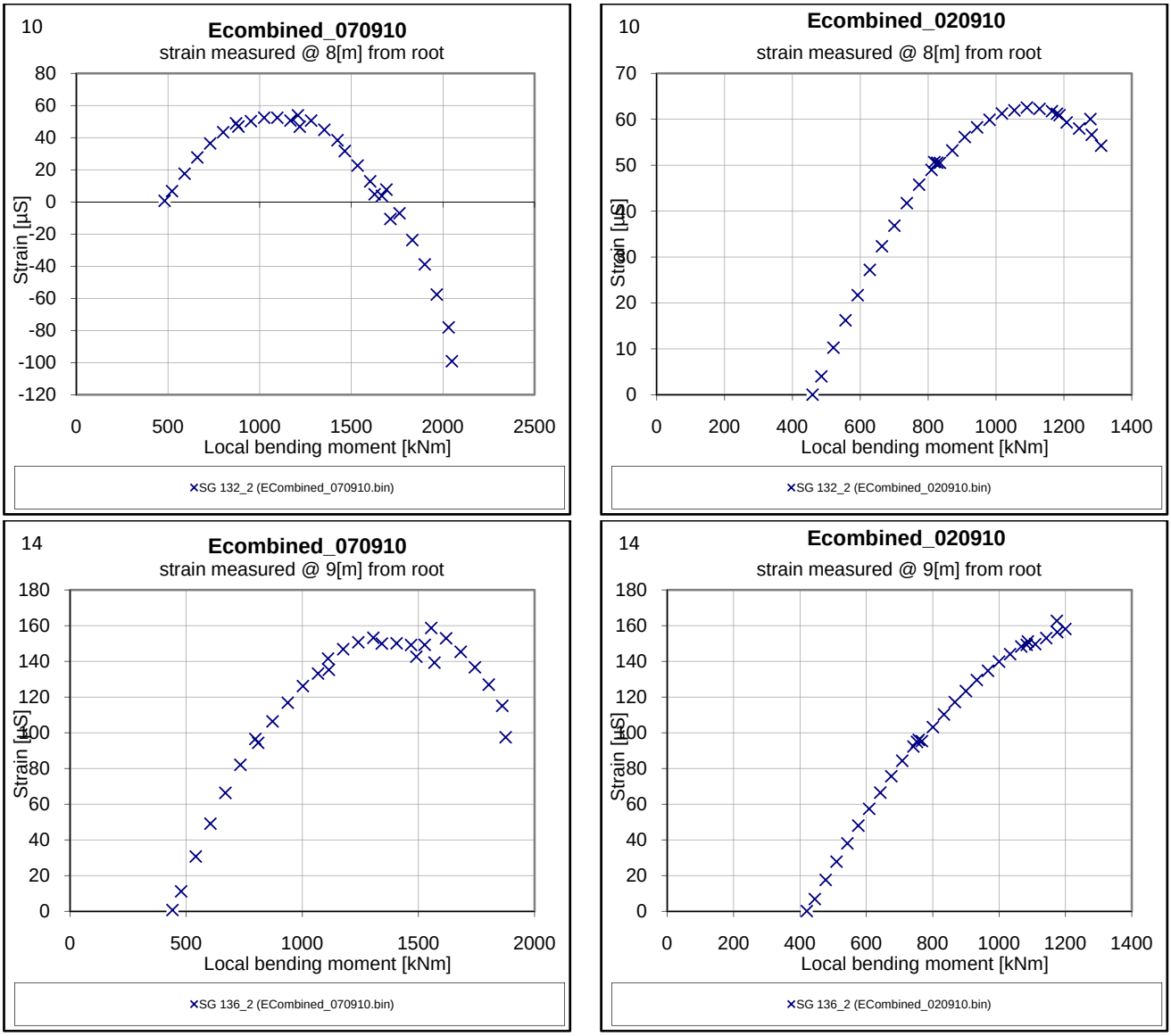

Figure 4.35. Strain measurements at the transition between the box and the trailing edge panels (position E). Pull *Ecombined_070910* is presented at 55% Risø load and pull *Econbined_020910* is at 35% Risø load.

The strain measurements on the web at 35% Risø load are presented in . The notation N, O, L and M corresponds to the strain measurement placement on the web, see . At the root region, the strain in positions O and L are small compared to N and M. This reflects the loading direction (combined, flap- and edgewise).

Table 4.8. Strain measurements on the web at 35% Risø load

	Position N			Position O		
Distance						
3 m in	-700	680	-100	-25	180	45
4 m in	-800	800	60	100	10	10
7 m in	-800	590	10	250	-50	60
10 m in	-1000	600	-50	180	-100	180
	Position L			Position M		
3 m	-10	10	-140	700	-300	180
4 m out	-160	50	-100	650	0	220
4 m in	-200	135	-100		-450	0
7 m out	-490	190	-250	680	-230	280
7 m in	-400	210	-200	720	-275	250
10 m out	-750	120	-350	400	-510	0
10 m in	-510	280	-75	700	-410	180

The strain measurements at the mid-point of the panels (position D) were taken at of the 35% Risø load, see .

The strain measured on the suction side is significantly lower than on the pressure side. The strains on the pressure side panel have the same magnitude as on the cap. The small strain values at the suction side are in agreement with small deformations of the suction side panel, see , , and Apendix D.

Table 4.9. Strain measurement at panel midpoint (position D) at 35% of the Risø load.

	Suction side strain gauge D_s [μS]				Pressure side strain gauge D_p [μS]			
	Outer L	Inner L	Outer T	Inner T	Outer L	Inner L	Outer T	Inner T
3 m	-10	-10	100	5	1000	900	- 700	-250
3.5 m						950	- 720	-180
3.75m					920	1050	-1000	-150
4 m	-50	≈0	- 50	50	920	1050	- 900	100
4.25m					1150	900	-975	≈0
4.5 m					1225	970	-850	-90
4.75m					1000	1000	-790	≈0
5 m	30	65	-225	-40	850	900		-55
5.25m					1000	900	-1000	-100
6 m	-70	-15	-120	-10	850	790	-650	-200
7 m	-55		- 60	-55	850	700	-600	-200
8 m	-110	-42	- 40	30	700	550	-320	-250
9 m	-120	-40	- 18	50	590	620	-310	-340
10 m		-90	- 60	60	950	820	-450	-450

The strains close to or at the trailing edge are presented for 35% Risø load. The strains in this region are of the same magnitude as at the cap, see , and .

Table 4.10. Strain measurements on the panels close to the trailing edge at 35% Risø load.

	Suction side strain gauge B_s [μS]				Pressure side strain gauge B_p [μS]			
	Outer L	Inner L	Outer T	Inner T	Outer L	Inner L	Outer T	Inner T
7 m	600	650	-700	250	850	800	-150	-1000
8 m	625	575	-400	-70	750	650	- 200	-500
9 m	600	600	-290	-200	600	700	-300	-420
10 m	630	550	- 220	-275	1000	800		-370

Table 4.11. Strain measurements at the trailing edge close to the root at 35% Risø load.

	Trailing edge root part A [μS]			
	Outer L	Inner L	Outer T	Inner T
3 m	920		800	
4 m	850	≈0	750	-600
5 m	850		890	

Table 4.12 Strain measurements at the trailing edge from 7m section, 35% Risø load

	Trailing edge	
	Suction side SG A_s [μS]	Pressure side SG A_p [μS]
	Outer L	Outer L
7 m	680	800
7.5m	750	750
8 m	740	760
8.5m	780	710
9.5m		970
10 m	790	950
10.5m	800	850
11 m	800	950
11.5m	790	950
12 m	790	900
12.5m	800	870
13.5m	690	790
14.5m	720	820
15.5m	700	880
16 m		800
22 m	450	500

In order to present all measurements the strain at the trailing edge panel is presented as well, see showing results for 35% of Risø load.

Table 4.13. Strain measurements at the leading edge at 35% Risø load

	Leading edge	
	H [μS] Outer L	H [μS] Outer T
4 m	-700	300
7 m	-600	300
10 m	-650	250
16 m	-400	
22 m	-25	5

5. Summary

This report presents tests carried out on a truncated blade from SSP technology A/S under a combined flap and edgewise load. The blade was tested with 55 % of a Risø extreme load at angle of 30° from the flapwise plane in direction towards the leading edge. The load was applied to the suction side of the blade using a new loading technique. The newly developed loading method uses anchor plates and the loads were applied on the suction side only.

The influence of the load adjustment was examined revealing that the deformations of panels and web were reluctant to follow (decrease) when the bending moment was reduced. The deflection measurements were repeated three times and compared to each other. These results showed that there was some variation between the first test performed after the blade has been rotated and the following ones. The results from the investigations indicate that the blade is not a perfectly elastic structure. It is suggested that the blade had been pre-deformed slightly from the loading direction it has been exposed to, and the adjustment of the shape to the current load case is included in the measurement.

The local deformation of the trailing edge showed that in 10m section the blade was twisted first clockwise and then counter clockwise as the loads increased and that in 22m section the trailing edge deforms considerably.

The transverse shear distortion phenomenon was examined and in the measured sections it was observed. The load will be increased in a forthcoming test to investigate whether this unstable behaviour will continue to failure or it will stabilize.

6. References

[1] Nielsen, M., Jensen, F. M., Nielsen, P. H., Berring, P., Martyniuk, K., Roczek, A., Sieradzan, T., Roudnitski, V., Kucio, P., Bitsche, R., Andreasen, P., Lukassen, T., Andrlová, Z., Branner, K., Bak, C., Kallesøe, B., McGugan M. "*Full Scale Test of SSP 34m blade, edgewise loading LTT. Data Report 1*" Risø-R-1718(EN). (January 2010)

[2] Magda Nielsen, Agnieszka Roczek-Sieradzan, Find M. Jensen, Per H. Nielsen, Peter Berring, Tomasz Sieradzan, Vatslav Roudnitski, Robert Bitsche, Henrik Knudsen, Anders Rasmussen, Jens Rasmussen, Ulla Uldahl, Zuzana Andrlová, Kim Branner, Christian Bak, Bjarne Kallesøe, Malcolm McGugan, Mikkel Lagerbon. "*Full Scale Test SSP 34m blade, edgewise loading LTT. Extreme load and PoC_InvE Data report*" Risø-R 1748(EN) (September 2010)

[3] Jensen, F. M. *"Ultimate strength of a large wind turbine blade"*, Risø-PhD-34(EN) (May 2008)

[4] Jensen, F. M., Falzon, B.G., Ankersen, J., Stang, H. *"Structural testing and numerical simulation of a 34m composite wind turbine blade",* Composite Structures 76, 2006

[5] Thomsen, C. L., Eisenberg, Y. P. *"Blade Test SSP34#2. Edgewise and Flapwise Final Static test"* Risø National Laboratory, Denmark November 2003

[6] Thomsen C. L., Jørgensen E. R., Borum K. K., McGugan M., Debel C. P., Sørensen B., Jensen F. M. *"V52 Statisk Styrke".* Risø-I-Report. (April 2003)

7. Appendices

A Measurement equipment and its placements

B Strain and deflection measurement data

C Acoustic Emission

D Deformation of the sections

E Extracting horizontal deflection

F Graph with repeated deflection measurements

G FEM analysis of combined load.

A Measurement equipment at its placements

Displacement transducers Group 1

	1	2	3	4	5	6	7	8	9	10
A1	FT-1	FT-2	FT-3	ASM-2000-5	ASM-6000-1	ASM-2000-7	ASM-4000-2	ASM-2000-2	ASM-2000-3	ASM-2000-4
A2	ASM-4000-1	ASM-100-23	ASM-2000-8	ASM-2000-6	ASM-2000-1	NT-50-11	NT-100-6	NT-50-6	NT-50-7	NT-50-16
A3	NT-100-3	NT-100-2	NT-100-5	NT-50-8	NT-50-9	NT-50-10	NT-100-4	NT-50-15	NT-50-13	NT-50-14
A4	empty	empty	NT-50-1	NT-50-2	empty	NT-50-4	NT-50-5	*empty*	FT-4	ASM-100-9
A5	ASM-100-10	ASM-100-11	ASM-100-12	ASM-100-13	ASM-100-14	ASM-100-17	ASM-100-19	ASM-100-20	ASM-100-21	ASM-100-22
A6	ASM-100-1	ASM-100-2	ASM-100-15	FT-5	FT-6	ASM-100-5	ASM-100-16	ASM-100-6	ASM-100-18	ASM-100-7

Strain gauges positions Main section

		Group A-Global				Group B-TE-Panels						Group C-Shear Webs				Group D-Caps	
		A	**As**	**Ap**	**H**	**Bs**	**Bp**	**Ds**	**Dp**	**Es**	**Ep**	**Ls**	**Mp**	**Ns**	**Op**	**Fp**	**Fs**
Section					LE	SS_TE	PS_TE	PS_MID	SS_MID			SS_CAP	PS_CAP	SS_CAP	PS_CAP	PS_CAP	SS_CAP
3 m	Outer	SG1UD						SG67Bx	SG69Bx	SG111Bx	SG113Bx					SG201UD	SG203UD
	Inner	SG2UD						SG68Bx	SG70Bx	SG112Bx		SG151Tx	SG153Tx	SG152Tx	SG158Tx	SG202UD	SG204UD
3.5 m	Outer								SG251Bx		SG253Bx						
	Inner								SG250Bx								
3.75 m	Outer								SG303Bx								
	Inner								SG304Bx								
4 m	Outer	SG3Bx			SG41Bx			SG71Tx	SG73Tx	SG115Bx	SG117Bx	SG161Tx	SG163Tx			SG205UD	SG207UD
	Inner	SG4Bx						SG72Tx	SG74Tx	SG116Bx		SG162Tx	SG164Tx	SG166Tx	SG168Tx	SG206UD	SG208UD
4.25 m	Outer								SG307Bx								
	Inner								SG308Bx								
4.5 m	Outer								SG255Bx		SG257Bx						
	Inner								SG254Bx		SG256Bx						
4.75 m	Outer								SG311Bx								
	Inner								SG312Bx								
5 m	Outer	SG5UD						SG75Bx	SG77Bx	SG119Bx	SG121Bx					SG209UD	SG211UD
	Inner	SG6UD						SG76Bx	SG78Bx	SG120Bx	SG122Bx					SG210UD	SG212UD
5.25 m	Outer								SG315Bx								
	Inner								SG316Bx								
6 m	Outer	SG7UD						SG79Bx	SG81Bx	SG123Bx	SG125Bx					SG213UD	SG215UD
	Inner	SG8UD						SG80Bx	SG82Bx	SG124Bx	SG126Bx					SG214UD	SG216UD
7 m	Outer		SG9UD	SG11UD	SG43Bx	SG51Bx	SG53Bx	SG83Tx	SG85Tx	SG127Bx	SG129Bx	SG171Tx	SG173Tx			SG217Bx	SG219Bx
	Inner					SG52Bx	SG54Bx	SG84Tx	SG86Tx	SG128Bx	SG130Bx	SG172Tx	SG174Tx	SG176Tx	SG178Tx	SG218Bx	SG220Bx
7.5 m	Outer		SG297UD	SG299UD													
	Inner																
8 m	Outer		SG13UD	SG15UD		SG55Bx	SG57Bx	SG87Bx	SG89Bx	SG131Bx	SG133Bx					SG221UD	SG223UD
	Inner					SG56Bx	SG58Bx	SG88Bx	SG90Bx	SG132Bx	SG134Bx					SG222UD	SG224UD
8.5 m	Outer		SG261UD	SG263UD													
	Inner																
9 m	Outer		SG17UD	SG19UD		SG59Bx	SG61Bx	SG91Bx	SG93Bx	SG135Bx	SG137Bx					SG225UD	SG227UD
	Inner					SG60Bx	SG62Bx	SG92Bx	SG94Bx	SG136Bx	SG138Bx					SG226UD	SG228UD
9.5 m	Outer		SG265UD	SG267UD													
	Inner																
10 m	Outer		SG21UD	SG23UD	SG45Bx	SG63Bx	SG65Bx	SG95Tx	SG97Tx	SG139Bx	SG141Bx	SG181Tx	SG183Tx			SG229Bx	SG231Bx
	Inner					SG64Bx	SG66Bx	SG96Tx	SG98Tx	SG140Bx	SG142Bx	SG182Tx	SG184Tx	SG186Tx	SG188Tx	SG230Bx	SG232Bx
10.5 m	Outer		SG269UD	SG271UD													
	Inner																
11 m	Outer		SG25UD	SG27UD												SG233UD	SG235UD
	Inner															SG234UD	SG236UD
11.5 m	Outer		SG273UD	SG275UD													
	Inner																
12 m	Outer		SG29UD	SG31UD												SG237UD	SG239UD
	Inner															SG238UD	SG240UD
12.5 m	Outer		SG277UD	SG279UD													
	Inner																
13.5 m	Outer		SG281UD	SG283UD													
	Inner																
14.5 m	Outer		SG285UD	SG287UD													
	Inner																
15.5 m	Outer		SG289UD	SG291UD													
	Inner																
16 m	Outer		SG33UD	SG35UD	SG47Bx			SG99Bx	SG101Bx							SG241UD	SG243UD
	Inner																
22 m	Outer		SG37UD	SG39UD	SG49Bx			SG103Bx	SG105Bx							SG245UD	SG247UD
	Inner																

	Unidirectionel (0 long.)
BX	Biax (0/90 long/vert. or trv.)
TX	Triax/Rosette(0/45/90)

	Group
Global edgewise bending	**A**
Trailing edge panel deflection	**B**
Shear webs	**C**
Caps	**D**

Strain gauges positions AED Section + Global

		Group A-Global				Group B-TE-Panels						Group C-Shear Webs				Group D-Caps	
		A	**As**	**Ap**	**H**	**Bs**	**Bp**	**Ds**	**Dp**	**Es**	**Ep**	**Ls**	**Mp**	**Ns**	**Op**	**Fp**	**Fs**
Section					LE	SS_TE	PS_TE	PS_MID	SS_MID			SS_CAP	PS_CAP	SS_CAP	PS_CAP	PS_CAP	SS_CAP
3 m	Outer	SG1UD						SG67Bx	SG69Bx	SG111Bx	SG113Bx					SG201UD	SG203UD
	Inner	SG2UD						SG68Bx	SG70Bx	SG112Bx		SG151Tx	SG153Tx	SG152Tx	SG158Tx	SG202UD	SG204UD
3.5 m	Outer								SG251Bx		SG253Bx						
	Inner								SG250Bx								
3.75 m	Outer								SG303Bx								
	Inner								SG304Bx								
4 m	Outer	SG3Bx			SG41Bx			SG71Tx	SG73Tx	SG115Bx	SG117Bx	SG161Tx	SG163Tx			SG205UD	SG207UD
	Inner	SG4Bx						SG72Tx	SG74Tx	SG116Bx		SG162Tx	SG164Tx	SG166Tx	SG168Tx	SG206UD	SG208UD
4.25 m	Outer								SG307Bx								
	Inner								SG308Bx								
4.5 m	Outer								SG255Bx		SG257Bx						
	Inner								SG254Bx		SG256Bx						
4.75 m	Outer								SG311Bx								
	Inner								SG312Bx								
5 m	Outer	SG5UD						SG75Bx	SG77Bx	SG119Bx	SG121Bx					SG209UD	SG211UD
	Inner	SG6UD						SG76Bx	SG78Bx	SG120Bx	SG122Bx					SG210UD	SG212UD
5.25 m	Outer								SG315Bx								
	Inner								SG316Bx								
6 m	Outer	SG7UD						SG79Bx	SG81Bx	SG123Bx	SG125Bx					SG213UD	SG215UD
	Inner	SG8UD						SG80Bx	SG82Bx	SG124Bx	SG126Bx					SG214UD	SG216UD
7 m	Outer		SG9UD	SG11UD	SG43Bx	SG51Bx	SG53Bx	SG83Tx	SG85Tx	SG127Bx	SG129Bx	SG171Tx	SG173Tx			SG217Bx	SG219Bx
	Inner					SG52Bx	SG54Bx	SG84Tx	SG86Tx	SG128Bx	SG130Bx	SG172Tx	SG174Tx	SG176Tx	SG178Tx	SG218Bx	SG220Bx
7.5 m	Outer		SG297UD	SG299UD													
	Inner																
8 m	Outer		SG13UD	SG15UD		SG55Bx	SG57Bx	SG87Bx	SG89Bx	SG131Bx	SG133Bx					SG221UD	SG223UD
	Inner					SG56Bx	SG58Bx	SG88Bx	SG90Bx	SG132Bx	SG134Bx					SG222UD	SG224UD
8.5 m	Outer		SG261UD	SG263UD													
	Inner																
9 m	Outer		SG17UD	SG19UD		SG59Bx	SG61Bx	SG91Bx	SG93Bx	SG135Bx	SG137Bx					SG225UD	SG227UD
	Inner					SG60Bx	SG62Bx	SG92Bx	SG94Bx	SG136Bx	SG138Bx					SG226UD	SG228UD
9.5 m	Outer		SG265UD	SG267UD													
	Inner																
10 m	Outer		SG21UD	SG23UD	SG45Bx	SG63Bx	SG65Bx	SG95Tx	SG97Tx	SG139Bx	SG141Bx	SG181Tx	SG183Tx			SG229Bx	SG231Bx
	Inner					SG64Bx	SG66Bx	SG96Tx	SG98Tx	SG140Bx	SG142Bx	SG182Tx	SG184Tx	SG186Tx	SG188Tx	SG230Bx	SG232Bx
10.5 m	Outer		SG269UD	SG271UD													
	Inner																
11 m	Outer		SG25UD	SG27UD												SG233UD	SG235UD
	Inner															SG234UD	SG236UD
11.5 m	Outer		SG273UD	SG275UD													
	Inner																
12 m	Outer		SG29UD	SG31UD												SG237UD	SG239UD
	Inner															SG238UD	SG240UD
12.5 m	Outer		SG277UD	SG279UD													
	Inner																
13.5 m	Outer		SG281UD	SG283UD													
	Inner																
14.5 m	Outer		SG285UD	SG287UD													
	Inner																
15.5 m	Outer		SG289UD	SG291UD													
	Inner																
16 m	Outer		SG33UD	SG35UD	SG47Bx			SG99Bx	SG101Bx							SG241UD	SG243UD
	Inner																
22 m	Outer		SG37UD	SG39UD	SG49Bx			SG103Bx	SG105Bx							SG245UD	SG247UD
	Inner																

	Unidirectionel (0 long.)
BX	Biax (0/90 long/vert. or trv.)
TX	Triax/Rosette(0/45/90)

	Group
Global edgewise bending	**A**
Trailing edge panel deflection	**B**
Shear webs	**C**
Caps	**D**

Strain gauges positions other groups

		Group A-Global				Group B-TE-Panels						Group C-Shear Webs				Group D-Caps	
		A	**As**	**Ap**	**H**	**Bs**	**Bp**	**Ds**	**Dp**	**Es**	**Ep**	**Ls**	**Mp**	**Ns**	**Op**	**Fp**	**Fs**
Section					LE	SS_TE	PS_TE	PS_MID	SS_MID			SS_CAP	PS_CAP	PS_CAP	PS_CAP	PS_CAP	SS_CAP
3 m	Outer	SG1UD						SG67Bx	SG69Bx	SG111Bx	SG113Bx					SG201UD	SG203UD
	Inner	SG2UD						SG68Bx	SG70Bx	SG112Bx		SG151Tx	SG153Tx	SG152Tx	SG158Tx	SG202UD	SG204UD
3.5 m	Outer								SG251Bx		SG253Bx						
	Inner								SG250Bx								
3.75 m	Outer								SG303Bx								
	Inner								SG304Bx								
4 m	Outer	SG3Bx			SG41Bx			SG71Tx	SG73Tx	SG115Bx	SG117Bx	SG161Tx	SG163Tx			SG205UD	SG207UD
	Inner	SG4Bx						SG72Tx	SG74Tx	SG116Bx		SG162Tx	SG164Tx	SG166Tx	SG168Tx	SG206UD	SG208UD
4.25 m	Outer								SG307Bx								
	Inner								SG308Bx								
4.5 m	Outer								SG255Bx		SG257Bx						
	Inner								SG254Bx		SG256Bx						
4.75 m	Outer								SG311Bx								
	Inner								SG312Bx								
5 m	Outer	SG5UD						SG75Bx	SG77Bx	SG119Bx	SG121Bx					SG209UD	SG211UD
	Inner	SG6UD						SG76Bx	SG78Bx	SG120Bx	SG122Bx					SG210UD	SG212UD
5.25 m	Outer								SG315Bx								
	Inner								SG316Bx								
6 m	Outer	SG7UD						SG79Bx	SG81Bx	SG123Bx	SG125Bx					SG213UD	SG215UD
	Inner	SG8UD						SG80Bx	SG82Bx	SG124Bx	SG126Bx					SG214UD	SG216UD
7 m	Outer		SG9UD	SG11UD	SG43Bx	SG51Bx	SG53Bx	SG83Tx	SG85Tx	SG127Bx	SG129Bx	SG171Tx	SG173Tx			SG217Bx	SG219Bx
	Inner					SG52Bx	SG54Bx	SG84Tx	SG86Tx	SG128Bx	SG130Bx	SG172Tx	SG174Tx	SG176Tx	SG178Tx	SG218Bx	SG220Bx
7.5 m	Outer		SG297UD	SG299UD													
	Inner																
8 m	Outer		SG13UD	SG15UD		SG55Bx	SG57Bx	SG87Bx	SG89Bx	SG131Bx	SG133Bx					SG221UD	SG223UD
	Inner					SG56Bx	SG58Bx	SG88Bx	SG90Bx	SG132Bx	SG134Bx					SG222UD	SG224UD
8.5 m	Outer		SG261UD	SG263UD													
	Inner																
9 m	Outer		SG17UD	SG19UD		SG59Bx	SG61Bx	SG91Bx	SG93Bx	SG135Bx	SG137Bx					SG225UD	SG227UD
	Inner					SG60Bx	SG62Bx	SG92Bx	SG94Bx	SG136Bx	SG138Bx					SG226UD	SG228UD
9.5 m	Outer		SG265UD	SG267UD													
	Inner																
10 m	Outer		SG21UD	SG23UD	SG45Bx	SG63Bx	SG65Bx	SG95Tx	SG97Tx	SG139Bx	SG141Bx	SG181Tx	SG183Tx			SG229Bx	SG231Bx
	Inner					SG64Bx	SG66Bx	SG96Tx	SG98Tx	SG140Bx	SG142Bx	SG182Tx	SG184Tx	SG186Tx	SG188Tx	SG230Bx	SG232Bx
10.5 m	Outer		SG269UD	SG271UD													
	Inner																
11 m	Outer		SG25UD	SG27UD												SG233UD	SG235UD
	Inner															SG234UD	SG236UD
11.5 m	Outer		SG273UD	SG275UD													
	Inner																
12 m	Outer		SG29UD	SG31UD												SG237UD	SG239UD
	Inner															SG238UD	SG240UD
12.5 m	Outer		SG277UD	SG279UD													
	Inner																
13.5 m	Outer		SG281UD	SG283UD													
	Inner																
14.5 m	Outer		SG285UD	SG287UD													
	Inner																
15.5 m	Outer		SG289UD	SG291UD													
	Inner																
16 m	Outer		SG33UD	SG35UD	SG47Bx			SG99Bx	SG101Bx							SG241UD	SG243UD
	Inner																
22 m	Outer		SG37UD	SG39UD	SG49Bx			SG103Bx	SG105Bx							SG245UD	SG247UD
	Inner																

	Unidirectionel (0 long.)
BX	Biax (0/90 long/vert. or trv.)
TX	Triax/Rosette(0/45/90)

	Group
Global edgewise bending	**A**
Trailing edge panel deflection	**B**
Shear webs	**C**
Caps	**D**

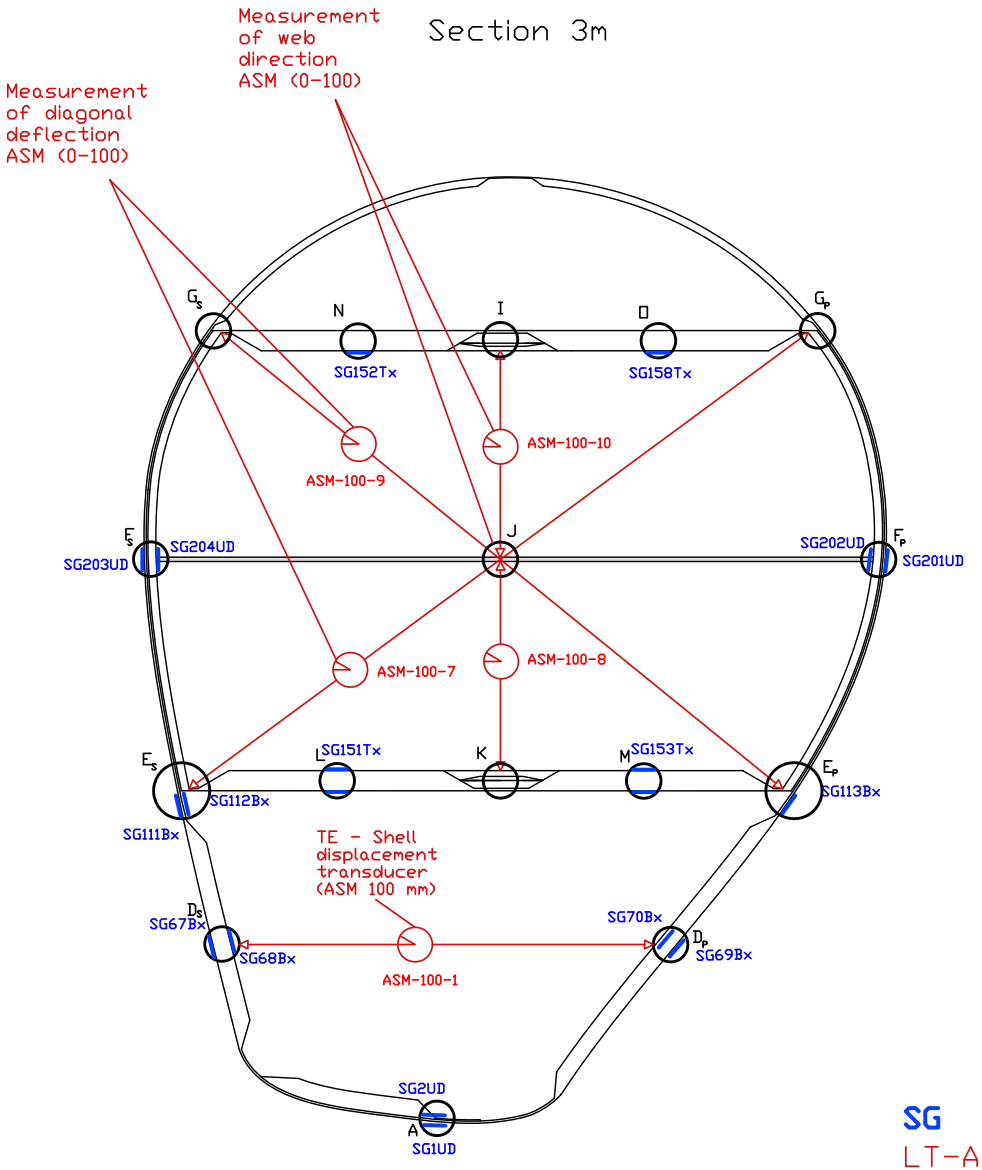
Section 3m
Measurement of web direction ASM (0-100)
Measurement of diagonal deflection ASM (0-100)
G_S
N
I
D
G_P
SG152Tx
SG158Tx
ASM-100-9
ASM-100-10
F_S
SG204UD
SG203UD
J
SG202UD
F_P
SG201UD
ASM-100-7
ASM-100-8
E_S
L
SG151Tx
K
M
SG153Tx
E_P
SG112Bx
SG113Bx
SG111Bx
TE - Shell displacement transducer (ASM 100 mm)
D_S
SG67Bx
SG70Bx
D_P
SG68Bx
ASM-100-1
SG69Bx
SG2UD
A
SG1UD

SG

LT-ASM

Section 3.5m based on the 3m. section

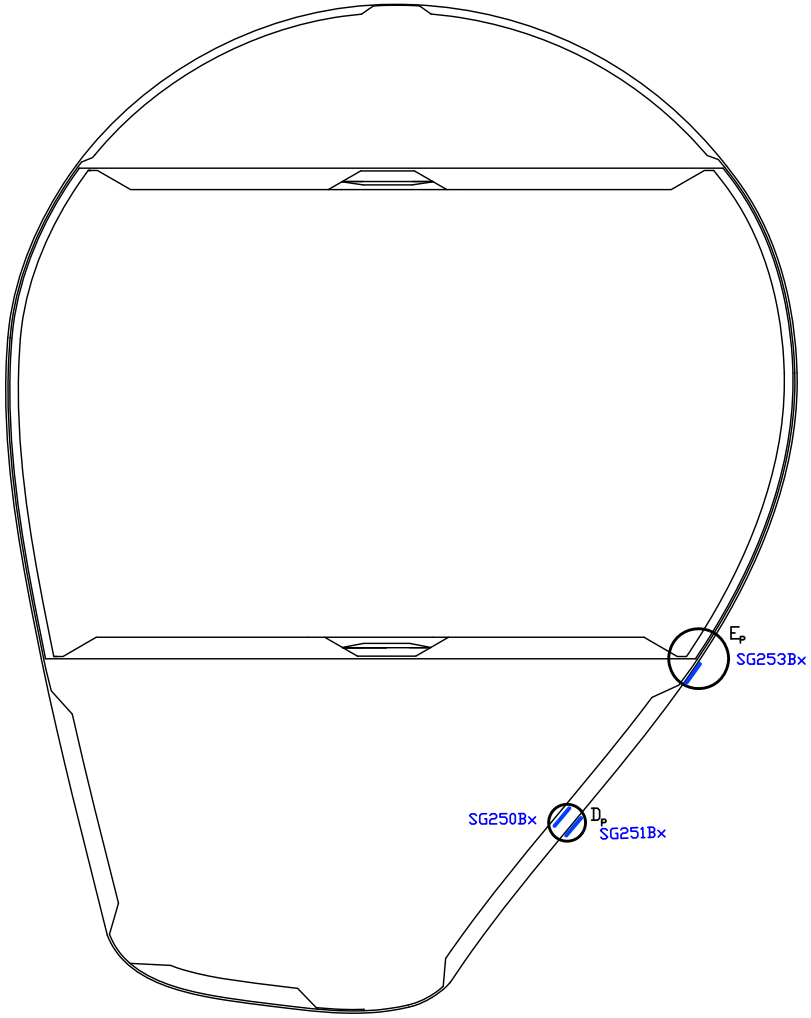

SG

Section 4m based on the 3m section

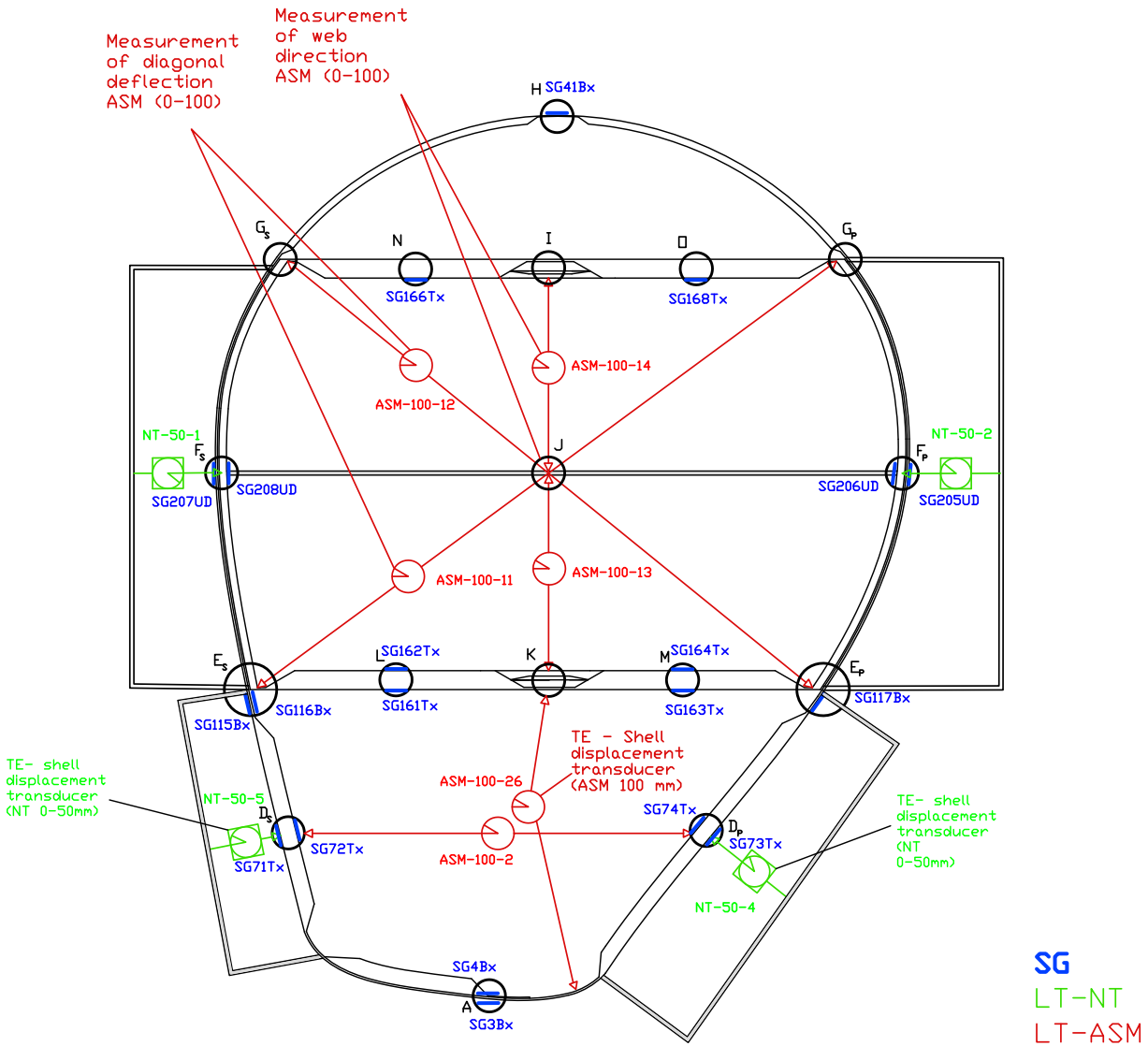

Section 4.5m based on the 3m. section

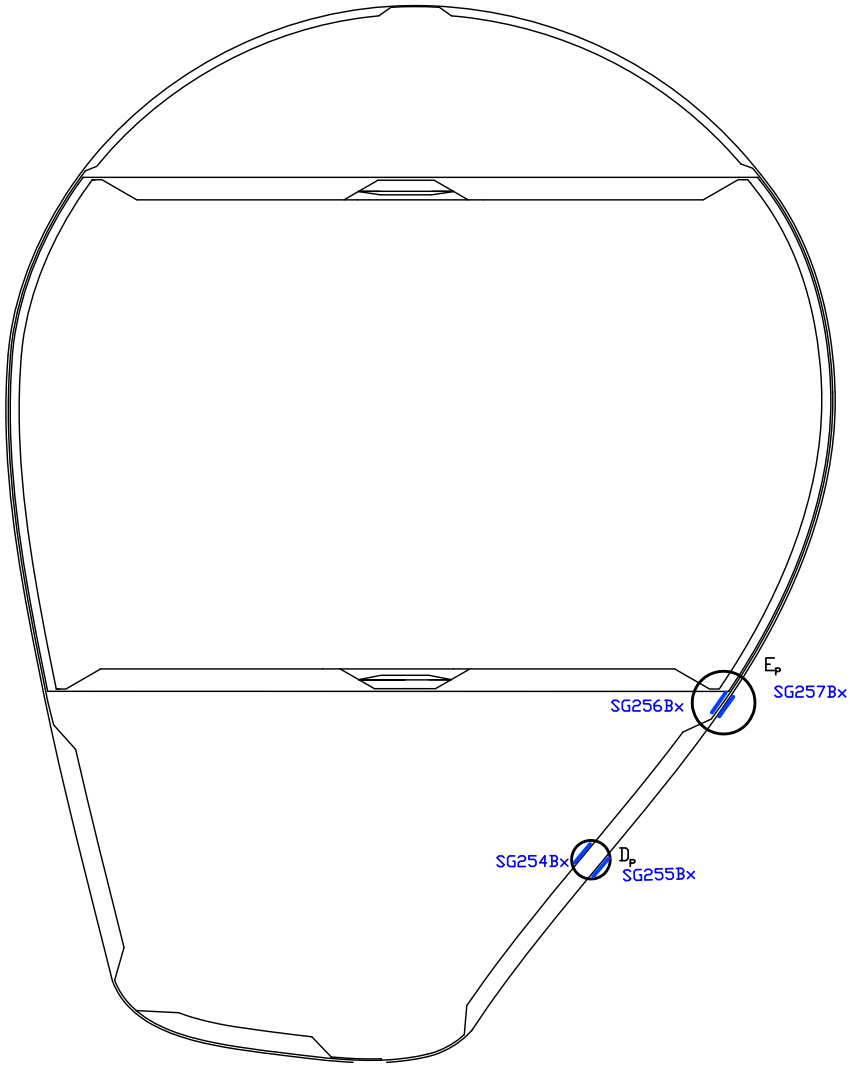

SG

Section 5m based on the 3m section

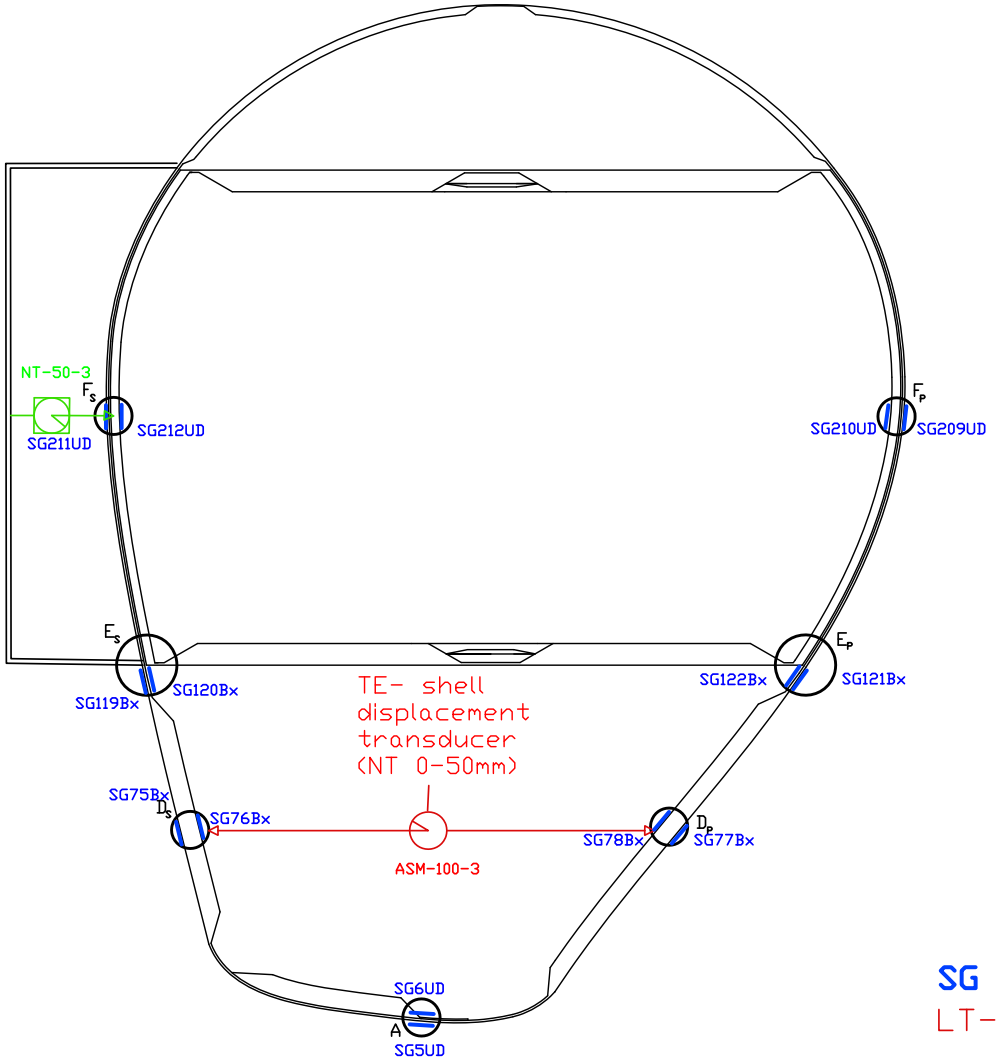

SG

LT-ASM

Section 6m based on the 3m section

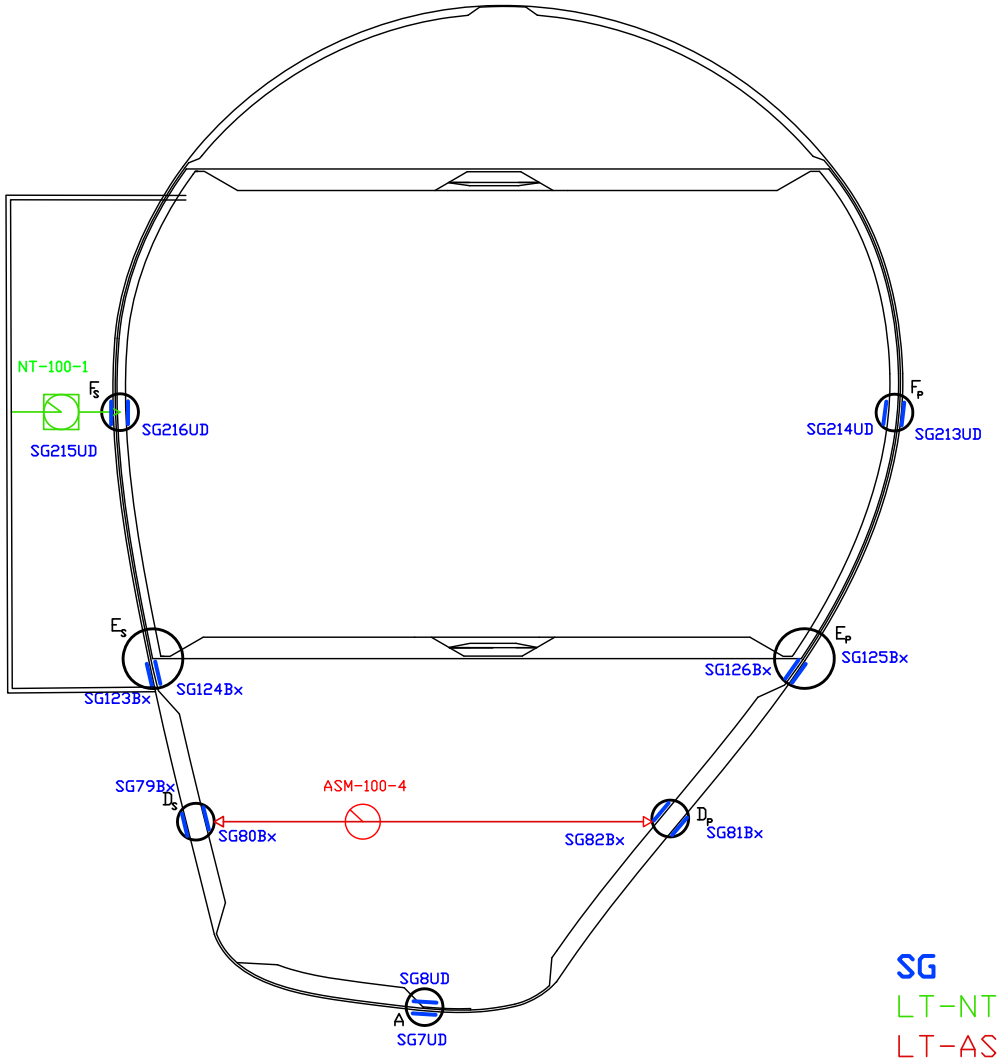

SG
LT-NT
LT-ASM

Section 7m Main section

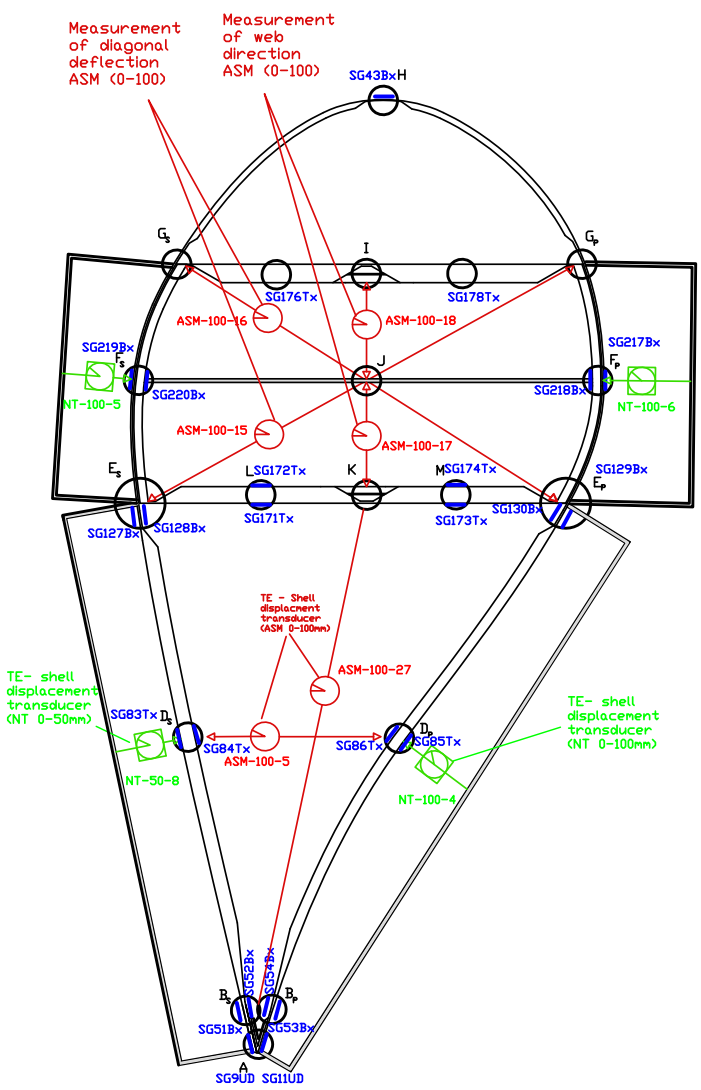

SG
LT-NT
LT-ASM

Section 8m based on 9m Section

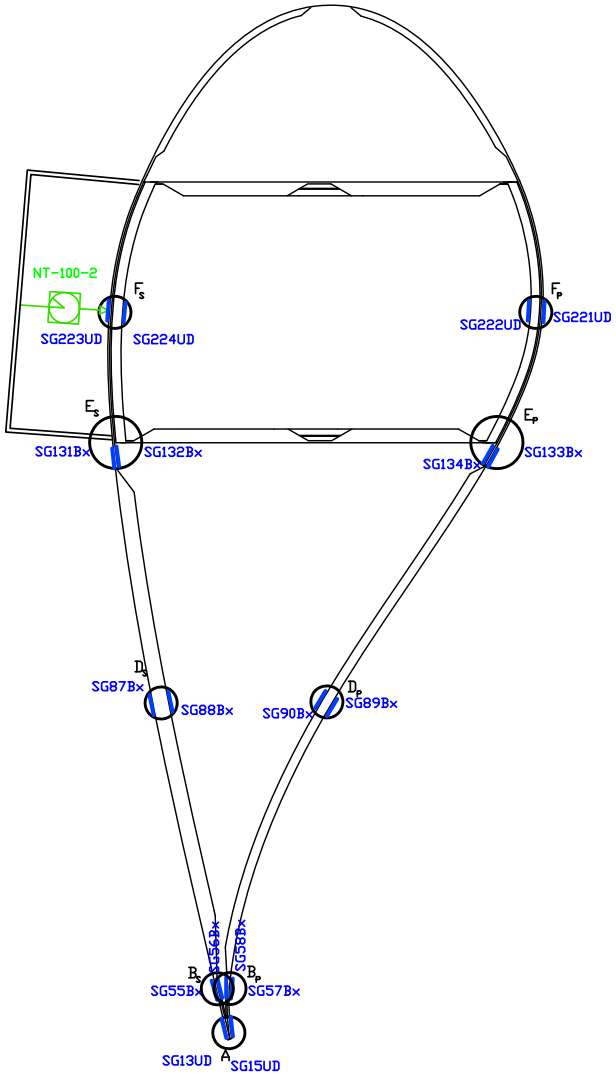

SG
LT-NT

Section 9m

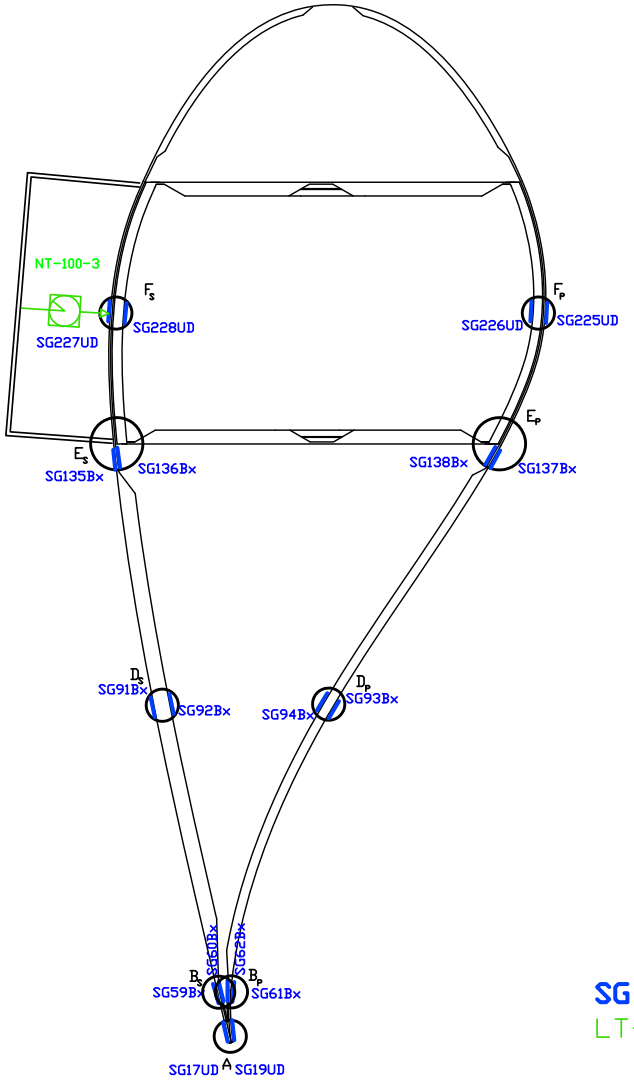

SG
LT-NT

Section 10m

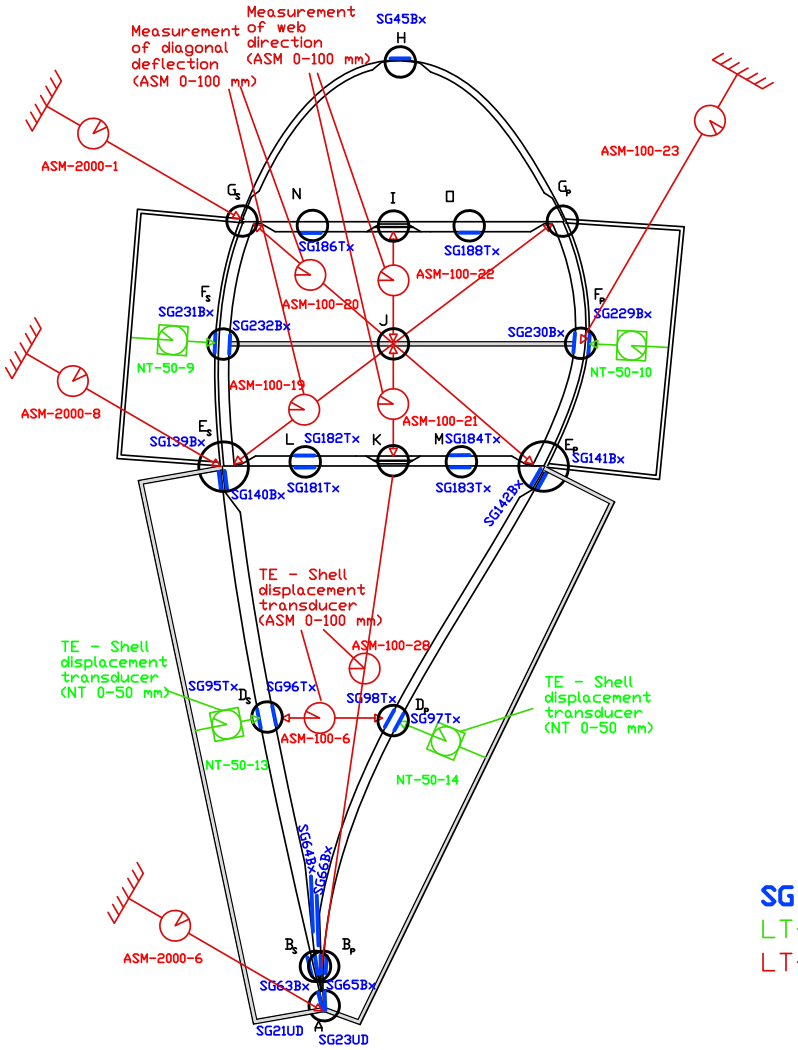

SG
LT-NT
LT-ASM

Section 11m based on 10m section

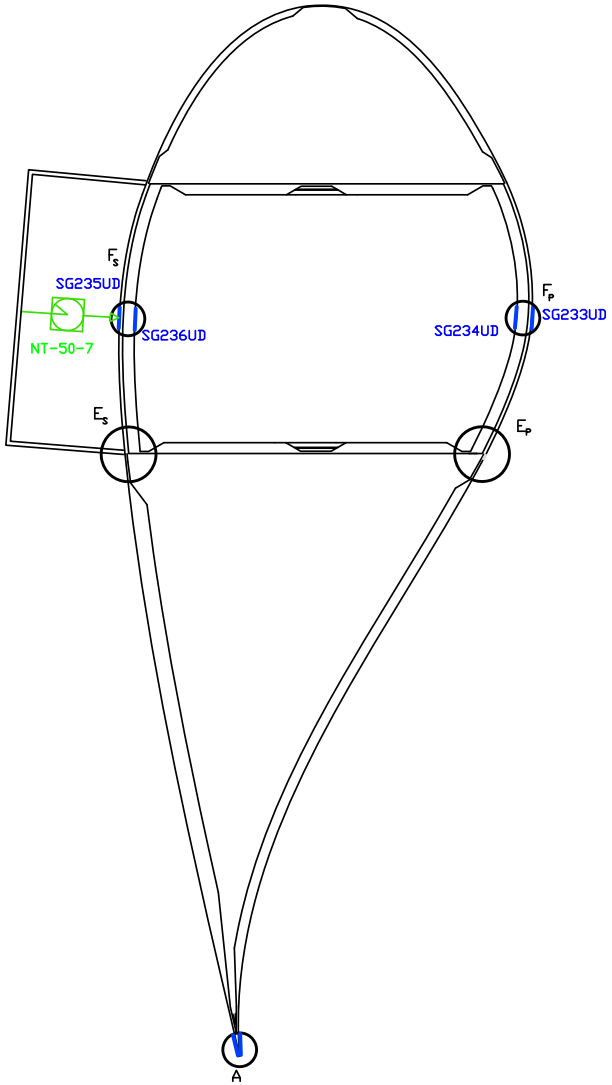

SG
LT-NT

Section 12m based on 10m section

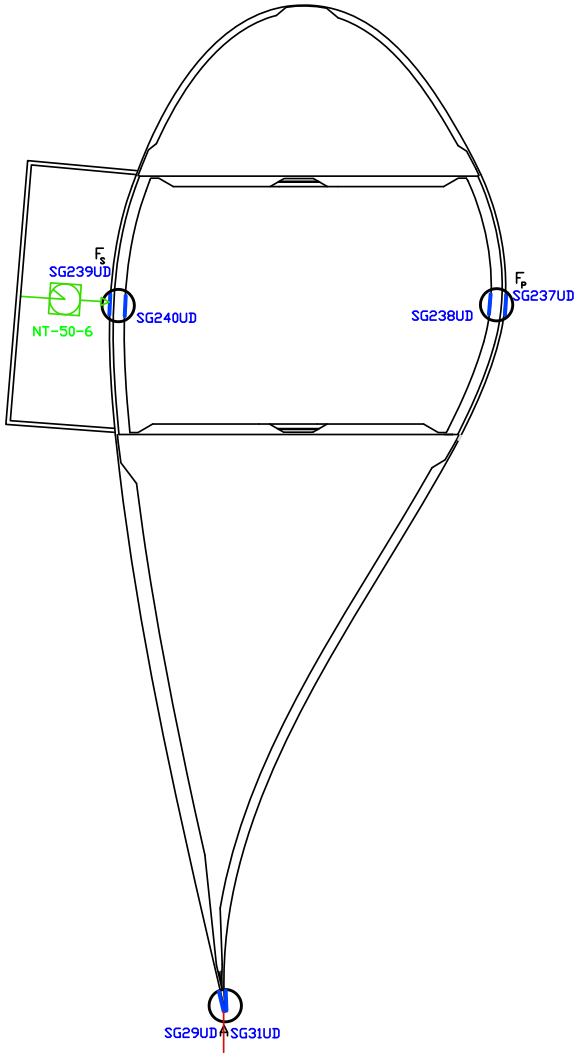

SG
LT-NT

Section 16m

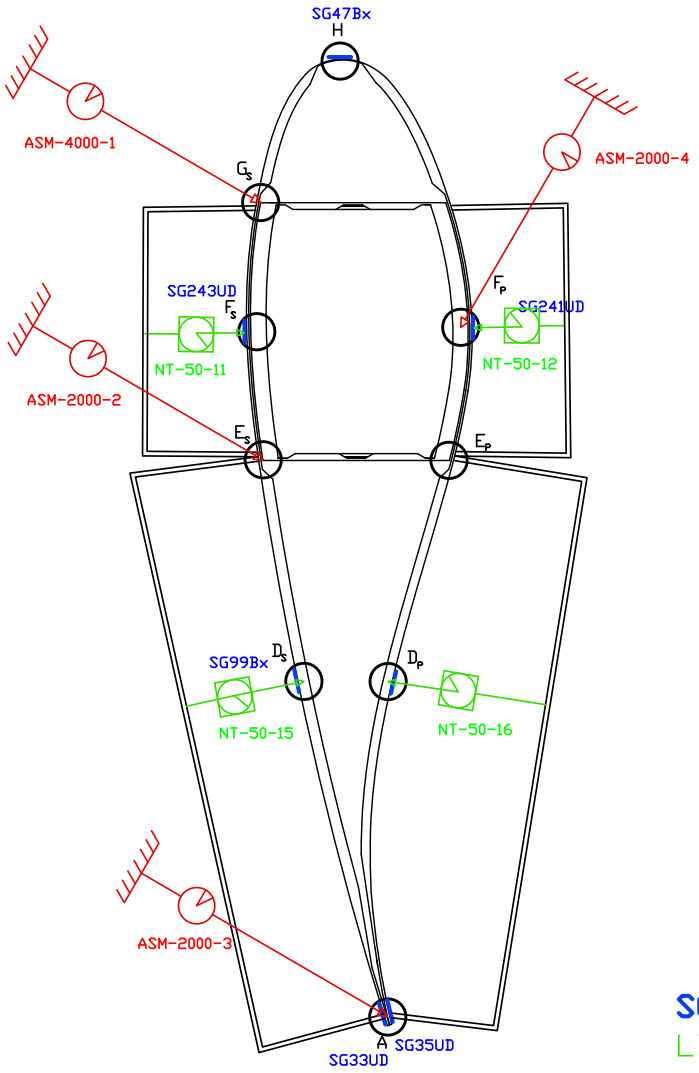

SG
LT-NT
LT-ASM

Section 22m

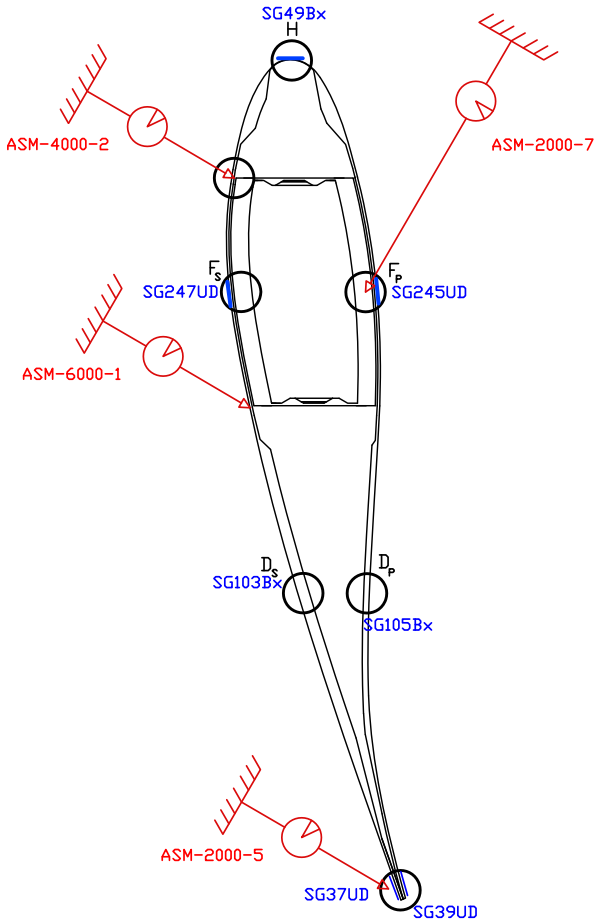

SG

LT-ASM

B Data presented by Graph tool

B.1.a Measurement of pull at 35% Risø load (Main section)

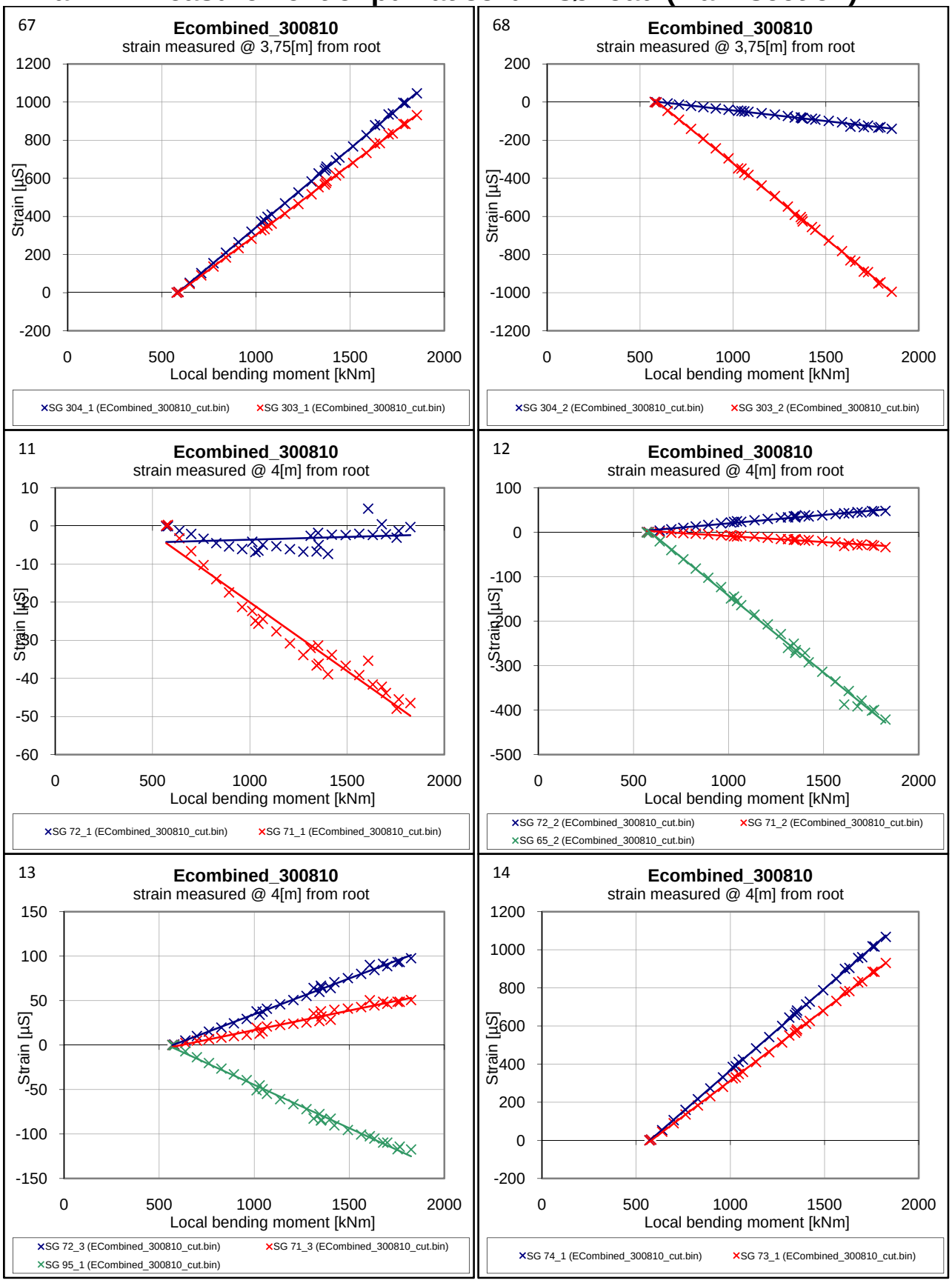

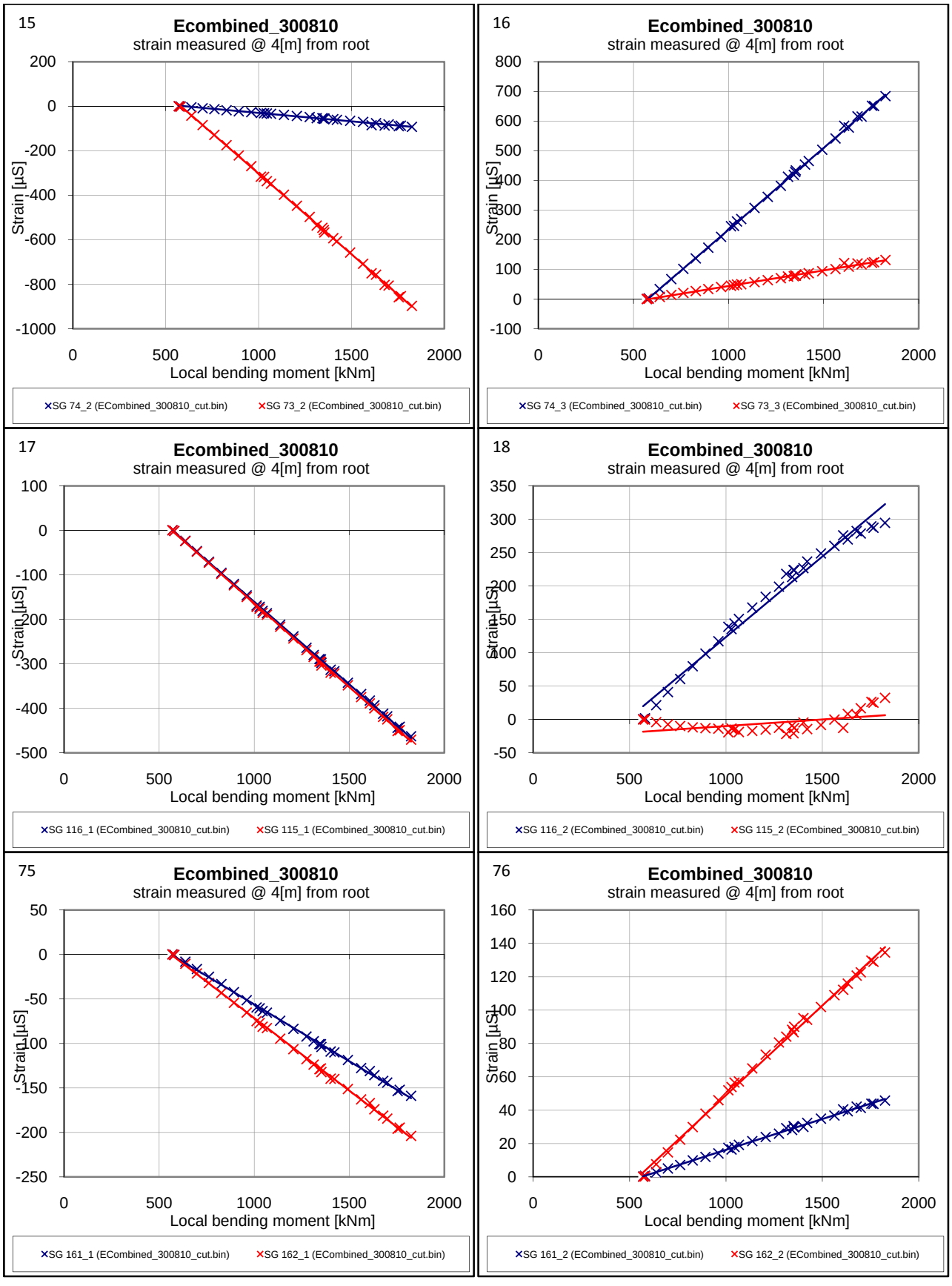
15
Ecombined_300810
strain measured @ 4[m] from root
Strain [µS]
Local bending moment [kNm]
SG 74_2 (ECombined_300810_cut.bin)
SG 73_2 (ECombined_300810_cut.bin)
16
Ecombined_300810
strain measured @ 4[m] from root
Strain [µS]
Local bending moment [kNm]
SG 74_3 (ECombined_300810_cut.bin)
SG 73_3 (ECombined_300810_cut.bin)
17
Ecombined_300810
strain measured @ 4[m] from root
Strain [µS]
Local bending moment [kNm]
SG 116_1 (ECombined_300810_cut.bin)
SG 115_1 (ECombined_300810_cut.bin)
18
Ecombined_300810
strain measured @ 4[m] from root
Strain [µS]
Local bending moment [kNm]
SG 116_2 (ECombined_300810_cut.bin)
SG 115_2 (ECombined_300810_cut.bin)
75
Ecombined_300810
strain measured @ 4[m] from root
Strain [µS]
Local bending moment [kNm]
SG 161_1 (ECombined_300810_cut.bin)
SG 162_1 (ECombined_300810_cut.bin)
76
Ecombined_300810
strain measured @ 4[m] from root
Strain [µS]
Local bending moment [kNm]
SG 161_2 (ECombined_300810_cut.bin)
SG 162_2 (ECombined_300810_cut.bin)

77

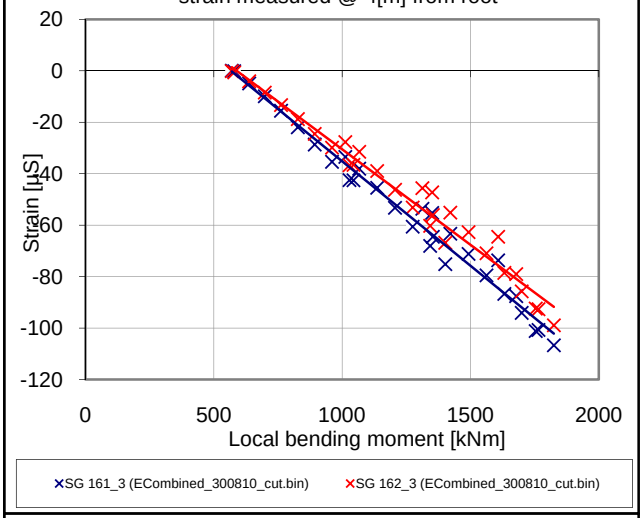

78

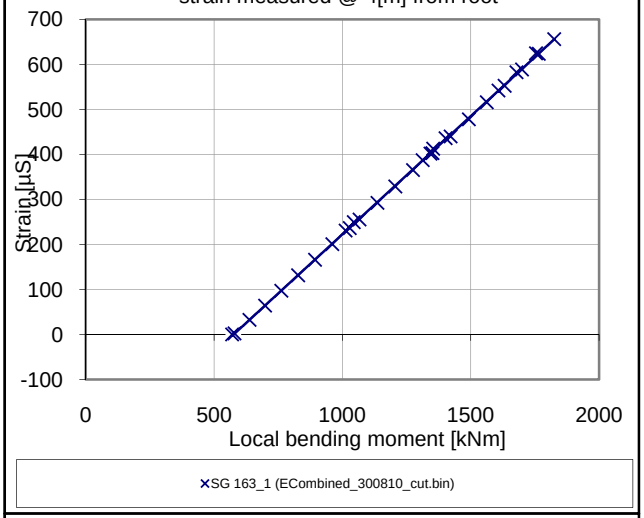

79

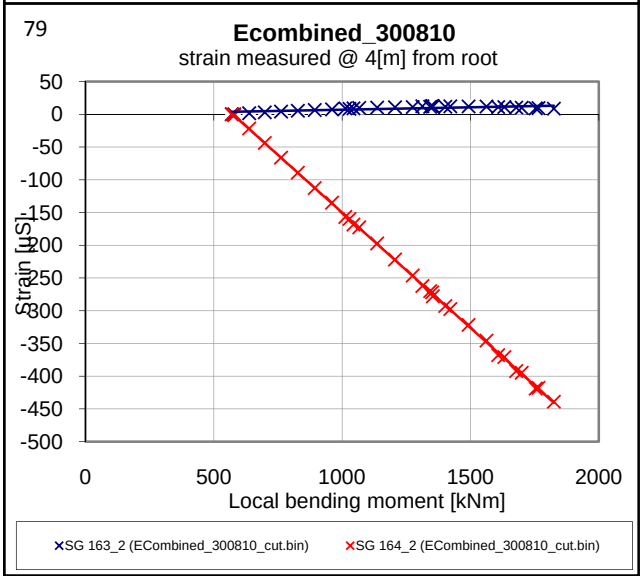

80

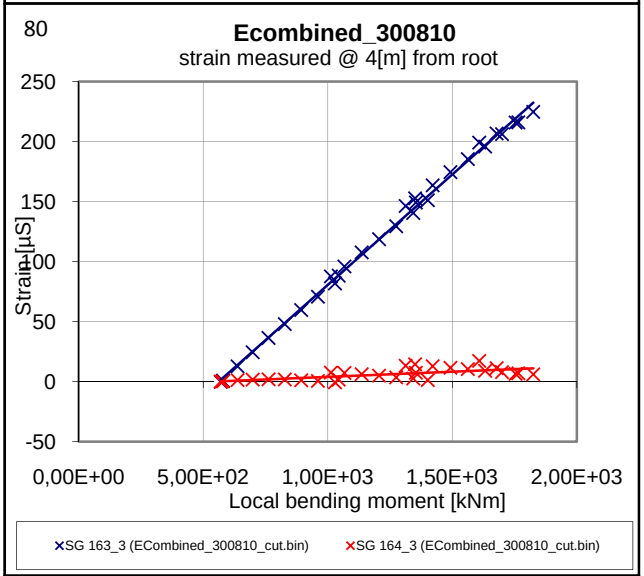

81

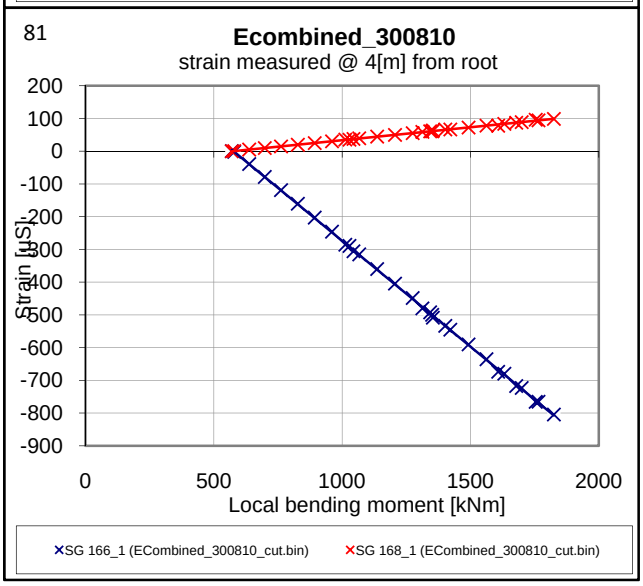

82

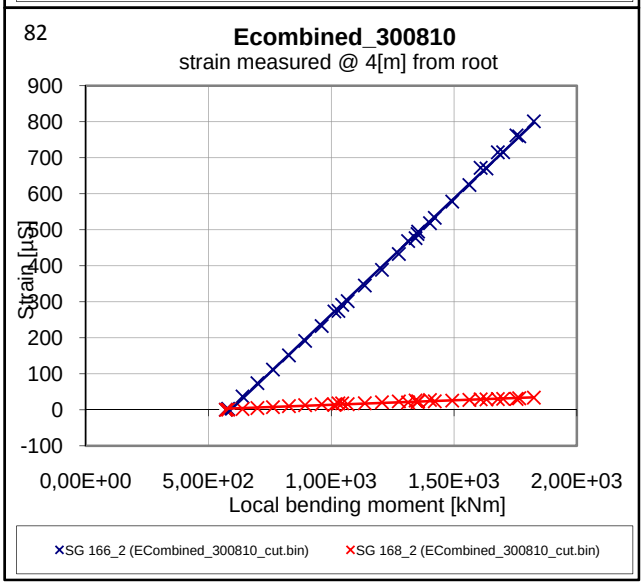

83

Ecombined_300810

strain measured @ 4[m] from root

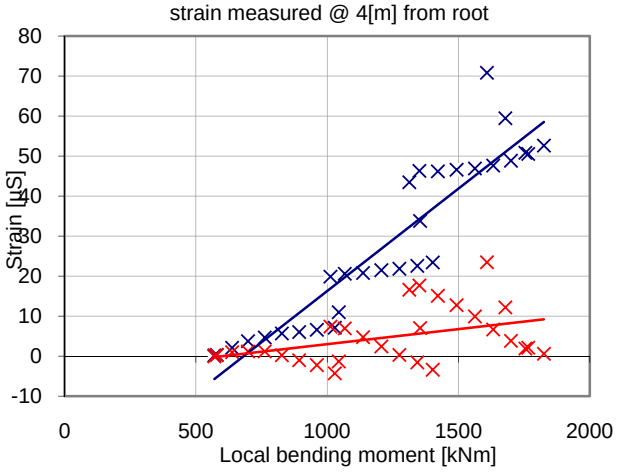

19

Ecombined_300810

strain measured @ 4[m] from root

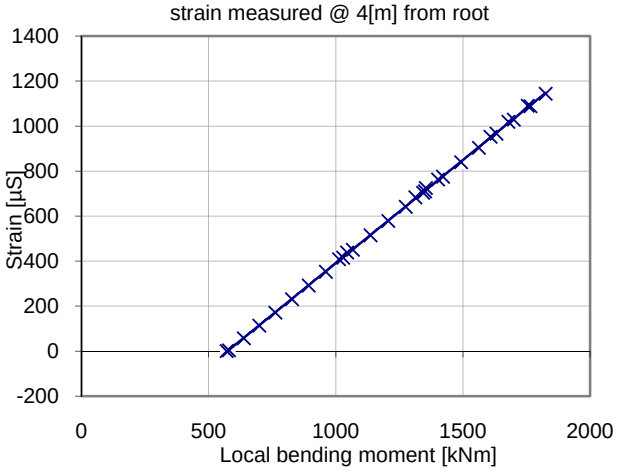

20

Ecombined_300810

strain measured @ 4[m] from root

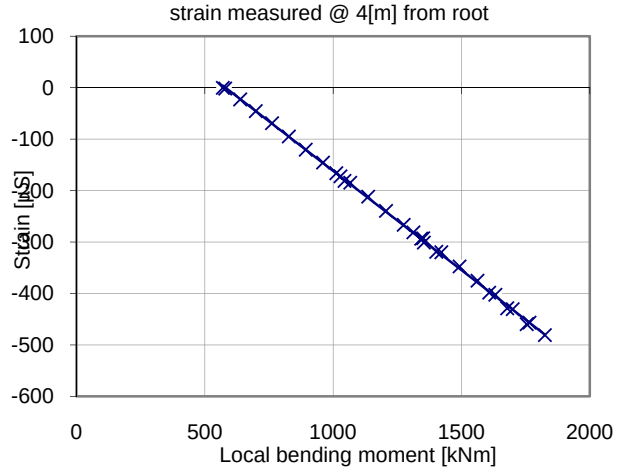

69

Ecombined_300810

strain measured @ 4,25[m] from root

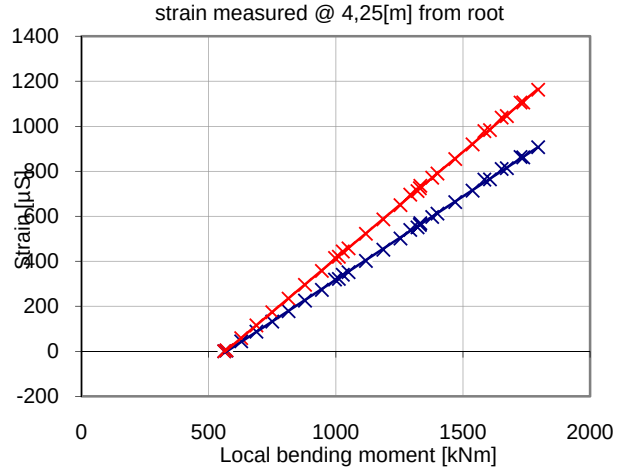

70

Ecombined_300810

strain measured @ 4,25[m] from root

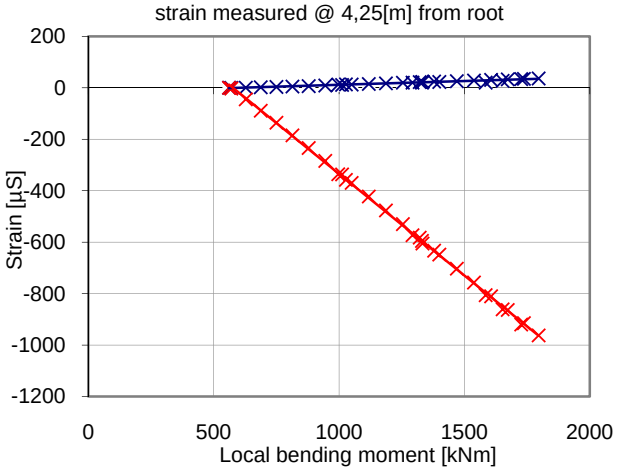

1

Ecombined_300810

strain measured @ 4,5[m] from root

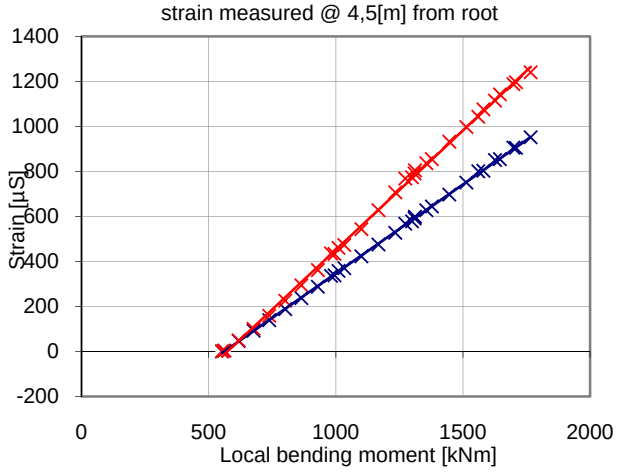

2

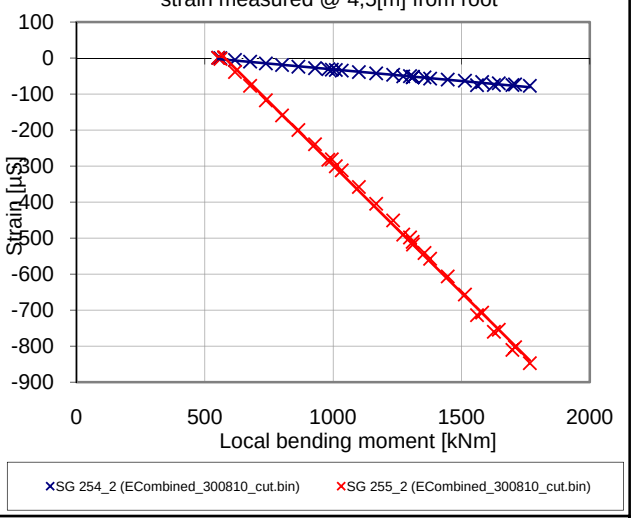
Ecombined_300810
strain measured @ 4,5[m] from root
Strain [µS]
Local bending moment [kNm]
SG 254_2 (ECombined_300810_cut.bin)
SG 255_2 (ECombined_300810_cut.bin)

71

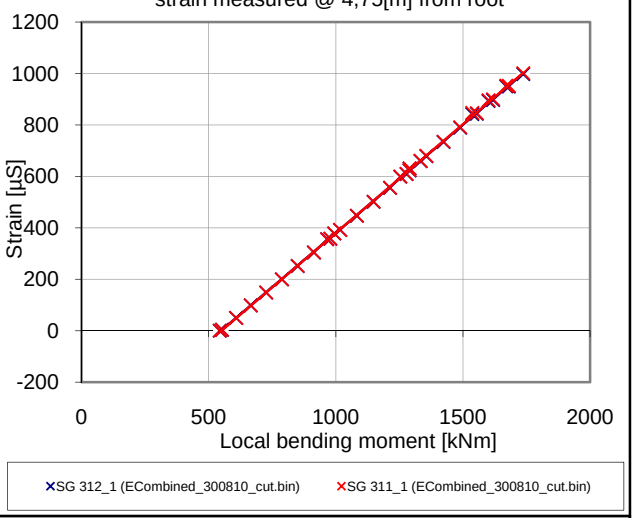
Ecombined_300810
strain measured @ 4,75[m] from root
Strain [µS]
Local bending moment [kNm]
SG 312_1 (ECombined_300810_cut.bin)
SG 311_1 (ECombined_300810_cut.bin)

72

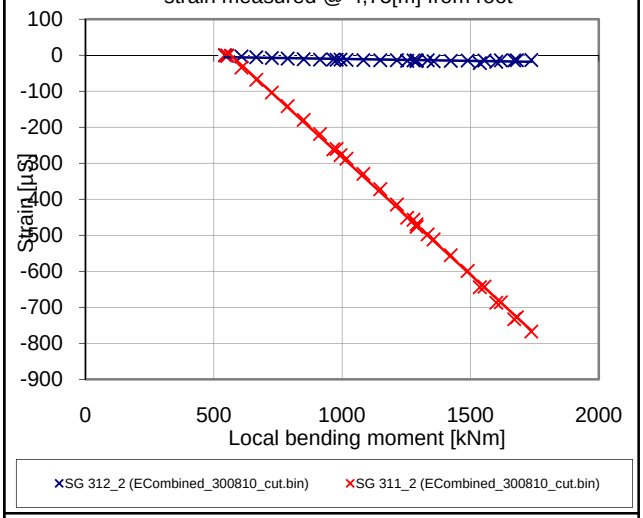
Ecombined_300810
strain measured @ 4,75[m] from root
Strain [µS]
Local bending moment [kNm]
SG 312_2 (ECombined_300810_cut.bin)
SG 311_2 (ECombined_300810_cut.bin)

3

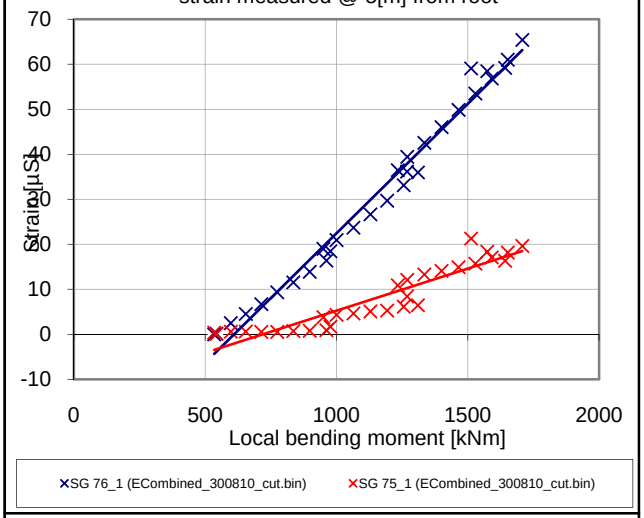
Ecombined_300810
strain measured @ 5[m] from root
Strain [µS]
Local bending moment [kNm]
SG 76_1 (ECombined_300810_cut.bin)
SG 75_1 (ECombined_300810_cut.bin)

4

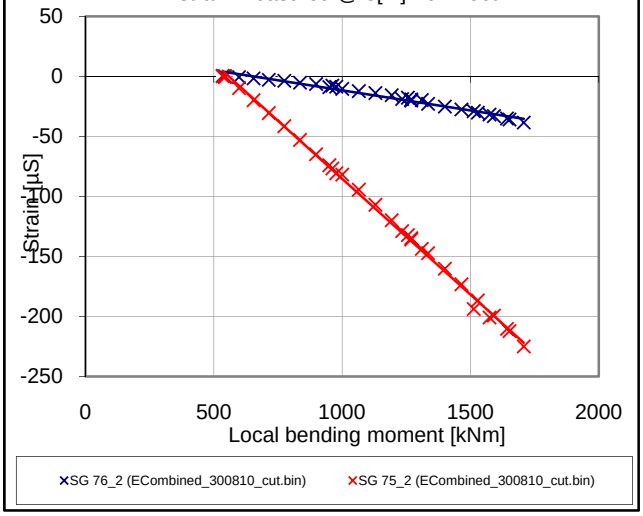
Ecombined_300810
strain measured @ 5[m] from root
Strain [µS]
Local bending moment [kNm]
SG 76_2 (ECombined_300810_cut.bin)
SG 75_2 (ECombined_300810_cut.bin)

5

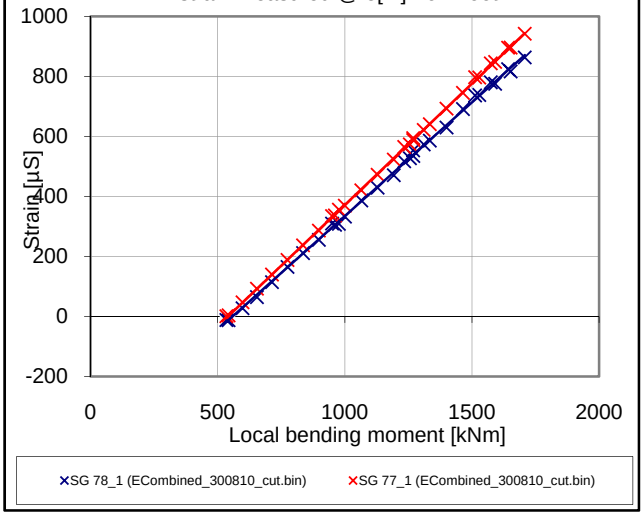
Ecombined_300810
strain measured @ 5[m] from root
Strain [µS]
Local bending moment [kNm]
SG 78_1 (ECombined_300810_cut.bin)
SG 77_1 (ECombined_300810_cut.bin)

6

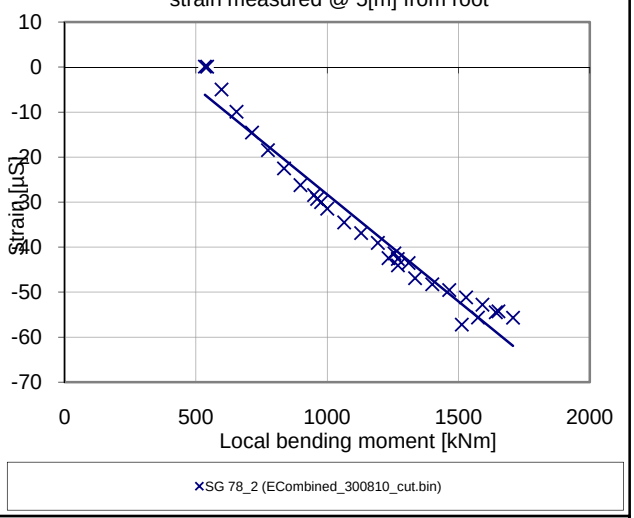
Ecombined_300810
strain measured @ 5[m] from root
Strain [µS]
Local bending moment [kNm]
SG 78_2 (ECombined_300810_cut.bin)

73

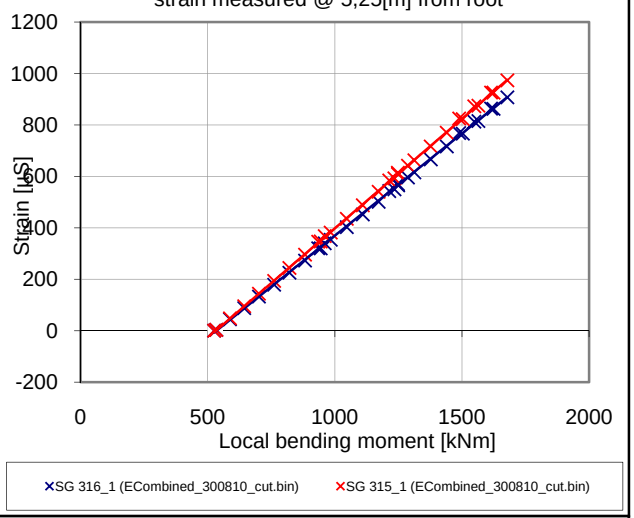
Ecombined_300810
strain measured @ 5,25[m] from root
Strain [µS]
Local bending moment [kNm]
SG 316_1 (ECombined_300810_cut.bin)
SG 315_1 (ECombined_300810_cut.bin)

74

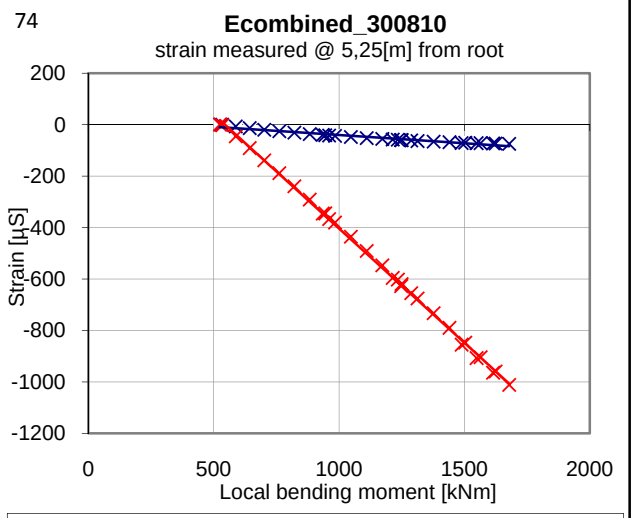
Ecombined_300810
strain measured @ 5,25[m] from root
Strain [µS]
Local bending moment [kNm]
SG 316_2 (ECombined_300810_cut.bin)
SG 315_2 (ECombined_300810_cut.bin)

7

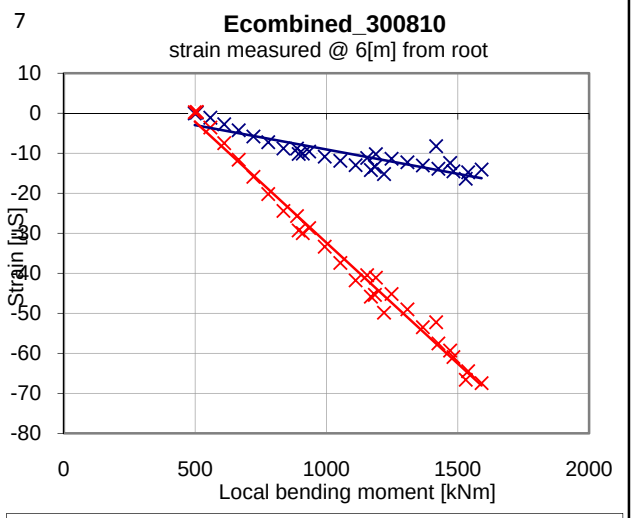
Ecombined_300810
strain measured @ 6[m] from root
Strain [µS]
Local bending moment [kNm]
SG 80_1 (ECombined_300810_cut.bin)
SG 79_1 (ECombined_300810_cut.bin)

8

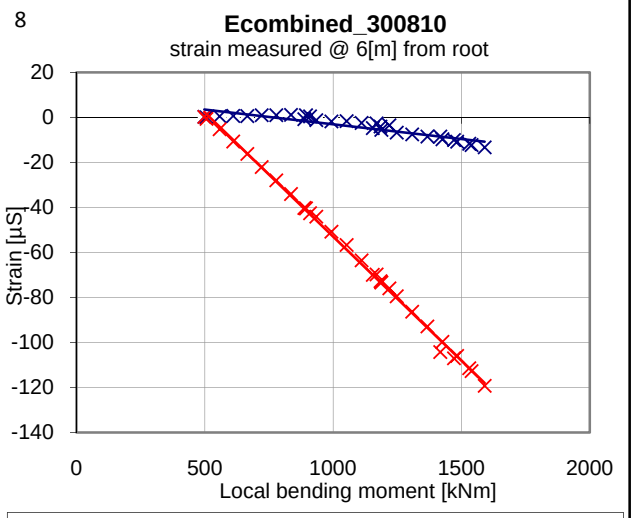
Ecombined_300810
strain measured @ 6[m] from root
Strain [µS]
Local bending moment [kNm]
SG 80_2 (ECombined_300810_cut.bin)
SG 79_2 (ECombined_300810_cut.bin)

9

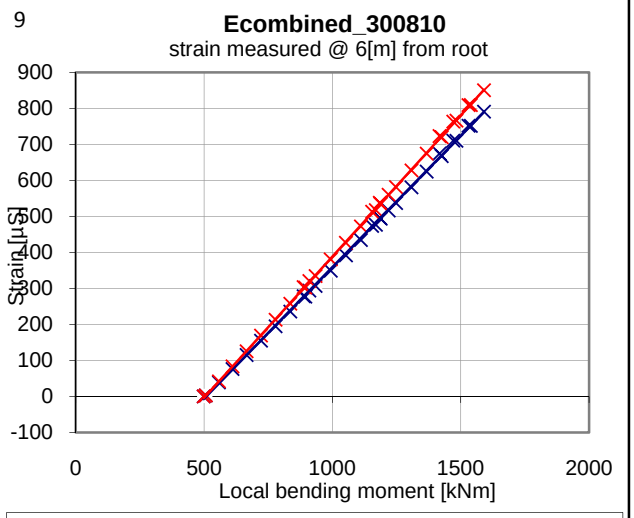
Ecombined_300810
strain measured @ 6[m] from root
Strain [µS]
Local bending moment [kNm]
SG 82_1 (ECombined_300810_cut.bin)
SG 81_1 (ECombined_300810_cut.bin)

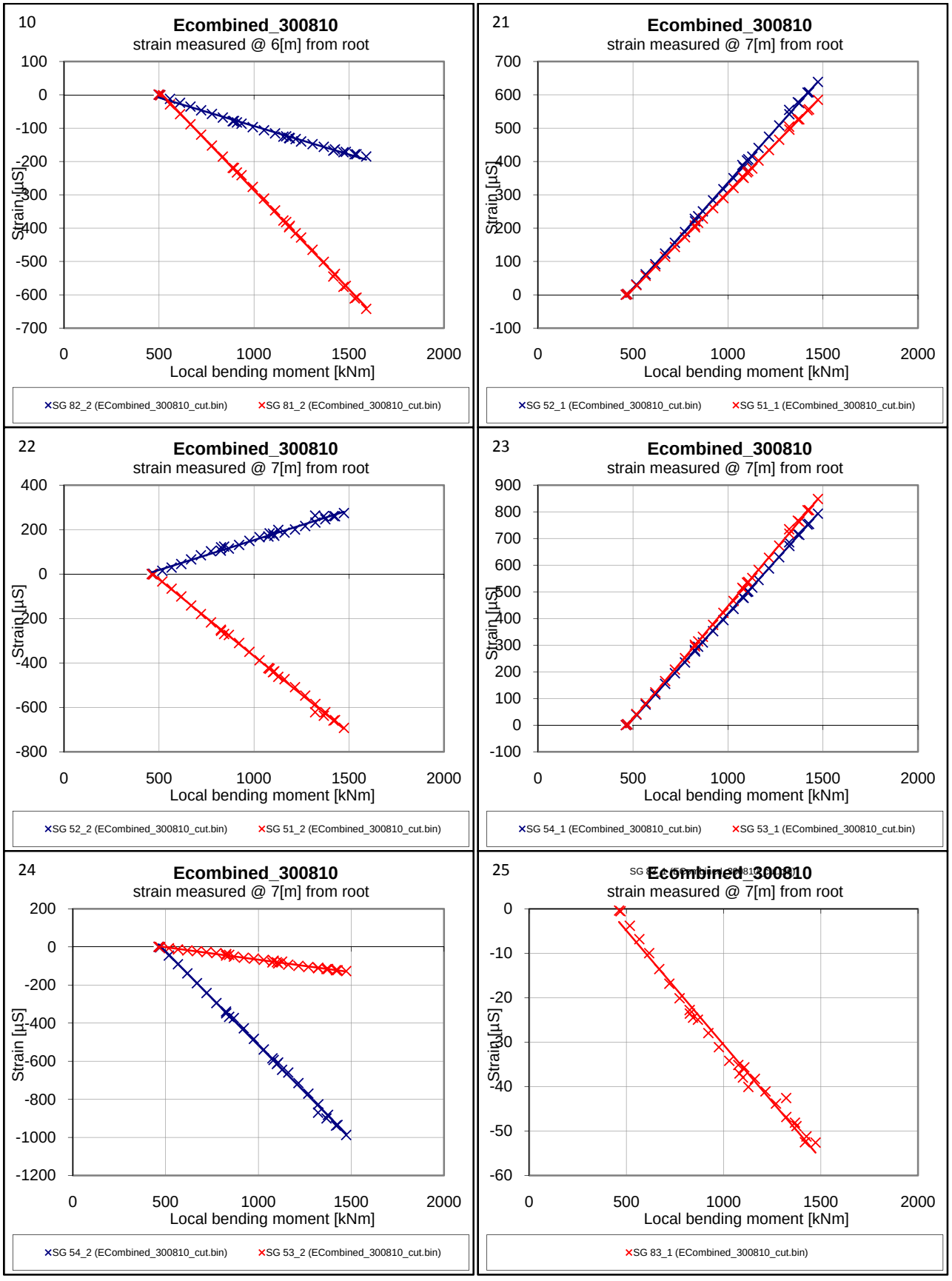
10
Ecombined_300810
strain measured @ 6[m] from root
Strain [µS]
Local bending moment [kNm]
SG 82_2 (ECombined_300810_cut.bin)
SG 81_2 (ECombined_300810_cut.bin)
21
Ecombined_300810
strain measured @ 7[m] from root
Strain [µS]
Local bending moment [kNm]
SG 52_1 (ECombined_300810_cut.bin)
SG 51_1 (ECombined_300810_cut.bin)
22
Ecombined_300810
strain measured @ 7[m] from root
Strain [µS]
Local bending moment [kNm]
SG 52_2 (ECombined_300810_cut.bin)
SG 51_2 (ECombined_300810_cut.bin)
23
Ecombined_300810
strain measured @ 7[m] from root
Strain [µS]
Local bending moment [kNm]
SG 54_1 (ECombined_300810_cut.bin)
SG 53_1 (ECombined_300810_cut.bin)
24
Ecombined_300810
strain measured @ 7[m] from root
Strain [µS]
Local bending moment [kNm]
SG 54_2 (ECombined_300810_cut.bin)
SG 53_2 (ECombined_300810_cut.bin)
25
Ecombined_300810
strain measured @ 7[m] from root
Strain [µS]
Local bending moment [kNm]
SG 83_1 (ECombined_300810_cut.bin)

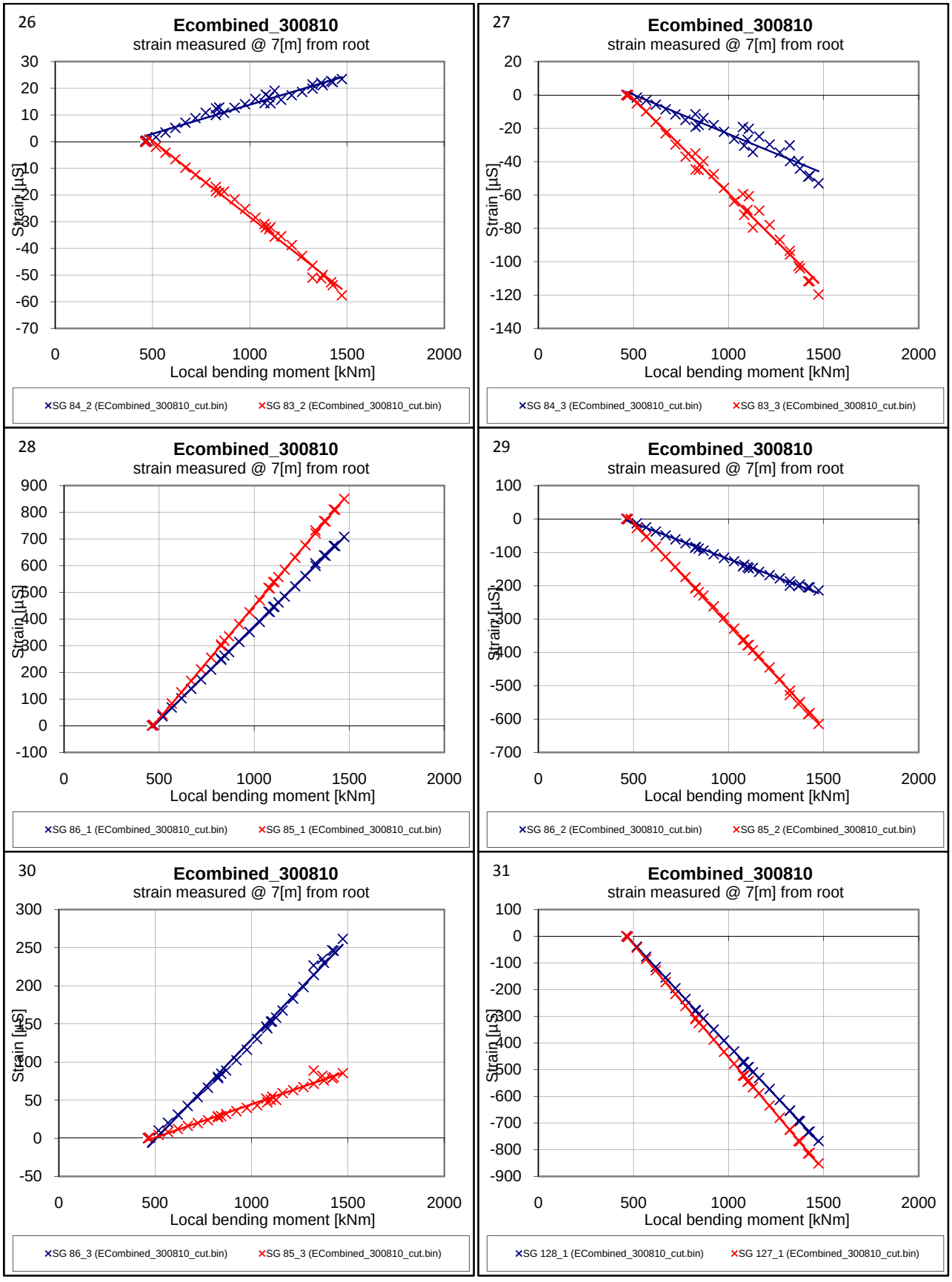
26
Ecombined_300810
strain measured @ 7[m] from root
Strain [µS]
Local bending moment [kNm]
SG 84_2 (ECombined_300810_cut.bin)
SG 83_2 (ECombined_300810_cut.bin)
27
Ecombined_300810
strain measured @ 7[m] from root
Strain [µS]
Local bending moment [kNm]
SG 84_3 (ECombined_300810_cut.bin)
SG 83_3 (ECombined_300810_cut.bin)
28
Ecombined_300810
strain measured @ 7[m] from root
Strain [µS]
Local bending moment [kNm]
SG 86_1 (ECombined_300810_cut.bin)
SG 85_1 (ECombined_300810_cut.bin)
29
Ecombined_300810
strain measured @ 7[m] from root
Strain [µS]
Local bending moment [kNm]
SG 86_2 (ECombined_300810_cut.bin)
SG 85_2 (ECombined_300810_cut.bin)
30
Ecombined_300810
strain measured @ 7[m] from root
Strain [µS]
Local bending moment [kNm]
SG 86_3 (ECombined_300810_cut.bin)
SG 85_3 (ECombined_300810_cut.bin)
31
Ecombined_300810
strain measured @ 7[m] from root
Strain [µS]
Local bending moment [kNm]
SG 128_1 (ECombined_300810_cut.bin)
SG 127_1 (ECombined_300810_cut.bin)

32

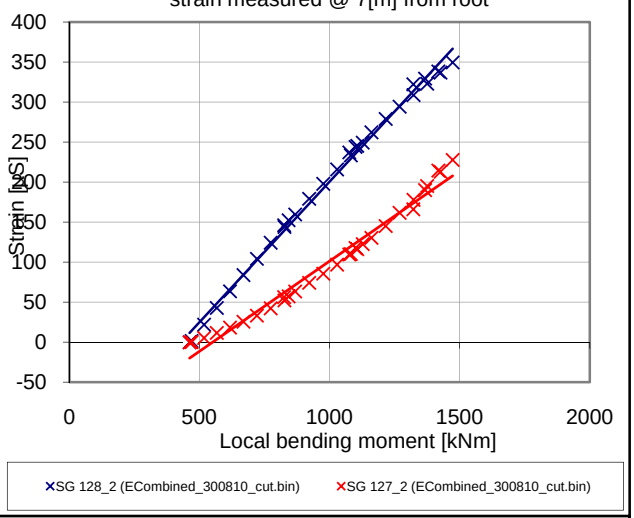

33

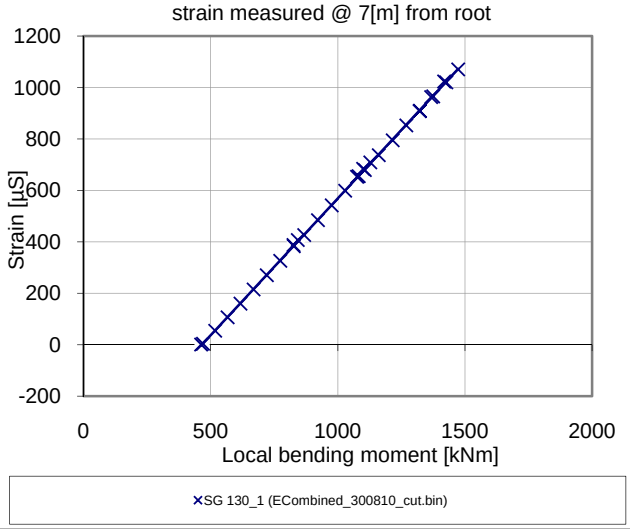

34

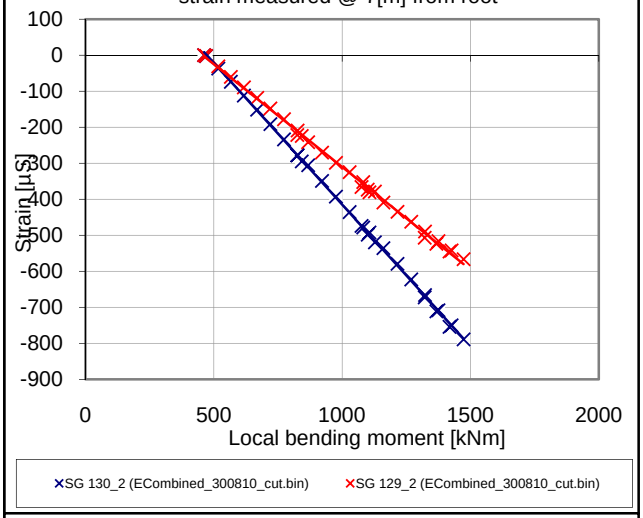

49

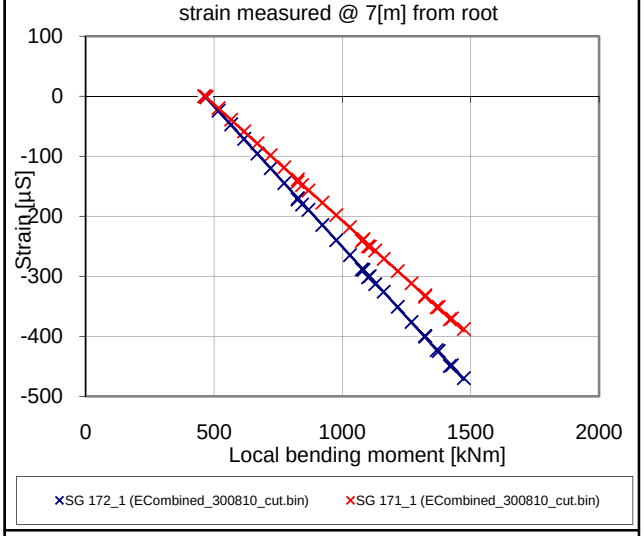

50

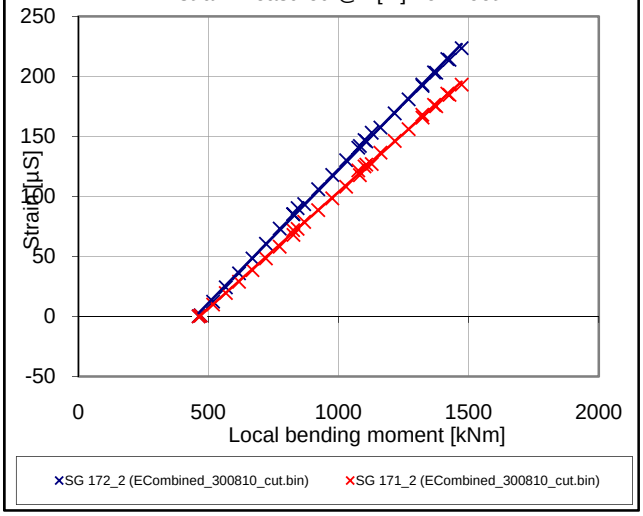

51

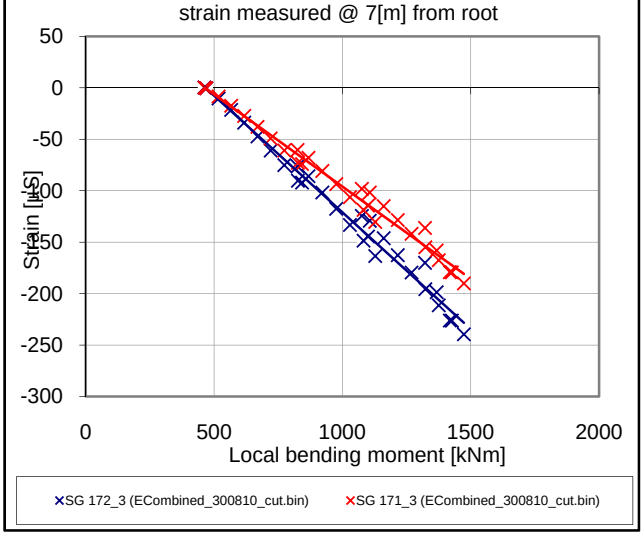

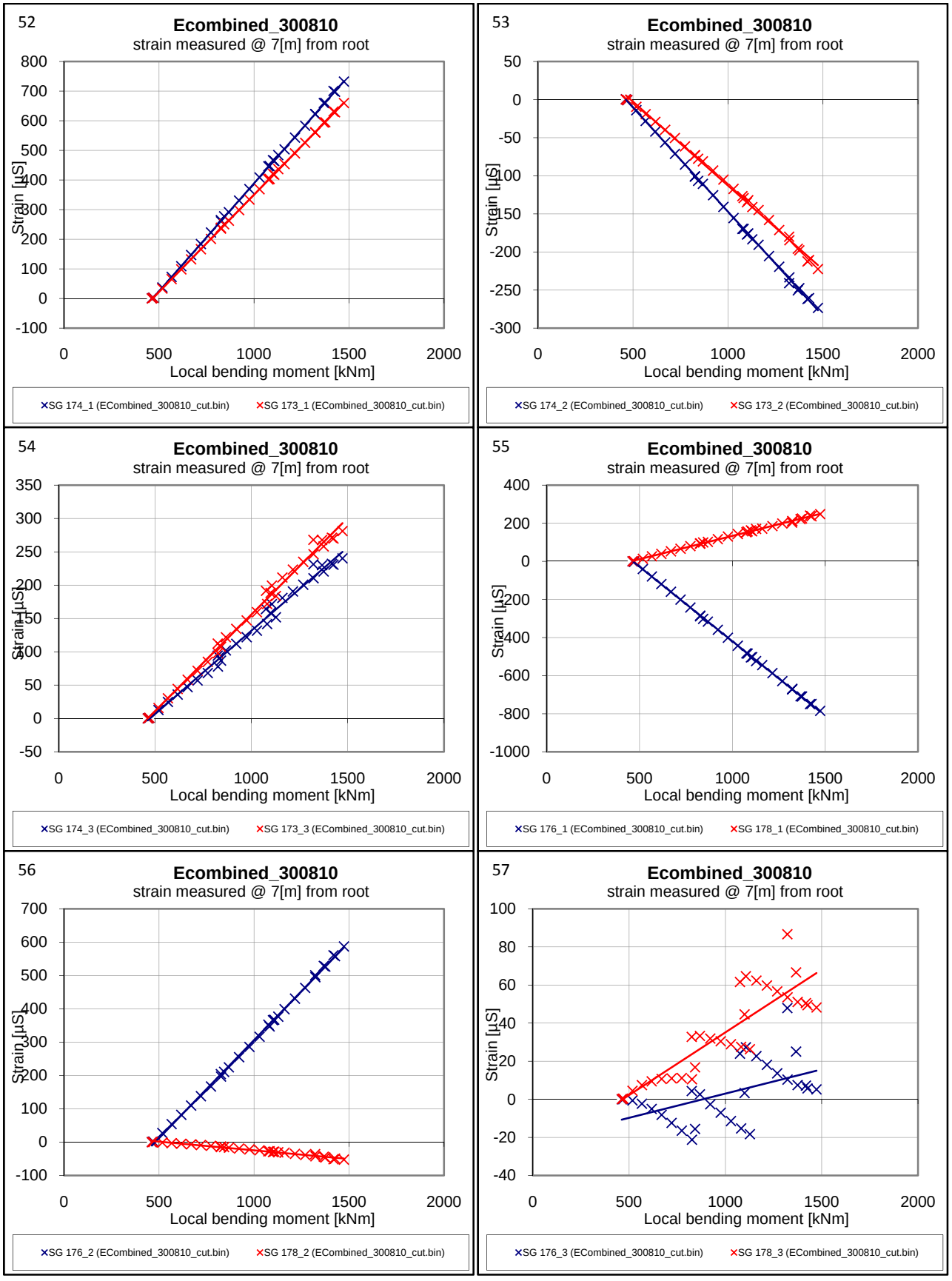
52
Ecombined_300810
strain measured @ 7[m] from root
Strain [µS]
Local bending moment [kNm]
SG 174_1 (ECombined_300810_cut.bin)
SG 173_1 (ECombined_300810_cut.bin)
53
Ecombined_300810
strain measured @ 7[m] from root
Strain [µS]
Local bending moment [kNm]
SG 174_2 (ECombined_300810_cut.bin)
SG 173_2 (ECombined_300810_cut.bin)
54
Ecombined_300810
strain measured @ 7[m] from root
Strain [µS]
Local bending moment [kNm]
SG 174_3 (ECombined_300810_cut.bin)
SG 173_3 (ECombined_300810_cut.bin)
55
Ecombined_300810
strain measured @ 7[m] from root
Strain [µS]
Local bending moment [kNm]
SG 176_1 (ECombined_300810_cut.bin)
SG 178_1 (ECombined_300810_cut.bin)
56
Ecombined_300810
strain measured @ 7[m] from root
Strain [µS]
Local bending moment [kNm]
SG 176_2 (ECombined_300810_cut.bin)
SG 178_2 (ECombined_300810_cut.bin)
57
Ecombined_300810
strain measured @ 7[m] from root
Strain [µS]
Local bending moment [kNm]
SG 176_3 (ECombined_300810_cut.bin)
SG 178_3 (ECombined_300810_cut.bin)

35

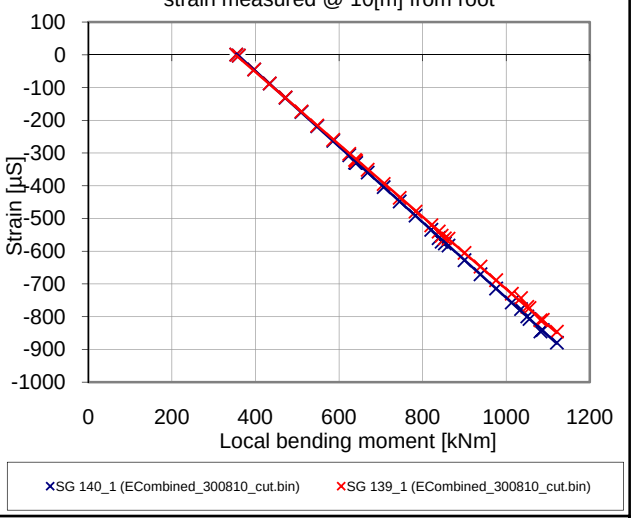

36

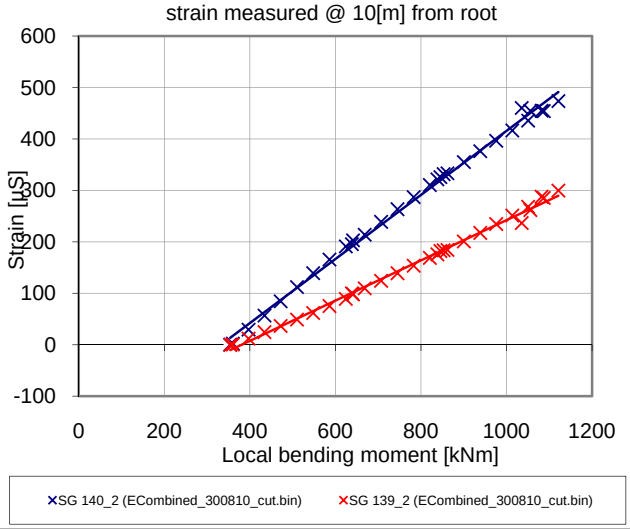

37

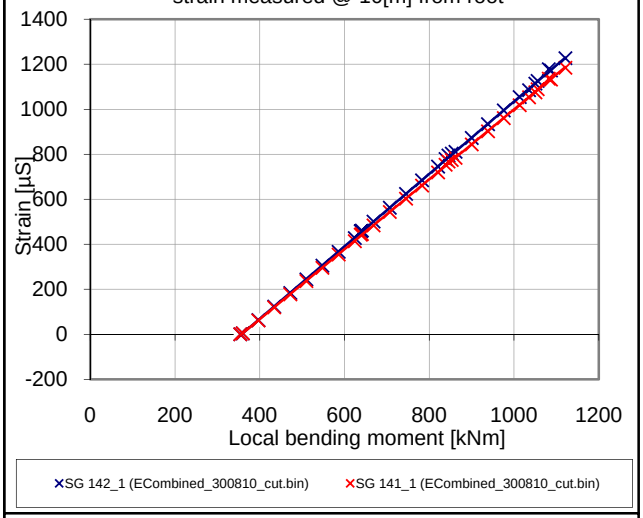

38

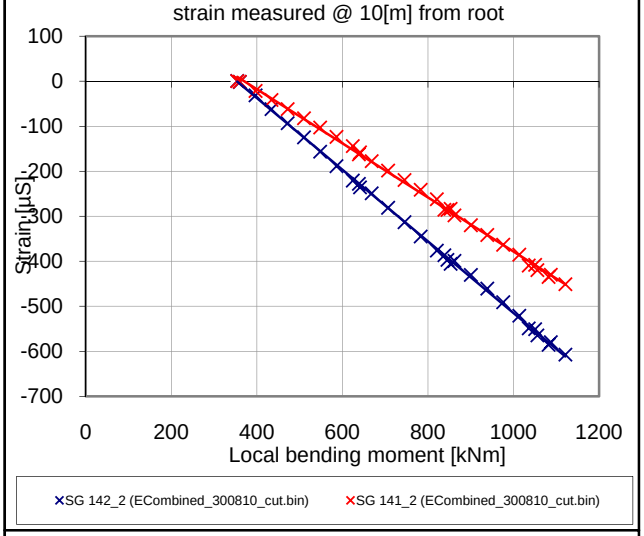

39

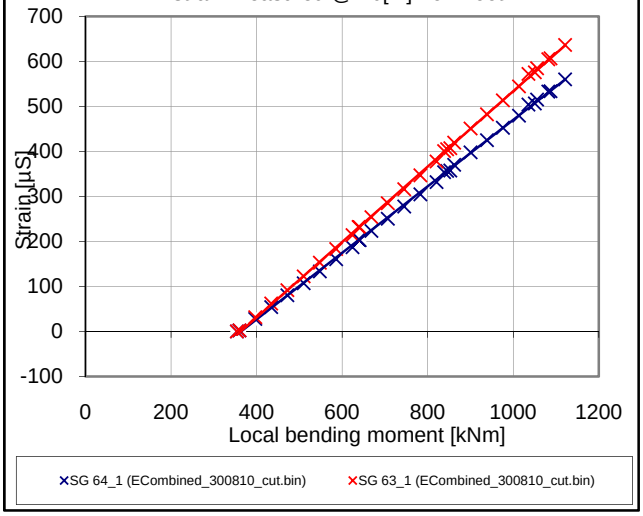

40

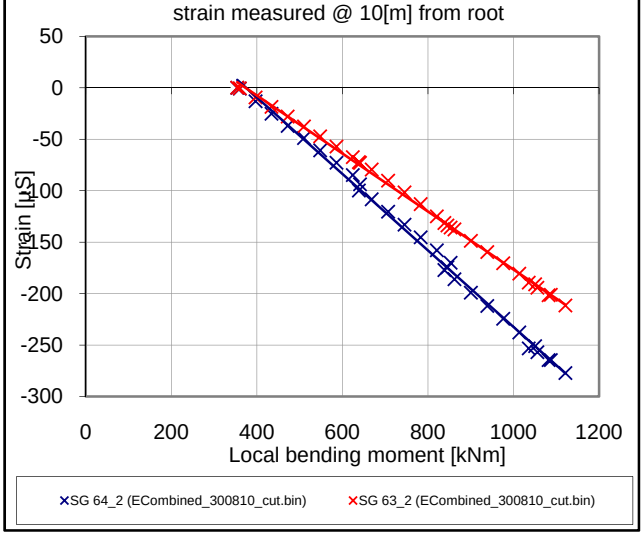

41

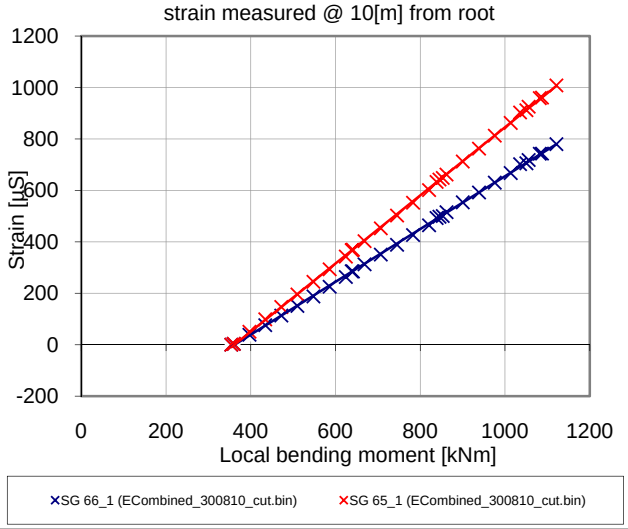

42

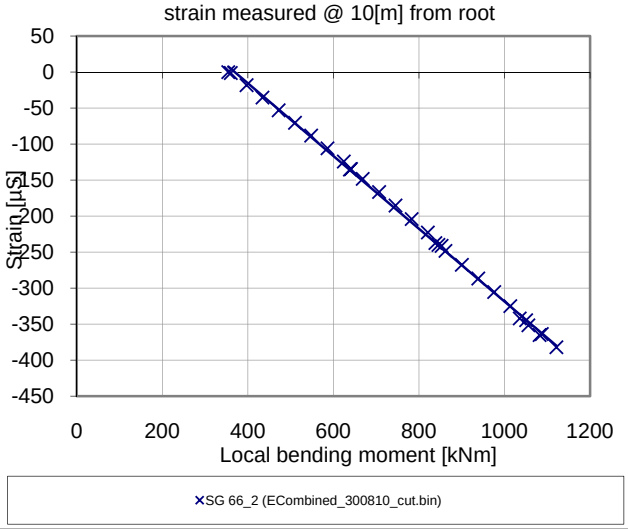

43

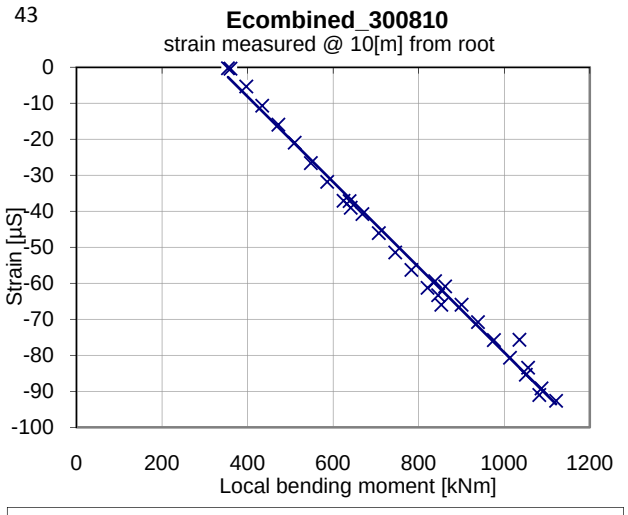

44

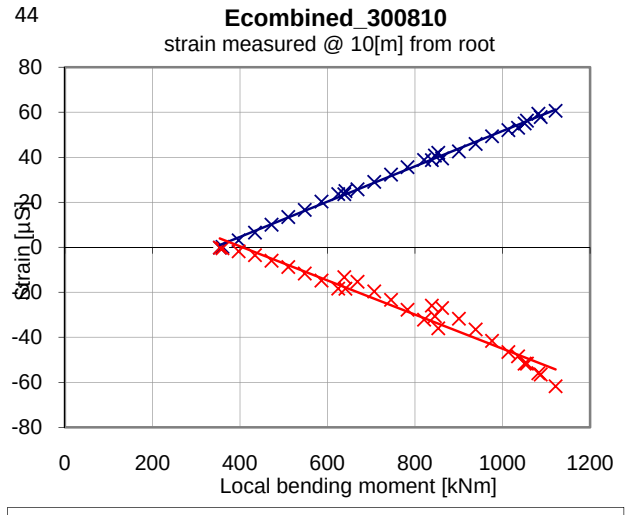

45

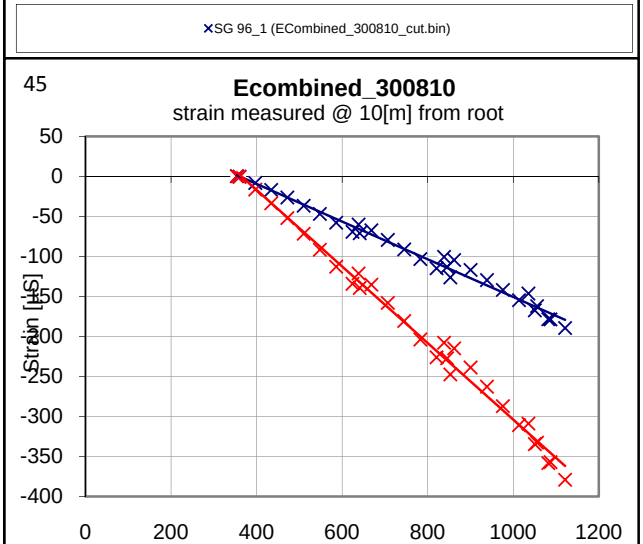

46

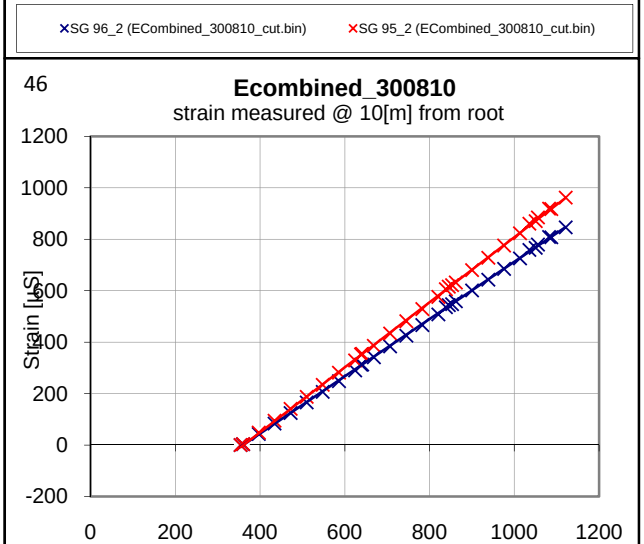

47

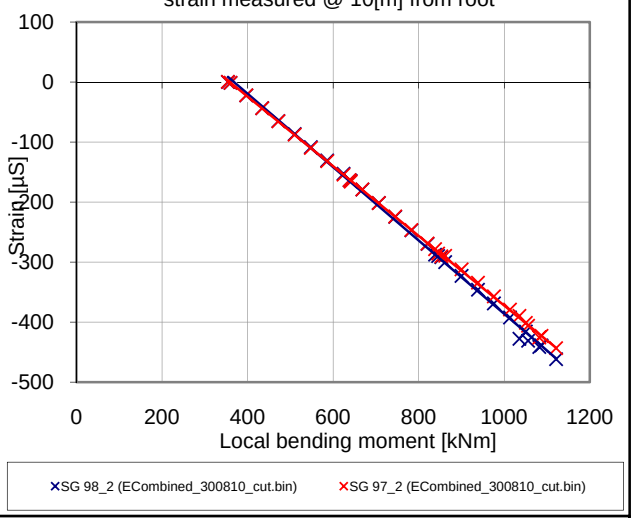

48

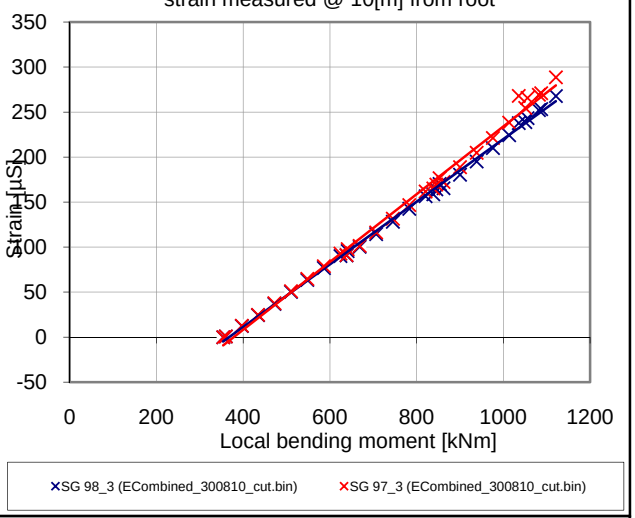

58

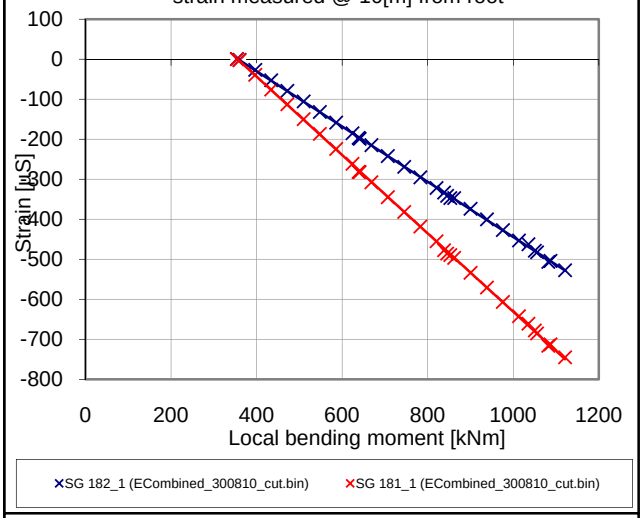

59

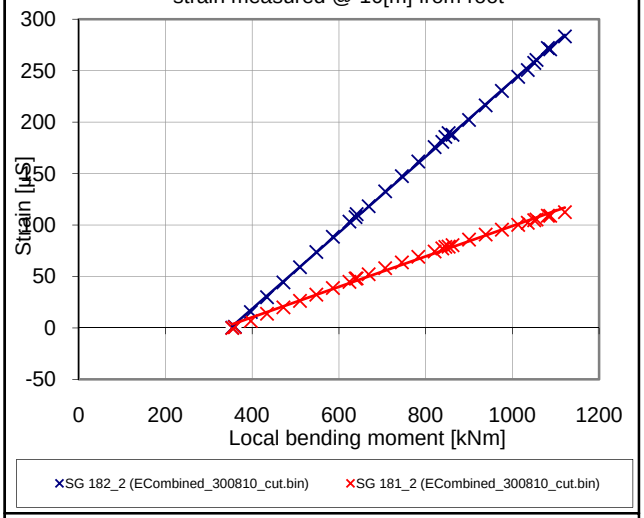

60

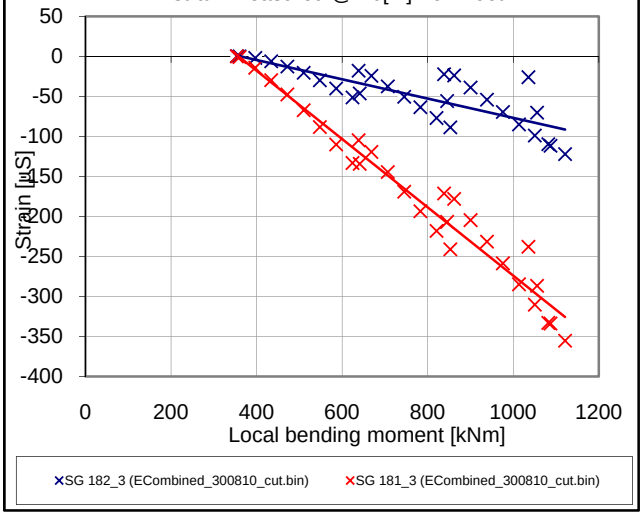

61

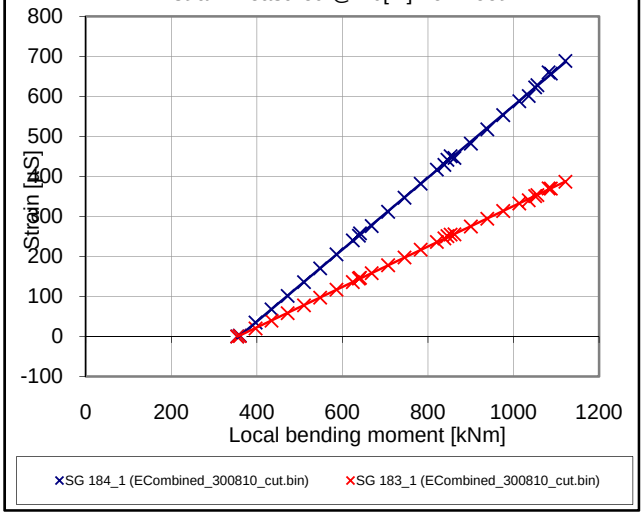

62

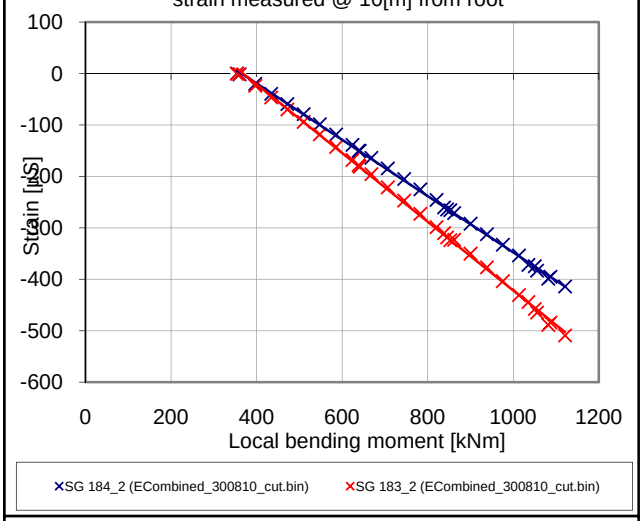
Ecombined_300810
strain measured @ 10[m] from root
Strain [µS]
Local bending moment [kNm]
SG 184_2 (ECombined_300810_cut.bin)
SG 183_2 (ECombined_300810_cut.bin)

63

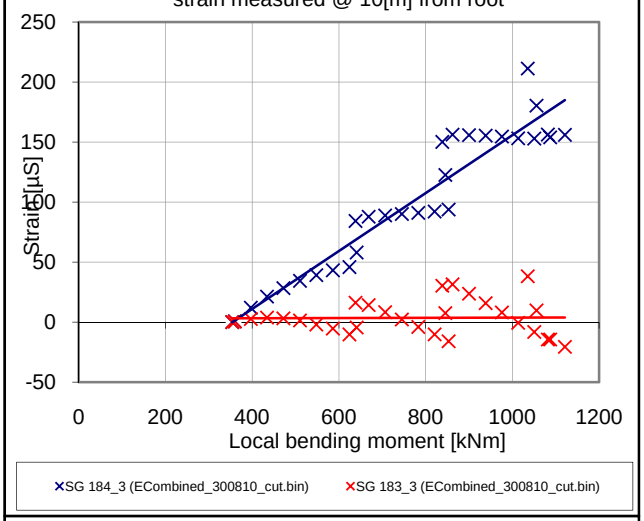
Ecombined_300810
strain measured @ 10[m] from root
Strain [µS]
Local bending moment [kNm]
SG 184_3 (ECombined_300810_cut.bin)
SG 183_3 (ECombined_300810_cut.bin)

64

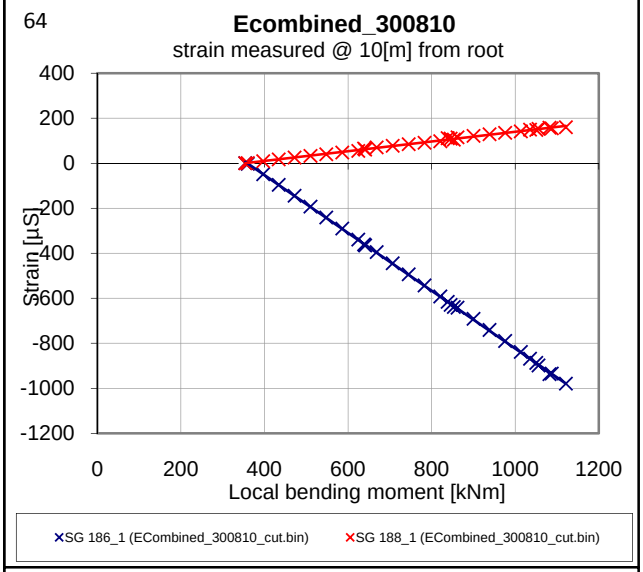
Ecombined_300810
strain measured @ 10[m] from root
Strain [µS]
Local bending moment [kNm]
SG 186_1 (ECombined_300810_cut.bin)
SG 188_1 (ECombined_300810_cut.bin)

65

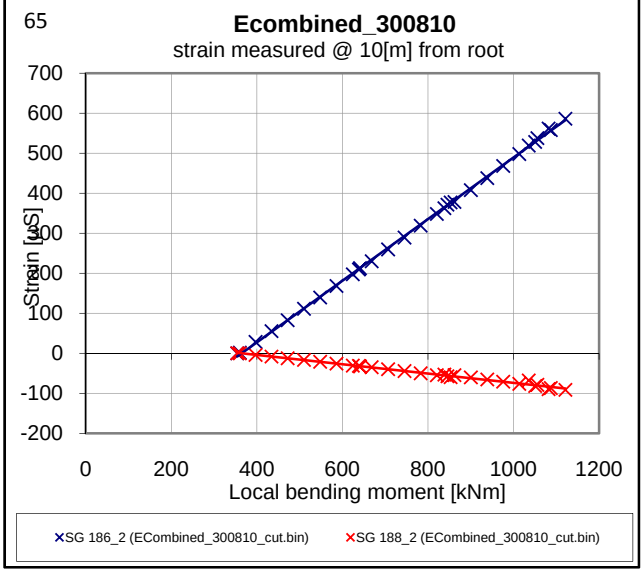
Ecombined_300810
strain measured @ 10[m] from root
Strain [µS]
Local bending moment [kNm]
SG 186_2 (ECombined_300810_cut.bin)
SG 188_2 (ECombined_300810_cut.bin)

66

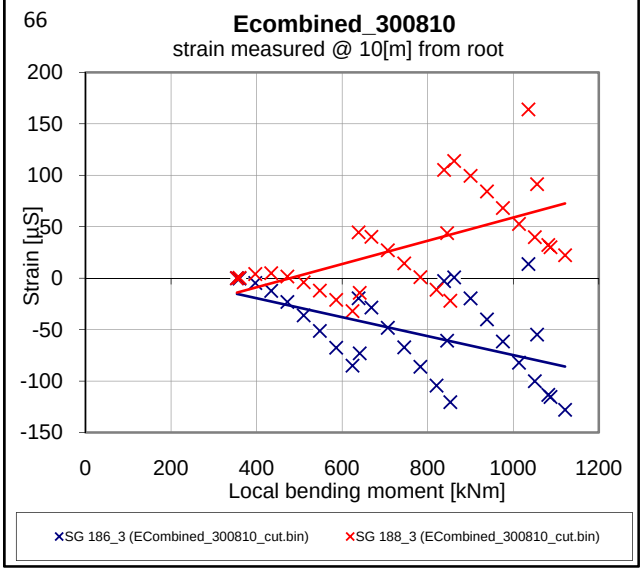
Ecombined_300810
strain measured @ 10[m] from root
Strain [µS]
Local bending moment [kNm]
SG 186_3 (ECombined_300810_cut.bin)
SG 188_3 (ECombined_300810_cut.bin)

B.1.b Measurement of pull at 35% Risø load (AED Section)

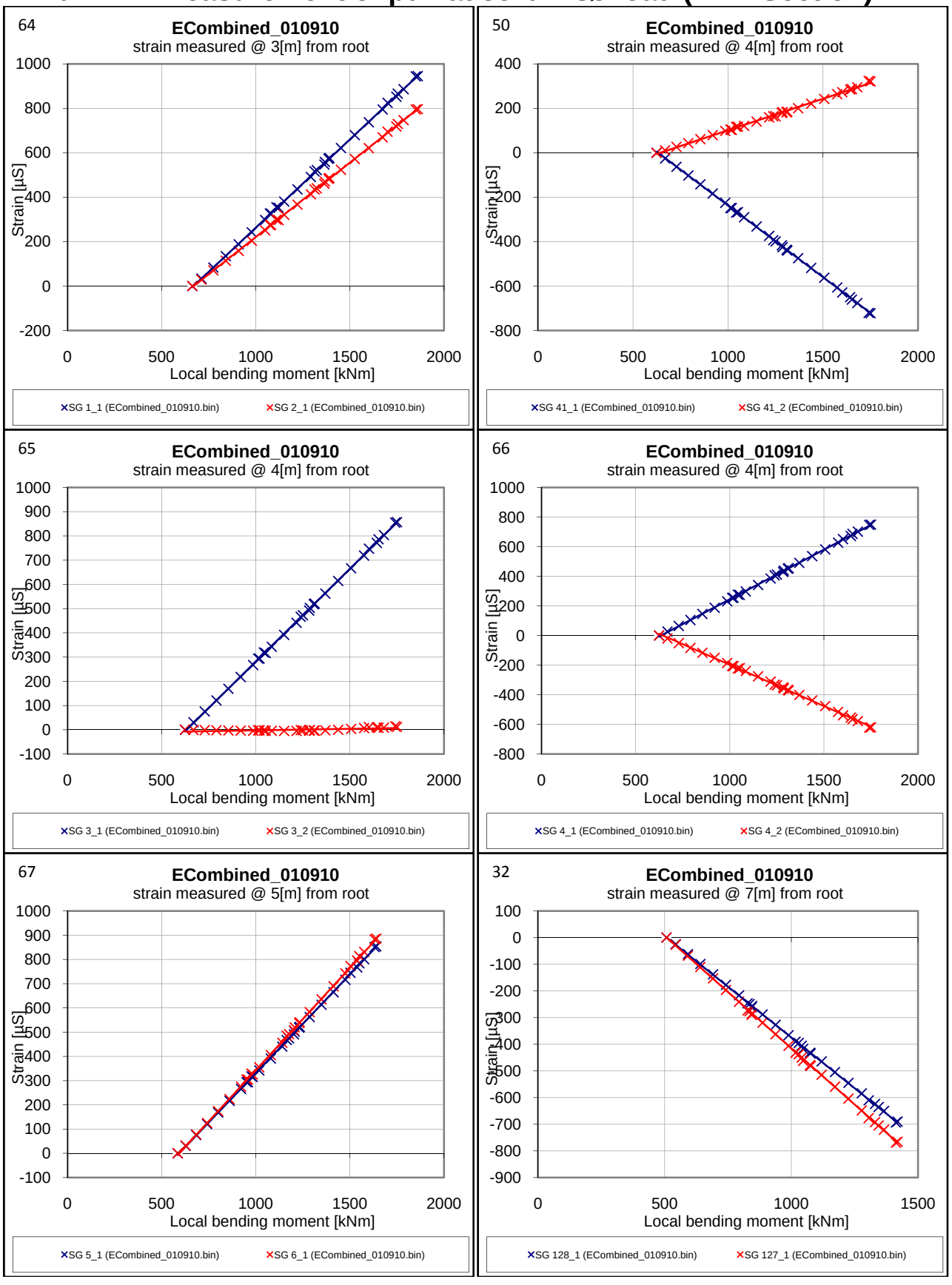

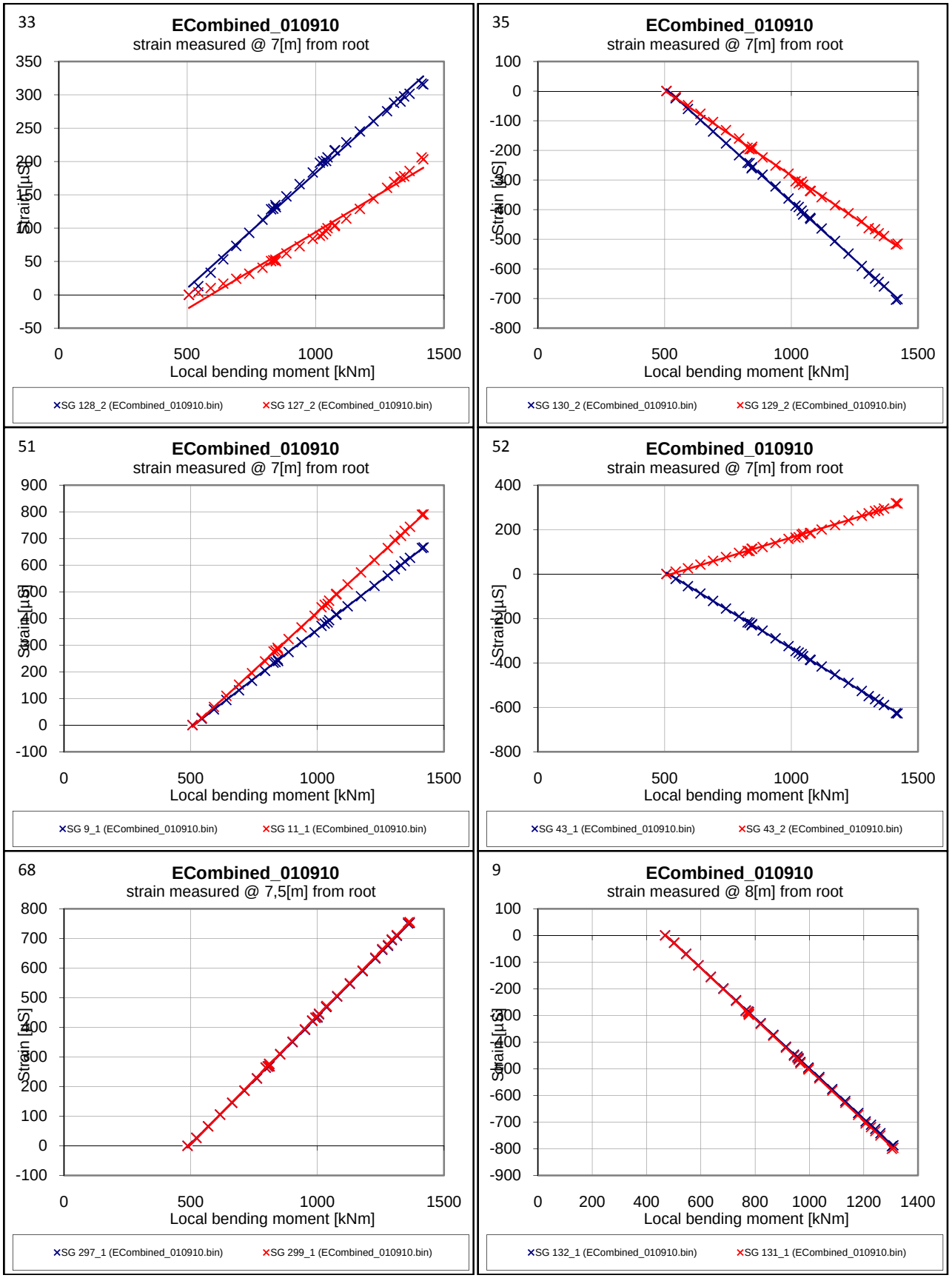
33
ECombined_010910
strain measured @ 7[m] from root
Strain [µS]
Local bending moment [kNm]
SG 128_2 (ECombined_010910.bin)
SG 127_2 (ECombined_010910.bin)
35
ECombined_010910
strain measured @ 7[m] from root
Strain [µS]
Local bending moment [kNm]
SG 130_2 (ECombined_010910.bin)
SG 129_2 (ECombined_010910.bin)
51
ECombined_010910
strain measured @ 7[m] from root
Strain [µS]
Local bending moment [kNm]
SG 9_1 (ECombined_010910.bin)
SG 11_1 (ECombined_010910.bin)
52
ECombined_010910
strain measured @ 7[m] from root
Strain [µS]
Local bending moment [kNm]
SG 43_1 (ECombined_010910.bin)
SG 43_2 (ECombined_010910.bin)
68
ECombined_010910
strain measured @ 7,5[m] from root
Strain [µS]
Local bending moment [kNm]
SG 297_1 (ECombined_010910.bin)
SG 299_1 (ECombined_010910.bin)
9
ECombined_010910
strain measured @ 8[m] from root
Strain [µS]
Local bending moment [kNm]
SG 132_1 (ECombined_010910.bin)
SG 131_1 (ECombined_010910.bin)

10

ECombined_010910

strain measured @ 8[m] from root

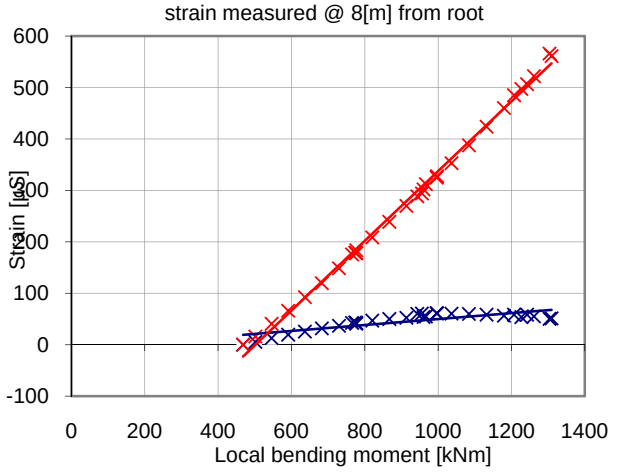

11

ECombined_010910

strain measured @ 8[m] from root

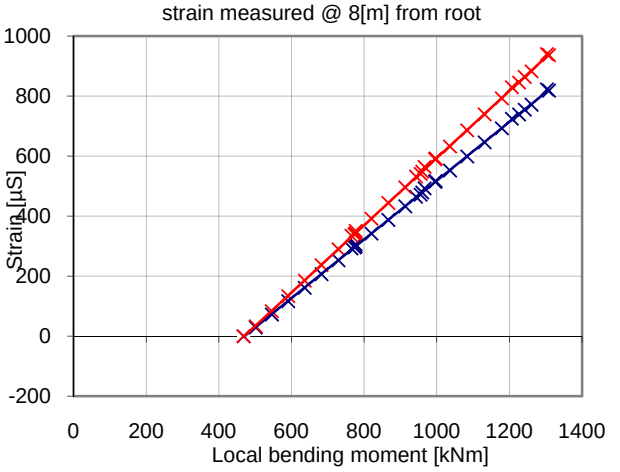

12

ECombined_010910

strain measured @ 8[m] from root

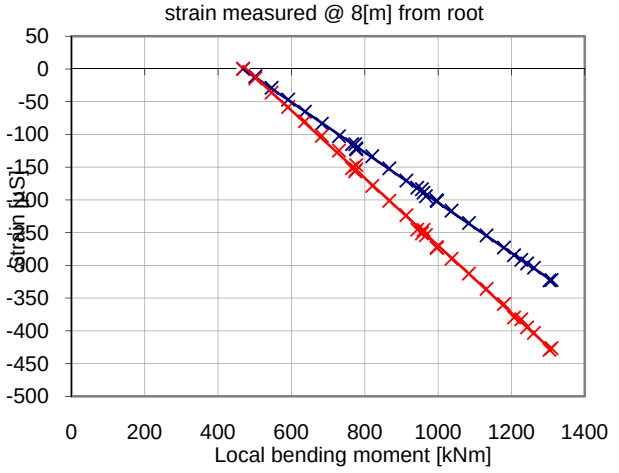

69

ECombined_010910

strain measured @ 8[m] from root

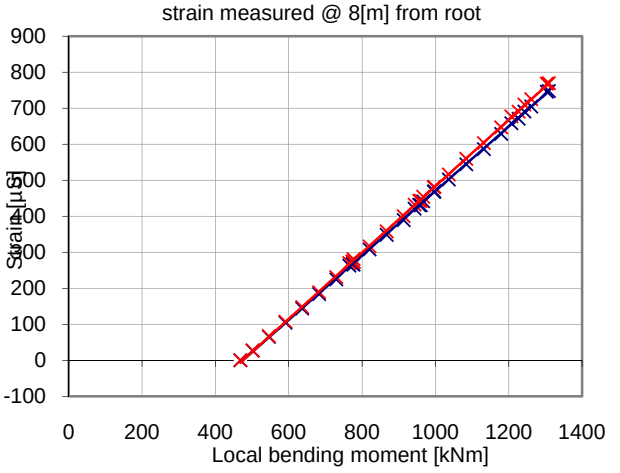

70

ECombined_010910

strain measured @ 8,5[m] from root

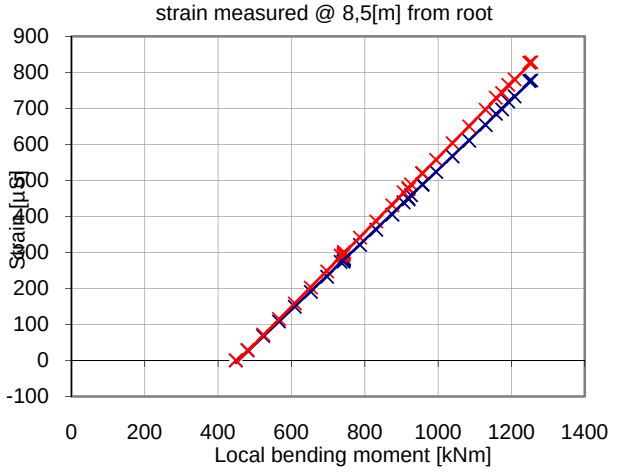

1

ECombined_010910

strain measured @ 9[m] from root

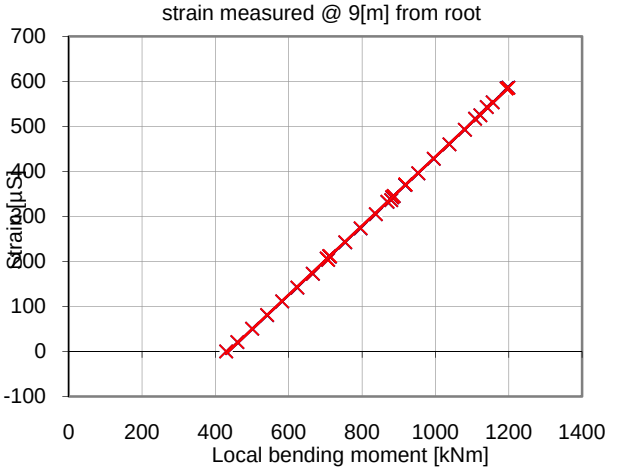

2

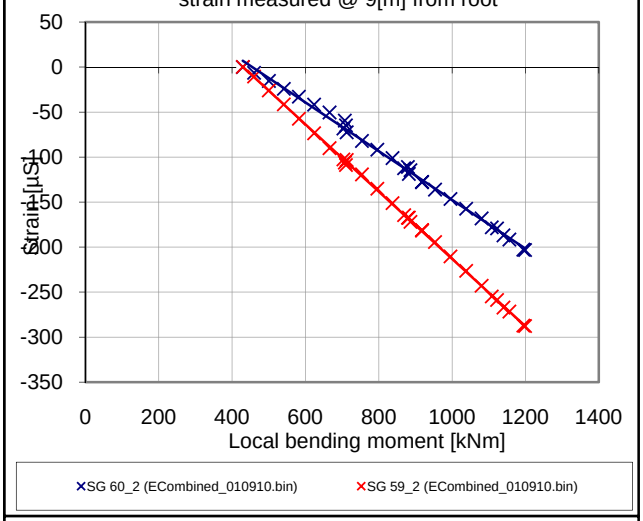
ECombined_010910
strain measured @ 9[m] from root
Strain [µS]
Local bending moment [kNm]
SG 60_2 (ECombined_010910.bin)
SG 59_2 (ECombined_010910.bin)

3

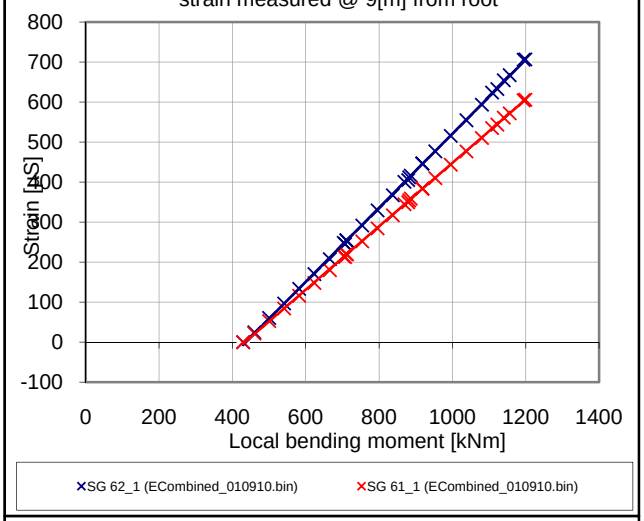
ECombined_010910
strain measured @ 9[m] from root
Strain [µS]
Local bending moment [kNm]
SG 62_1 (ECombined_010910.bin)
SG 61_1 (ECombined_010910.bin)

4

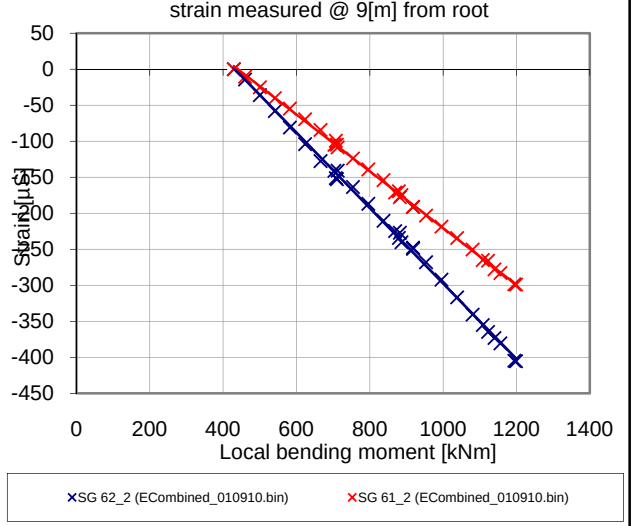
ECombined_010910
strain measured @ 9[m] from root
Strain [µS]
Local bending moment [kNm]
SG 62_2 (ECombined_010910.bin)
SG 61_2 (ECombined_010910.bin)

6

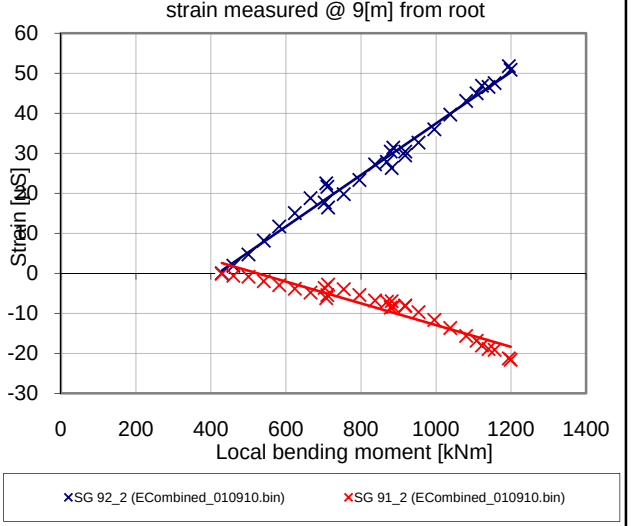
ECombined_010910
strain measured @ 9[m] from root
Strain [µS]
Local bending moment [kNm]
SG 92_2 (ECombined_010910.bin)
SG 91_2 (ECombined_010910.bin)

7

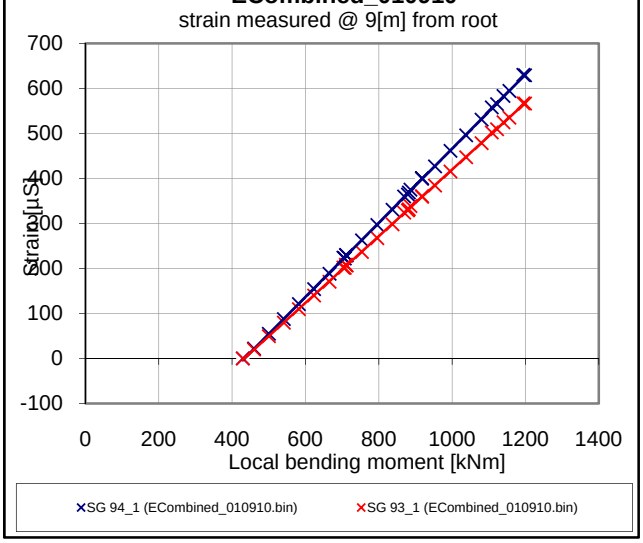
ECombined_010910
strain measured @ 9[m] from root
Strain [µS]
Local bending moment [kNm]
SG 94_1 (ECombined_010910.bin)
SG 93_1 (ECombined_010910.bin)

8

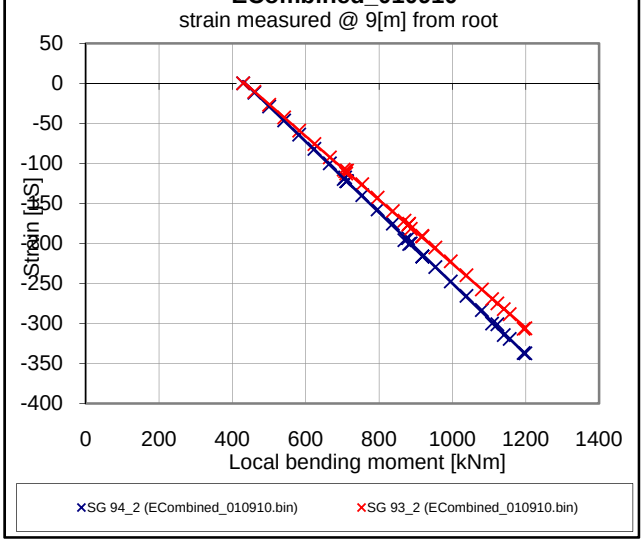
ECombined_010910
strain measured @ 9[m] from root
Strain [µS]
Local bending moment [kNm]
SG 94_2 (ECombined_010910.bin)
SG 93_2 (ECombined_010910.bin)

13

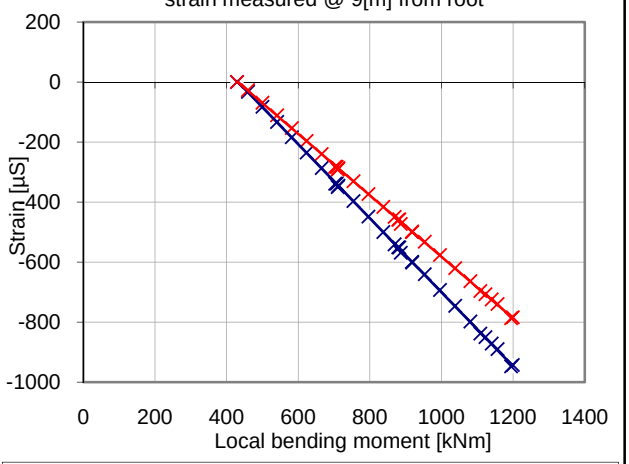

14

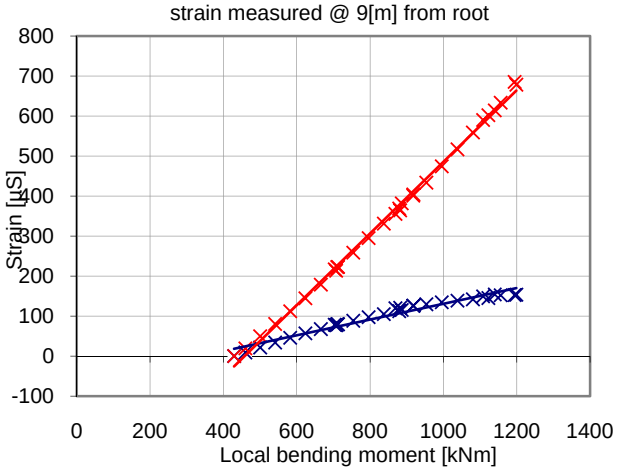

15

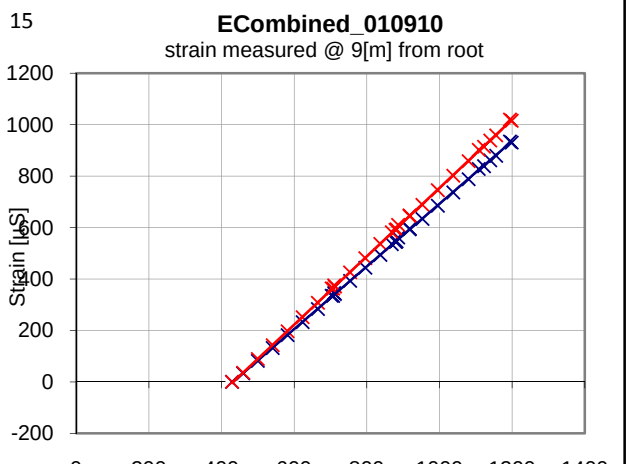

16

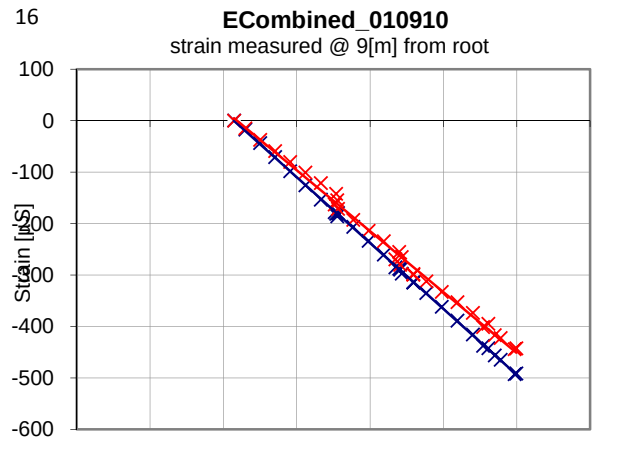

71

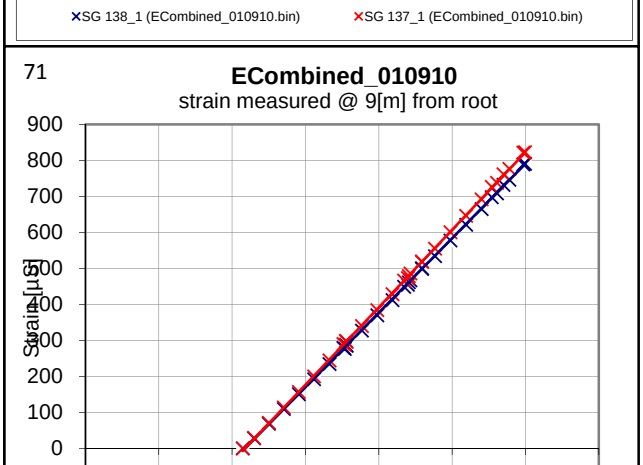

72

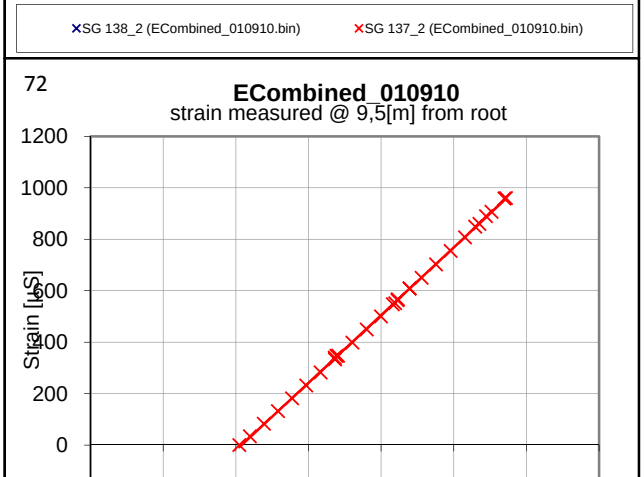

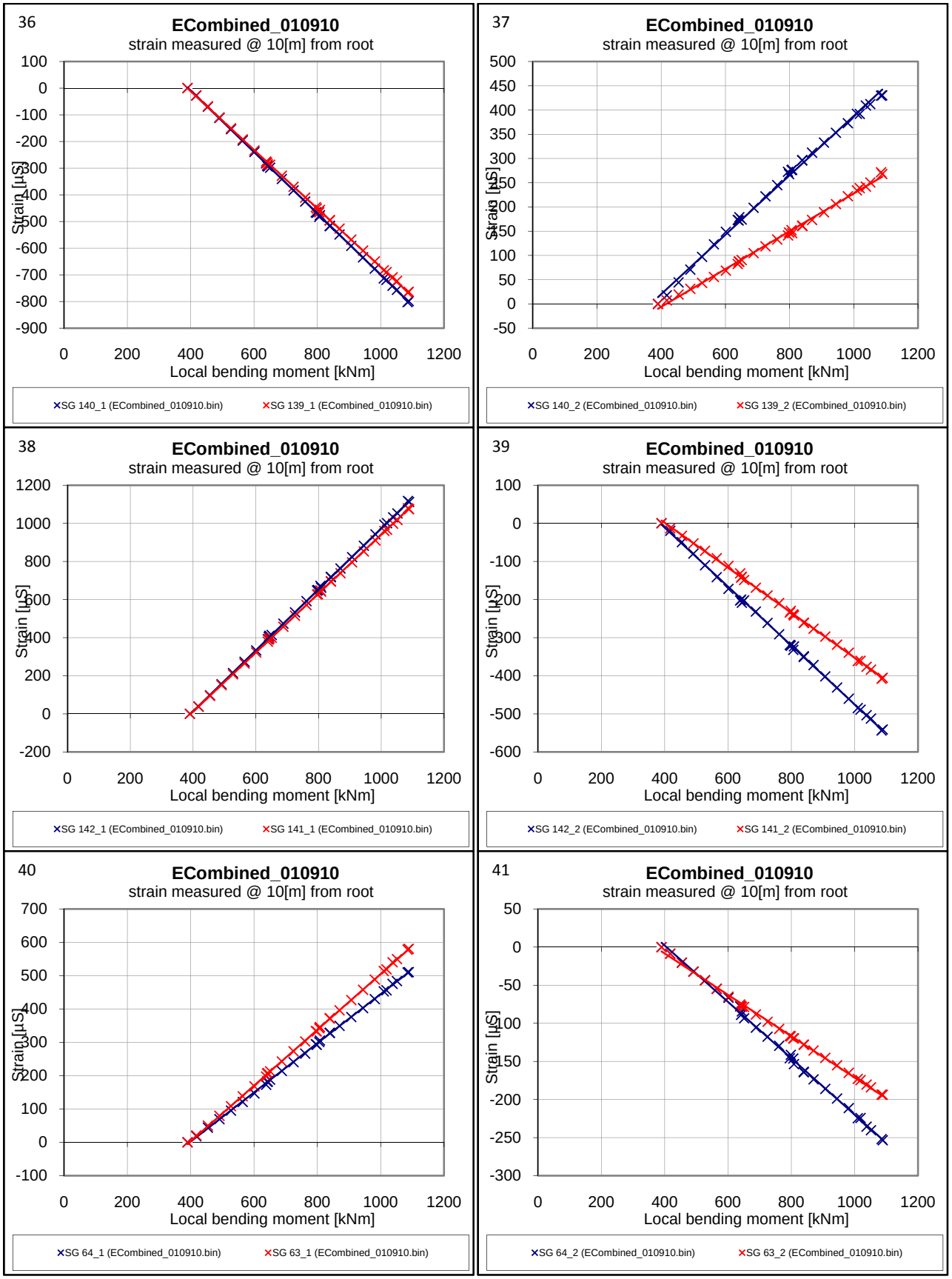
36
ECombined_010910
strain measured @ 10[m] from root
Strain [µS]
Local bending moment [kNm]
SG 140_1 (ECombined_010910.bin)
SG 139_1 (ECombined_010910.bin)
37
ECombined_010910
strain measured @ 10[m] from root
Strain [µS]
Local bending moment [kNm]
SG 140_2 (ECombined_010910.bin)
SG 139_2 (ECombined_010910.bin)
38
ECombined_010910
strain measured @ 10[m] from root
Strain [µS]
Local bending moment [kNm]
SG 142_1 (ECombined_010910.bin)
SG 141_1 (ECombined_010910.bin)
39
ECombined_010910
strain measured @ 10[m] from root
Strain [µS]
Local bending moment [kNm]
SG 142_2 (ECombined_010910.bin)
SG 141_2 (ECombined_010910.bin)
40
ECombined_010910
strain measured @ 10[m] from root
Strain [µS]
Local bending moment [kNm]
SG 64_1 (ECombined_010910.bin)
SG 63_1 (ECombined_010910.bin)
41
ECombined_010910
strain measured @ 10[m] from root
Strain [µS]
Local bending moment [kNm]
SG 64_2 (ECombined_010910.bin)
SG 63_2 (ECombined_010910.bin)

42

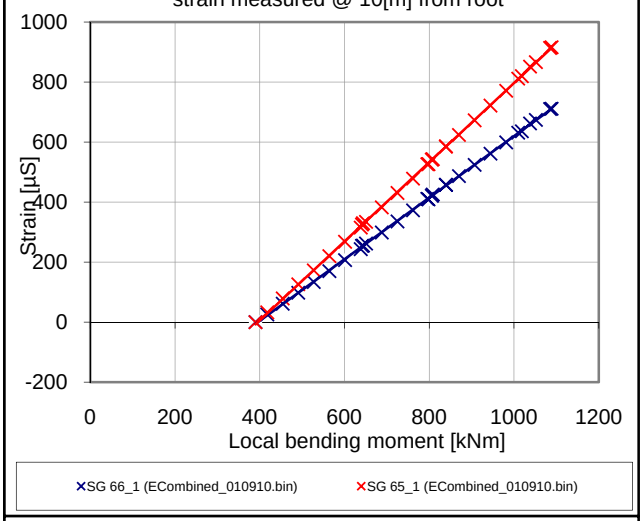

43

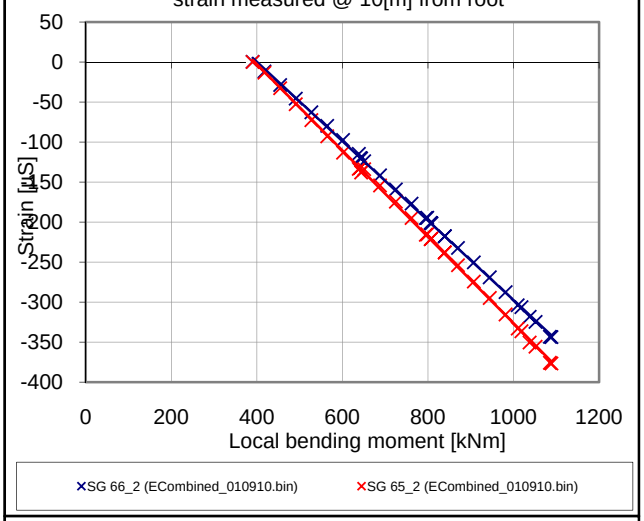

44

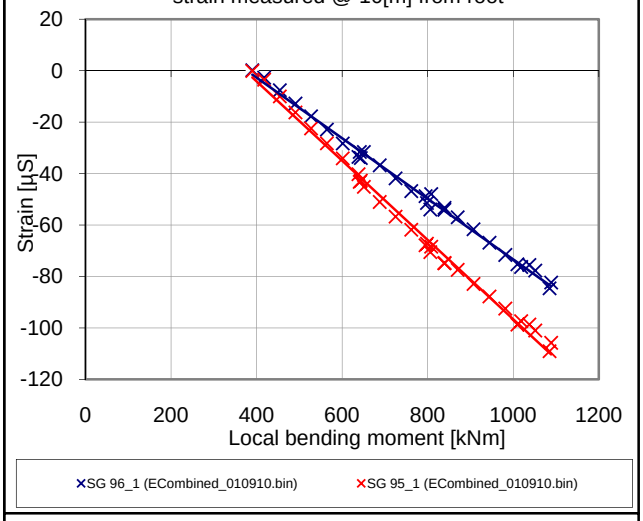

45

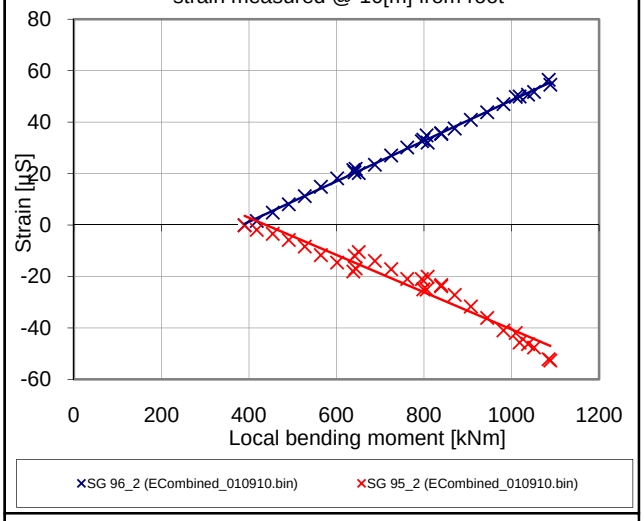

46

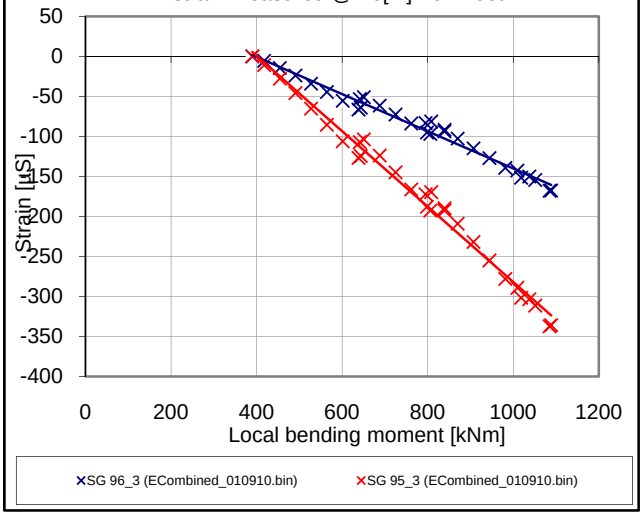

47

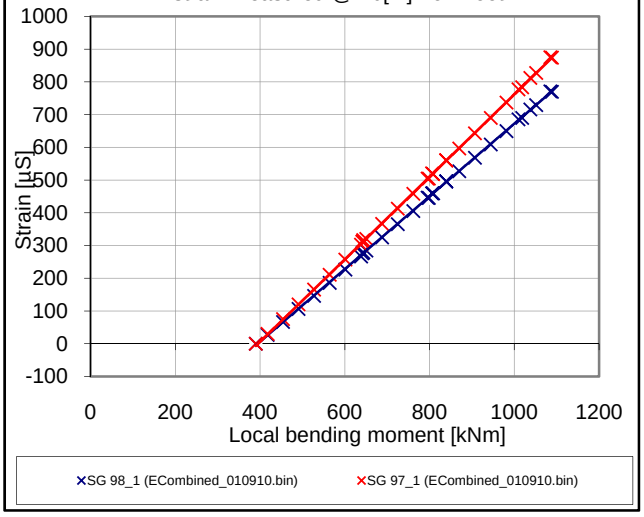

48

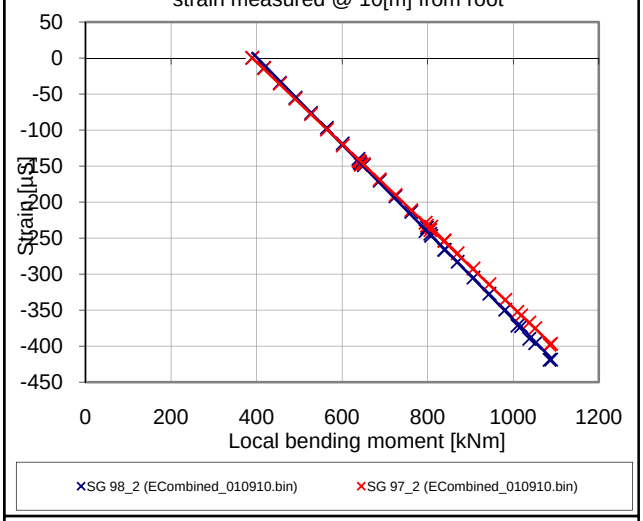

49

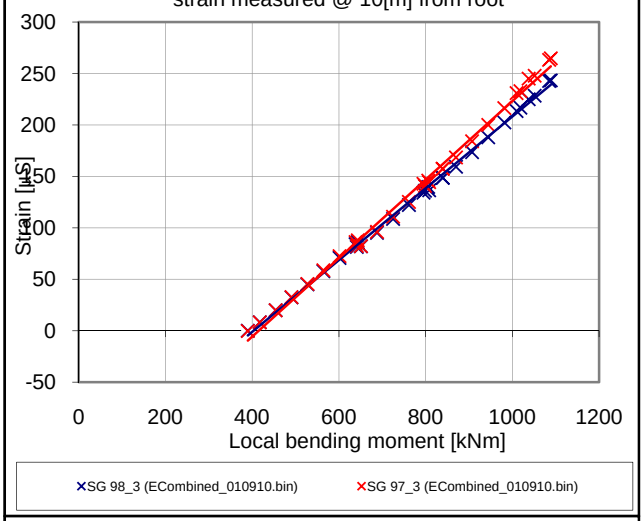

53

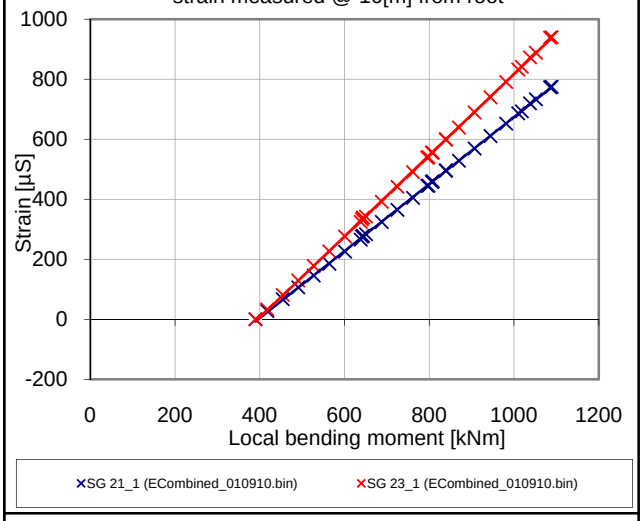

54

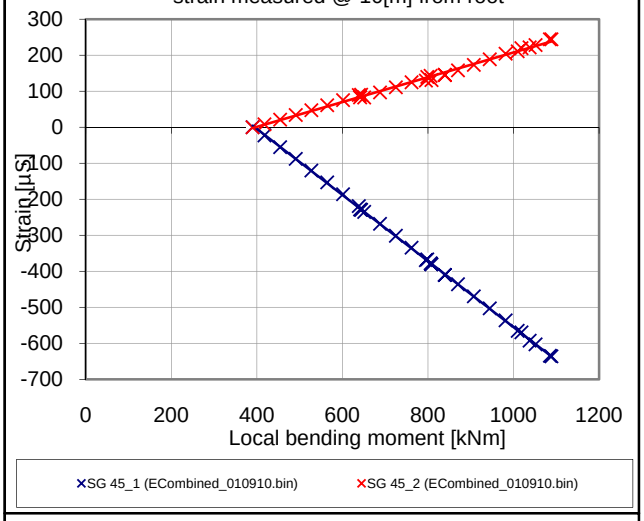

55

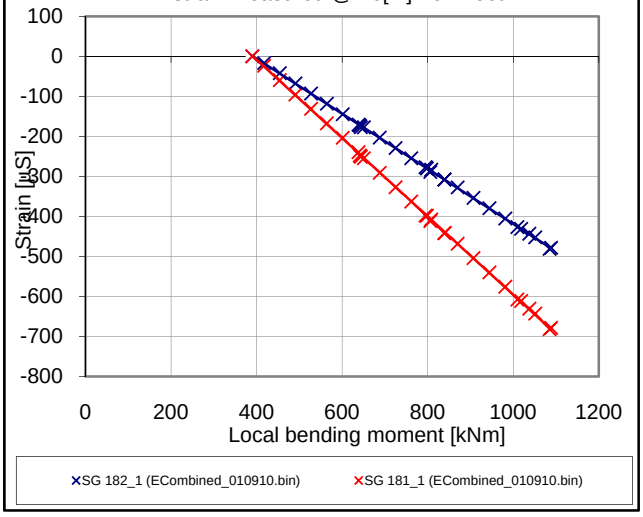

56

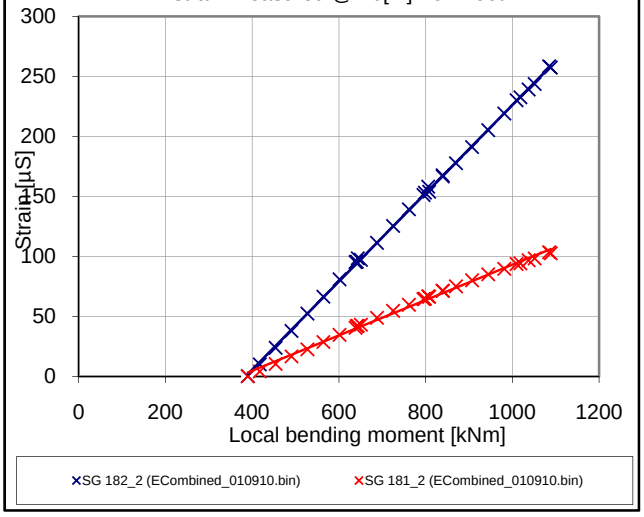

57

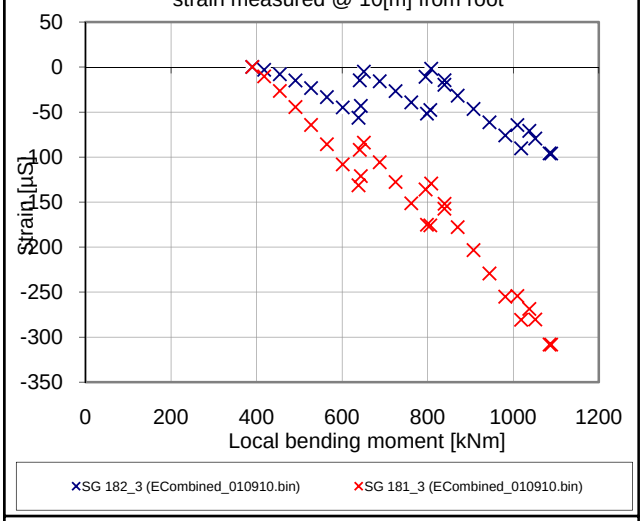

58

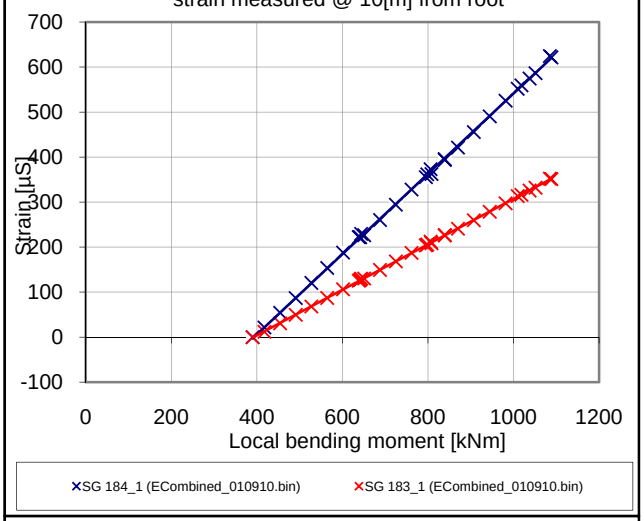

59

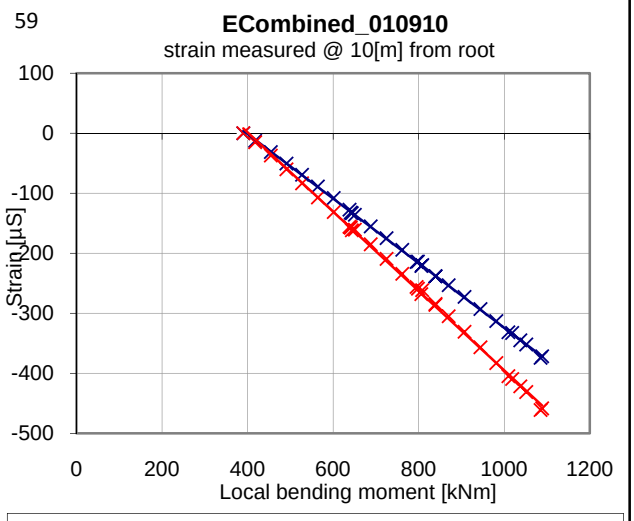

60

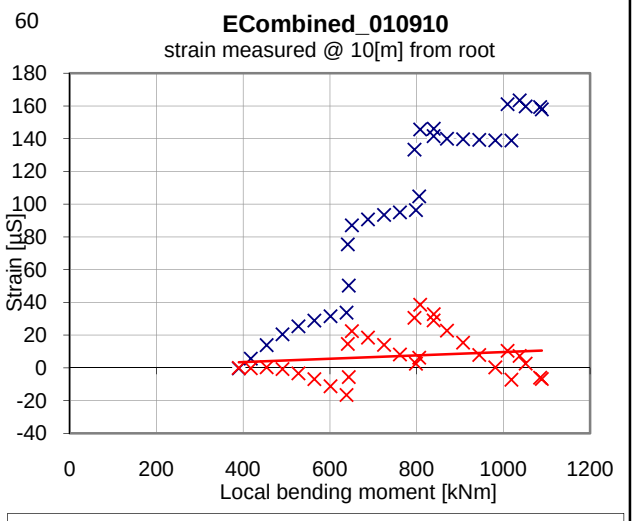

61

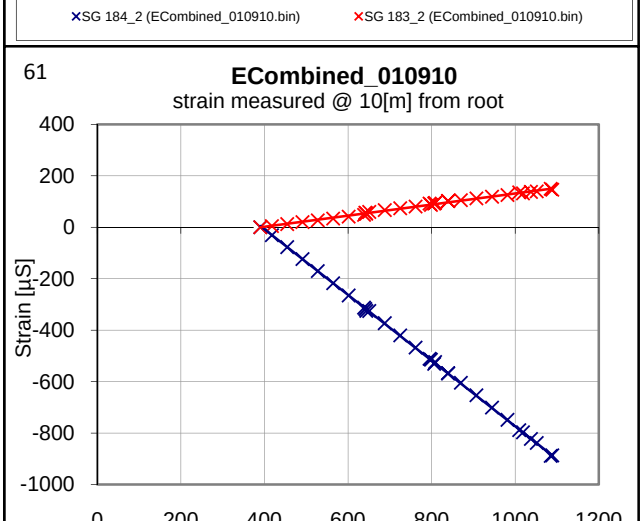

62

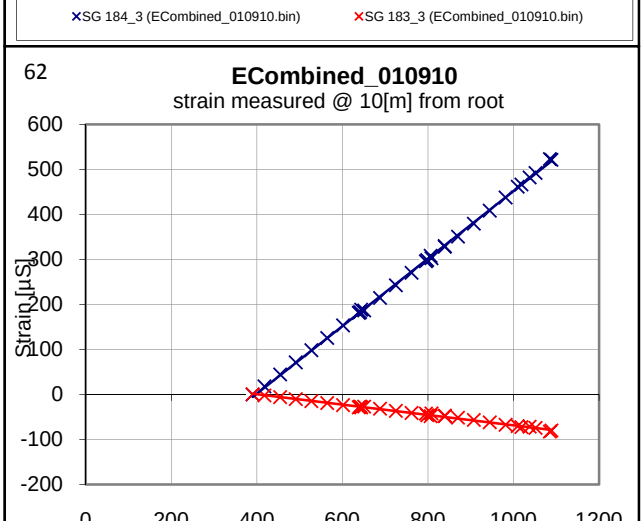

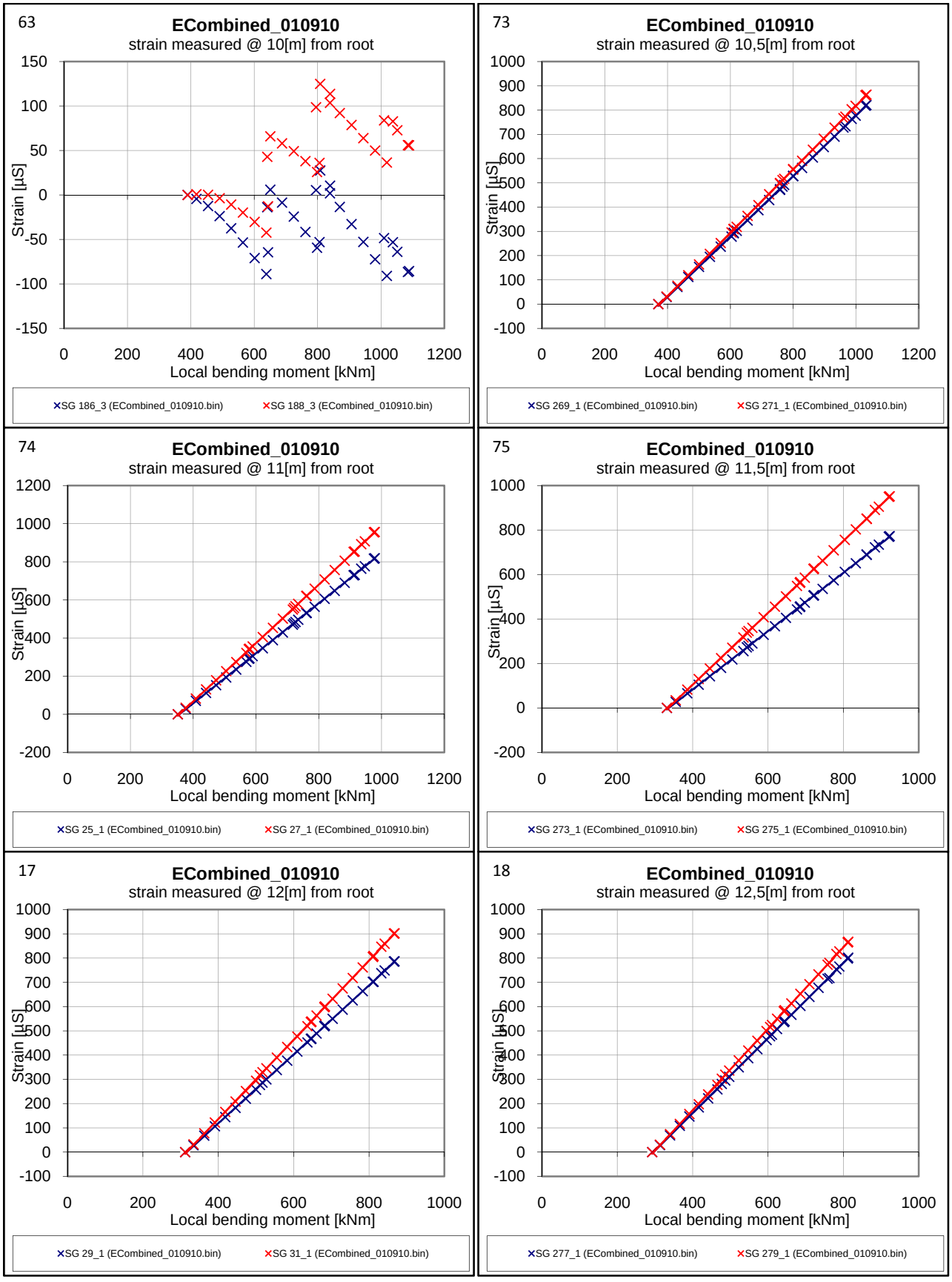
63
ECombined_010910
strain measured @ 10[m] from root
Strain [µS]
Local bending moment [kNm]
SG 186_3 (ECombined_010910.bin)
SG 188_3 (ECombined_010910.bin)
73
ECombined_010910
strain measured @ 10,5[m] from root
Strain [µS]
Local bending moment [kNm]
SG 269_1 (ECombined_010910.bin)
SG 271_1 (ECombined_010910.bin)
74
ECombined_010910
strain measured @ 11[m] from root
Strain [µS]
Local bending moment [kNm]
SG 25_1 (ECombined_010910.bin)
SG 27_1 (ECombined_010910.bin)
75
ECombined_010910
strain measured @ 11,5[m] from root
Strain [µS]
Local bending moment [kNm]
SG 273_1 (ECombined_010910.bin)
SG 275_1 (ECombined_010910.bin)
17
ECombined_010910
strain measured @ 12[m] from root
Strain [µS]
Local bending moment [kNm]
SG 29_1 (ECombined_010910.bin)
SG 31_1 (ECombined_010910.bin)
18
ECombined_010910
strain measured @ 12,5[m] from root
Strain [µS]
Local bending moment [kNm]
SG 277_1 (ECombined_010910.bin)
SG 279_1 (ECombined_010910.bin)

19

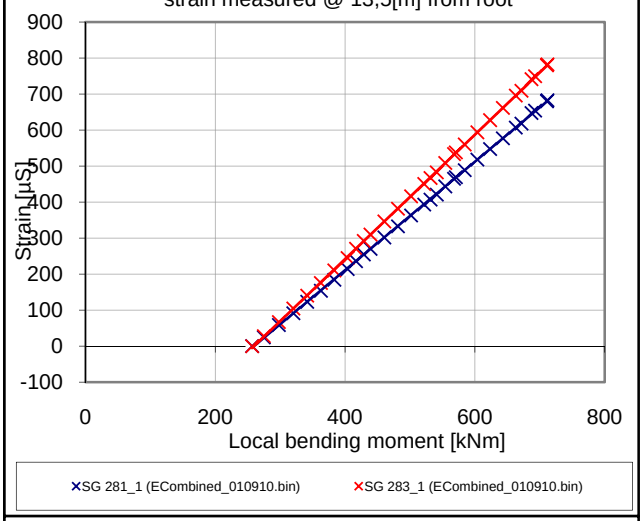

20

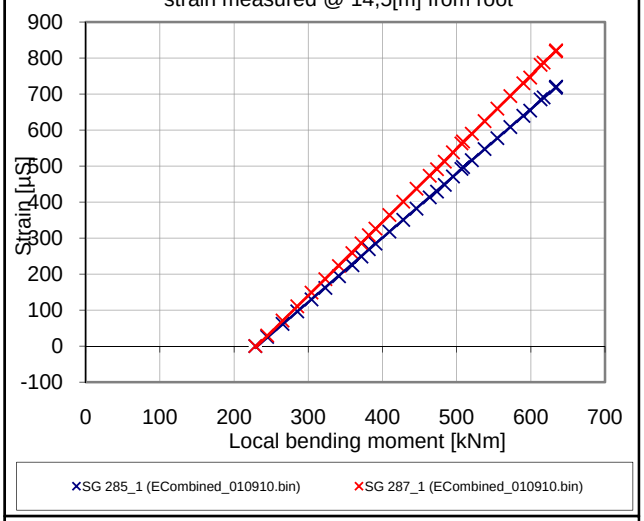

21

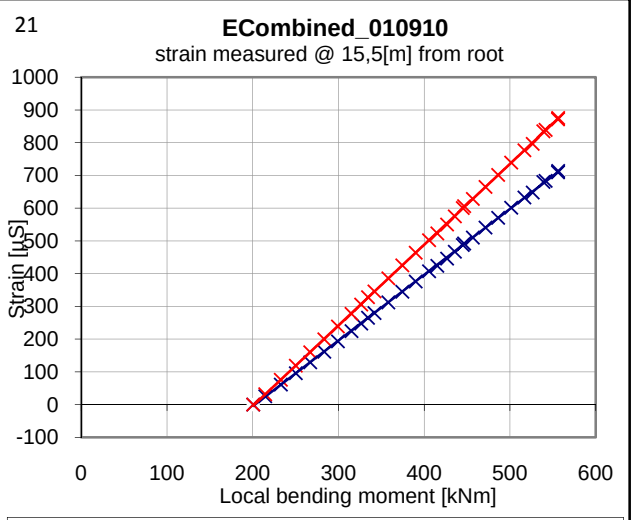

22

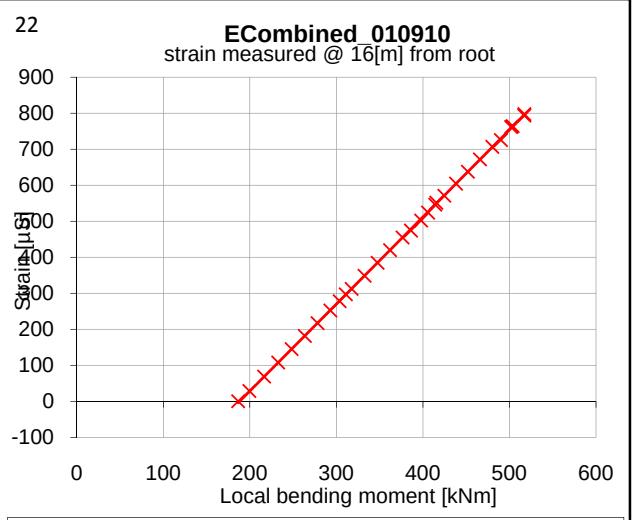

23

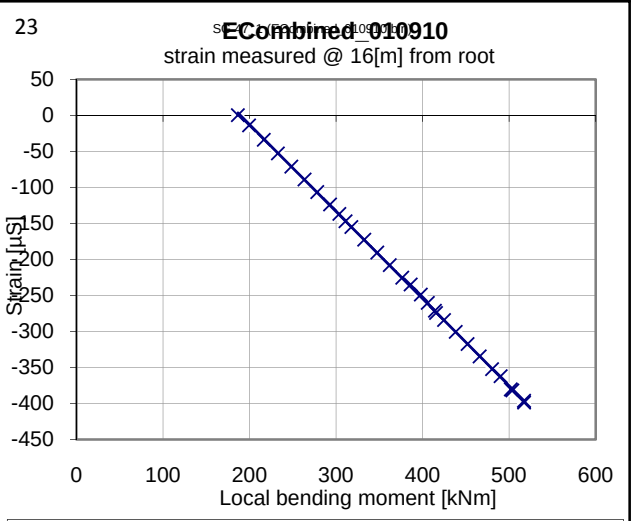

24

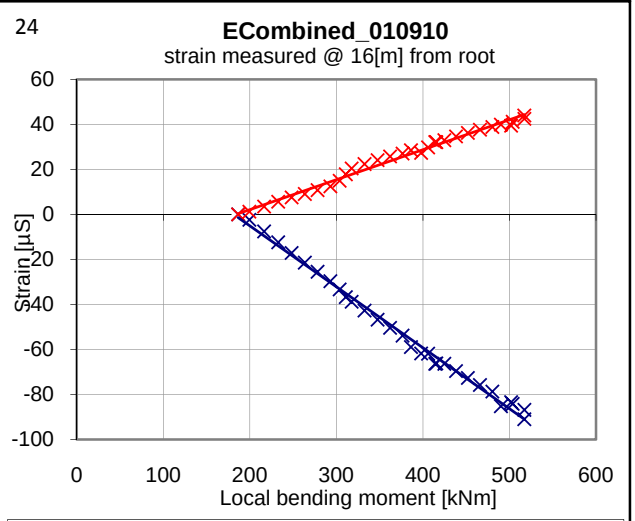

19

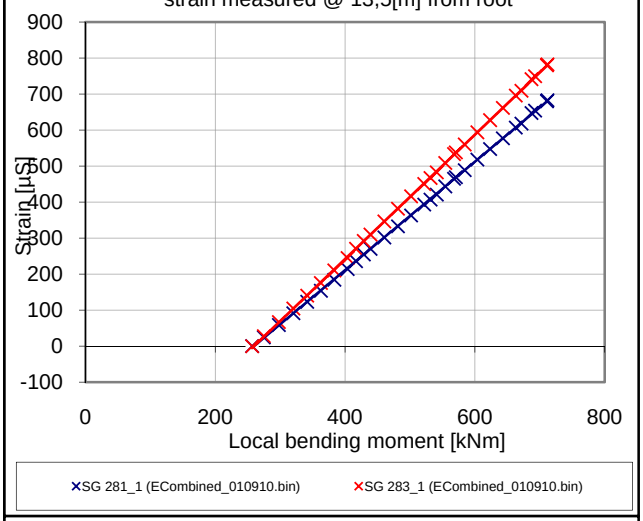

20

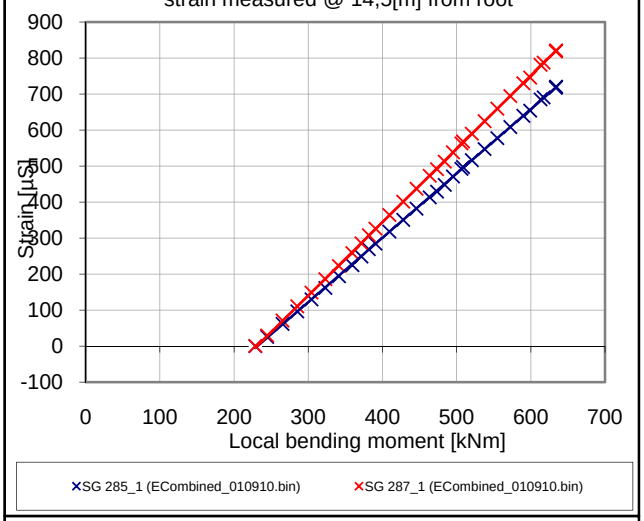

21

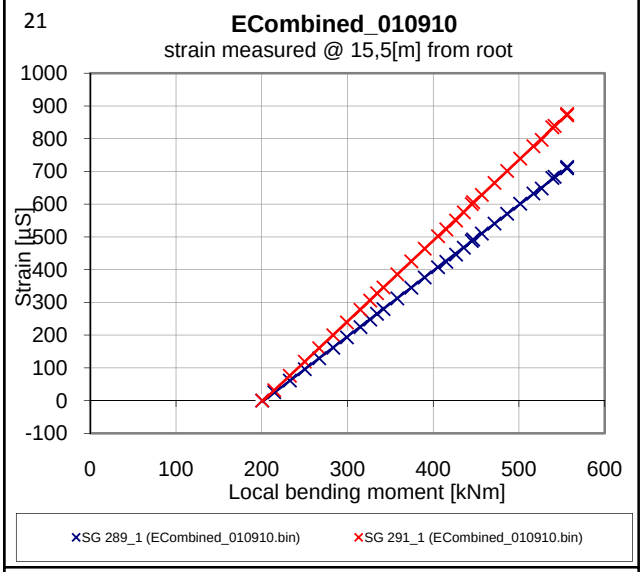

22

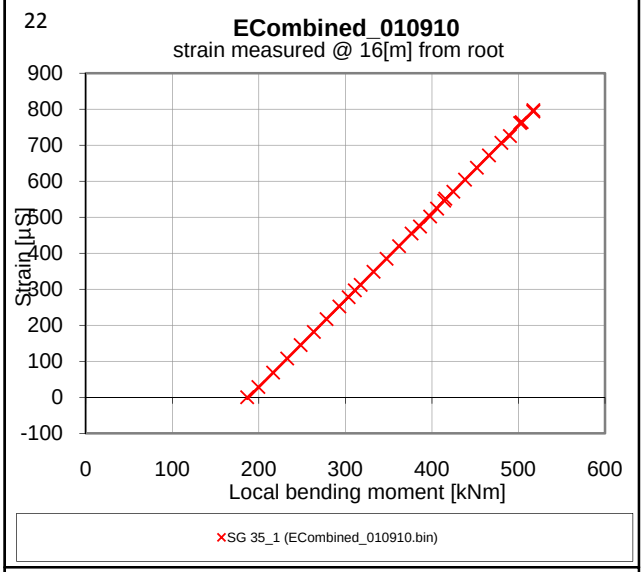

23

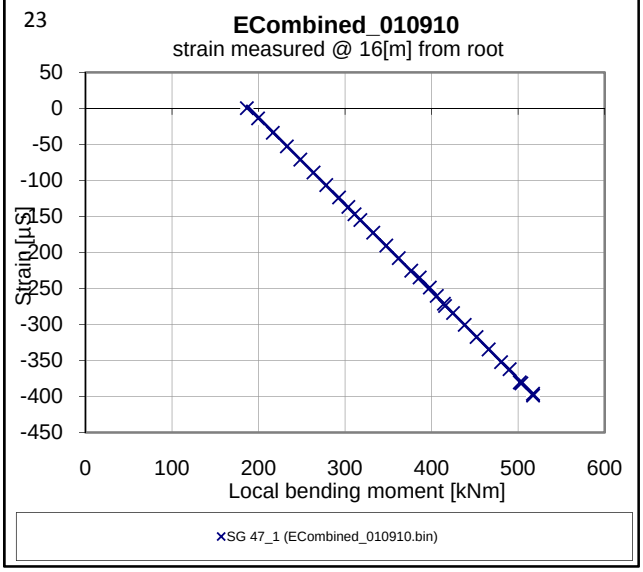

24

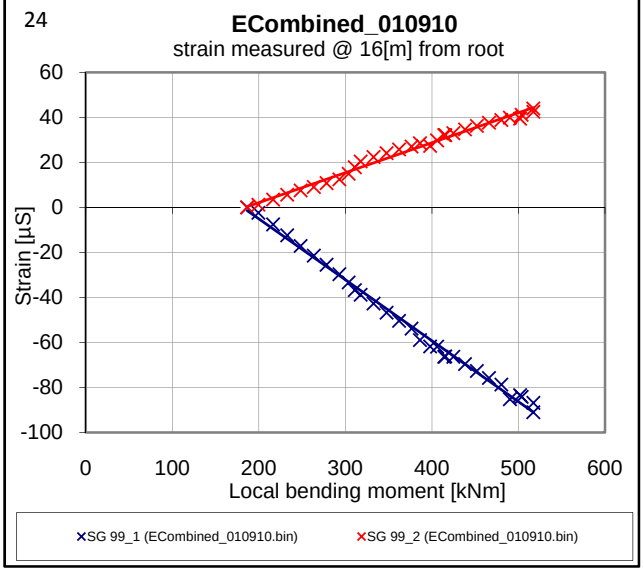

25

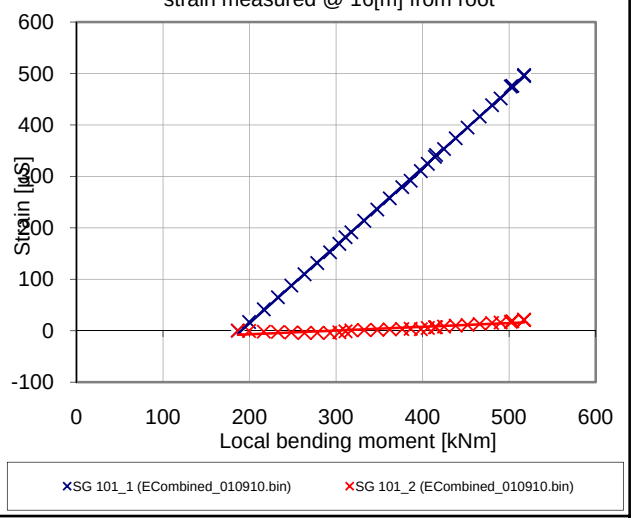

26

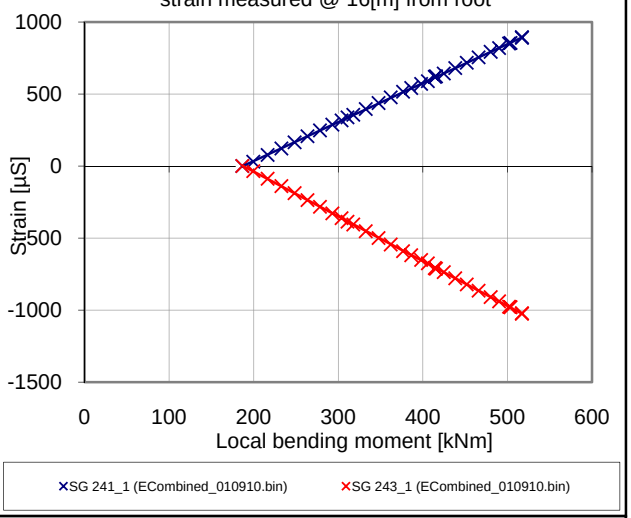

27

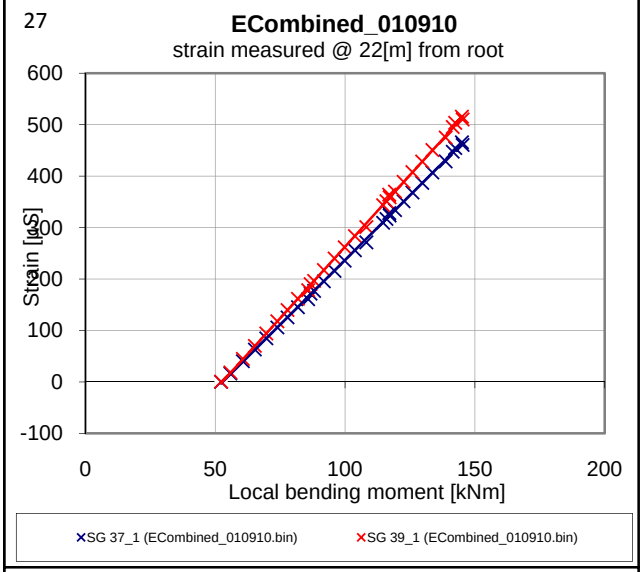

28

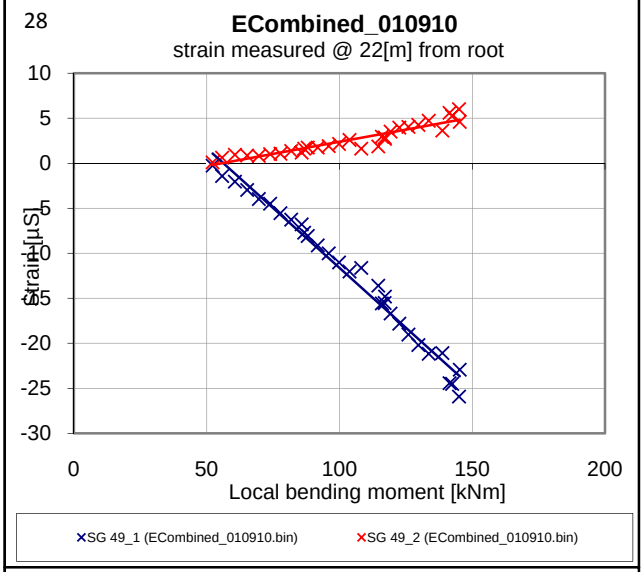

29

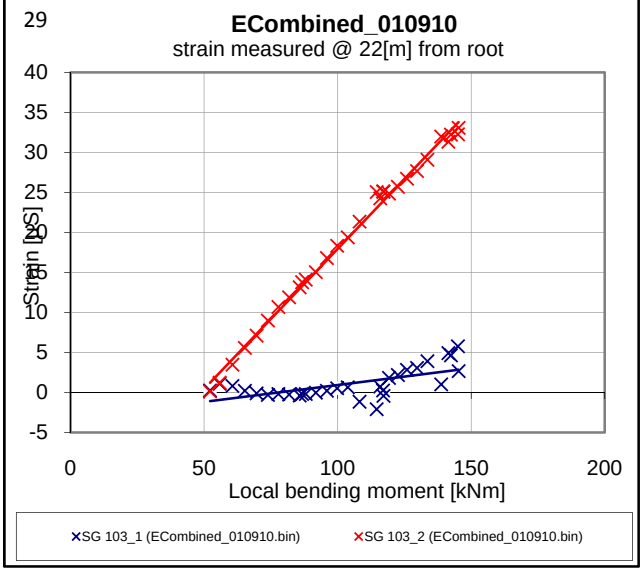

30

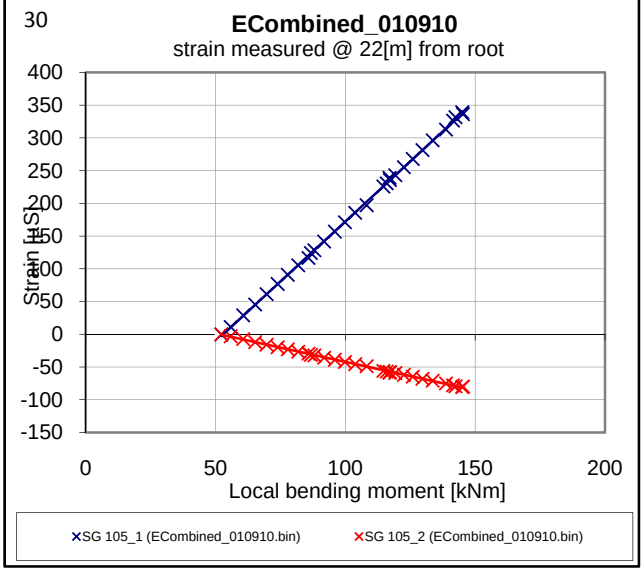

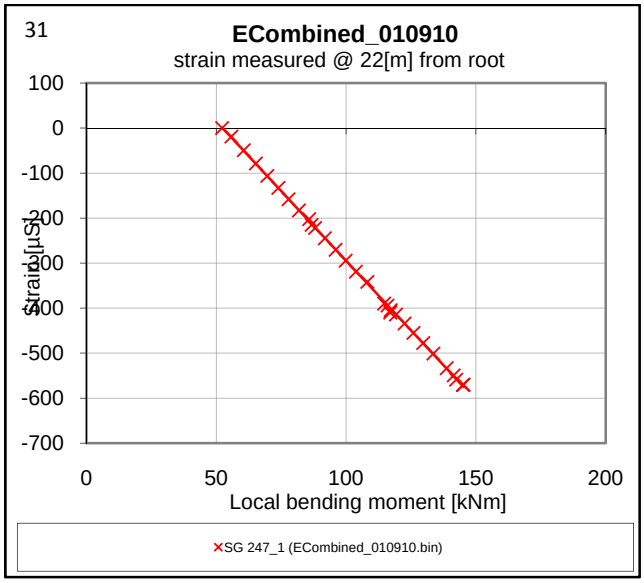
31
ECombined_010910
strain measured @ 22[m] from root
100
0
-100
-200
-300
-400
-500
-600
-700
Strain [µSt]
0
50
100
150
200
Local bending moment [kNm]
SG 247_1 (ECombined_010910.bin)

B.1.c Measurement of pull at 35% Risø load (Other groups)

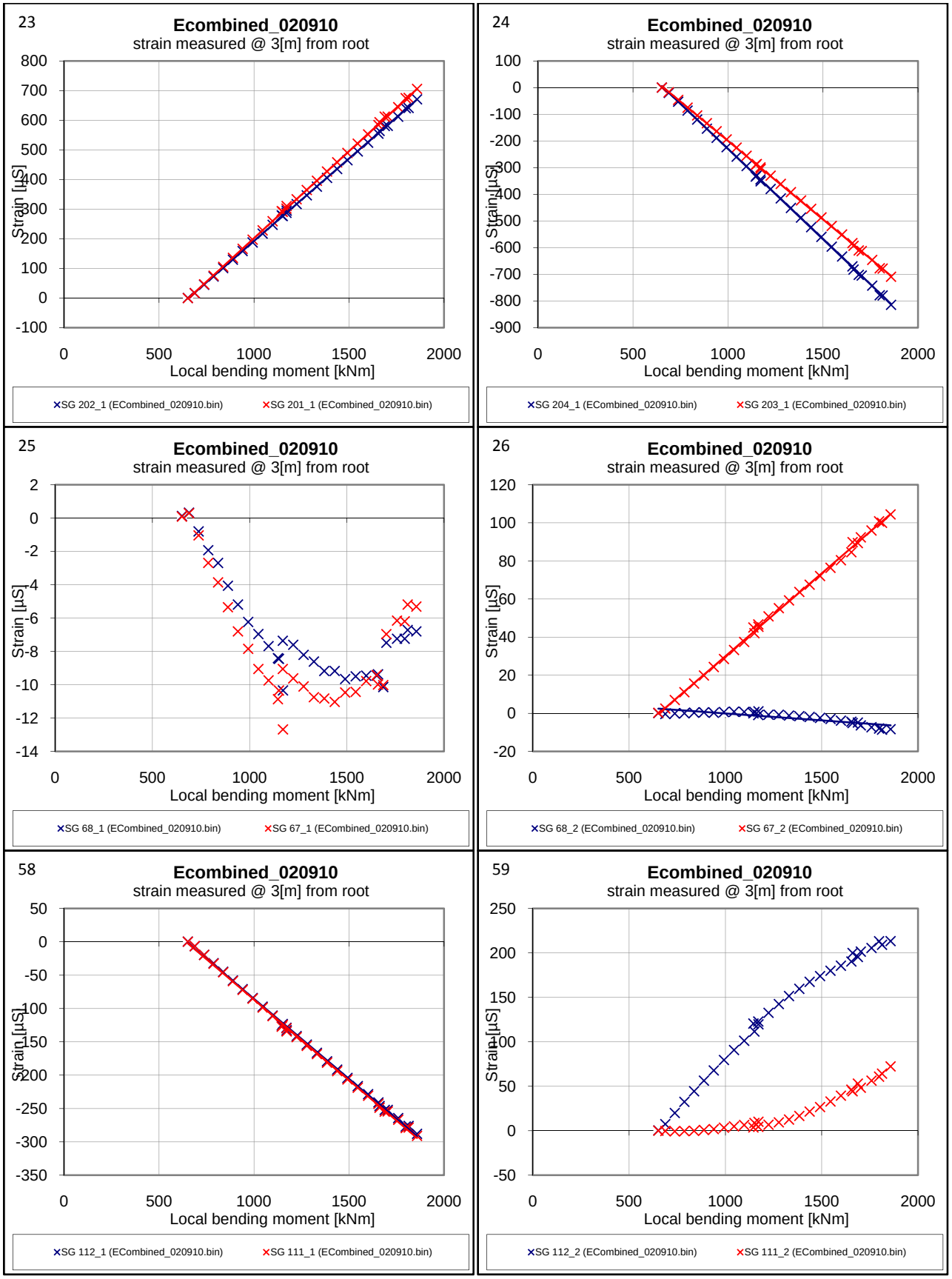

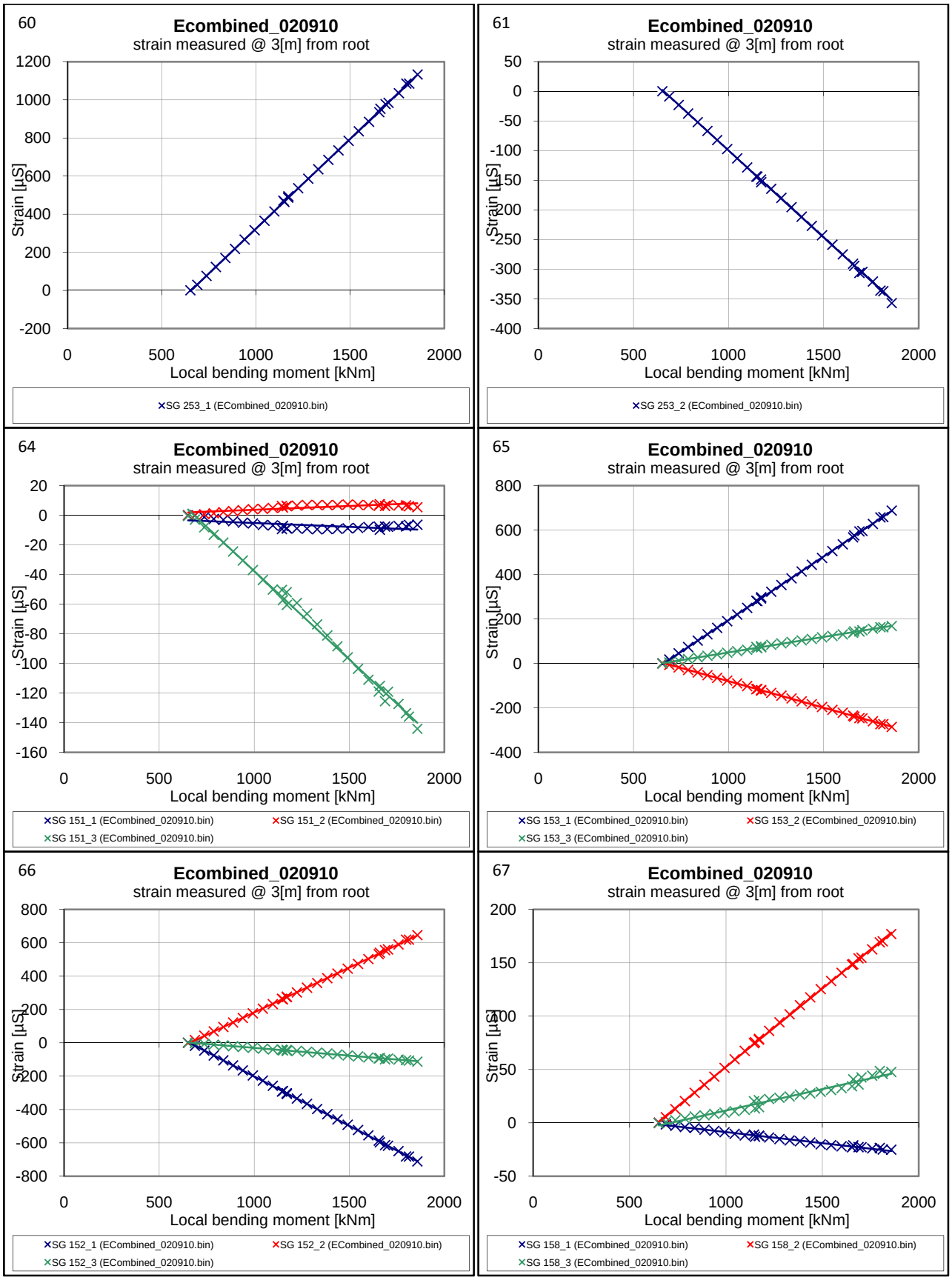
60
Ecombined_020910
strain measured @ 3[m] from root
Strain [µS]
Local bending moment [kNm]
SG 253_1 (ECombined_020910.bin)
61
Ecombined_020910
strain measured @ 3[m] from root
Strain [µS]
Local bending moment [kNm]
SG 253_2 (ECombined_020910.bin)
64
Ecombined_020910
strain measured @ 3[m] from root
Strain [µS]
Local bending moment [kNm]
SG 151_1 (ECombined_020910.bin)
SG 151_2 (ECombined_020910.bin)
SG 151_3 (ECombined_020910.bin)
65
Ecombined_020910
strain measured @ 3[m] from root
Strain [µS]
Local bending moment [kNm]
SG 153_1 (ECombined_020910.bin)
SG 153_2 (ECombined_020910.bin)
SG 153_3 (ECombined_020910.bin)
66
Ecombined_020910
strain measured @ 3[m] from root
Strain [µS]
Local bending moment [kNm]
SG 152_1 (ECombined_020910.bin)
SG 152_2 (ECombined_020910.bin)
SG 152_3 (ECombined_020910.bin)
67
Ecombined_020910
strain measured @ 3[m] from root
Strain [µS]
Local bending moment [kNm]
SG 158_1 (ECombined_020910.bin)
SG 158_2 (ECombined_020910.bin)
SG 158_3 (ECombined_020910.bin)

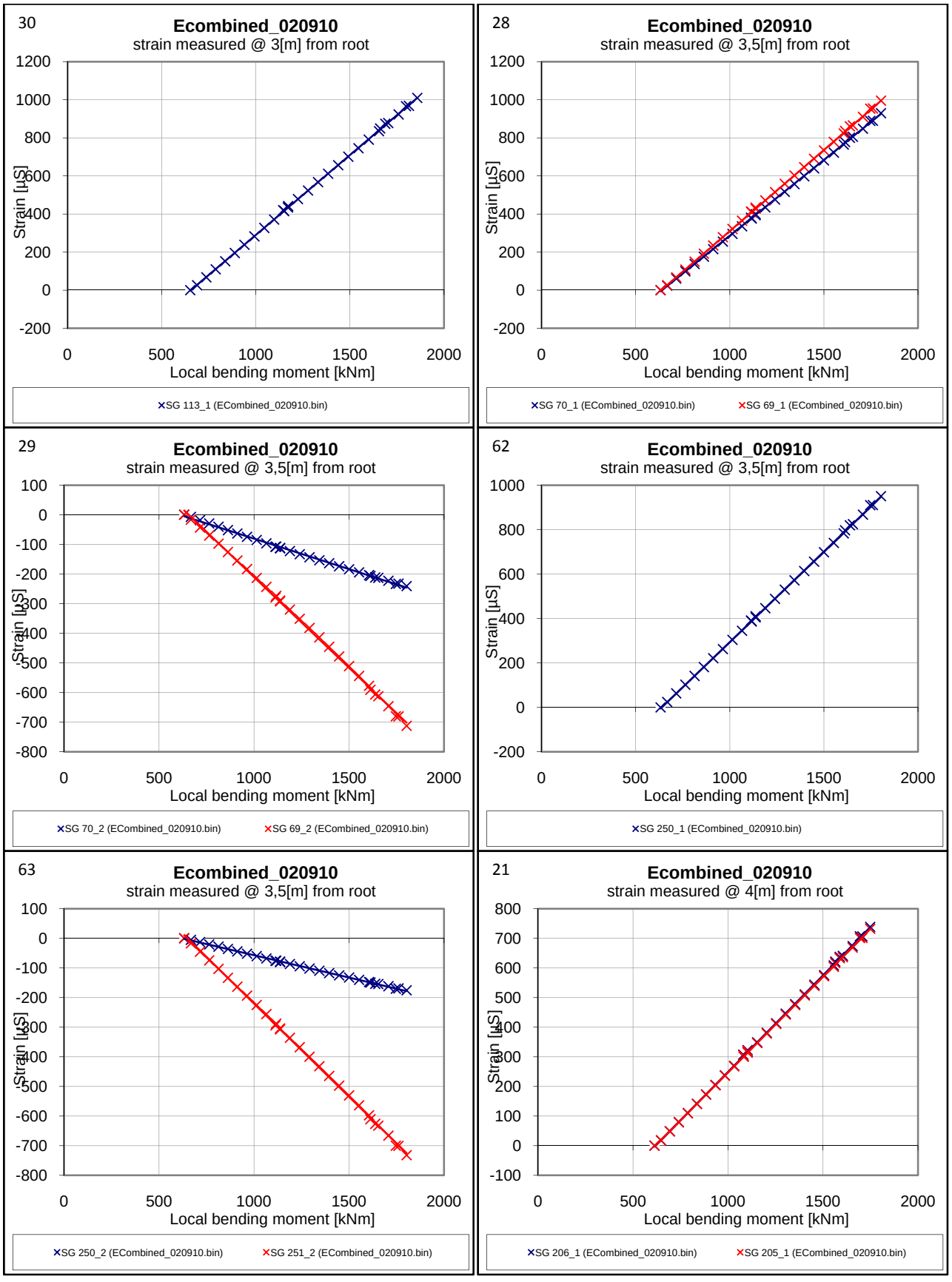
30
Ecombined_020910
strain measured @ 3[m] from root
Strain [µS]
Local bending moment [kNm]
SG 113_1 (ECombined_020910.bin)
28
Ecombined_020910
strain measured @ 3,5[m] from root
Strain [µS]
Local bending moment [kNm]
SG 70_1 (ECombined_020910.bin)
SG 69_1 (ECombined_020910.bin)
29
Ecombined_020910
strain measured @ 3,5[m] from root
Strain [µS]
Local bending moment [kNm]
SG 70_2 (ECombined_020910.bin)
SG 69_2 (ECombined_020910.bin)
62
Ecombined_020910
strain measured @ 3,5[m] from root
Strain [µS]
Local bending moment [kNm]
SG 250_1 (ECombined_020910.bin)
63
Ecombined_020910
strain measured @ 3,5[m] from root
Strain [µS]
Local bending moment [kNm]
SG 250_2 (ECombined_020910.bin)
SG 251_2 (ECombined_020910.bin)
21
Ecombined_020910
strain measured @ 4[m] from root
Strain [µS]
Local bending moment [kNm]
SG 206_1 (ECombined_020910.bin)
SG 205_1 (ECombined_020910.bin)

22

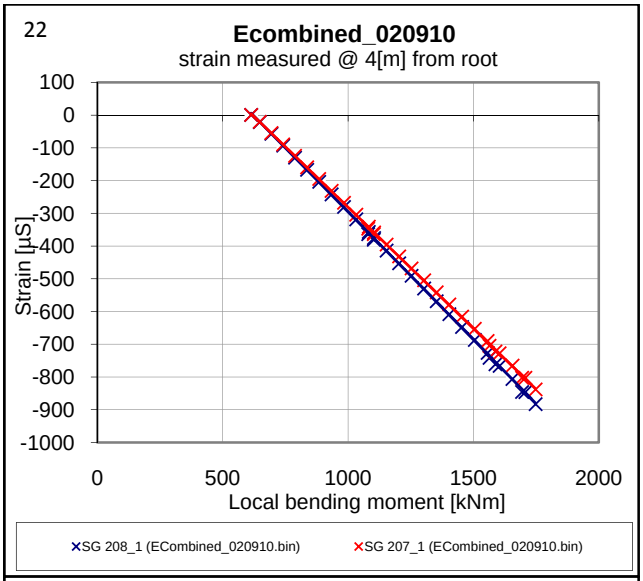

40

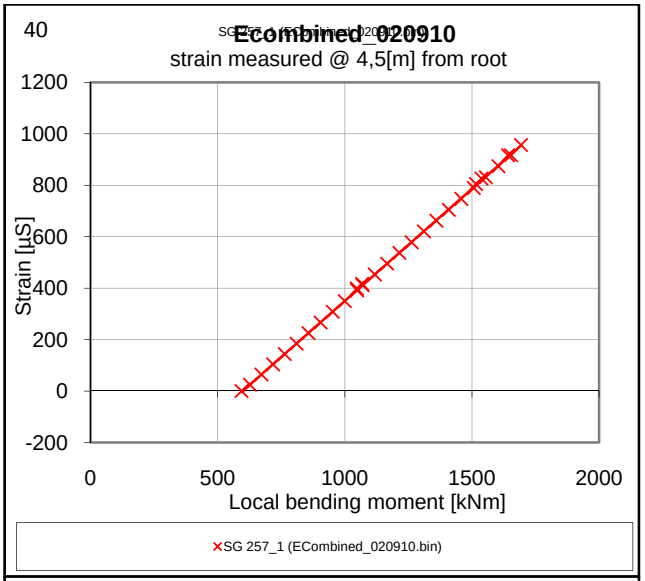

41

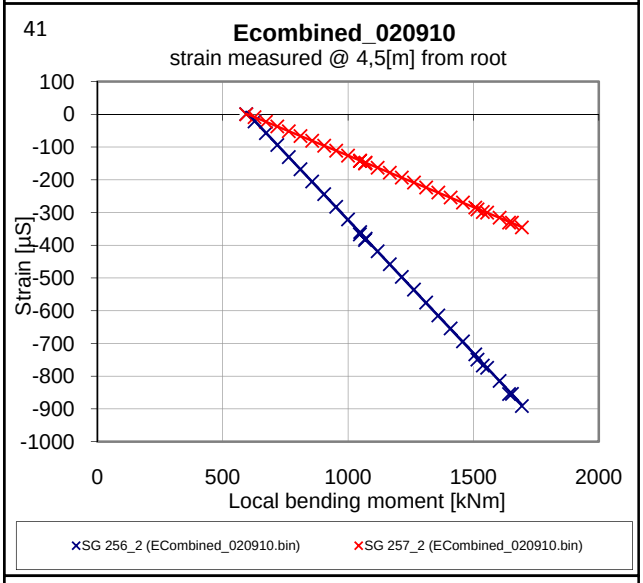

42

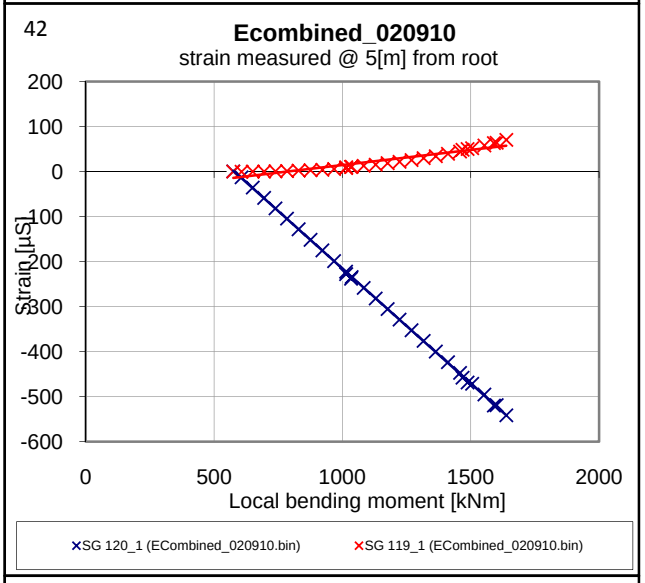

43

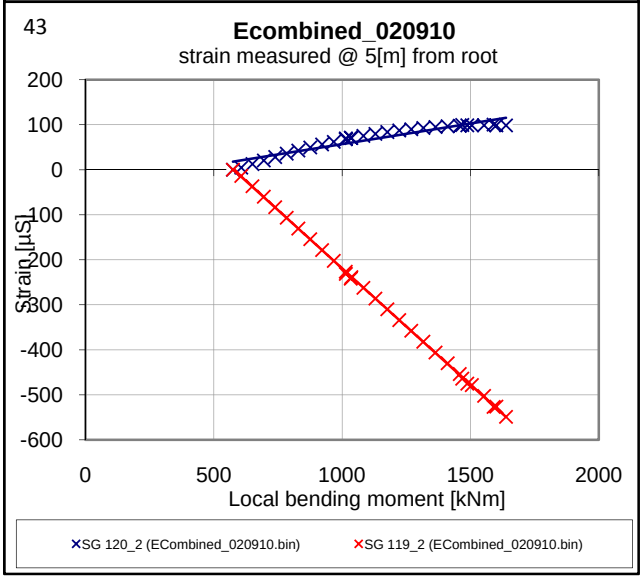

44

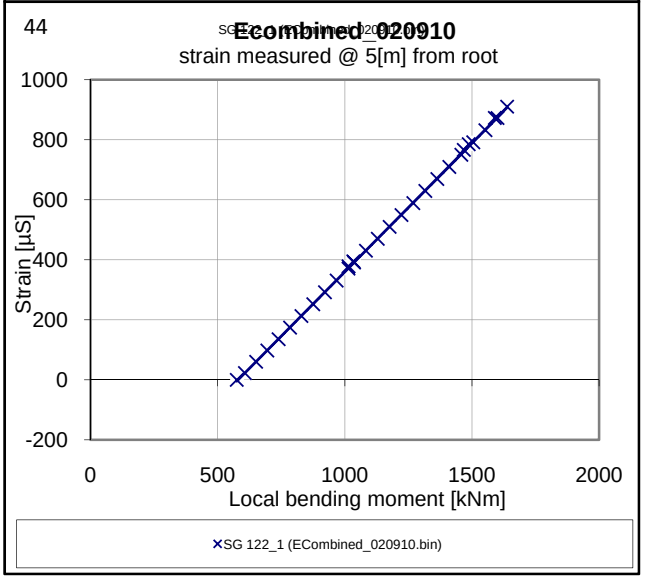

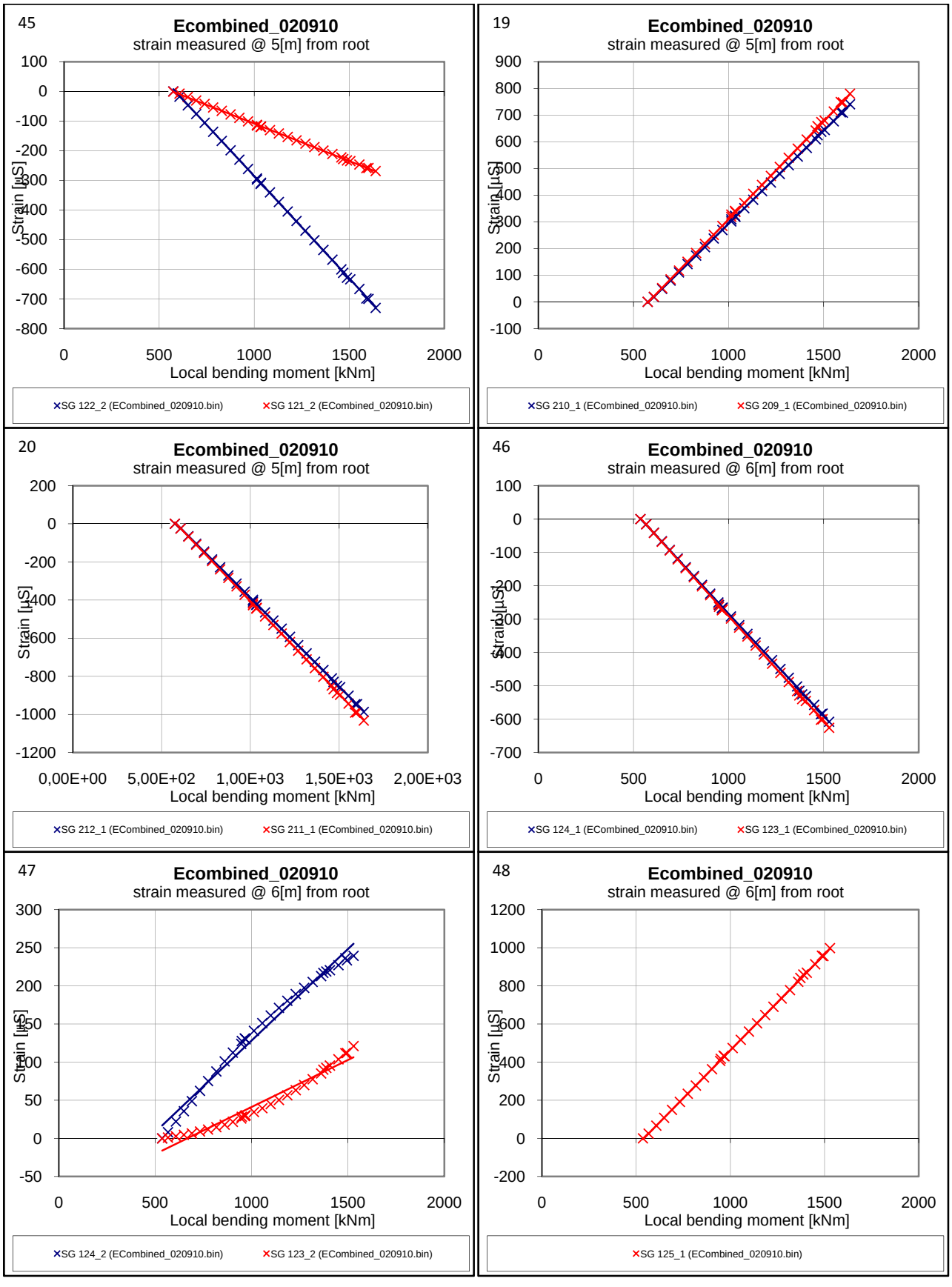
45
Ecombined_020910
strain measured @ 5[m] from root
Strain [µS]
Local bending moment [kNm]
SG 122_2 (ECombined_020910.bin)
SG 121_2 (ECombined_020910.bin)
19
Ecombined_020910
strain measured @ 5[m] from root
Strain [µS]
Local bending moment [kNm]
SG 210_1 (ECombined_020910.bin)
SG 209_1 (ECombined_020910.bin)
20
Ecombined_020910
strain measured @ 5[m] from root
Strain [µS]
Local bending moment [kNm]
SG 212_1 (ECombined_020910.bin)
SG 211_1 (ECombined_020910.bin)
46
Ecombined_020910
strain measured @ 6[m] from root
Strain [µS]
Local bending moment [kNm]
SG 124_1 (ECombined_020910.bin)
SG 123_1 (ECombined_020910.bin)
47
Ecombined_020910
strain measured @ 6[m] from root
Strain [µS]
Local bending moment [kNm]
SG 124_2 (ECombined_020910.bin)
SG 123_2 (ECombined_020910.bin)
48
Ecombined_020910
strain measured @ 6[m] from root
Strain [µS]
Local bending moment [kNm]
SG 125_1 (ECombined_020910.bin)

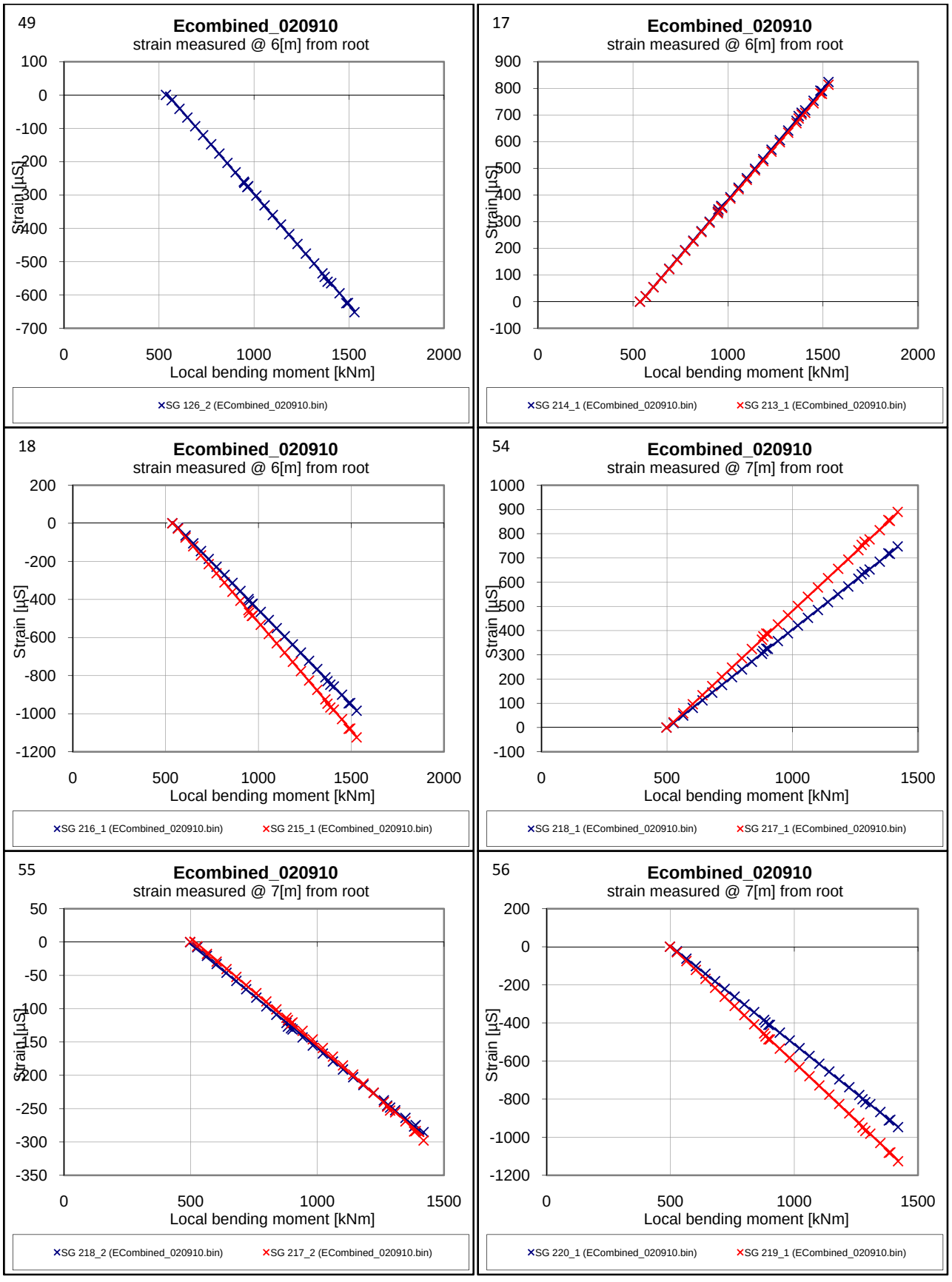
49
Ecombined_020910
strain measured @ 6[m] from root
Strain [µS]
Local bending moment [kNm]
SG 126_2 (ECombined_020910.bin)
17
Ecombined_020910
strain measured @ 6[m] from root
Strain [µS]
Local bending moment [kNm]
SG 214_1 (ECombined_020910.bin)
SG 213_1 (ECombined_020910.bin)
18
Ecombined_020910
strain measured @ 6[m] from root
Strain [µS]
Local bending moment [kNm]
SG 216_1 (ECombined_020910.bin)
SG 215_1 (ECombined_020910.bin)
54
Ecombined_020910
strain measured @ 7[m] from root
Strain [µS]
Local bending moment [kNm]
SG 218_1 (ECombined_020910.bin)
SG 217_1 (ECombined_020910.bin)
55
Ecombined_020910
strain measured @ 7[m] from root
Strain [µS]
Local bending moment [kNm]
SG 218_2 (ECombined_020910.bin)
SG 217_2 (ECombined_020910.bin)
56
Ecombined_020910
strain measured @ 7[m] from root
Strain [µS]
Local bending moment [kNm]
SG 220_1 (ECombined_020910.bin)
SG 219_1 (ECombined_020910.bin)

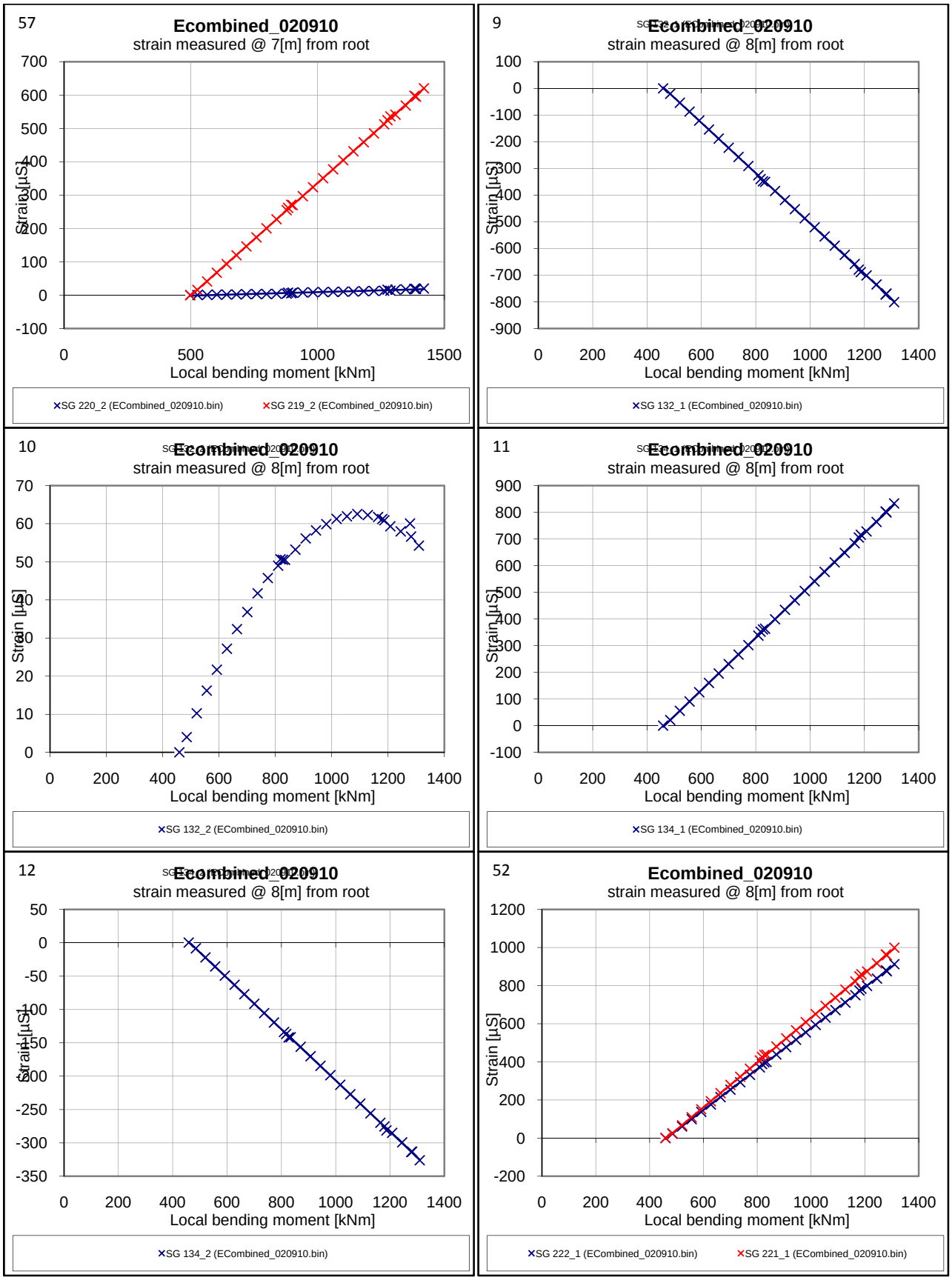
57
Ecombined_020910
strain measured @ 7[m] from root
Strain [µS]
Local bending moment [kNm]
SG 220_2 (ECombined_020910.bin)
SG 219_2 (ECombined_020910.bin)
9
Ecombined_020910
strain measured @ 8[m] from root
Strain [µS]
Local bending moment [kNm]
SG 132_1 (ECombined_020910.bin)
10
Ecombined_020910
strain measured @ 8[m] from root
Strain [µS]
Local bending moment [kNm]
SG 132_2 (ECombined_020910.bin)
11
Ecombined_020910
strain measured @ 8[m] from root
Strain [µS]
Local bending moment [kNm]
SG 134_1 (ECombined_020910.bin)
12
Ecombined_020910
strain measured @ 8[m] from root
Strain [µS]
Local bending moment [kNm]
SG 134_2 (ECombined_020910.bin)
52
Ecombined_020910
strain measured @ 8[m] from root
Strain [µS]
Local bending moment [kNm]
SG 222_1 (ECombined_020910.bin)
SG 221_1 (ECombined_020910.bin)

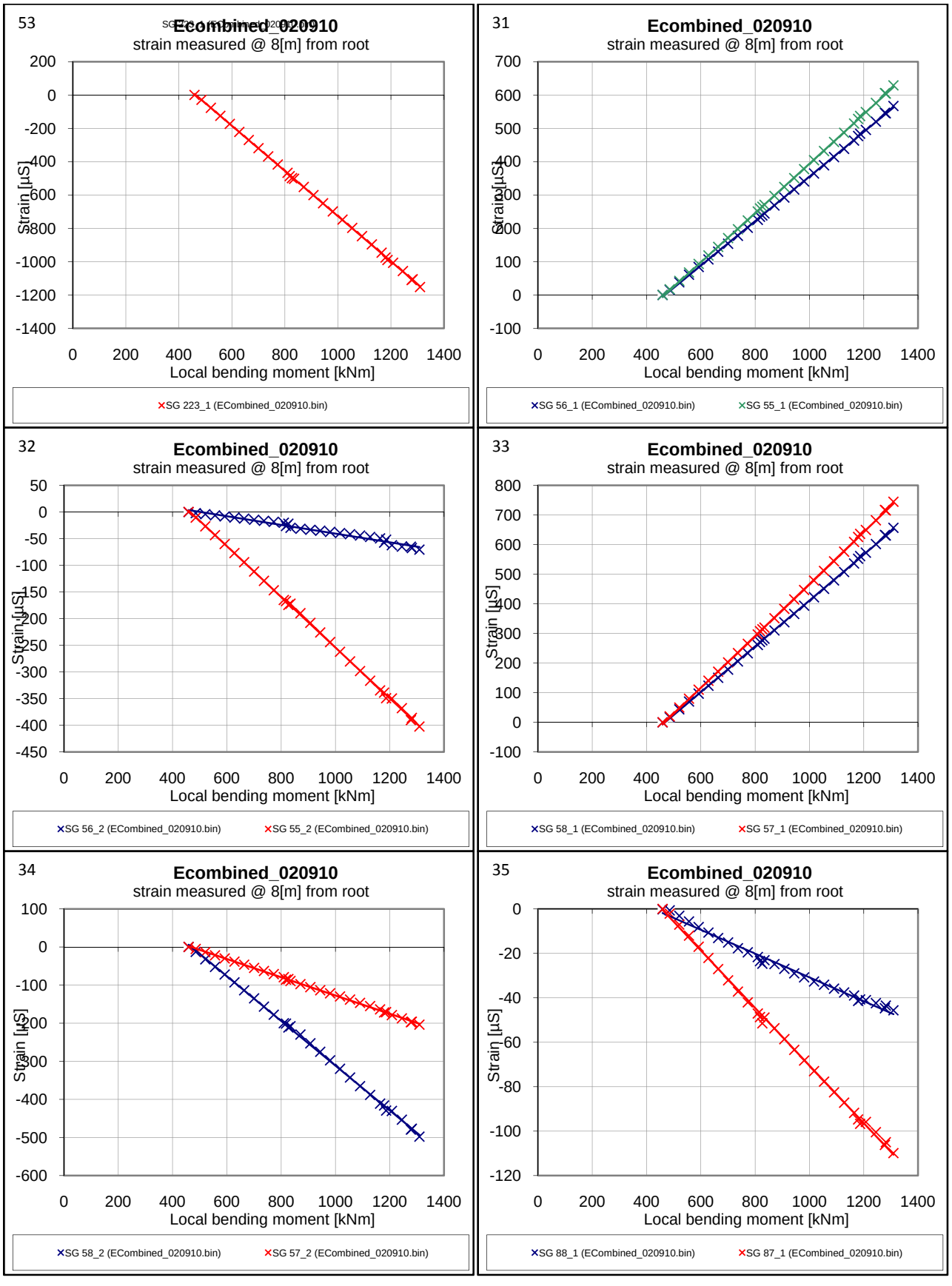
53
Ecombined_020910
strain measured @ 8[m] from root
Strain [µS]
Local bending moment [kNm]
SG 223_1 (ECombined_020910.bin)
31
Ecombined_020910
strain measured @ 8[m] from root
Strain [µS]
Local bending moment [kNm]
SG 56_1 (ECombined_020910.bin)
SG 55_1 (ECombined_020910.bin)
32
Ecombined_020910
strain measured @ 8[m] from root
Strain [µS]
Local bending moment [kNm]
SG 56_2 (ECombined_020910.bin)
SG 55_2 (ECombined_020910.bin)
33
Ecombined_020910
strain measured @ 8[m] from root
Strain [µS]
Local bending moment [kNm]
SG 58_1 (ECombined_020910.bin)
SG 57_1 (ECombined_020910.bin)
34
Ecombined_020910
strain measured @ 8[m] from root
Strain [µS]
Local bending moment [kNm]
SG 58_2 (ECombined_020910.bin)
SG 57_2 (ECombined_020910.bin)
35
Ecombined_020910
strain measured @ 8[m] from root
Strain [µS]
Local bending moment [kNm]
SG 88_1 (ECombined_020910.bin)
SG 87_1 (ECombined_020910.bin)

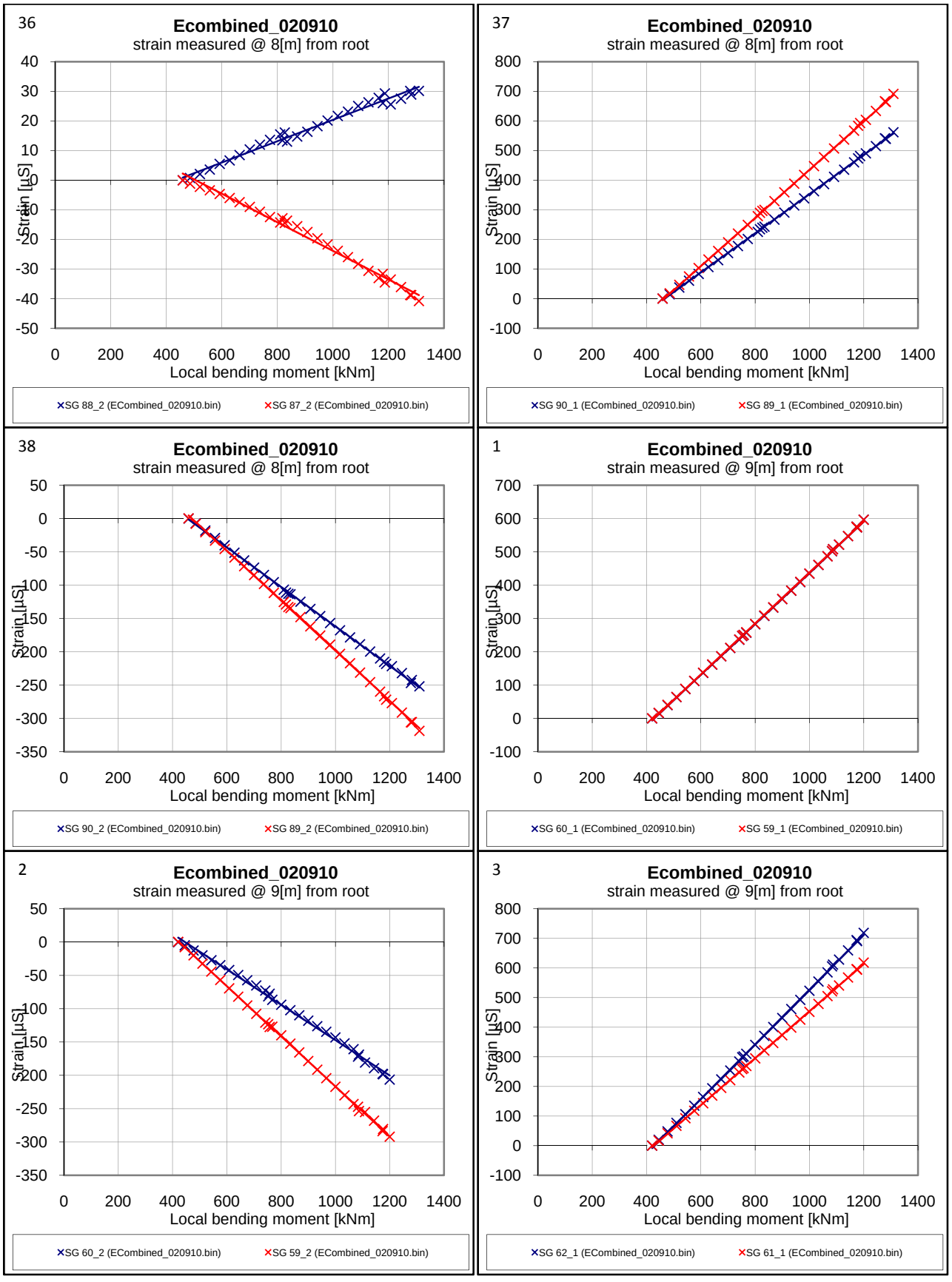
36
Ecombined_020910
strain measured @ 8[m] from root
Strain [µS]
Local bending moment [kNm]
SG 88_2 (ECombined_020910.bin)
SG 87_2 (ECombined_020910.bin)
37
Ecombined_020910
strain measured @ 8[m] from root
Strain [µS]
Local bending moment [kNm]
SG 90_1 (ECombined_020910.bin)
SG 89_1 (ECombined_020910.bin)
38
Ecombined_020910
strain measured @ 8[m] from root
Strain [µS]
Local bending moment [kNm]
SG 90_2 (ECombined_020910.bin)
SG 89_2 (ECombined_020910.bin)
1
Ecombined_020910
strain measured @ 9[m] from root
Strain [µS]
Local bending moment [kNm]
SG 60_1 (ECombined_020910.bin)
SG 59_1 (ECombined_020910.bin)
2
Ecombined_020910
strain measured @ 9[m] from root
Strain [µS]
Local bending moment [kNm]
SG 60_2 (ECombined_020910.bin)
SG 59_2 (ECombined_020910.bin)
3
Ecombined_020910
strain measured @ 9[m] from root
Strain [µS]
Local bending moment [kNm]
SG 62_1 (ECombined_020910.bin)
SG 61_1 (ECombined_020910.bin)

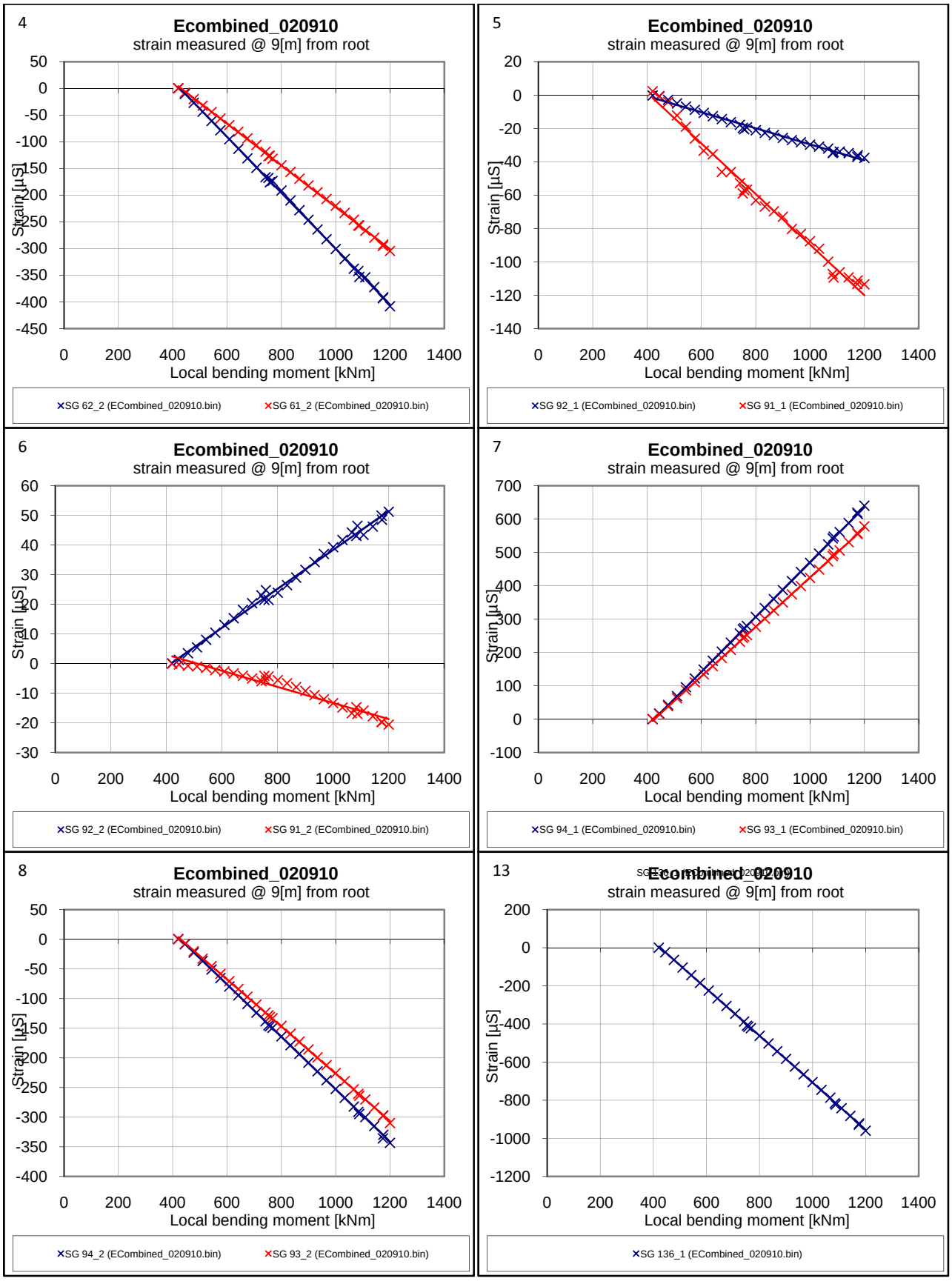
4
Ecombined_020910
strain measured @ 9[m] from root
Strain [µS]
Local bending moment [kNm]
SG 62_2 (ECombined_020910.bin)
SG 61_2 (ECombined_020910.bin)
5
Ecombined_020910
strain measured @ 9[m] from root
Strain [µS]
Local bending moment [kNm]
SG 92_1 (ECombined_020910.bin)
SG 91_1 (ECombined_020910.bin)
6
Ecombined_020910
strain measured @ 9[m] from root
Strain [µS]
Local bending moment [kNm]
SG 92_2 (ECombined_020910.bin)
SG 91_2 (ECombined_020910.bin)
7
Ecombined_020910
strain measured @ 9[m] from root
Strain [µS]
Local bending moment [kNm]
SG 94_1 (ECombined_020910.bin)
SG 93_1 (ECombined_020910.bin)
8
Ecombined_020910
strain measured @ 9[m] from root
Strain [µS]
Local bending moment [kNm]
SG 94_2 (ECombined_020910.bin)
SG 93_2 (ECombined_020910.bin)
13
Ecombined_020910
strain measured @ 9[m] from root
Strain [µS]
Local bending moment [kNm]
SG 136_1 (ECombined_020910.bin)

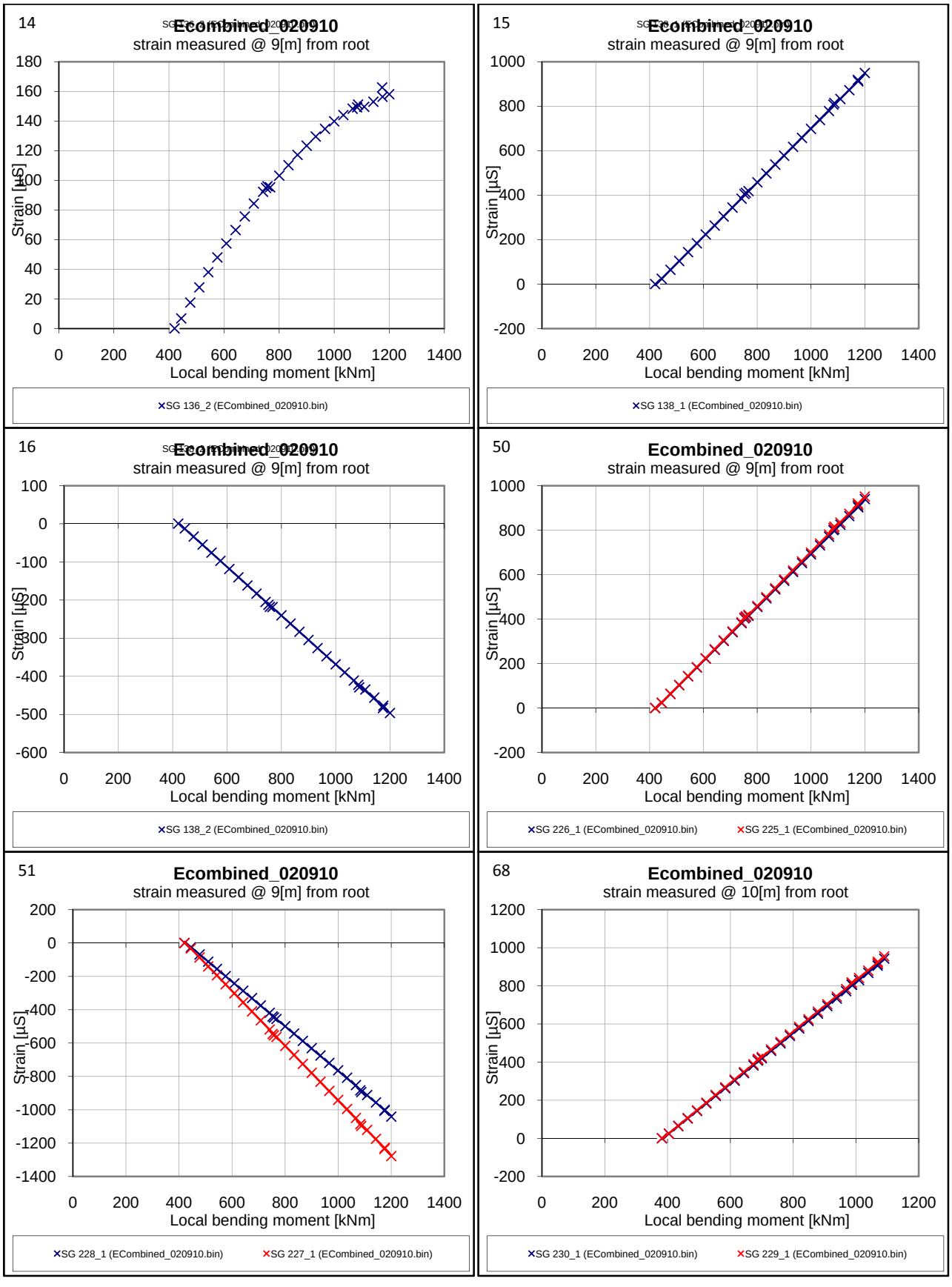
14
Ecombined_020910
strain measured @ 9[m] from root
Strain [µS]
Local bending moment [kNm]
SG 136_2 (ECombined_020910.bin)
15
Ecombined_020910
strain measured @ 9[m] from root
Strain [µS]
Local bending moment [kNm]
SG 138_1 (ECombined_020910.bin)
16
Ecombined_020910
strain measured @ 9[m] from root
Strain [µS]
Local bending moment [kNm]
SG 138_2 (ECombined_020910.bin)
50
Ecombined_020910
strain measured @ 9[m] from root
Strain [µS]
Local bending moment [kNm]
SG 226_1 (ECombined_020910.bin)
SG 225_1 (ECombined_020910.bin)
51
Ecombined_020910
strain measured @ 9[m] from root
Strain [µS]
Local bending moment [kNm]
SG 228_1 (ECombined_020910.bin)
SG 227_1 (ECombined_020910.bin)
68
Ecombined_020910
strain measured @ 10[m] from root
Strain [µS]
Local bending moment [kNm]
SG 230_1 (ECombined_020910.bin)
SG 229_1 (ECombined_020910.bin)

69

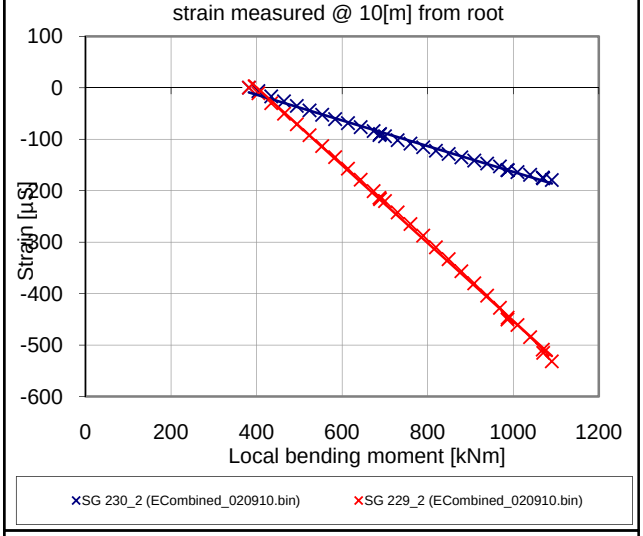

70

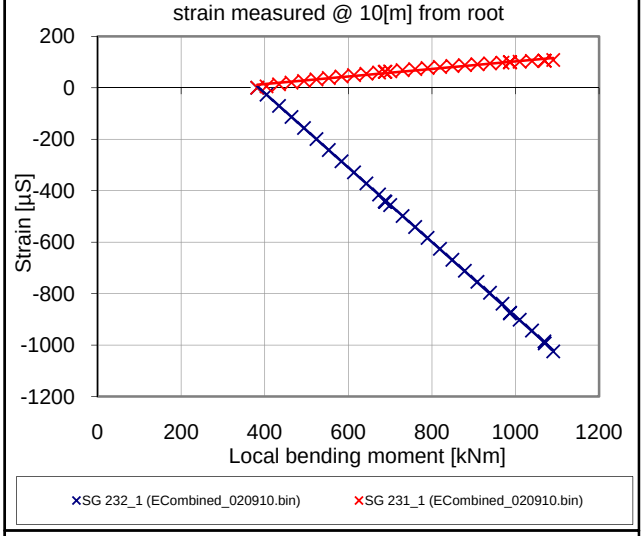

71

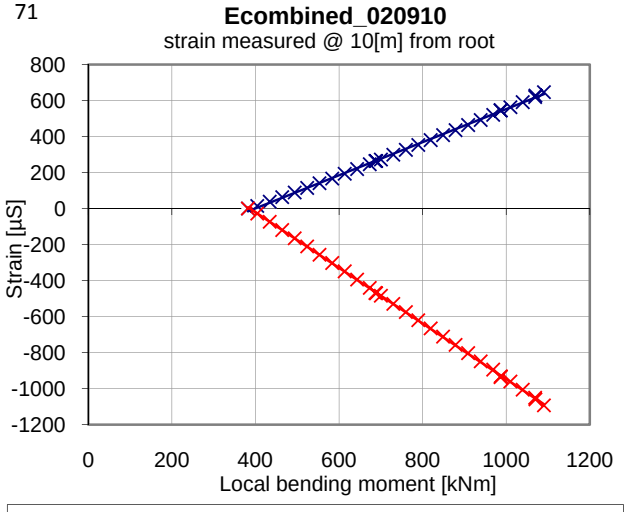

72

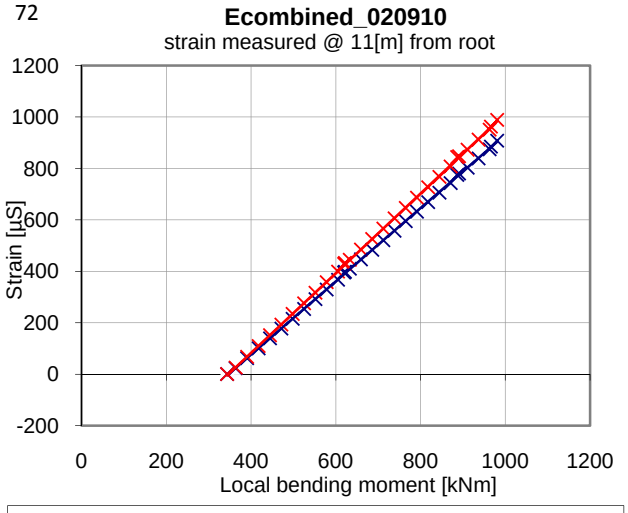

73

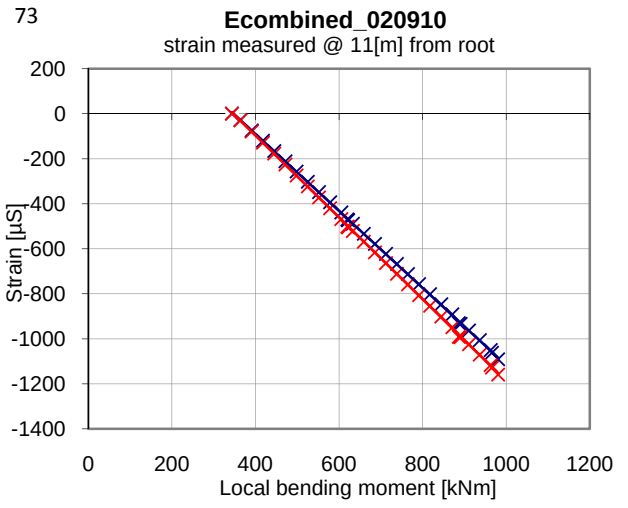

74

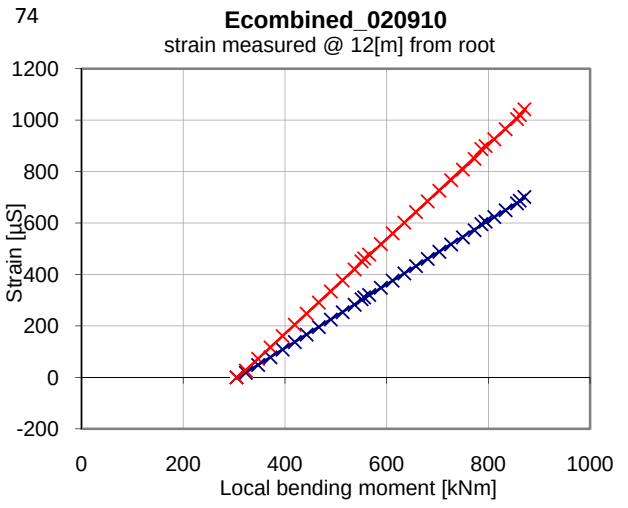

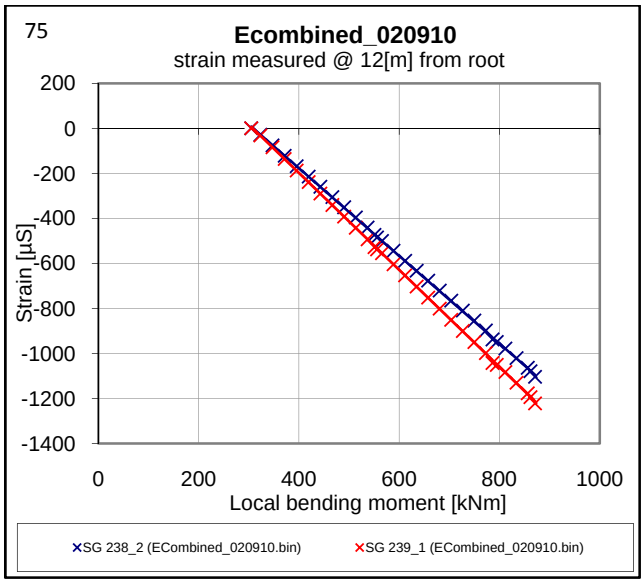
75
Ecombined_020910
strain measured @ 12[m] from root
200
0
-200
-400
-600
-800
-1000
-1200
-1400
Strain [µS]
0
200
400
600
800
1000
Local bending moment [kNm]
SG 238_2 (ECombined_020910.bin)
SG 239_1 (ECombined_020910.bin)

B.2.a Measurement of pull at 35% Risø load (Main section)

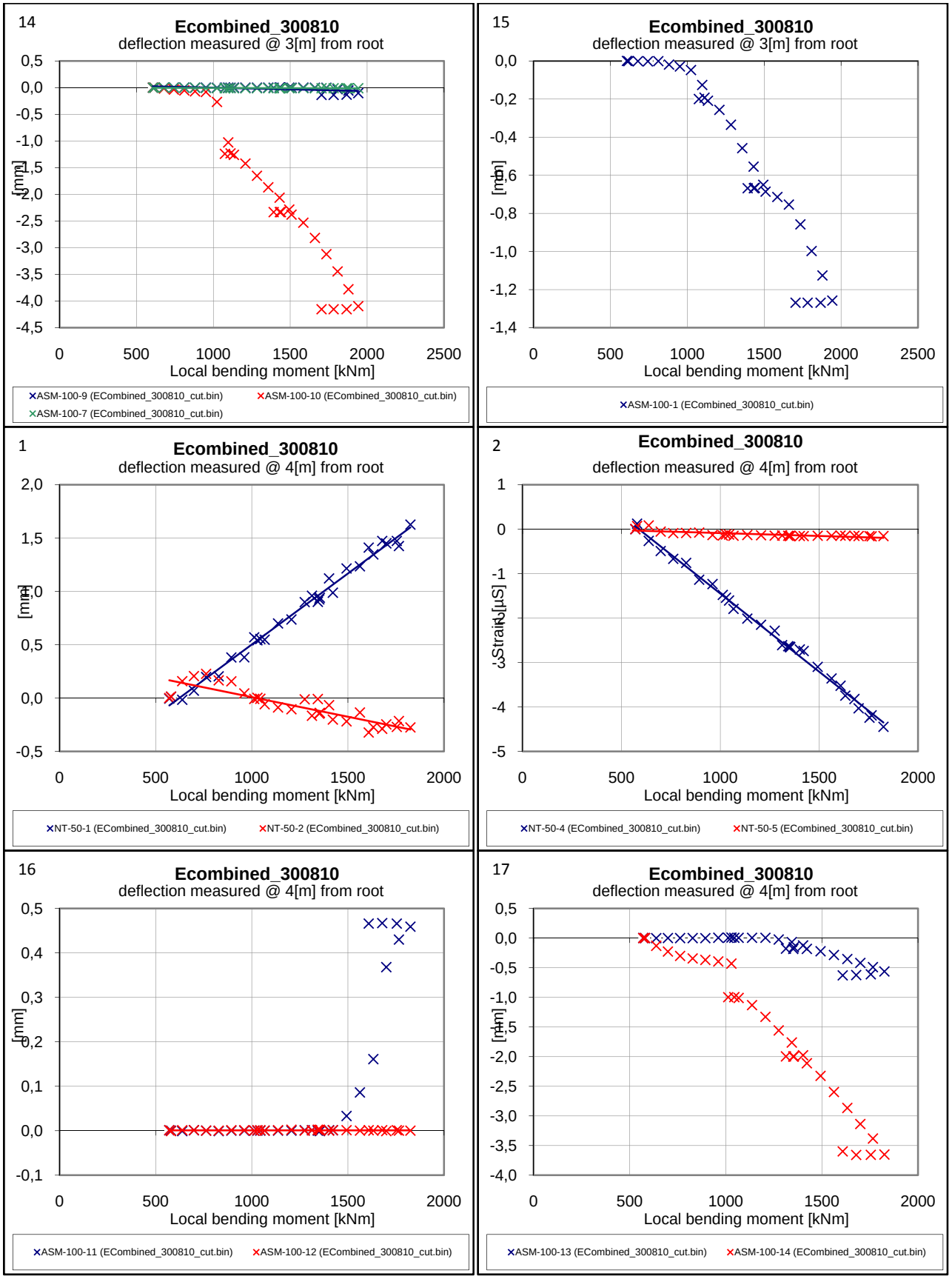

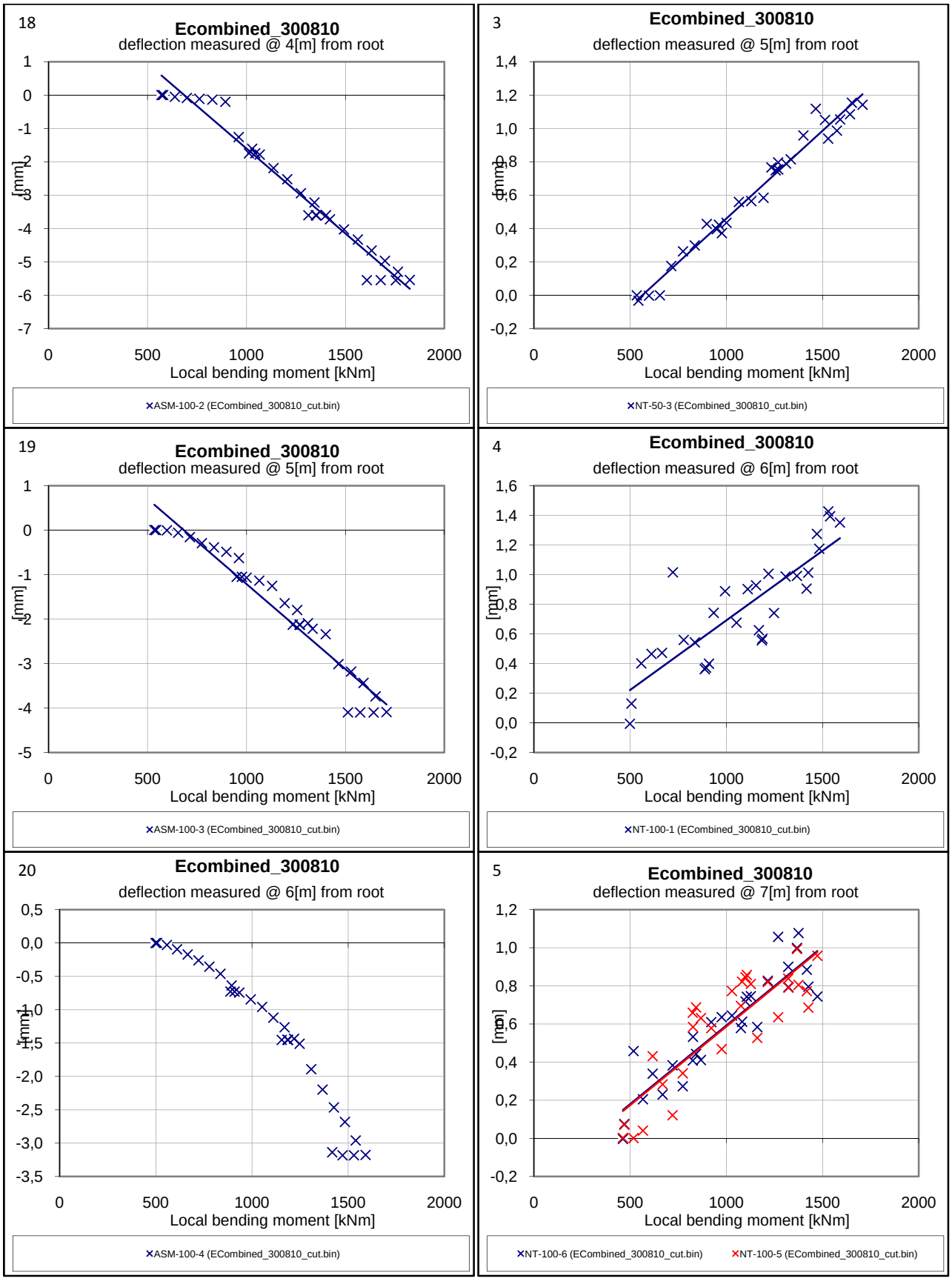
18
Ecombined_300810
deflection measured @ 4[m] from root
[mm]
Local bending moment [kNm]
ASM-100-2 (ECombined_300810_cut.bin)
3
Ecombined_300810
deflection measured @ 5[m] from root
[mm]
Local bending moment [kNm]
NT-50-3 (ECombined_300810_cut.bin)
19
Ecombined_300810
deflection measured @ 5[m] from root
[mm]
Local bending moment [kNm]
ASM-100-3 (ECombined_300810_cut.bin)
4
Ecombined_300810
deflection measured @ 6[m] from root
[mm]
Local bending moment [kNm]
NT-100-1 (ECombined_300810_cut.bin)
20
Ecombined_300810
deflection measured @ 6[m] from root
[mm]
Local bending moment [kNm]
ASM-100-4 (ECombined_300810_cut.bin)
5
Ecombined_300810
deflection measured @ 7[m] from root
[mm]
Local bending moment [kNm]
NT-100-6 (ECombined_300810_cut.bin)
NT-100-5 (ECombined_300810_cut.bin)

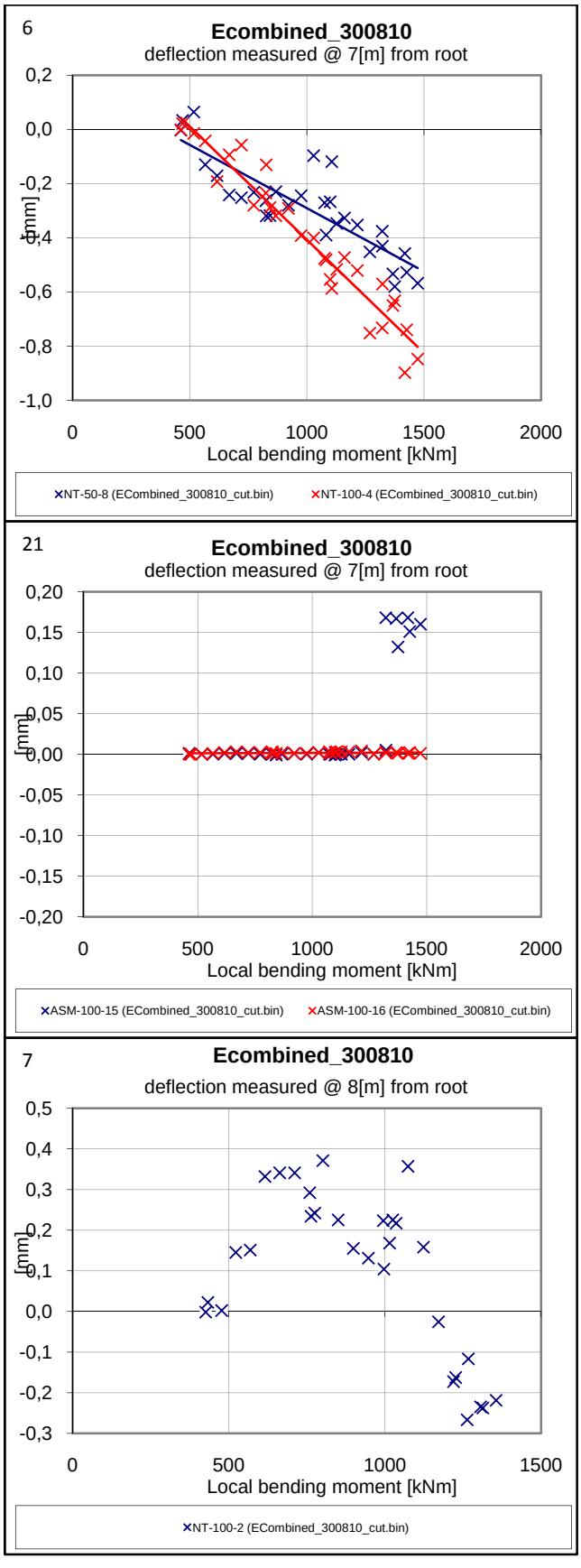
6
Ecombined_300810
deflection measured @ 7[m] from root
[mm]
Local bending moment [kNm]
NT-50-8 (ECombined_300810_cut.bin)
NT-100-4 (ECombined_300810_cut.bin)
22
Ecombined_300810
deflection measured @ 7[m] from root
[mm]
Local bending moment [kNm]
ASM-100-17 (ECombined_300810_cut.bin)
ASM-100-18 (ECombined_300810_cut.bin)
21
Ecombined_300810
deflection measured @ 7[m] from root
[mm]
Local bending moment [kNm]
ASM-100-15 (ECombined_300810_cut.bin)
ASM-100-16 (ECombined_300810_cut.bin)
23
Ecombined_300810
deflection measured @ 7[m] from root
[mm]
Local bending moment [kNm]
ASM-100-5 (ECombined_300810_cut.bin)
7
Ecombined_300810
deflection measured @ 8[m] from root
[mm]
Local bending moment [kNm]
NT-100-2 (ECombined_300810_cut.bin)
8
Ecombined_300810
deflection measured @ 9[m] from root
[mm]
Local bending moment [kNm]
NT-100-3 (ECombined_300810_cut.bin)

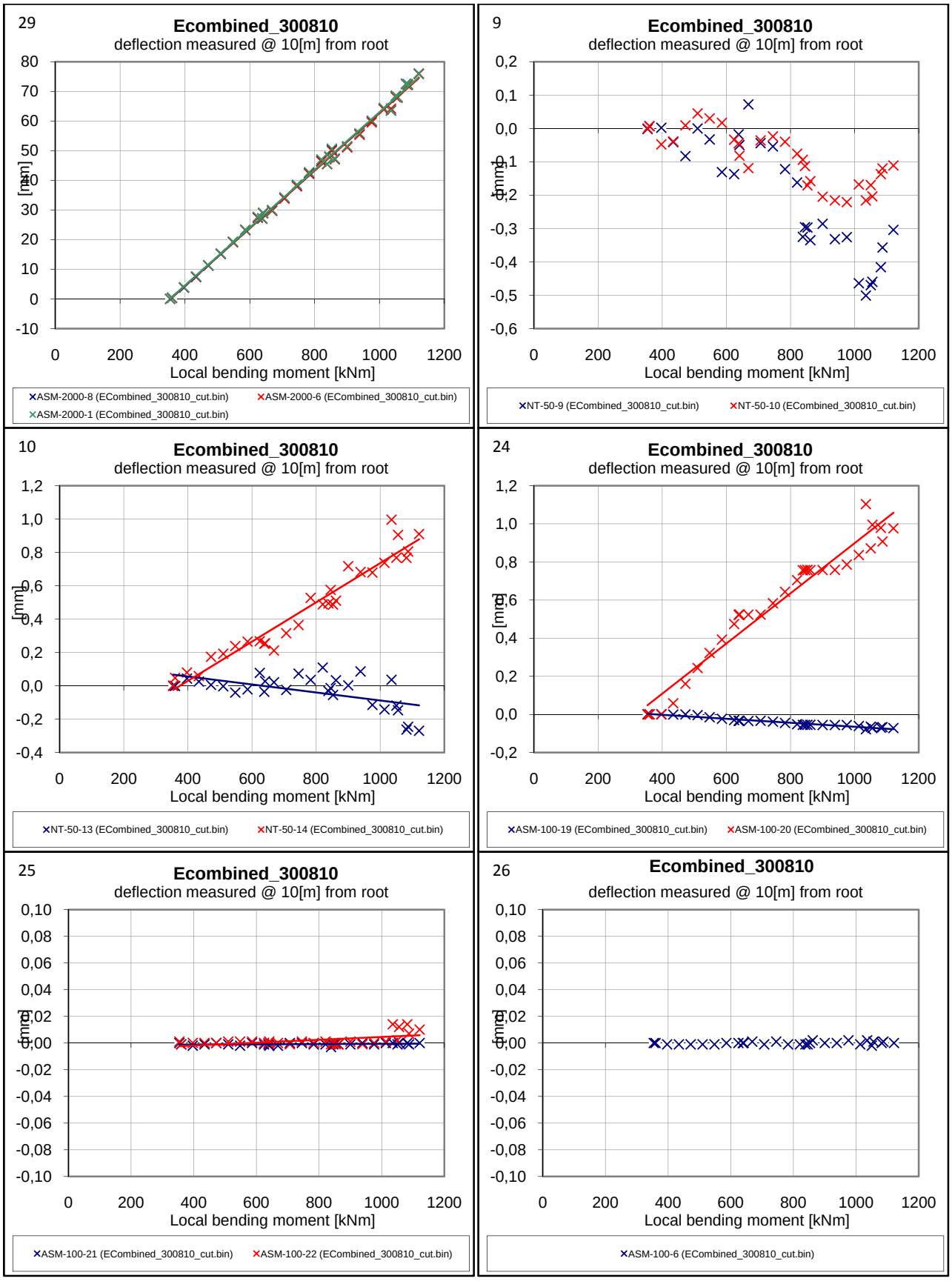
29
Ecombined_300810
deflection measured @ 10[m] from root
[mm]
Local bending moment [kNm]
ASM-2000-8 (ECombined_300810_cut.bin)
ASM-2000-6 (ECombined_300810_cut.bin)
ASM-2000-1 (ECombined_300810_cut.bin)
9
Ecombined_300810
deflection measured @ 10[m] from root
[mm]
Local bending moment [kNm]
NT-50-9 (ECombined_300810_cut.bin)
NT-50-10 (ECombined_300810_cut.bin)
10
Ecombined_300810
deflection measured @ 10[m] from root
[mm]
Local bending moment [kNm]
NT-50-13 (ECombined_300810_cut.bin)
NT-50-14 (ECombined_300810_cut.bin)
24
Ecombined_300810
deflection measured @ 10[m] from root
[mm]
Local bending moment [kNm]
ASM-100-19 (ECombined_300810_cut.bin)
ASM-100-20 (ECombined_300810_cut.bin)
25
Ecombined_300810
deflection measured @ 10[m] from root
[mm]
Local bending moment [kNm]
ASM-100-21 (ECombined_300810_cut.bin)
ASM-100-22 (ECombined_300810_cut.bin)
26
Ecombined_300810
deflection measured @ 10[m] from root
[mm]
Local bending moment [kNm]
ASM-100-6 (ECombined_300810_cut.bin)

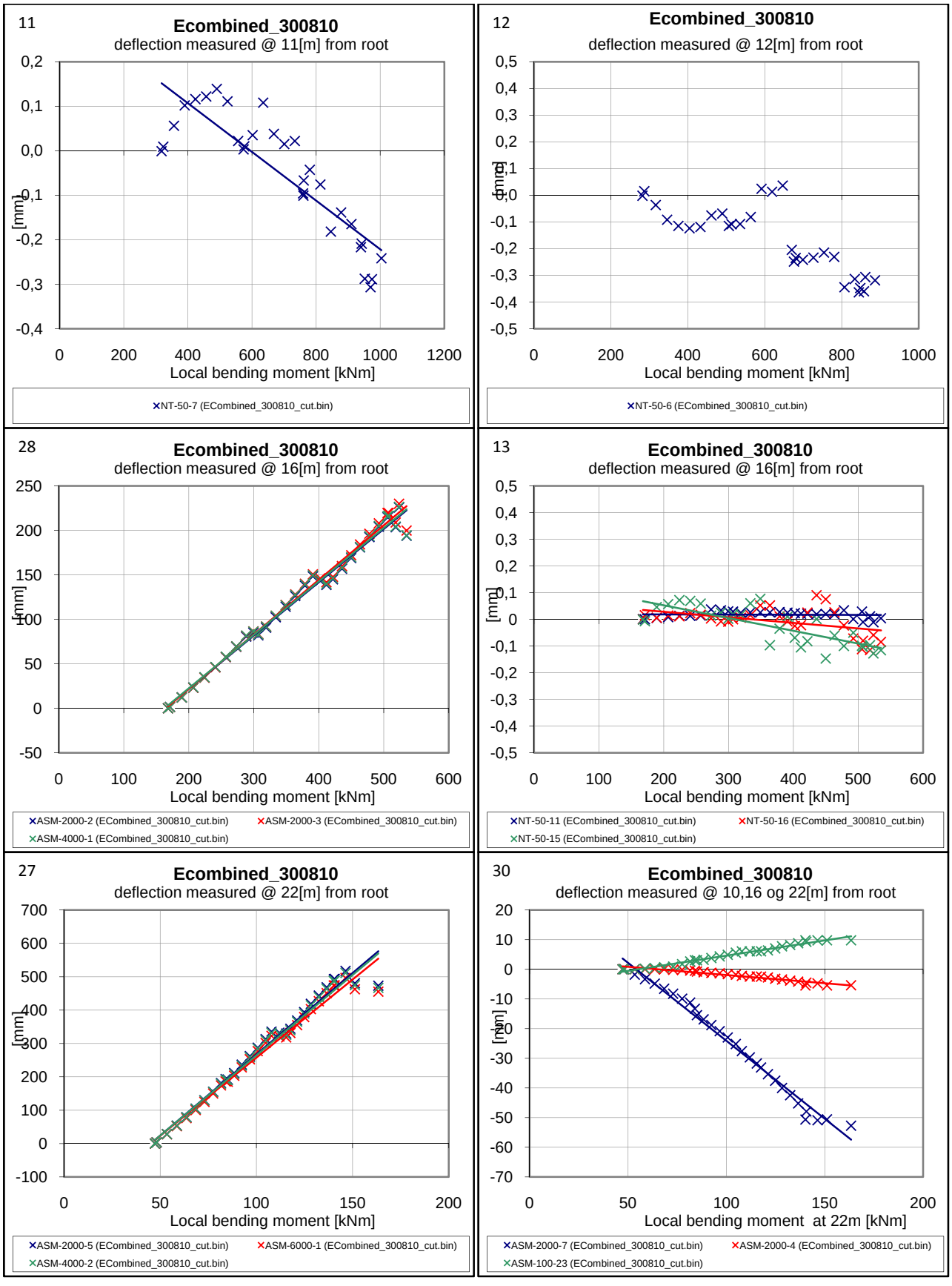
11
Ecombined_300810
deflection measured @ 11[m] from root
[mm]
Local bending moment [kNm]
NT-50-7 (ECombined_300810_cut.bin)
12
Ecombined_300810
deflection measured @ 12[m] from root
[mm]
Local bending moment [kNm]
NT-50-6 (ECombined_300810_cut.bin)
28
Ecombined_300810
deflection measured @ 16[m] from root
[mm]
Local bending moment [kNm]
ASM-2000-2 (ECombined_300810_cut.bin)
ASM-2000-3 (ECombined_300810_cut.bin)
ASM-4000-1 (ECombined_300810_cut.bin)
13
Ecombined_300810
deflection measured @ 16[m] from root
[mm]
Local bending moment [kNm]
NT-50-11 (ECombined_300810_cut.bin)
NT-50-16 (ECombined_300810_cut.bin)
NT-50-15 (ECombined_300810_cut.bin)
27
Ecombined_300810
deflection measured @ 22[m] from root
[mm]
Local bending moment [kNm]
ASM-2000-5 (ECombined_300810_cut.bin)
ASM-6000-1 (ECombined_300810_cut.bin)
ASM-4000-2 (ECombined_300810_cut.bin)
30
Ecombined_300810
deflection measured @ 10,16 og 22[m] from root
[mm]
Local bending moment at 22m [kNm]
ASM-2000-7 (ECombined_300810_cut.bin)
ASM-2000-4 (ECombined_300810_cut.bin)
ASM-100-23 (ECombined_300810_cut.bin)

B.2.b Measurement of pull at 35% Risø load (AED section)

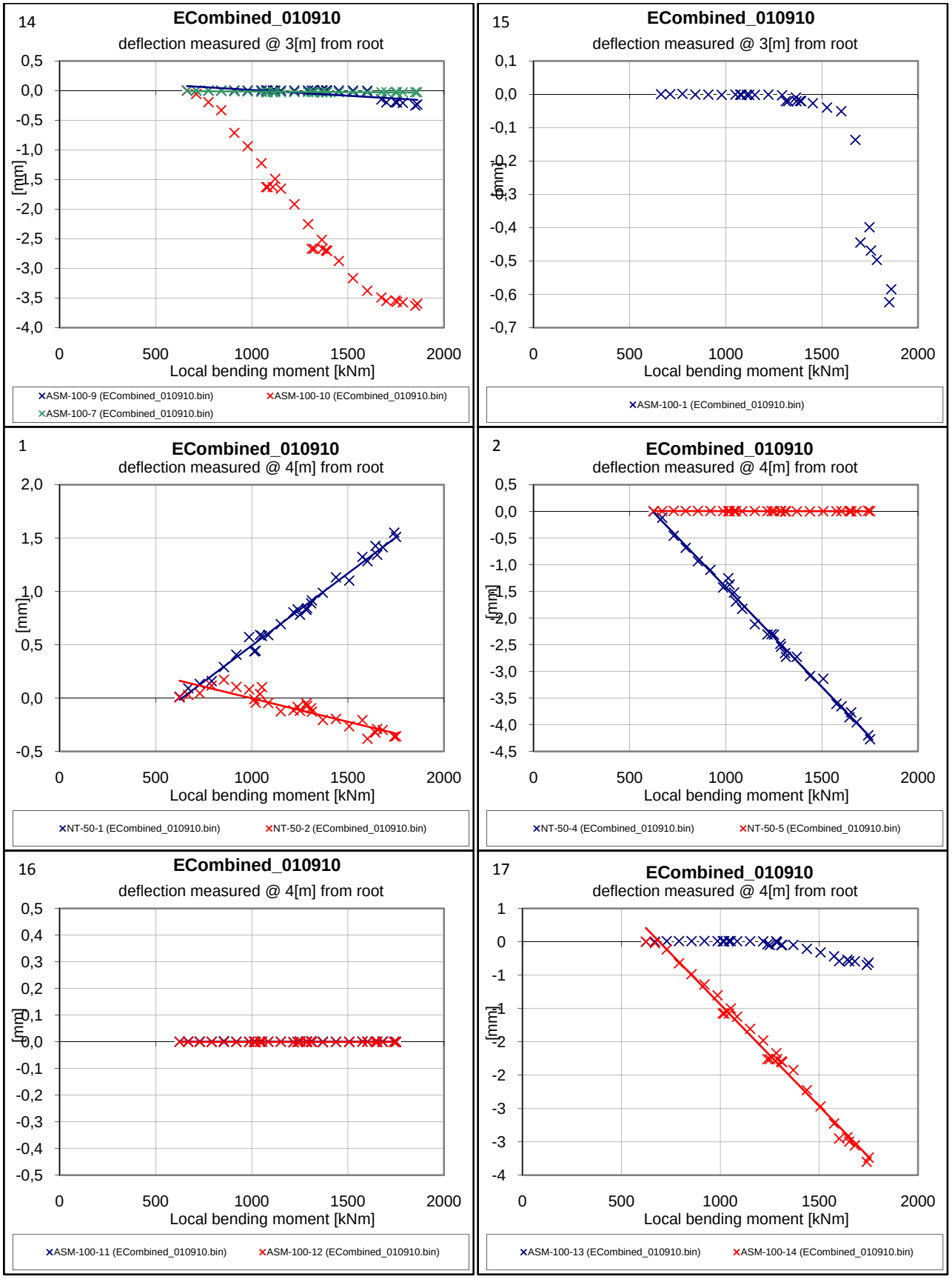

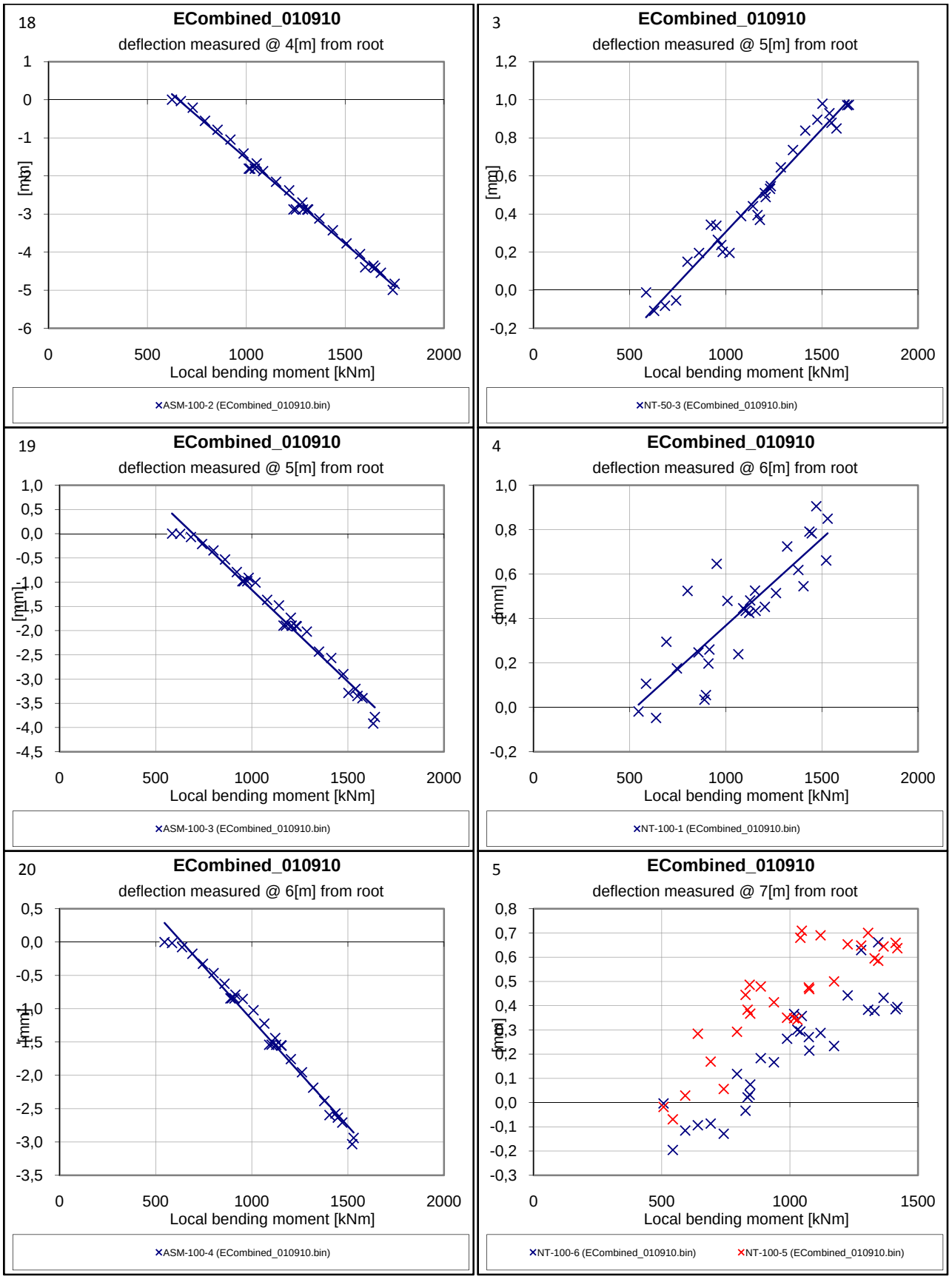
18
ECombined_010910
deflection measured @ 4[m] from root
[mm]
Local bending moment [kNm]
ASM-100-2 (ECombined_010910.bin)
3
ECombined_010910
deflection measured @ 5[m] from root
[mm]
Local bending moment [kNm]
NT-50-3 (ECombined_010910.bin)
19
ECombined_010910
deflection measured @ 5[m] from root
[mm]
Local bending moment [kNm]
ASM-100-3 (ECombined_010910.bin)
4
ECombined_010910
deflection measured @ 6[m] from root
[mm]
Local bending moment [kNm]
NT-100-1 (ECombined_010910.bin)
20
ECombined_010910
deflection measured @ 6[m] from root
[mm]
Local bending moment [kNm]
ASM-100-4 (ECombined_010910.bin)
5
ECombined_010910
deflection measured @ 7[m] from root
[mm]
Local bending moment [kNm]
NT-100-6 (ECombined_010910.bin)
NT-100-5 (ECombined_010910.bin)

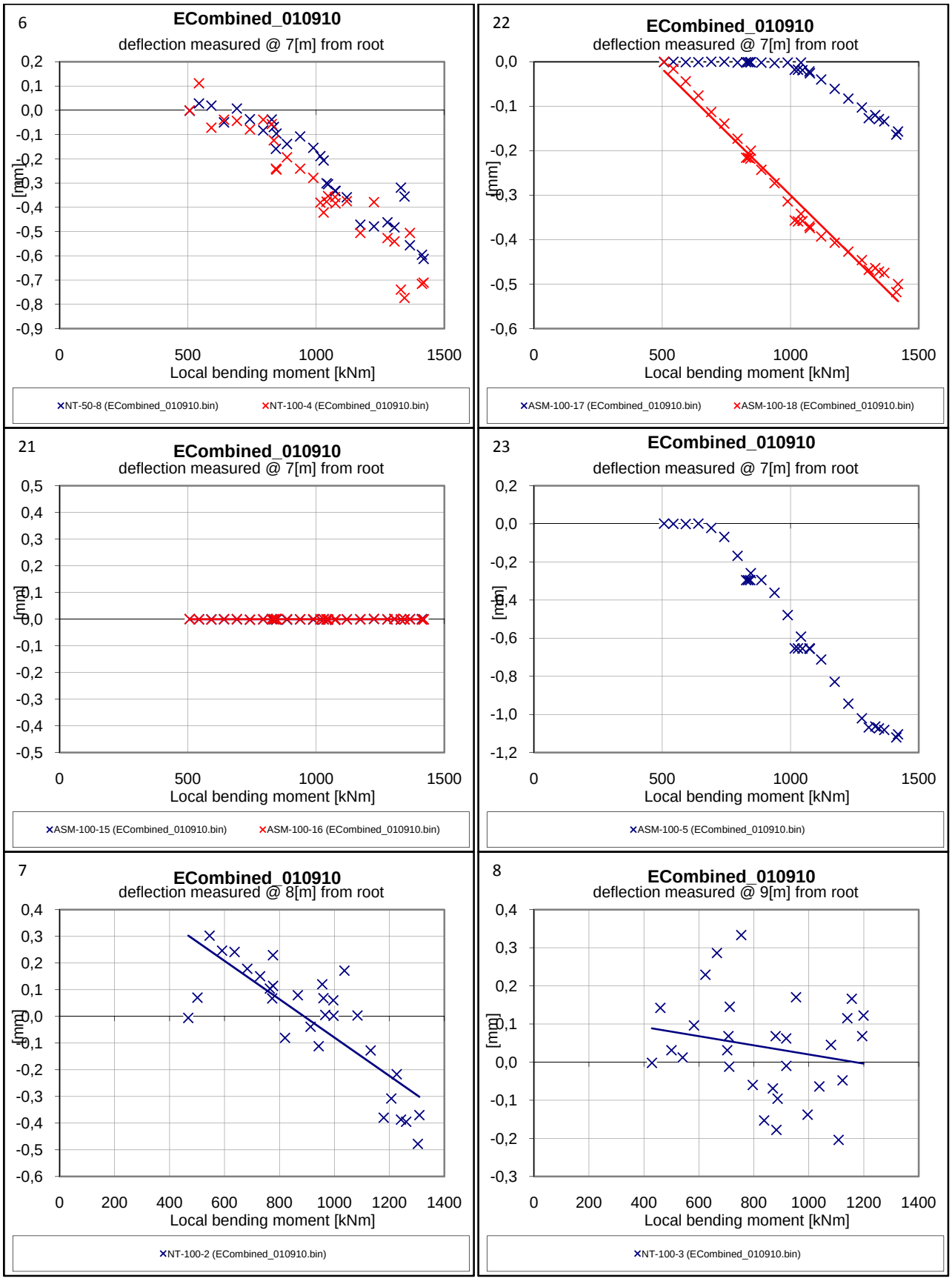
6
ECombined_010910
deflection measured @ 7[m] from root
[mm]
Local bending moment [kNm]
NT-50-8 (ECombined_010910.bin)
NT-100-4 (ECombined_010910.bin)
22
ECombined_010910
deflection measured @ 7[m] from root
[mm]
Local bending moment [kNm]
ASM-100-17 (ECombined_010910.bin)
ASM-100-18 (ECombined_010910.bin)
21
ECombined_010910
deflection measured @ 7[m] from root
[mm]
Local bending moment [kNm]
ASM-100-15 (ECombined_010910.bin)
ASM-100-16 (ECombined_010910.bin)
23
ECombined_010910
deflection measured @ 7[m] from root
[mm]
Local bending moment [kNm]
ASM-100-5 (ECombined_010910.bin)
7
ECombined_010910
deflection measured @ 8[m] from root
[mm]
Local bending moment [kNm]
NT-100-2 (ECombined_010910.bin)
8
ECombined_010910
deflection measured @ 9[m] from root
[mm]
Local bending moment [kNm]
NT-100-3 (ECombined_010910.bin)

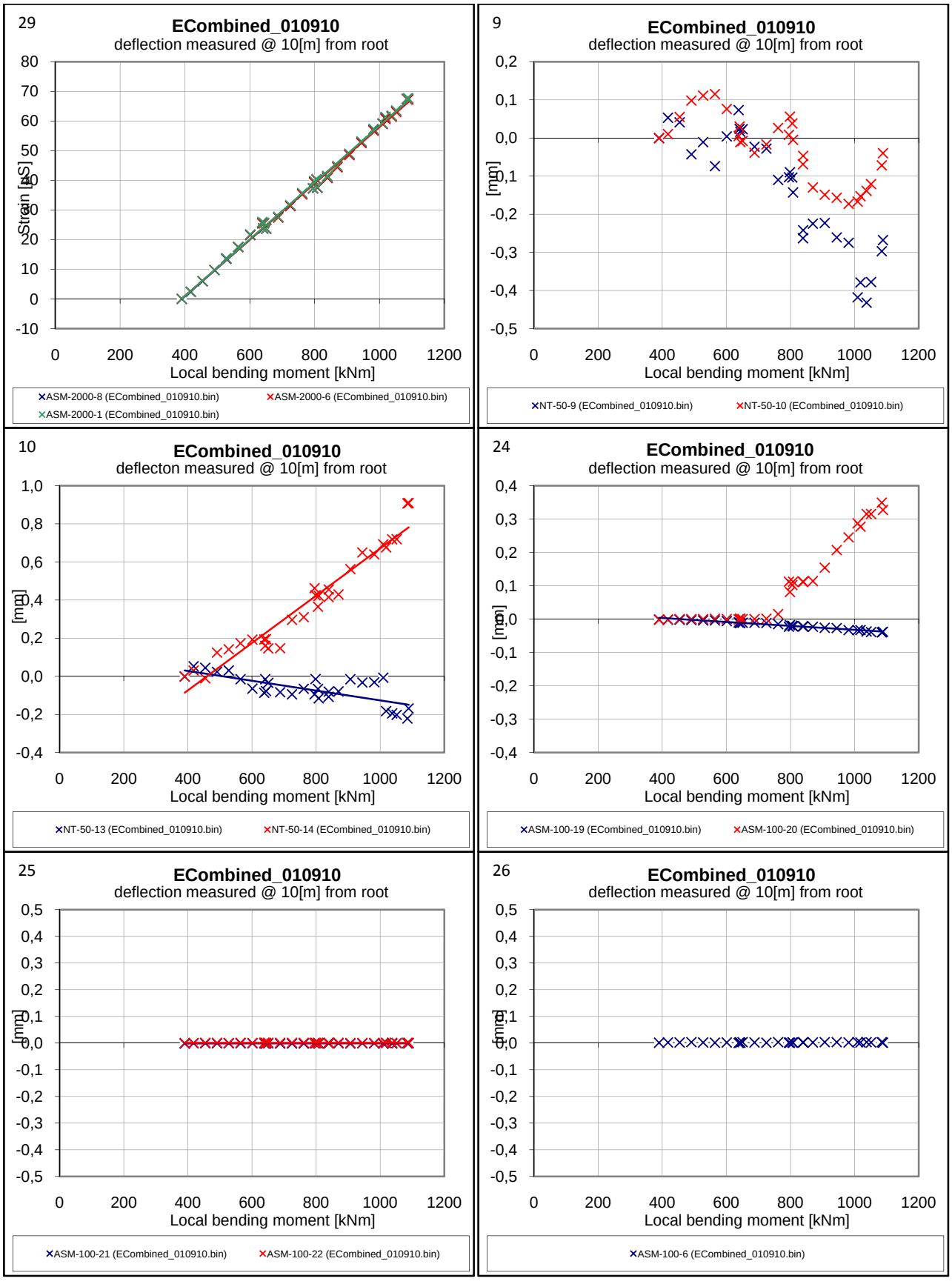
29
ECombined_010910
deflection measured @ 10[m] from root
Strain [µS]
Local bending moment [kNm]
ASM-2000-8 (ECombined_010910.bin)
ASM-2000-6 (ECombined_010910.bin)
ASM-2000-1 (ECombined_010910.bin)
9
ECombined_010910
deflection measured @ 10[m] from root
[mm]
Local bending moment [kNm]
NT-50-9 (ECombined_010910.bin)
NT-50-10 (ECombined_010910.bin)
10
ECombined_010910
deflecton measured @ 10[m] from root
[mm]
Local bending moment [kNm]
NT-50-13 (ECombined_010910.bin)
NT-50-14 (ECombined_010910.bin)
24
ECombined_010910
deflection measured @ 10[m] from root
[mm]
Local bending moment [kNm]
ASM-100-19 (ECombined_010910.bin)
ASM-100-20 (ECombined_010910.bin)
25
ECombined_010910
deflection measured @ 10[m] from root
[mm]
Local bending moment [kNm]
ASM-100-21 (ECombined_010910.bin)
ASM-100-22 (ECombined_010910.bin)
26
ECombined_010910
deflection measured @ 10[m] from root
[mm]
Local bending moment [kNm]
ASM-100-6 (ECombined_010910.bin)

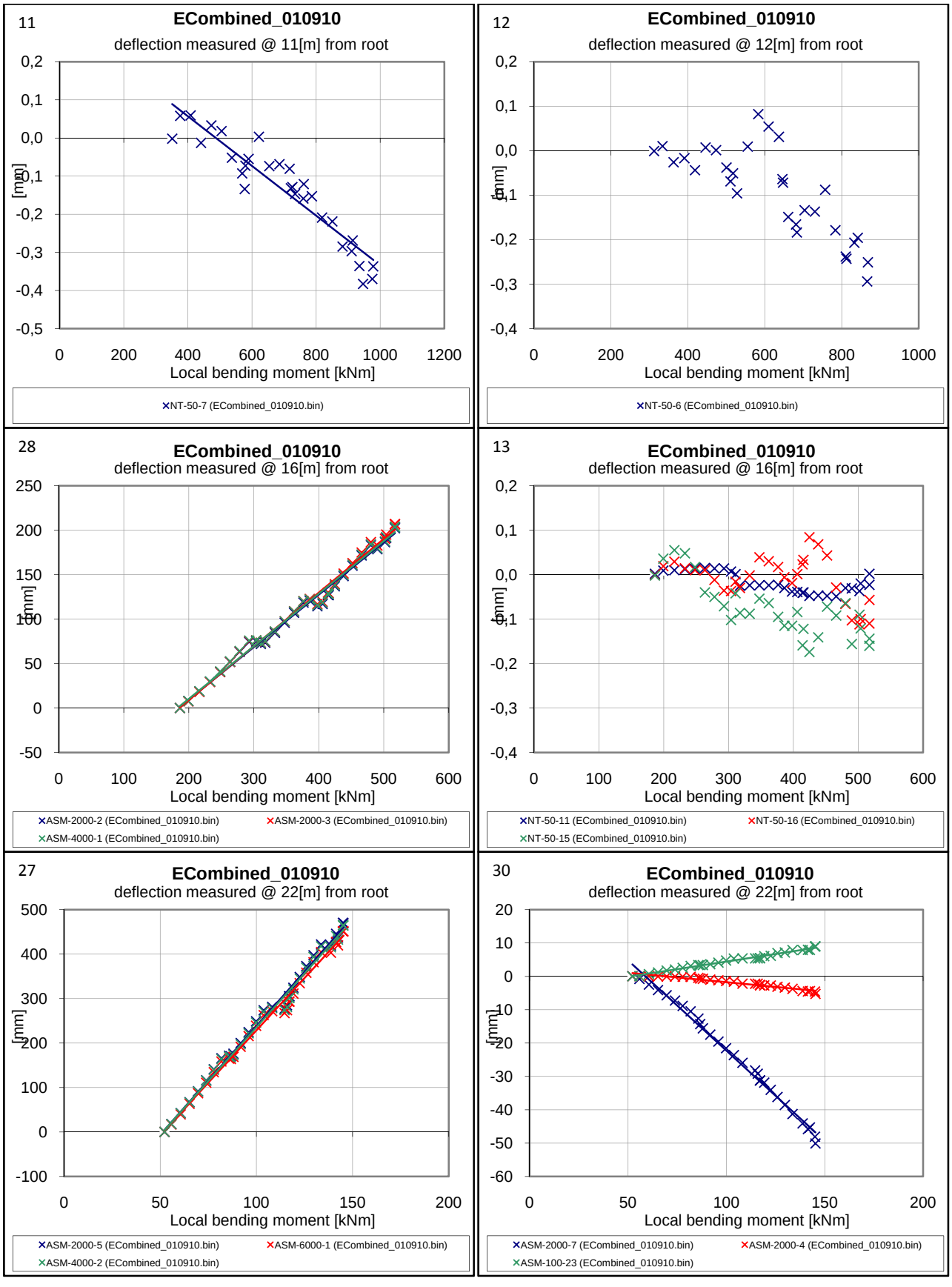
11
ECombined_010910
deflection measured @ 11[m] from root
[mm]
Local bending moment [kNm]
NT-50-7 (ECombined_010910.bin)
12
ECombined_010910
deflection measured @ 12[m] from root
[mm]
Local bending moment [kNm]
NT-50-6 (ECombined_010910.bin)
28
ECombined_010910
deflection measured @ 16[m] from root
[mm]
Local bending moment [kNm]
ASM-2000-2 (ECombined_010910.bin)
ASM-2000-3 (ECombined_010910.bin)
ASM-4000-1 (ECombined_010910.bin)
13
ECombined_010910
deflection measured @ 16[m] from root
[mm]
Local bending moment [kNm]
NT-50-11 (ECombined_010910.bin)
NT-50-16 (ECombined_010910.bin)
NT-50-15 (ECombined_010910.bin)
27
ECombined_010910
deflection measured @ 22[m] from root
[mm]
Local bending moment [kNm]
ASM-2000-5 (ECombined_010910.bin)
ASM-6000-1 (ECombined_010910.bin)
ASM-4000-2 (ECombined_010910.bin)
30
ECombined_010910
deflection measured @ 22[m] from root
[mm]
Local bending moment [kNm]
ASM-2000-7 (ECombined_010910.bin)
ASM-2000-4 (ECombined_010910.bin)
ASM-100-23 (ECombined_010910.bin)

B.2.c Measurement of pull at 35% Risø load (Other groups)

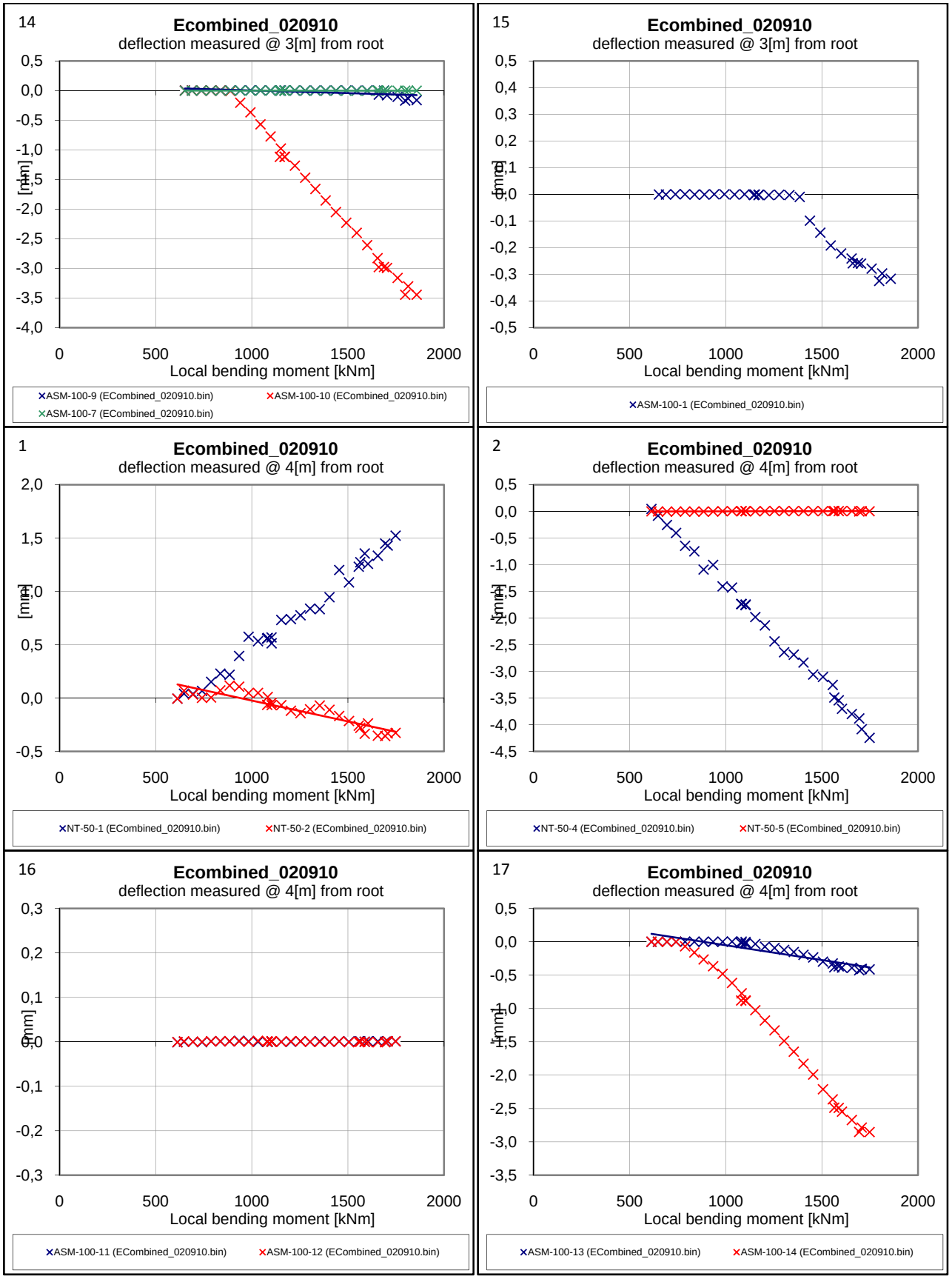

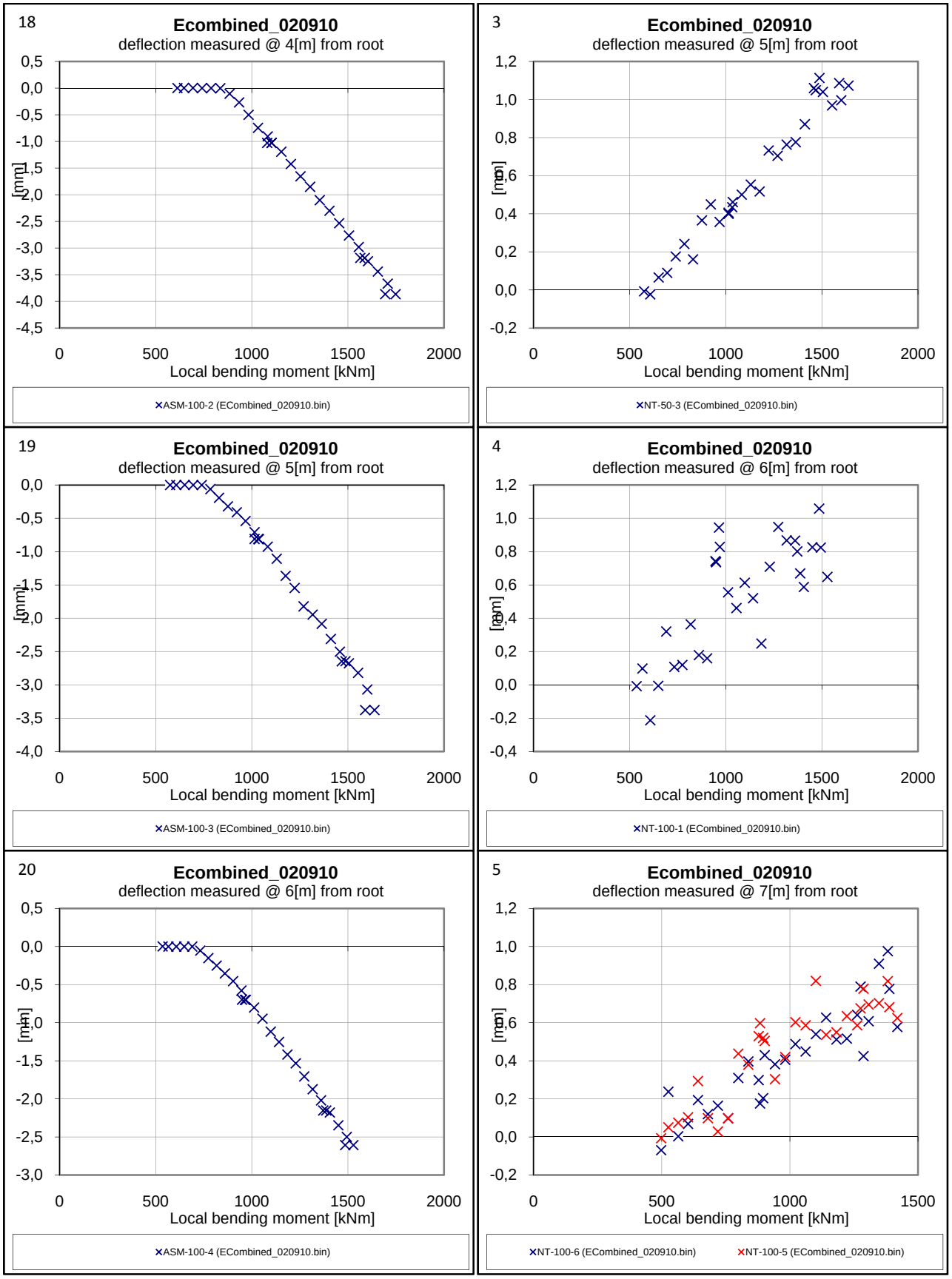
18
Ecombined_020910
deflection measured @ 4[m] from root
[mm]
Local bending moment [kNm]
ASM-100-2 (ECombined_020910.bin)
3
Ecombined_020910
deflection measured @ 5[m] from root
[mm]
Local bending moment [kNm]
NT-50-3 (ECombined_020910.bin)
19
Ecombined_020910
deflection measured @ 5[m] from root
[mm]
Local bending moment [kNm]
ASM-100-3 (ECombined_020910.bin)
4
Ecombined_020910
deflection measured @ 6[m] from root
[mm]
Local bending moment [kNm]
NT-100-1 (ECombined_020910.bin)
20
Ecombined_020910
deflection measured @ 6[m] from root
[mm]
Local bending moment [kNm]
ASM-100-4 (ECombined_020910.bin)
5
Ecombined_020910
deflection measured @ 7[m] from root
[mm]
Local bending moment [kNm]
NT-100-6 (ECombined_020910.bin)
NT-100-5 (ECombined_020910.bin)

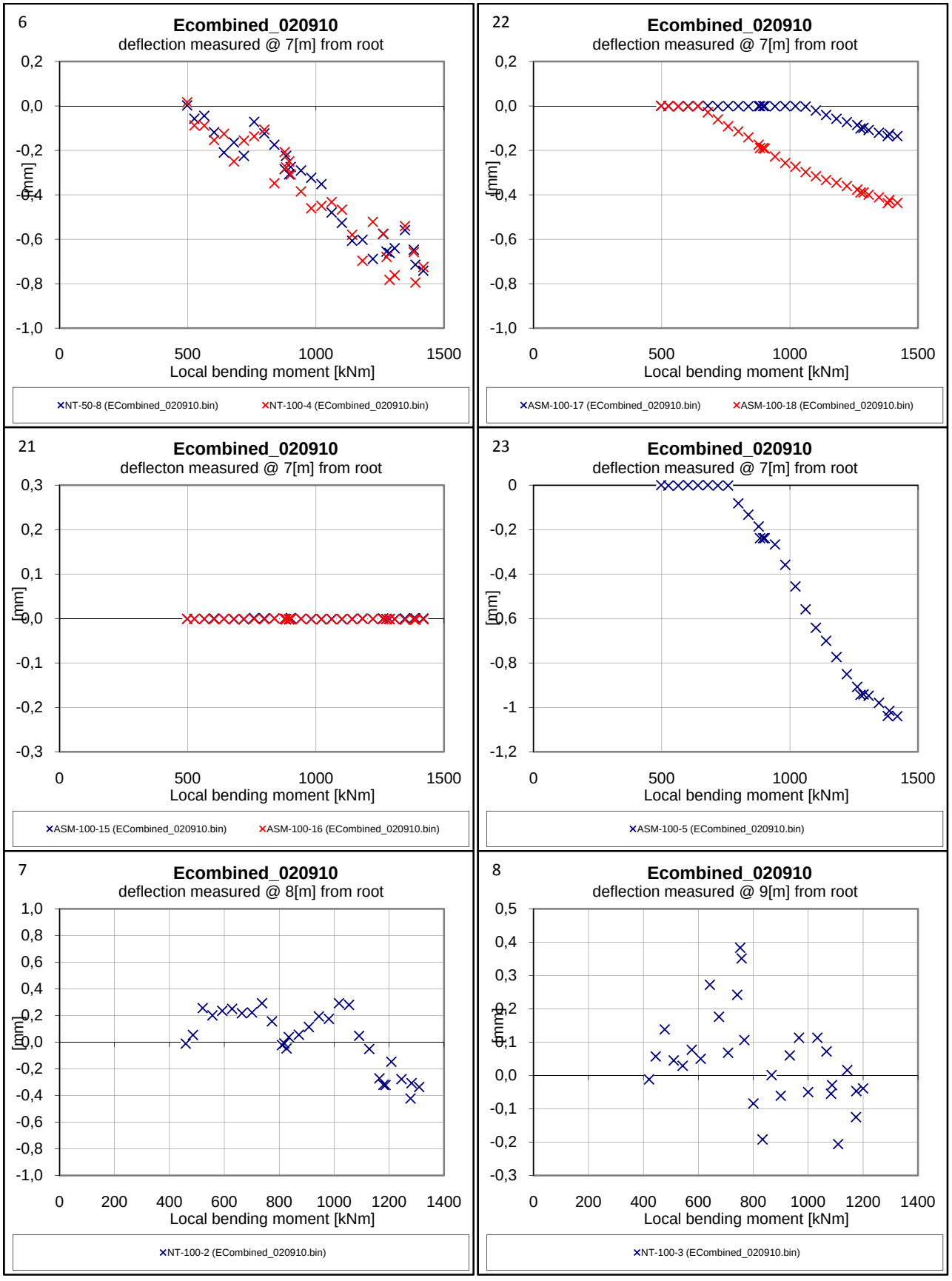
6
Ecombined_020910
deflection measured @ 7[m] from root
0,2
0,0
-0,2
-0,4
-0,6
-0,8
-1,0
[mm]
0
500
1000
1500
Local bending moment [kNm]
NT-50-8 (ECombined_020910.bin)
NT-100-4 (ECombined_020910.bin)
22
Ecombined_020910
deflection measured @ 7[m] from root
0,2
0,0
-0,2
-0,4
-0,6
-0,8
-1,0
[mm]
0
500
1000
1500
Local bending moment [kNm]
ASM-100-17 (ECombined_020910.bin)
ASM-100-18 (ECombined_020910.bin)
21
Ecombined_020910
deflecton measured @ 7[m] from root
0,3
0,2
0,1
0,0
-0,1
-0,2
-0,3
[mm]
0
500
1000
1500
Local bending moment [kNm]
ASM-100-15 (ECombined_020910.bin)
ASM-100-16 (ECombined_020910.bin)
23
Ecombined_020910
deflection measured @ 7[m] from root
0
-0,2
-0,4
-0,6
-0,8
-1
-1,2
[mm]
0
500
1000
1500
Local bending moment [kNm]
ASM-100-5 (ECombined_020910.bin)
7
Ecombined_020910
deflection measured @ 8[m] from root
1,0
0,8
0,6
0,4
0,2
0,0
-0,2
-0,4
-0,6
-0,8
-1,0
[mm]
0
200
400
600
800
1000
1200
1400
Local bending moment [kNm]
NT-100-2 (ECombined_020910.bin)
8
Ecombined_020910
deflection measured @ 9[m] from root
0,5
0,4
0,3
0,2
0,1
0,0
-0,1
-0,2
-0,3
[mm]
0
200
400
600
800
1000
1200
1400
Local bending moment [kNm]
NT-100-3 (ECombined_020910.bin)

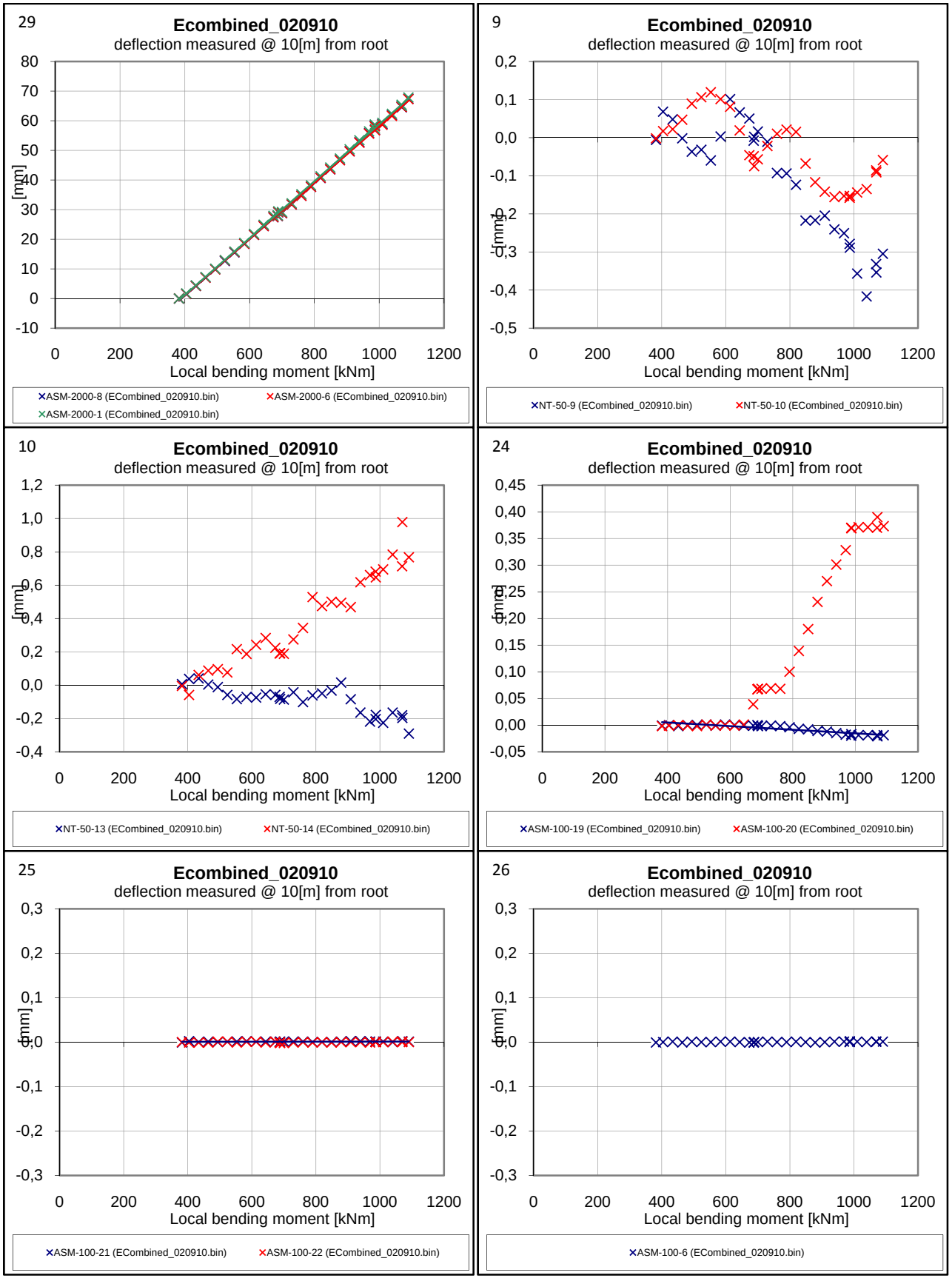
29
Ecombined_020910
deflection measured @ 10[m] from root
[mm]
Local bending moment [kNm]
ASM-2000-8 (ECombined_020910.bin)
ASM-2000-6 (ECombined_020910.bin)
ASM-2000-1 (ECombined_020910.bin)
9
Ecombined_020910
deflection measured @ 10[m] from root
[mm]
Local bending moment [kNm]
NT-50-9 (ECombined_020910.bin)
NT-50-10 (ECombined_020910.bin)
10
Ecombined_020910
deflection measured @ 10[m] from root
[mm]
Local bending moment [kNm]
NT-50-13 (ECombined_020910.bin)
NT-50-14 (ECombined_020910.bin)
24
Ecombined_020910
deflection measured @ 10[m] from root
[mm]
Local bending moment [kNm]
ASM-100-19 (ECombined_020910.bin)
ASM-100-20 (ECombined_020910.bin)
25
Ecombined_020910
deflection measured @ 10[m] from root
[mm]
Local bending moment [kNm]
ASM-100-21 (ECombined_020910.bin)
ASM-100-22 (ECombined_020910.bin)
26
Ecombined_020910
deflection measured @ 10[m] from root
[mm]
Local bending moment [kNm]
ASM-100-6 (ECombined_020910.bin)

11

Ecombined_020910

deflectopn measured @ 11[m] from root

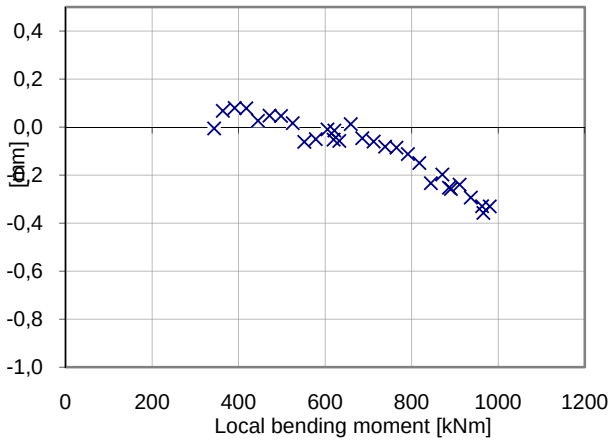

12

Ecombined_020910

deflection measured @ 12[m] from root

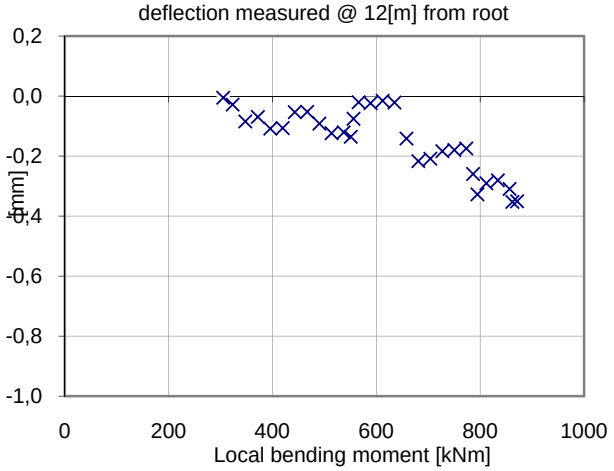

28

Ecombined_020910

deflection measured @ 16[m] from root

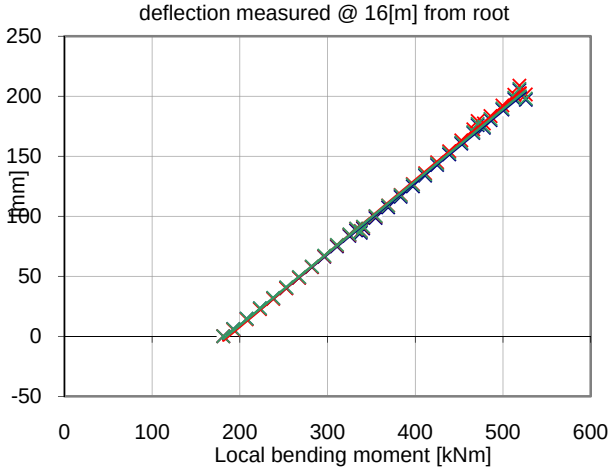

13

Ecombined_020910

deflection measured @ 16[m] from root

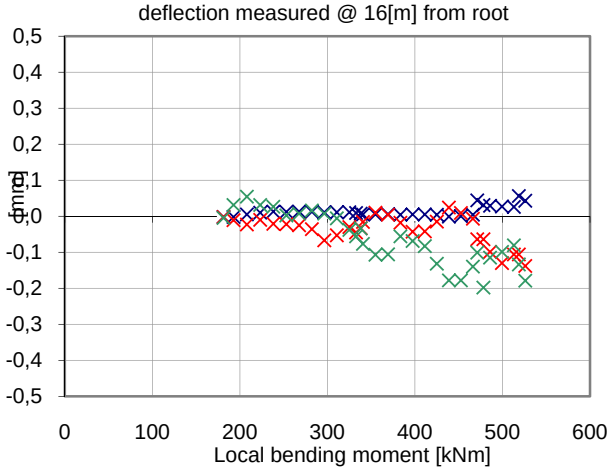

27

Ecombined_020910

deflection measured @ 22[m] from root

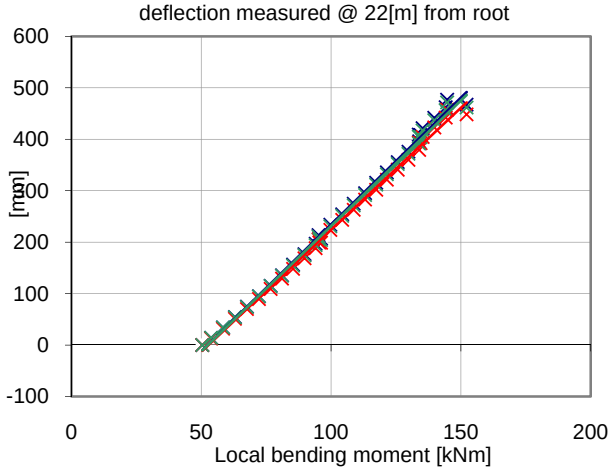

30

Ecombined_020910

defletion measured @ 10,16 and 22[m] from root

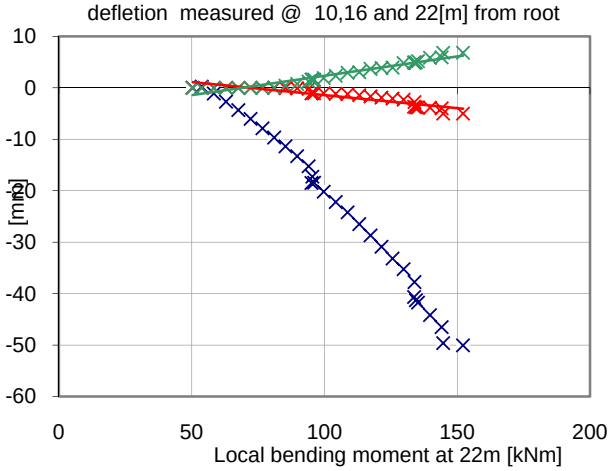

B.3 Measurement of pull at 55% Risø load (Other groups)

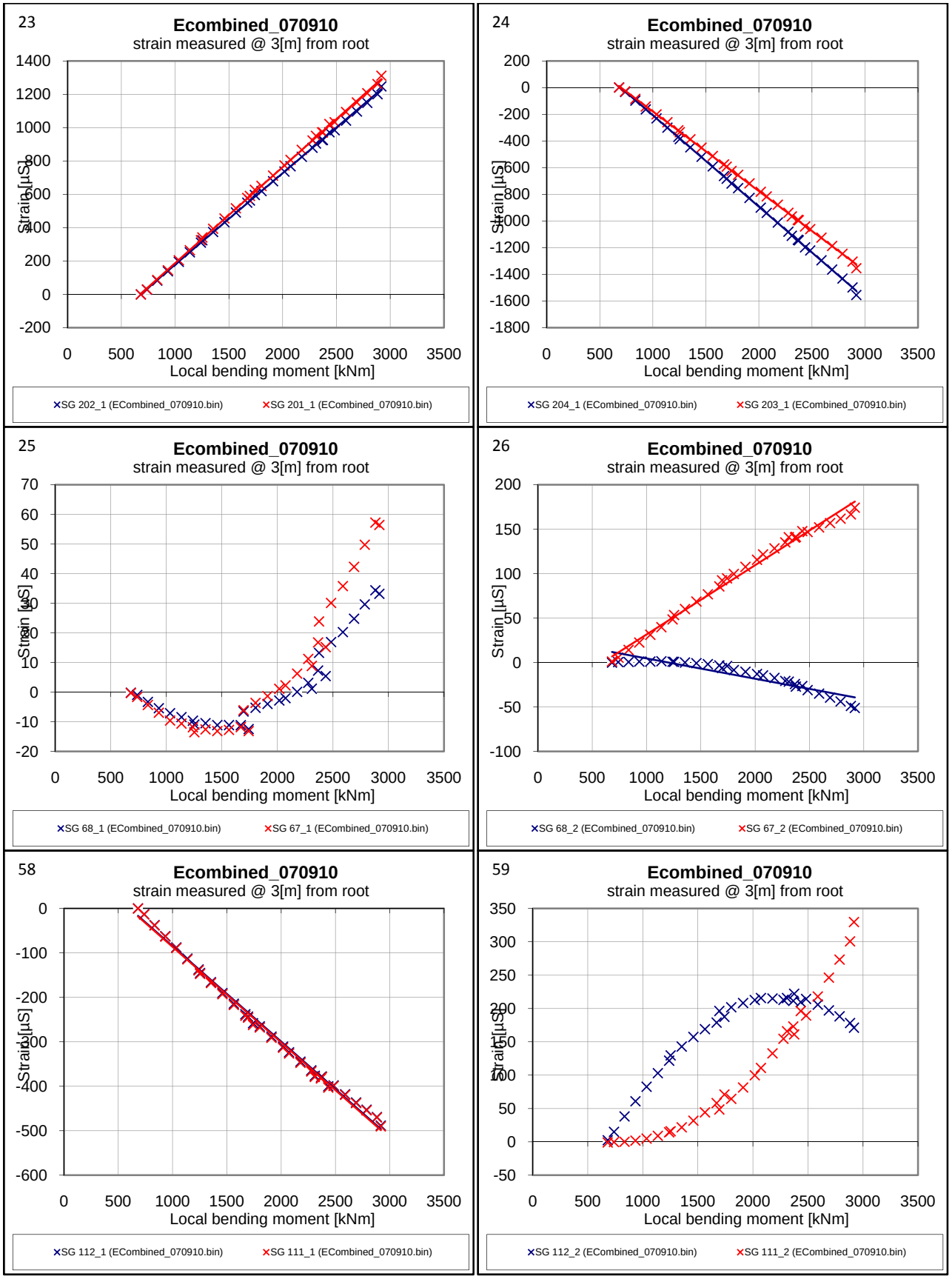

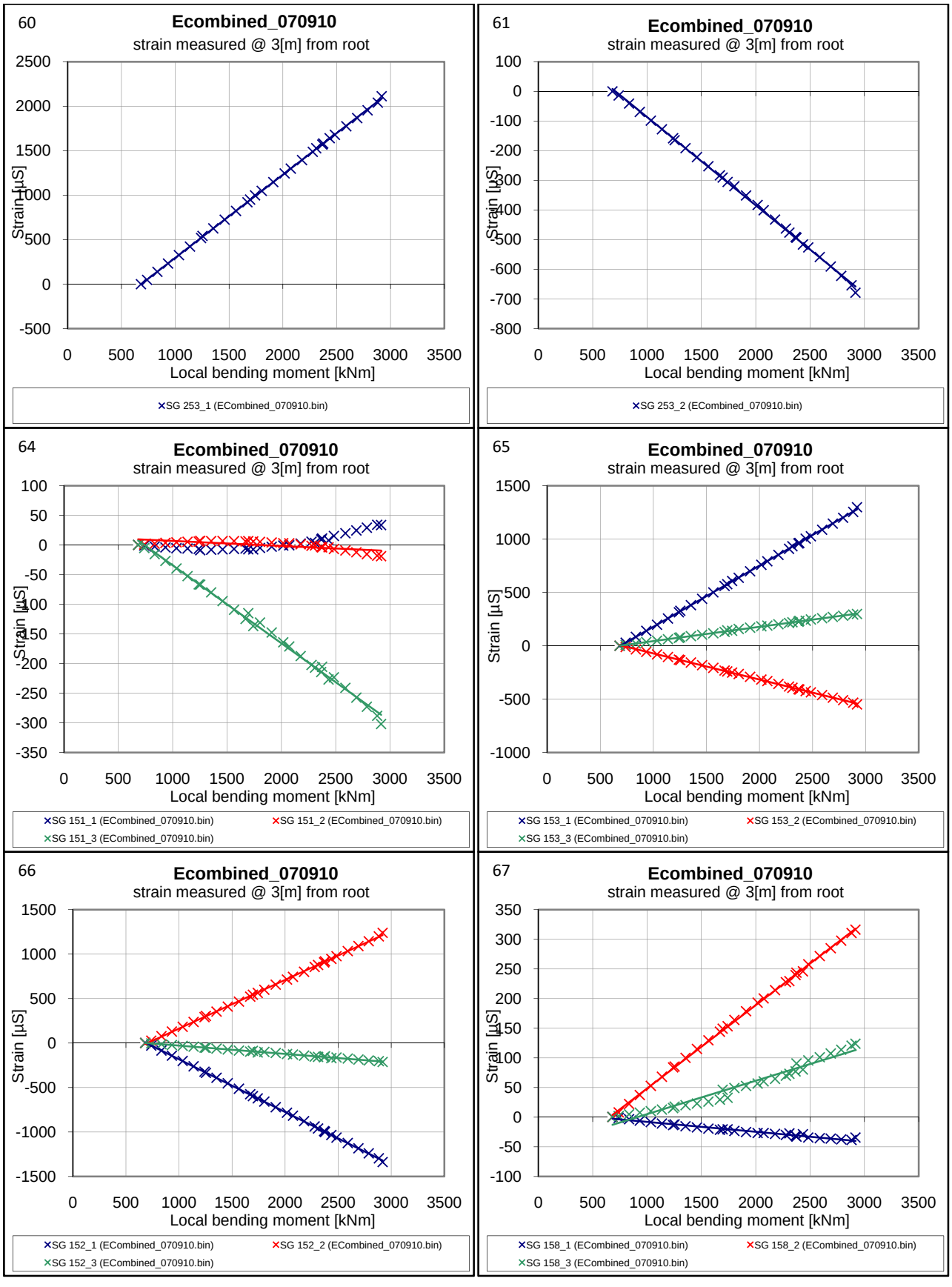
60
Ecombined_070910
strain measured @ 3[m] from root
Strain [µS]
Local bending moment [kNm]
SG 253_1 (ECombined_070910.bin)
61
Ecombined_070910
strain measured @ 3[m] from root
Strain [µS]
Local bending moment [kNm]
SG 253_2 (ECombined_070910.bin)
64
Ecombined_070910
strain measured @ 3[m] from root
Strain [µS]
Local bending moment [kNm]
SG 151_1 (ECombined_070910.bin)
SG 151_2 (ECombined_070910.bin)
SG 151_3 (ECombined_070910.bin)
65
Ecombined_070910
strain measured @ 3[m] from root
Strain [µS]
Local bending moment [kNm]
SG 153_1 (ECombined_070910.bin)
SG 153_2 (ECombined_070910.bin)
SG 153_3 (ECombined_070910.bin)
66
Ecombined_070910
strain measured @ 3[m] from root
Strain [µS]
Local bending moment [kNm]
SG 152_1 (ECombined_070910.bin)
SG 152_2 (ECombined_070910.bin)
SG 152_3 (ECombined_070910.bin)
67
Ecombined_070910
strain measured @ 3[m] from root
Strain [µS]
Local bending moment [kNm]
SG 158_1 (ECombined_070910.bin)
SG 158_2 (ECombined_070910.bin)
SG 158_3 (ECombined_070910.bin)

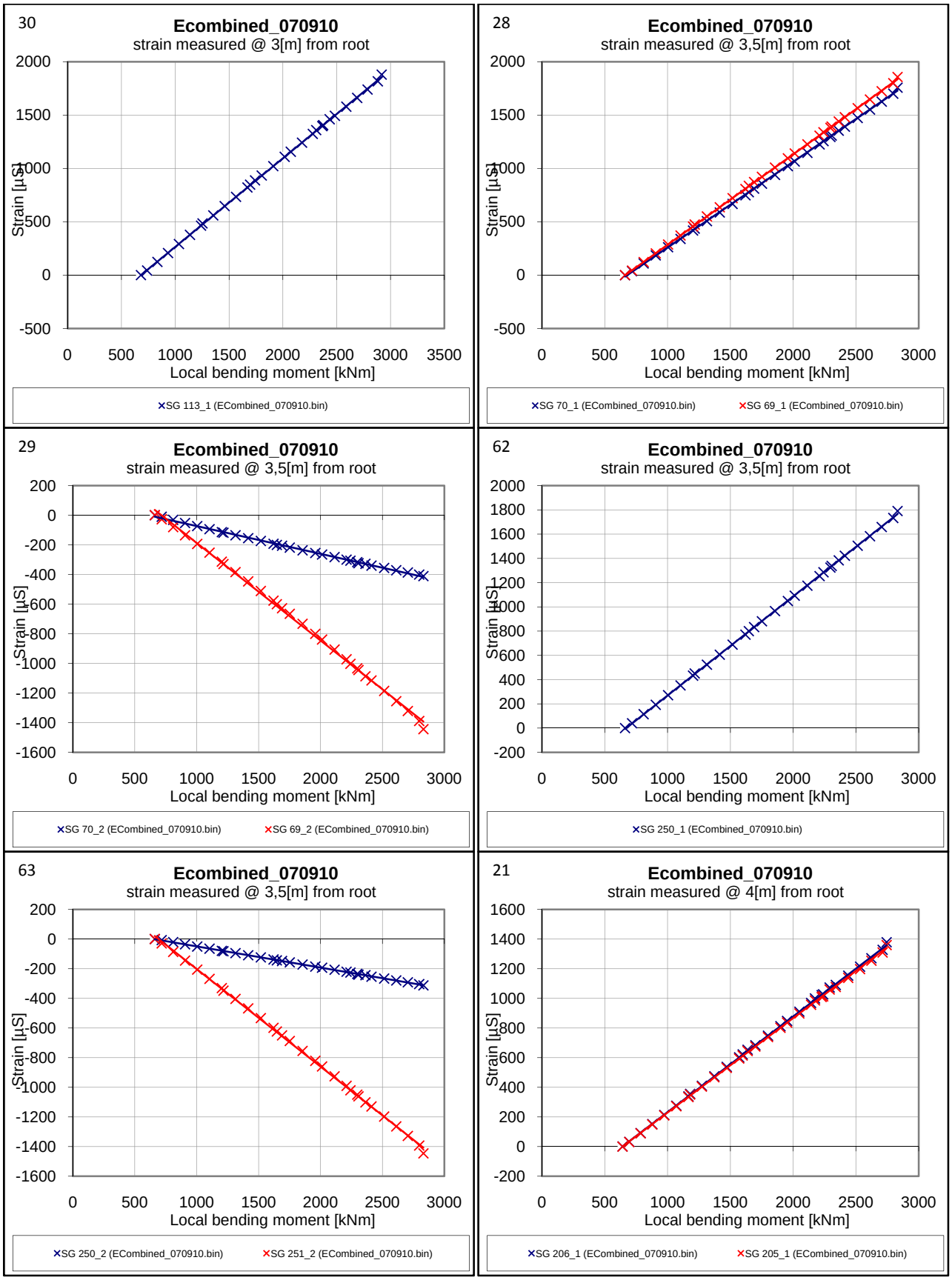
30
Ecombined_070910
strain measured @ 3[m] from root
Strain [µS]
Local bending moment [kNm]
SG 113_1 (ECombined_070910.bin)
28
Ecombined_070910
strain measured @ 3,5[m] from root
Strain [µS]
Local bending moment [kNm]
SG 70_1 (ECombined_070910.bin)
SG 69_1 (ECombined_070910.bin)
29
Ecombined_070910
strain measured @ 3,5[m] from root
Strain [µS]
Local bending moment [kNm]
SG 70_2 (ECombined_070910.bin)
SG 69_2 (ECombined_070910.bin)
62
Ecombined_070910
strain measured @ 3,5[m] from root
Strain [µS]
Local bending moment [kNm]
SG 250_1 (ECombined_070910.bin)
63
Ecombined_070910
strain measured @ 3,5[m] from root
Strain [µS]
Local bending moment [kNm]
SG 250_2 (ECombined_070910.bin)
SG 251_2 (ECombined_070910.bin)
21
Ecombined_070910
strain measured @ 4[m] from root
Strain [µS]
Local bending moment [kNm]
SG 206_1 (ECombined_070910.bin)
SG 205_1 (ECombined_070910.bin)

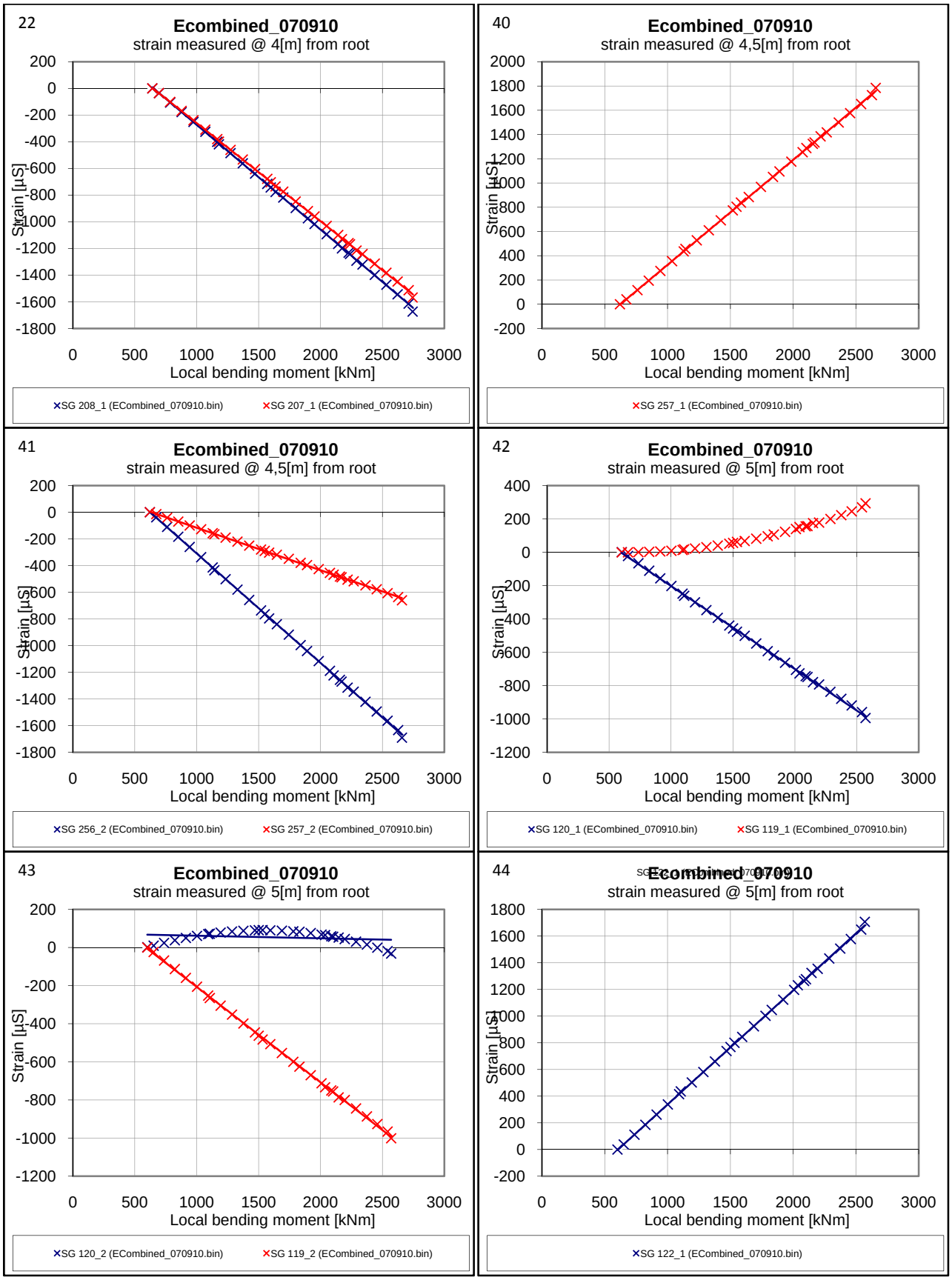
22
Ecombined_070910
strain measured @ 4[m] from root
Strain [µS]
Local bending moment [kNm]
SG 208_1 (ECombined_070910.bin)
SG 207_1 (ECombined_070910.bin)
40
Ecombined_070910
strain measured @ 4,5[m] from root
Strain [µS]
Local bending moment [kNm]
SG 257_1 (ECombined_070910.bin)
41
Ecombined_070910
strain measured @ 4,5[m] from root
Strain [µS]
Local bending moment [kNm]
SG 256_2 (ECombined_070910.bin)
SG 257_2 (ECombined_070910.bin)
42
Ecombined_070910
strain measured @ 5[m] from root
Strain [µS]
Local bending moment [kNm]
SG 120_1 (ECombined_070910.bin)
SG 119_1 (ECombined_070910.bin)
43
Ecombined_070910
strain measured @ 5[m] from root
Strain [µS]
Local bending moment [kNm]
SG 120_2 (ECombined_070910.bin)
SG 119_2 (ECombined_070910.bin)
44
Ecombined_070910
strain measured @ 5[m] from root
Strain [µS]
Local bending moment [kNm]
SG 122_1 (ECombined_070910.bin)

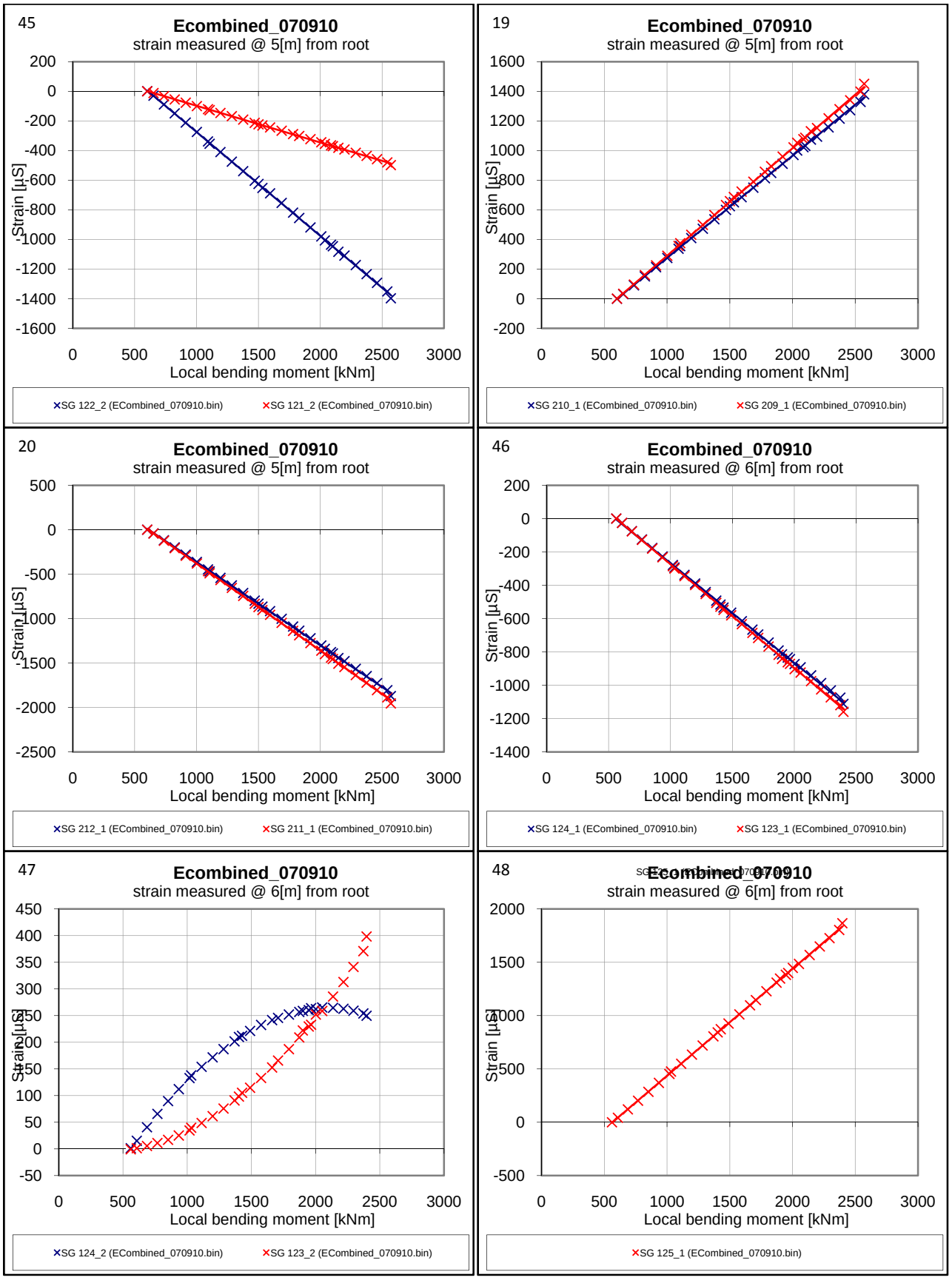
45
Ecombined_070910
strain measured @ 5[m] from root
Strain [µS]
Local bending moment [kNm]
SG 122_2 (ECombined_070910.bin)
SG 121_2 (ECombined_070910.bin)
19
Ecombined_070910
strain measured @ 5[m] from root
Strain [µS]
Local bending moment [kNm]
SG 210_1 (ECombined_070910.bin)
SG 209_1 (ECombined_070910.bin)
20
Ecombined_070910
strain measured @ 5[m] from root
Strain [µS]
Local bending moment [kNm]
SG 212_1 (ECombined_070910.bin)
SG 211_1 (ECombined_070910.bin)
46
Ecombined_070910
strain measured @ 6[m] from root
Strain [µS]
Local bending moment [kNm]
SG 124_1 (ECombined_070910.bin)
SG 123_1 (ECombined_070910.bin)
47
Ecombined_070910
strain measured @ 6[m] from root
Strain [µS]
Local bending moment [kNm]
SG 124_2 (ECombined_070910.bin)
SG 123_2 (ECombined_070910.bin)
48
Ecombined_070910
strain measured @ 6[m] from root
Strain [µS]
Local bending moment [kNm]
SG 125_1 (ECombined_070910.bin)

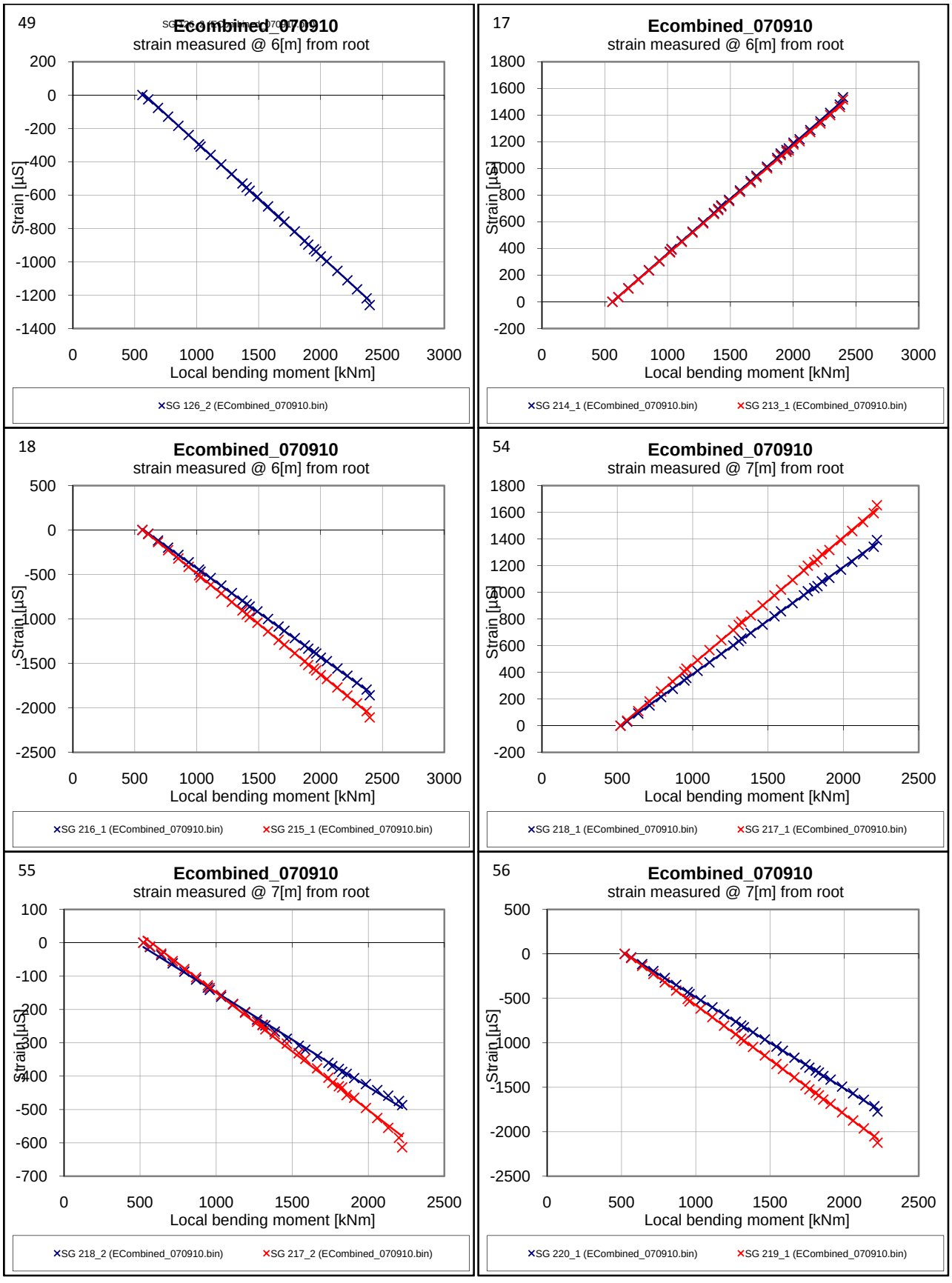
49
Ecombined_070910
strain measured @ 6[m] from root
Strain [µS]
Local bending moment [kNm]
SG 126_2 (ECombined_070910.bin)
17
Ecombined_070910
strain measured @ 6[m] from root
Strain [µS]
Local bending moment [kNm]
SG 214_1 (ECombined_070910.bin)
SG 213_1 (ECombined_070910.bin)
18
Ecombined_070910
strain measured @ 6[m] from root
Strain [µS]
Local bending moment [kNm]
SG 216_1 (ECombined_070910.bin)
SG 215_1 (ECombined_070910.bin)
54
Ecombined_070910
strain measured @ 7[m] from root
Strain [µS]
Local bending moment [kNm]
SG 218_1 (ECombined_070910.bin)
SG 217_1 (ECombined_070910.bin)
55
Ecombined_070910
strain measured @ 7[m] from root
Strain [µS]
Local bending moment [kNm]
SG 218_2 (ECombined_070910.bin)
SG 217_2 (ECombined_070910.bin)
56
Ecombined_070910
strain measured @ 7[m] from root
Strain [µS]
Local bending moment [kNm]
SG 220_1 (ECombined_070910.bin)
SG 219_1 (ECombined_070910.bin)

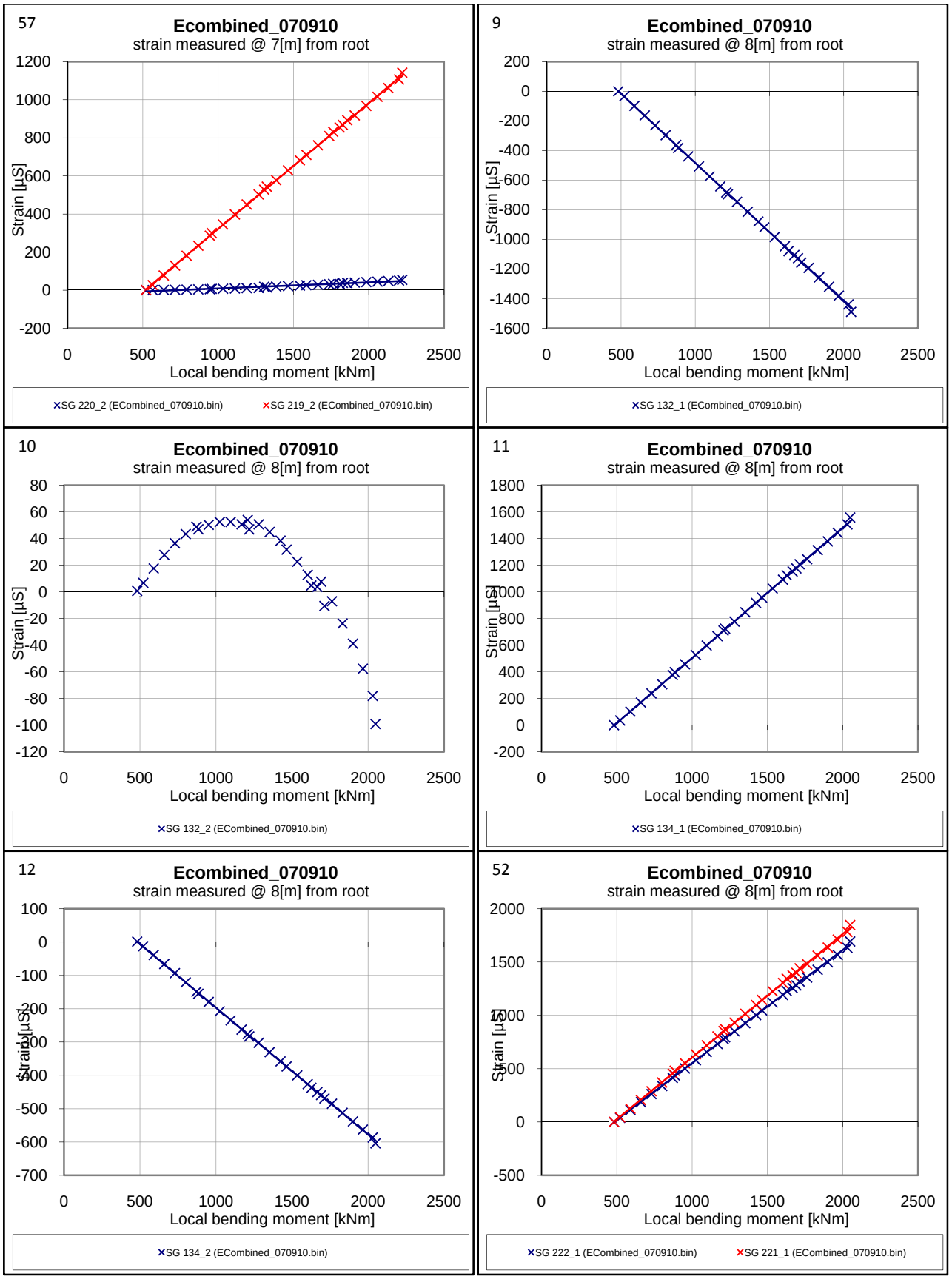
57
Ecombined_070910
strain measured @ 7[m] from root
Strain [µS]
Local bending moment [kNm]
SG 220_2 (ECombined_070910.bin)
SG 219_2 (ECombined_070910.bin)
9
Ecombined_070910
strain measured @ 8[m] from root
Strain [µS]
Local bending moment [kNm]
SG 132_1 (ECombined_070910.bin)
10
Ecombined_070910
strain measured @ 8[m] from root
Strain [µS]
Local bending moment [kNm]
SG 132_2 (ECombined_070910.bin)
11
Ecombined_070910
strain measured @ 8[m] from root
Strain [µS]
Local bending moment [kNm]
SG 134_1 (ECombined_070910.bin)
12
Ecombined_070910
strain measured @ 8[m] from root
Strain [µS]
Local bending moment [kNm]
SG 134_2 (ECombined_070910.bin)
52
Ecombined_070910
strain measured @ 8[m] from root
Strain [µS]
Local bending moment [kNm]
SG 222_1 (ECombined_070910.bin)
SG 221_1 (ECombined_070910.bin)

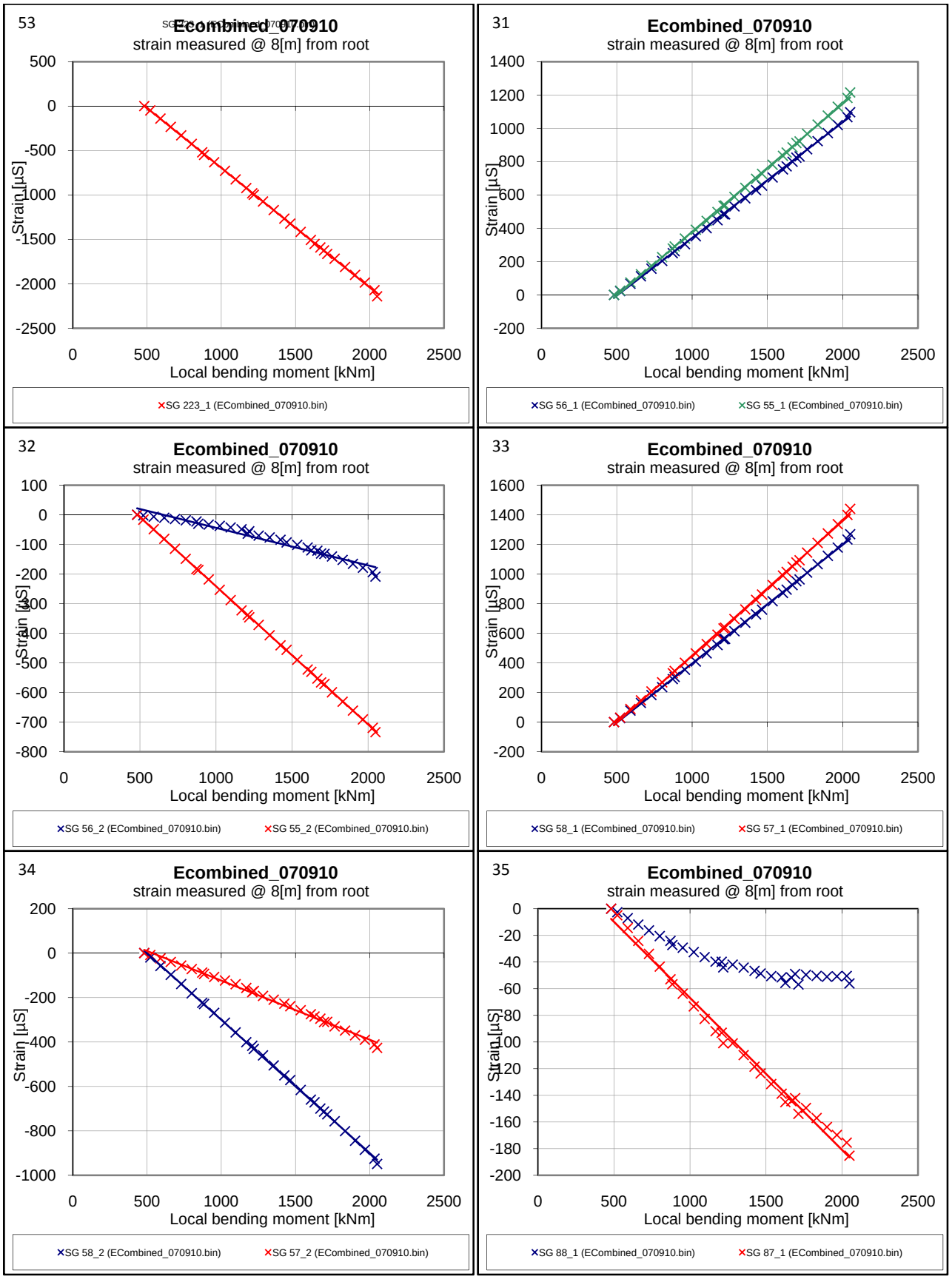
53
Ecombined_070910
strain measured @ 8[m] from root
Strain [µS]
Local bending moment [kNm]
SG 223_1 (ECombined_070910.bin)
31
Ecombined_070910
strain measured @ 8[m] from root
Strain [µS]
Local bending moment [kNm]
SG 56_1 (ECombined_070910.bin)
SG 55_1 (ECombined_070910.bin)
32
Ecombined_070910
strain measured @ 8[m] from root
Strain [µS]
Local bending moment [kNm]
SG 56_2 (ECombined_070910.bin)
SG 55_2 (ECombined_070910.bin)
33
Ecombined_070910
strain measured @ 8[m] from root
Strain [µS]
Local bending moment [kNm]
SG 58_1 (ECombined_070910.bin)
SG 57_1 (ECombined_070910.bin)
34
Ecombined_070910
strain measured @ 8[m] from root
Strain [µS]
Local bending moment [kNm]
SG 58_2 (ECombined_070910.bin)
SG 57_2 (ECombined_070910.bin)
35
Ecombined_070910
strain measured @ 8[m] from root
Strain [µS]
Local bending moment [kNm]
SG 88_1 (ECombined_070910.bin)
SG 87_1 (ECombined_070910.bin)

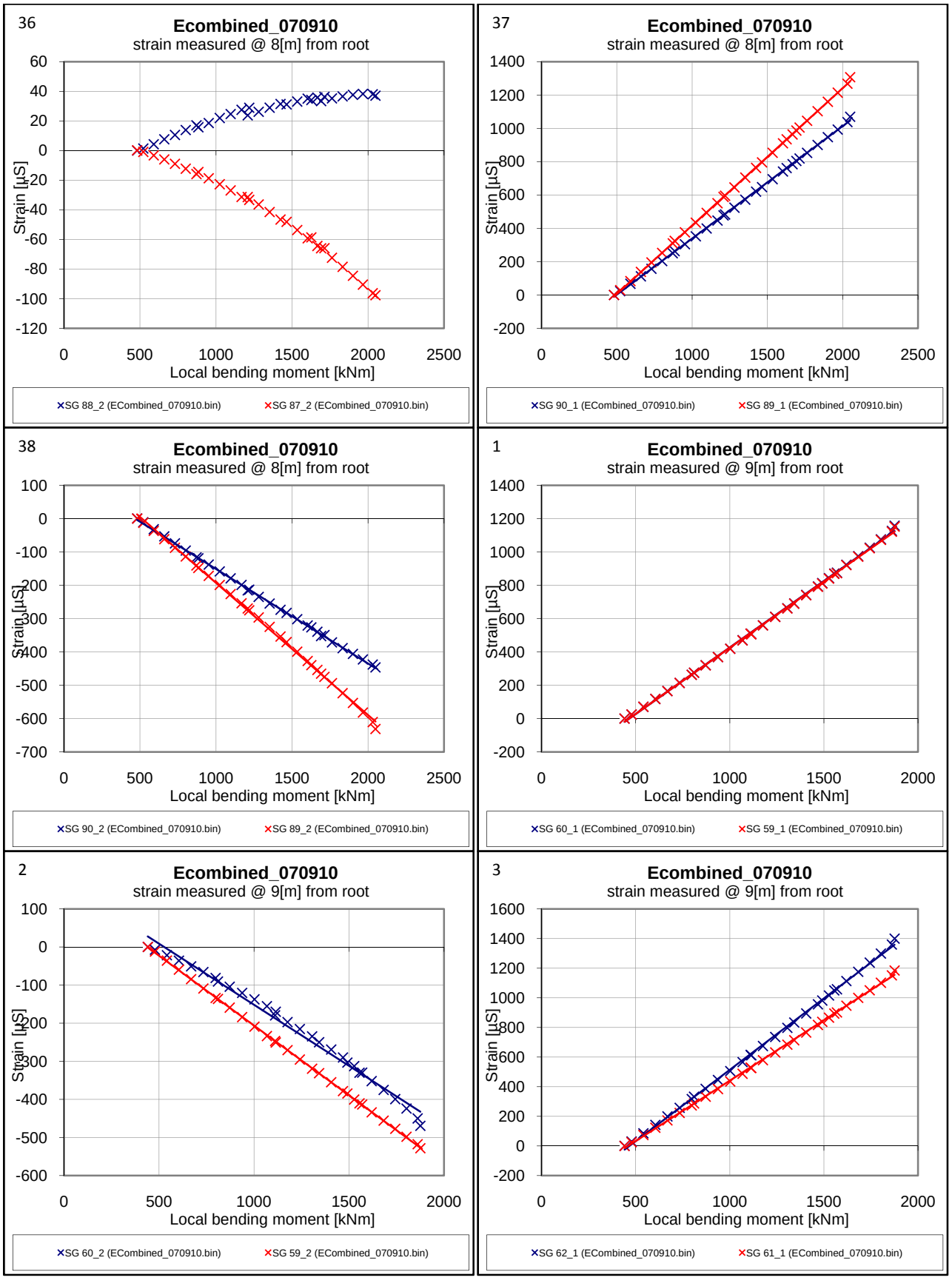
36
Ecombined_070910
strain measured @ 8[m] from root
Strain [µS]
Local bending moment [kNm]
SG 88_2 (ECombined_070910.bin)
SG 87_2 (ECombined_070910.bin)
37
Ecombined_070910
strain measured @ 8[m] from root
Strain [µS]
Local bending moment [kNm]
SG 90_1 (ECombined_070910.bin)
SG 89_1 (ECombined_070910.bin)
38
Ecombined_070910
strain measured @ 8[m] from root
Strain [µS]
Local bending moment [kNm]
SG 90_2 (ECombined_070910.bin)
SG 89_2 (ECombined_070910.bin)
1
Ecombined_070910
strain measured @ 9[m] from root
Strain [µS]
Local bending moment [kNm]
SG 60_1 (ECombined_070910.bin)
SG 59_1 (ECombined_070910.bin)
2
Ecombined_070910
strain measured @ 9[m] from root
Strain [µS]
Local bending moment [kNm]
SG 60_2 (ECombined_070910.bin)
SG 59_2 (ECombined_070910.bin)
3
Ecombined_070910
strain measured @ 9[m] from root
Strain [µS]
Local bending moment [kNm]
SG 62_1 (ECombined_070910.bin)
SG 61_1 (ECombined_070910.bin)

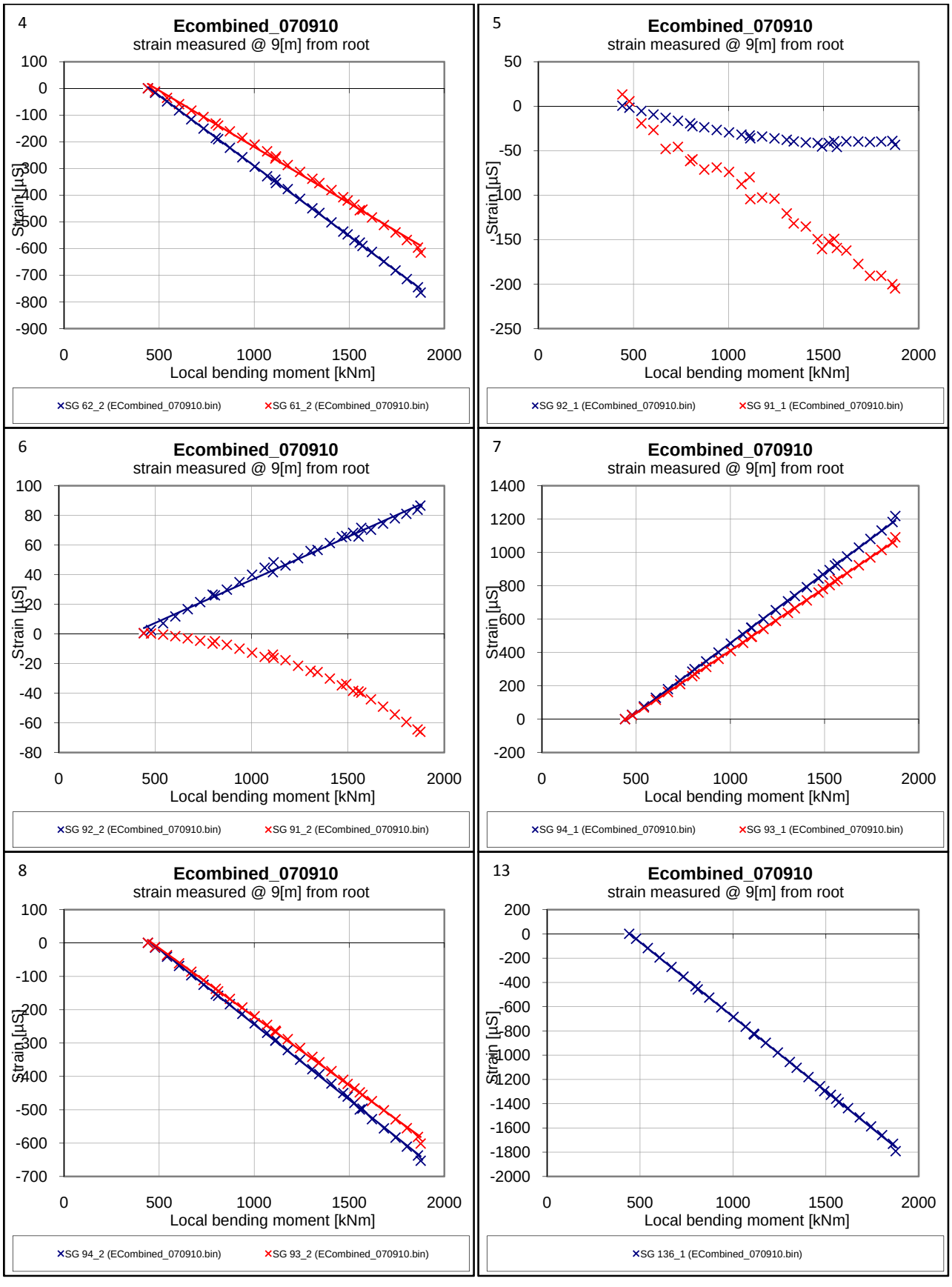
4
Ecombined_070910
strain measured @ 9[m] from root
Strain [µS]
Local bending moment [kNm]
SG 62_2 (ECombined_070910.bin)
SG 61_2 (ECombined_070910.bin)
5
Ecombined_070910
strain measured @ 9[m] from root
Strain [µS]
Local bending moment [kNm]
SG 92_1 (ECombined_070910.bin)
SG 91_1 (ECombined_070910.bin)
6
Ecombined_070910
strain measured @ 9[m] from root
Strain [µS]
Local bending moment [kNm]
SG 92_2 (ECombined_070910.bin)
SG 91_2 (ECombined_070910.bin)
7
Ecombined_070910
strain measured @ 9[m] from root
Strain [µS]
Local bending moment [kNm]
SG 94_1 (ECombined_070910.bin)
SG 93_1 (ECombined_070910.bin)
8
Ecombined_070910
strain measured @ 9[m] from root
Strain [µS]
Local bending moment [kNm]
SG 94_2 (ECombined_070910.bin)
SG 93_2 (ECombined_070910.bin)
13
Ecombined_070910
strain measured @ 9[m] from root
Strain [µS]
Local bending moment [kNm]
SG 136_1 (ECombined_070910.bin)

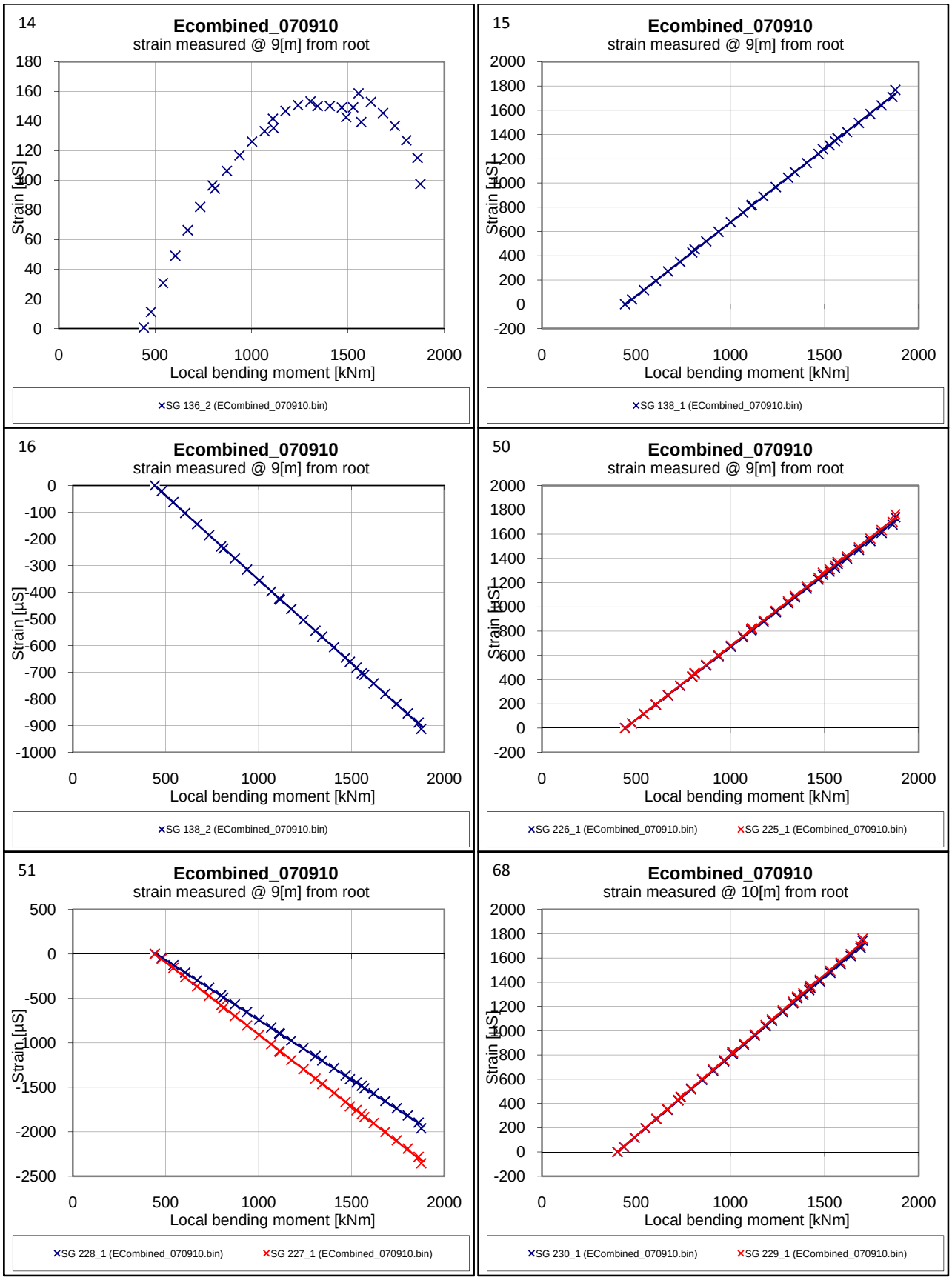
14
Ecombined_070910
strain measured @ 9[m] from root
Strain [µS]
Local bending moment [kNm]
SG 136_2 (ECombined_070910.bin)
15
Ecombined_070910
strain measured @ 9[m] from root
Strain [µS]
Local bending moment [kNm]
SG 138_1 (ECombined_070910.bin)
16
Ecombined_070910
strain measured @ 9[m] from root
Strain [µS]
Local bending moment [kNm]
SG 138_2 (ECombined_070910.bin)
50
Ecombined_070910
strain measured @ 9[m] from root
Strain [µS]
Local bending moment [kNm]
SG 226_1 (ECombined_070910.bin)
SG 225_1 (ECombined_070910.bin)
51
Ecombined_070910
strain measured @ 9[m] from root
Strain [µS]
Local bending moment [kNm]
SG 228_1 (ECombined_070910.bin)
SG 227_1 (ECombined_070910.bin)
68
Ecombined_070910
strain measured @ 10[m] from root
Strain [µS]
Local bending moment [kNm]
SG 230_1 (ECombined_070910.bin)
SG 229_1 (ECombined_070910.bin)

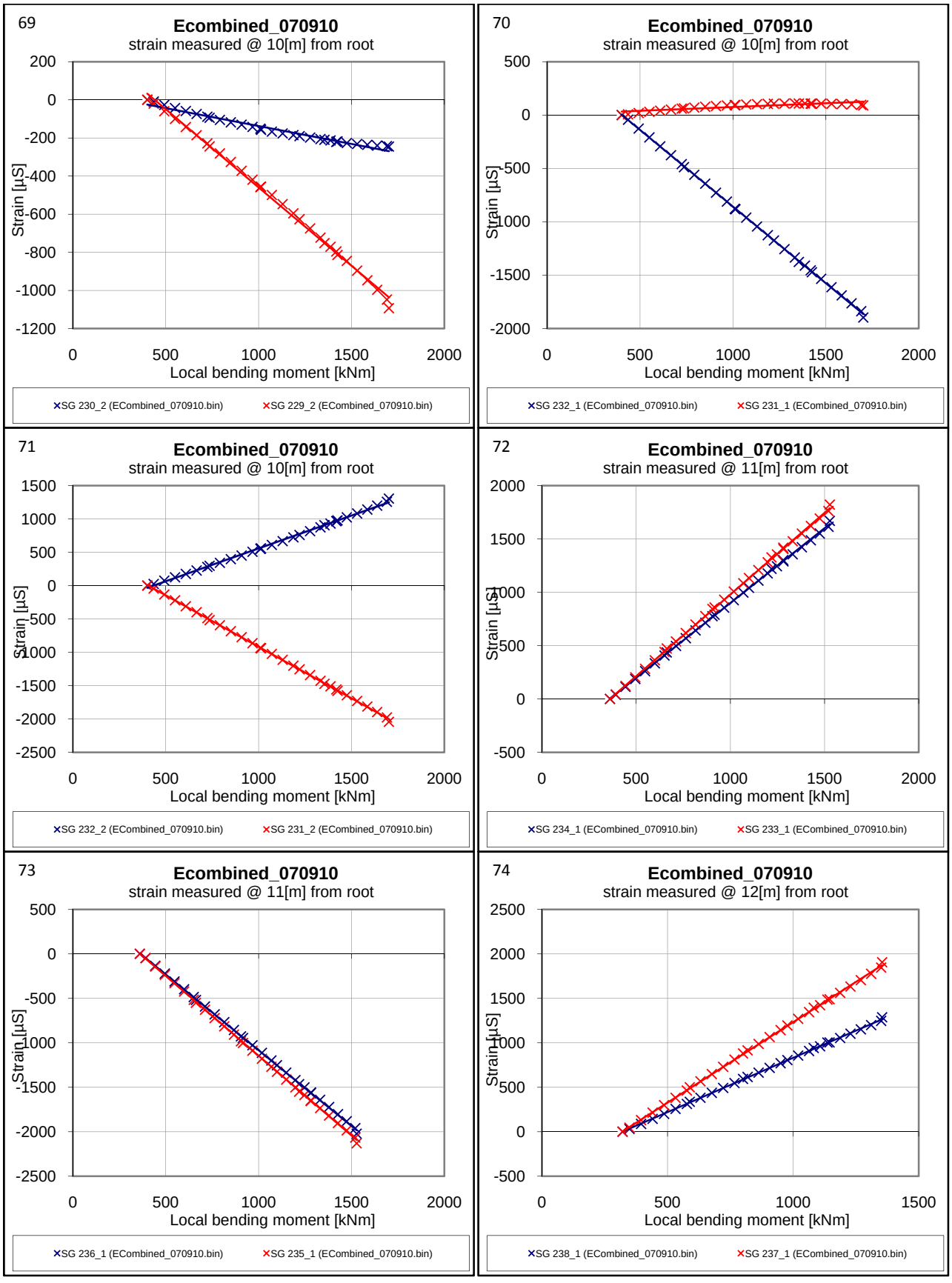
69
Ecombined_070910
strain measured @ 10[m] from root
Strain [µS]
Local bending moment [kNm]
SG 230_2 (ECombined_070910.bin)
SG 229_2 (ECombined_070910.bin)
70
Ecombined_070910
strain measured @ 10[m] from root
Strain [µS]
Local bending moment [kNm]
SG 232_1 (ECombined_070910.bin)
SG 231_1 (ECombined_070910.bin)
71
Ecombined_070910
strain measured @ 10[m] from root
Strain [µS]
Local bending moment [kNm]
SG 232_2 (ECombined_070910.bin)
SG 231_2 (ECombined_070910.bin)
72
Ecombined_070910
strain measured @ 11[m] from root
Strain [µS]
Local bending moment [kNm]
SG 234_1 (ECombined_070910.bin)
SG 233_1 (ECombined_070910.bin)
73
Ecombined_070910
strain measured @ 11[m] from root
Strain [µS]
Local bending moment [kNm]
SG 236_1 (ECombined_070910.bin)
SG 235_1 (ECombined_070910.bin)
74
Ecombined_070910
strain measured @ 12[m] from root
Strain [µS]
Local bending moment [kNm]
SG 238_1 (ECombined_070910.bin)
SG 237_1 (ECombined_070910.bin)

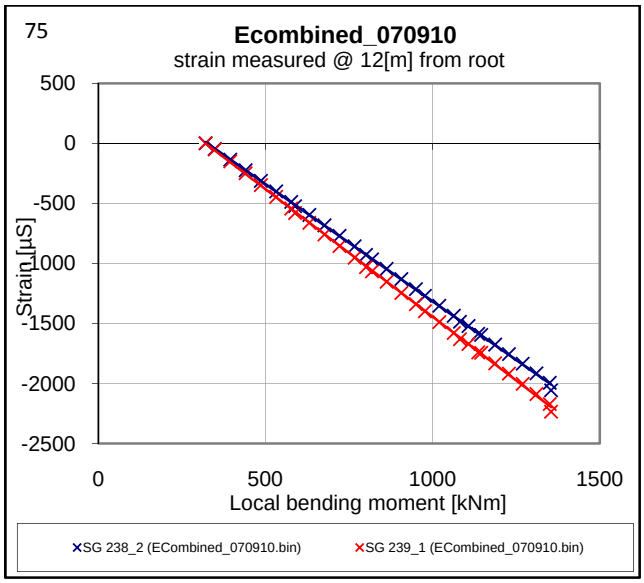
75
Ecombined_070910
strain measured @ 12[m] from root
500
0
-500
-1000
-1500
-2000
-2500
Strain [µS]
0
500
1000
1500
Local bending moment [kNm]
SG 238_2 (ECombined_070910.bin)
SG 239_1 (ECombined_070910.bin)

B.4 Measurement of pull at 55% Risø load (Other groups)

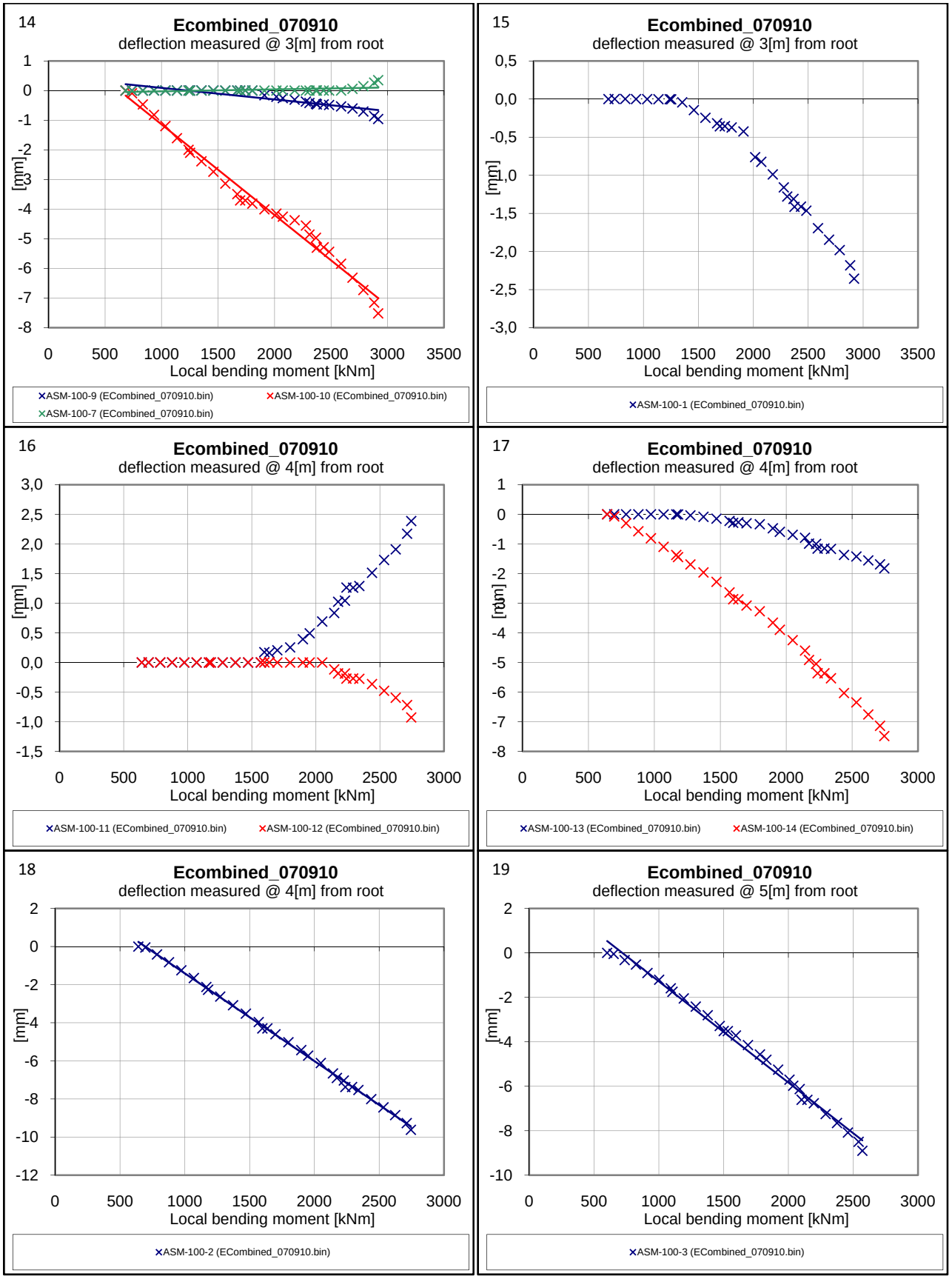

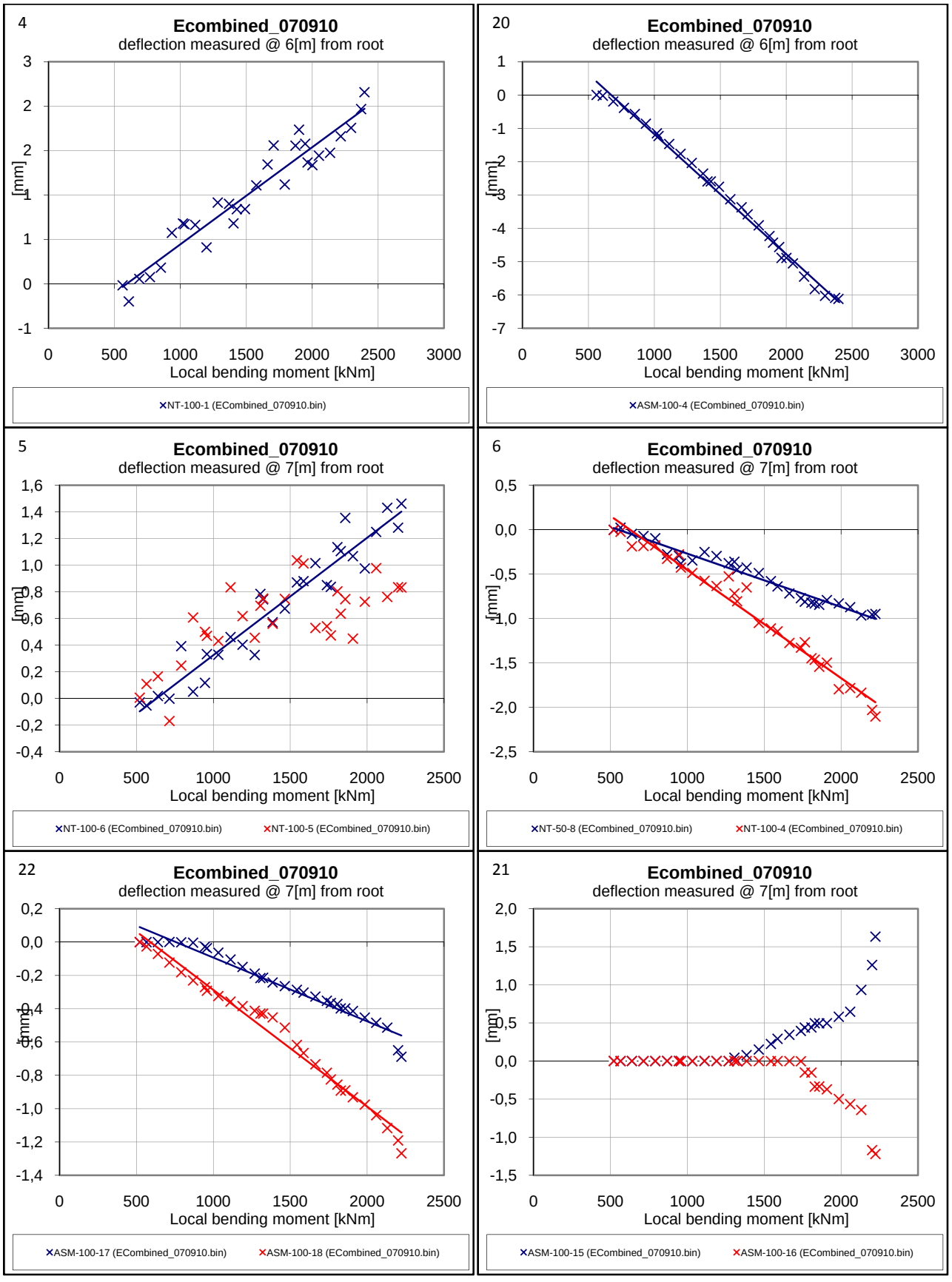
4
Ecombined_070910
deflection measured @ 6[m] from root
[mm]
Local bending moment [kNm]
NT-100-1 (ECombined_070910.bin)
20
Ecombined_070910
deflection measured @ 6[m] from root
[mm]
Local bending moment [kNm]
ASM-100-4 (ECombined_070910.bin)
5
Ecombined_070910
deflection measured @ 7[m] from root
[mm]
Local bending moment [kNm]
NT-100-6 (ECombined_070910.bin)
NT-100-5 (ECombined_070910.bin)
6
Ecombined_070910
deflection measured @ 7[m] from root
[mm]
Local bending moment [kNm]
NT-50-8 (ECombined_070910.bin)
NT-100-4 (ECombined_070910.bin)
22
Ecombined_070910
deflection measured @ 7[m] from root
[mm]
Local bending moment [kNm]
ASM-100-17 (ECombined_070910.bin)
ASM-100-18 (ECombined_070910.bin)
21
Ecombined_070910
deflection measured @ 7[m] from root
[mm]
Local bending moment [kNm]
ASM-100-15 (ECombined_070910.bin)
ASM-100-16 (ECombined_070910.bin)

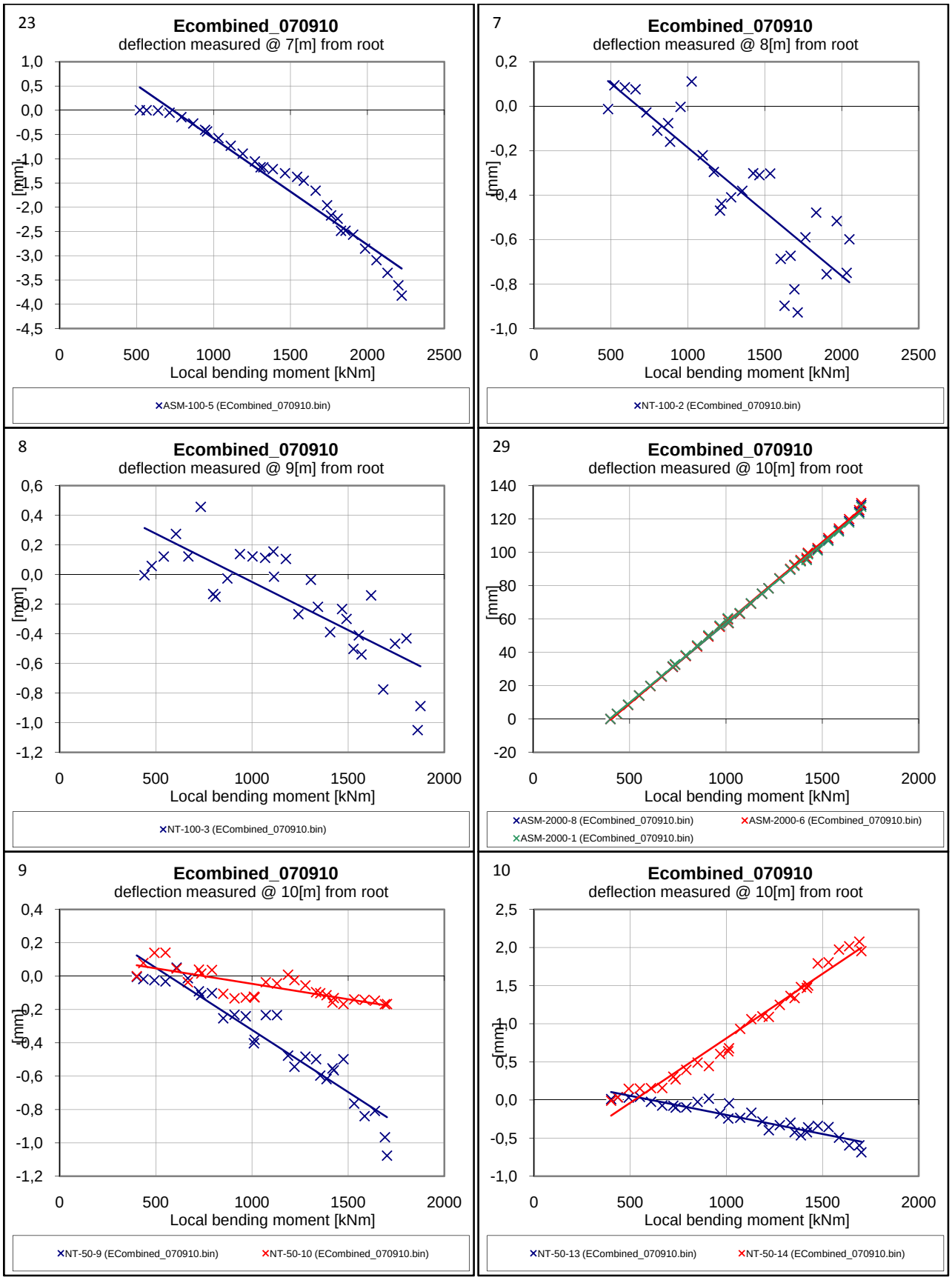
23
Ecombined_070910
deflection measured @ 7[m] from root
[mm]
Local bending moment [kNm]
ASM-100-5 (ECombined_070910.bin)
7
Ecombined_070910
deflection measured @ 8[m] from root
[mm]
Local bending moment [kNm]
NT-100-2 (ECombined_070910.bin)
8
Ecombined_070910
deflection measured @ 9[m] from root
[mm]
Local bending moment [kNm]
NT-100-3 (ECombined_070910.bin)
29
Ecombined_070910
deflection measured @ 10[m] from root
[mm]
Local bending moment [kNm]
ASM-2000-8 (ECombined_070910.bin)
ASM-2000-6 (ECombined_070910.bin)
ASM-2000-1 (ECombined_070910.bin)
9
Ecombined_070910
deflection measured @ 10[m] from root
[mm]
Local bending moment [kNm]
NT-50-9 (ECombined_070910.bin)
NT-50-10 (ECombined_070910.bin)
10
Ecombined_070910
deflection measured @ 10[m] from root
[mm]
Local bending moment [kNm]
NT-50-13 (ECombined_070910.bin)
NT-50-14 (ECombined_070910.bin)

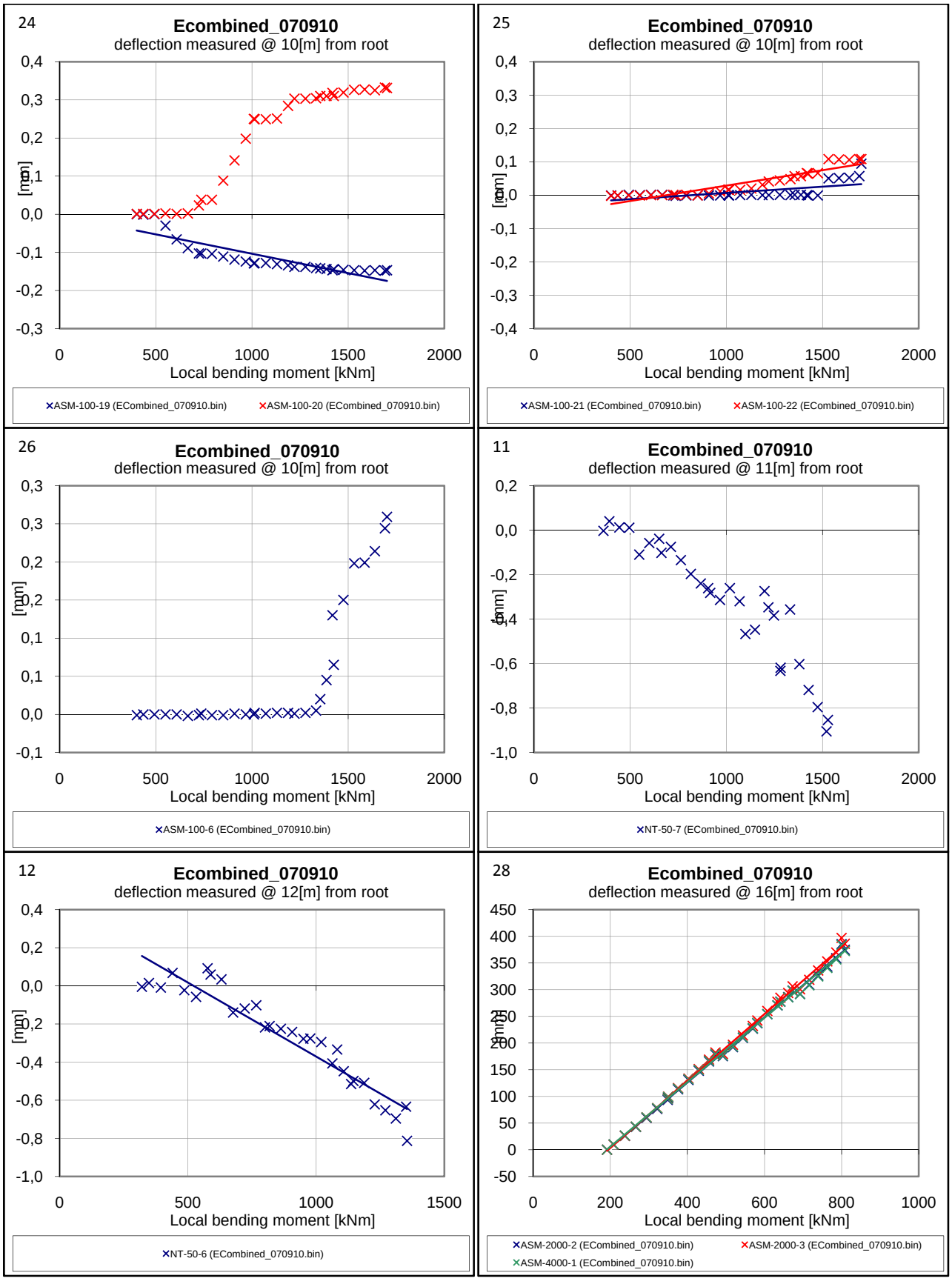
24
Ecombined_070910
deflection measured @ 10[m] from root
[mm]
Local bending moment [kNm]
ASM-100-19 (ECombined_070910.bin)
ASM-100-20 (ECombined_070910.bin)
25
Ecombined_070910
deflection measured @ 10[m] from root
[mm]
Local bending moment [kNm]
ASM-100-21 (ECombined_070910.bin)
ASM-100-22 (ECombined_070910.bin)
26
Ecombined_070910
deflection measured @ 10[m] from root
[mm]
Local bending moment [kNm]
ASM-100-6 (ECombined_070910.bin)
11
Ecombined_070910
deflection measured @ 11[m] from root
[mm]
Local bending moment [kNm]
NT-50-7 (ECombined_070910.bin)
12
Ecombined_070910
deflection measured @ 12[m] from root
[mm]
Local bending moment [kNm]
NT-50-6 (ECombined_070910.bin)
28
Ecombined_070910
deflection measured @ 16[m] from root
[mm]
Local bending moment [kNm]
ASM-2000-2 (ECombined_070910.bin)
ASM-2000-3 (ECombined_070910.bin)
ASM-4000-1 (ECombined_070910.bin)

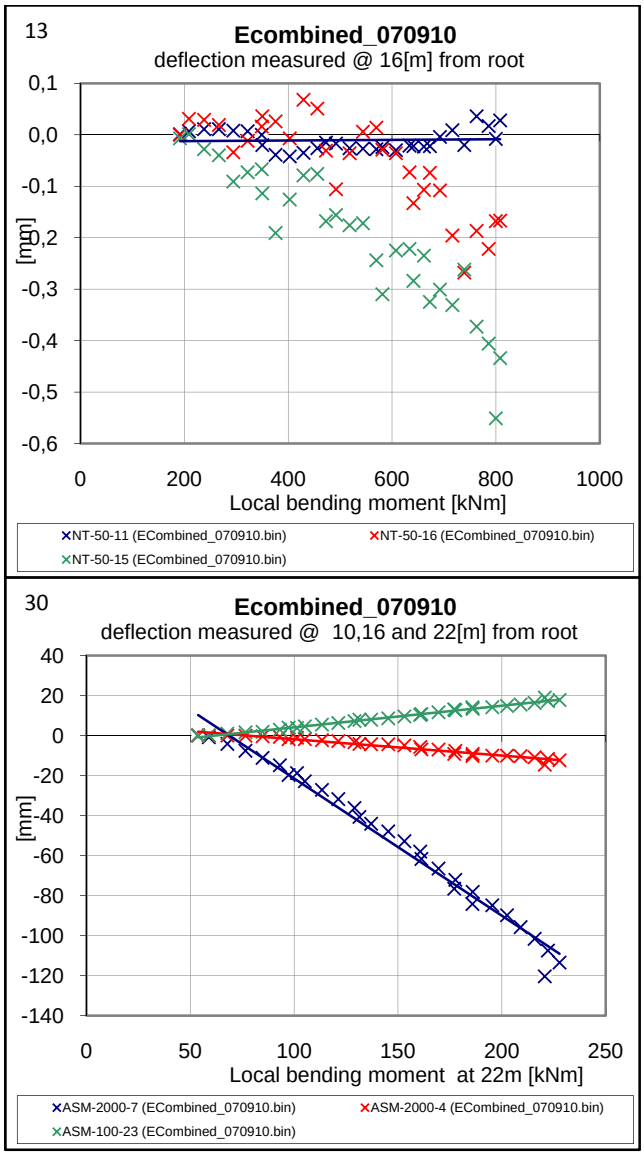
13
Ecombined_070910
deflection measured @ 16[m] from root
0,1
0,0
-0,1
-0,2
-0,3
-0,4
-0,5
-0,6
[mm]
0
200
400
600
800
1000
Local bending moment [kNm]
NT-50-11 (ECombined_070910.bin)
NT-50-16 (ECombined_070910.bin)
NT-50-15 (ECombined_070910.bin)

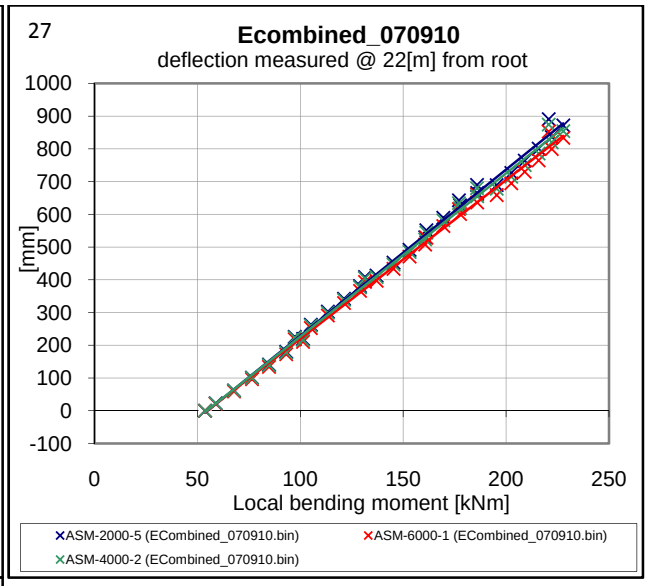
27
Ecombined_070910
deflection measured @ 22[m] from root
1000
900
800
700
600
500
400
300
200
100
0
-100
[mm]
0
50
100
150
200
250
Local bending moment [kNm]
ASM-2000-5 (ECombined_070910.bin)
ASM-6000-1 (ECombined_070910.bin)
ASM-4000-2 (ECombined_070910.bin)

30
Ecombined_070910
deflection measured @ 10,16 and 22[m] from root
40
20
0
-20
-40
-60
-80
-100
-120
-140
[mm]
0
50
100
150
200
250
Local bending moment at 22m [kNm]
ASM-2000-7 (ECombined_070910.bin)
ASM-2000-4 (ECombined_070910.bin)
ASM-100-23 (ECombined_070910.bin)

C Acoustic Emission

Blade test at VIM facility

1615140-00 (AFM PSP for this work)

Erik and Kaj use this, Malcolm uses SESS instead

Combined loading

Blade is twisted (120deg counterclockwise seen from the tip) with trailing edge up

Tuesday 07th September 2010

1100 Kaj and Erik set up sensors and cabling

1230 Malcolm arrives and sets up laptop and Pocket PAC

Pocket PAC running bladetest01.lay (40dB THS, 26dB gain from inline preamp)

100907SSP80.dta

CH1 4m S Central spar

C2 10,5m S Central spar

Both sensors are sensitive returning hits from strip flicks 1,0m away on sensor face

The blade will be tested to 55% load at 1400 this afternoon

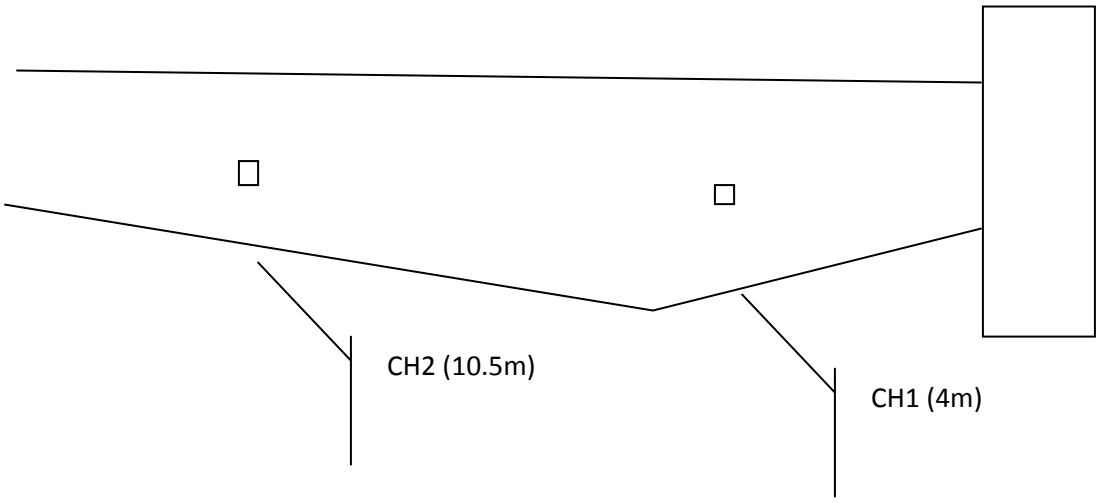

Test set up

1315 During the sensor check I notice that the cables take CH1 to 10m and CH2 to 4m. I'll swap the PIN connections at the Pocket PAC so we stay with the planned instrumentation described above. Otherwise both sensors seem to be connected well and ready to test.

1330 AV on (Erik Vogeley to help), then Test plan specifies load to 12,5% and then ARAMIS on and AE on. The test will be up to 50%, perhaps 55%, without pauses and then down again. Per loads and updates with load levels. Malcolm to advise AE responses; note that 4m is in focus for two reasons – the first that there may be damage present, also that buckling here is a possibility.

1420 No data acquisition → Load to 13%

1430 AV on and ARAMIS on

1438 13% and increasing

1439 20%

1440 25%

1441 30%

1442 35%

1443 40%

1445 45%

1446 50%

1447 55% AND UNLOAD

Unloading process in complex with only a few hits of long duration

Once at 40% (1505) the AE system is stopped

GRAPHS (extracted from DiSP system bladeviewer.lay)

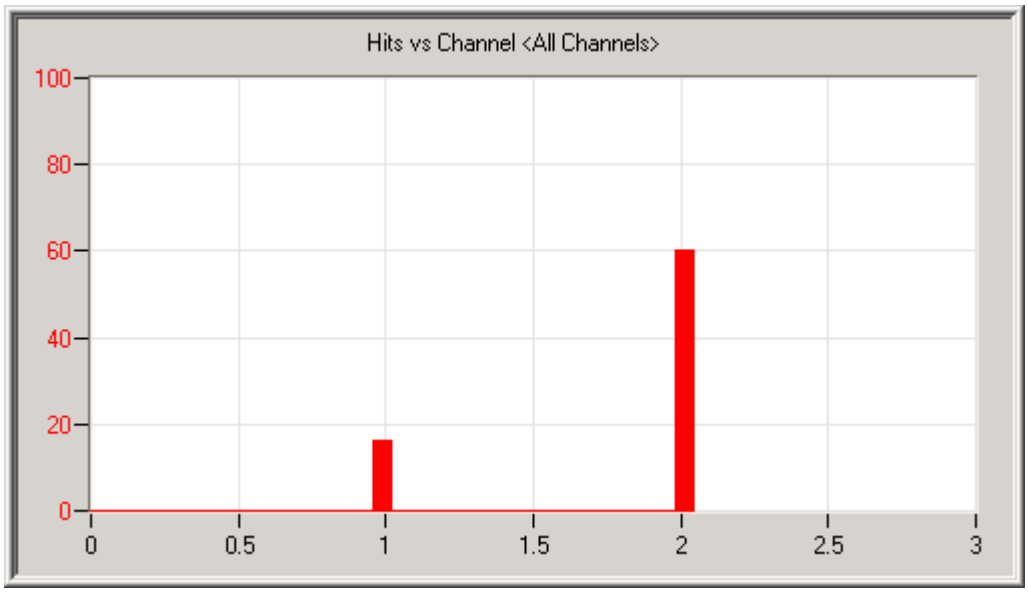

Graph showing hits at CH1 (4m) and CH2 (10,5m)

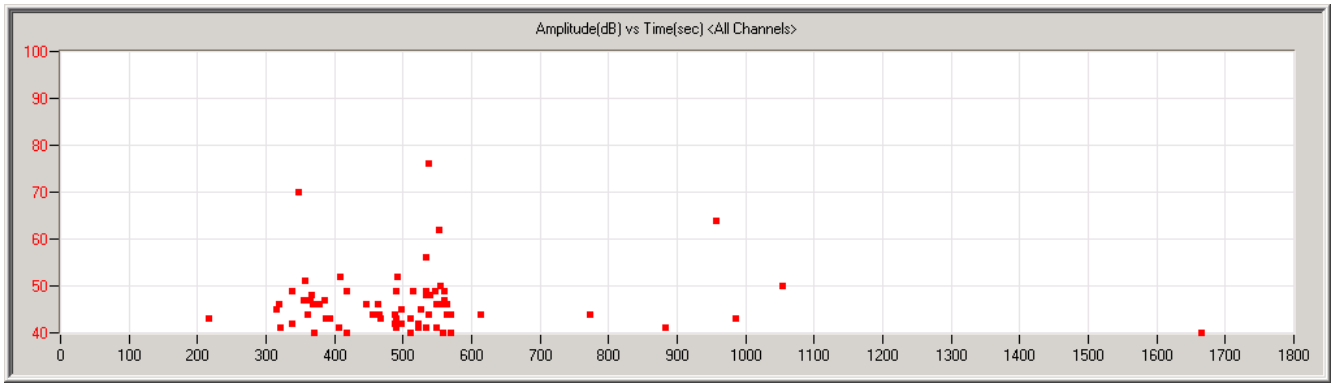

AMP vs time (point) All hits from Ch1 and 2

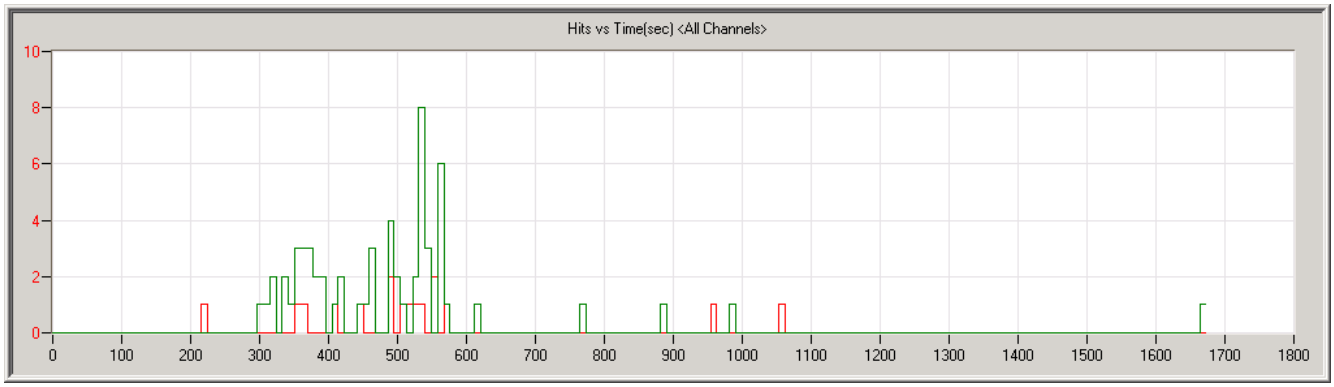

Hits vs time (Burst) Ch1/4m – RED, Ch2/11m - GREEN

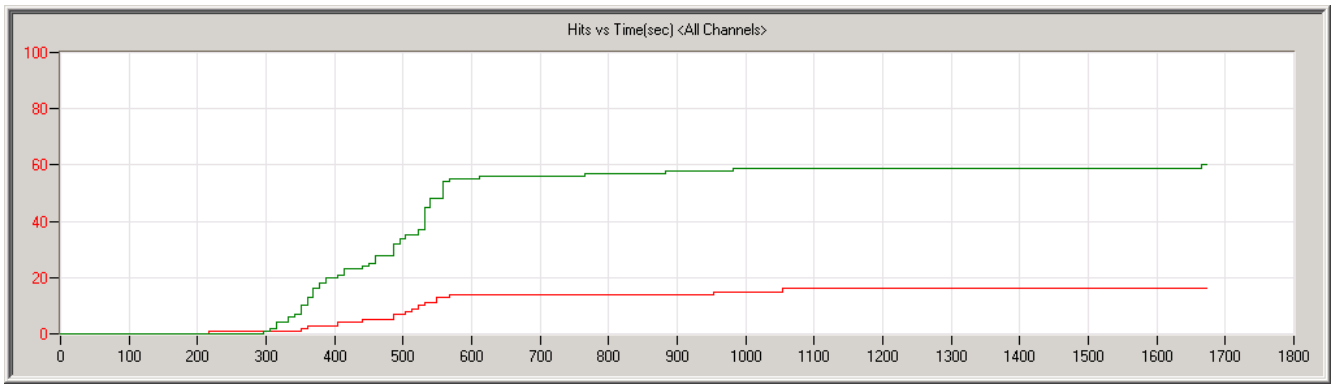

Hits vs time (CUM) Ch1/4m – RED, Ch2/11m - GREEN

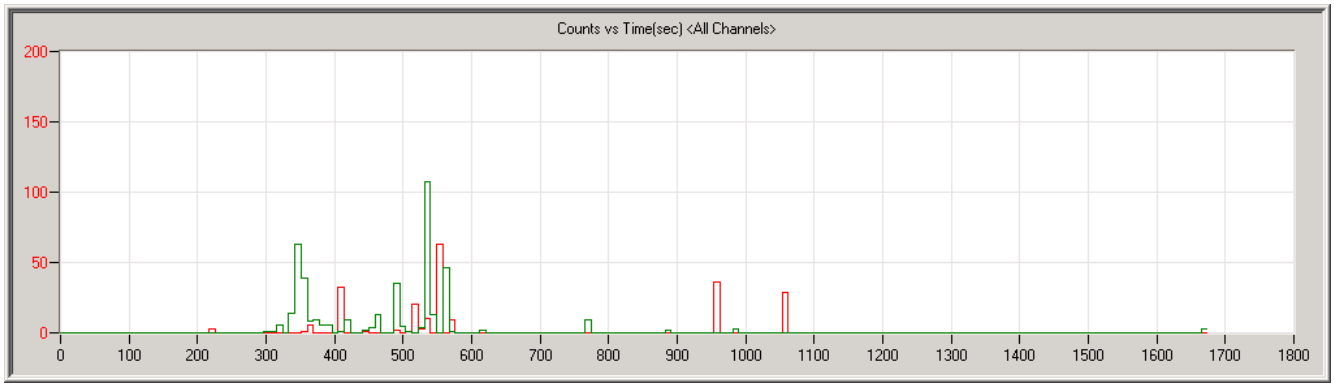

Cnts vs time (Burst) Ch1/4m – RED, Ch2/11m - GREEN

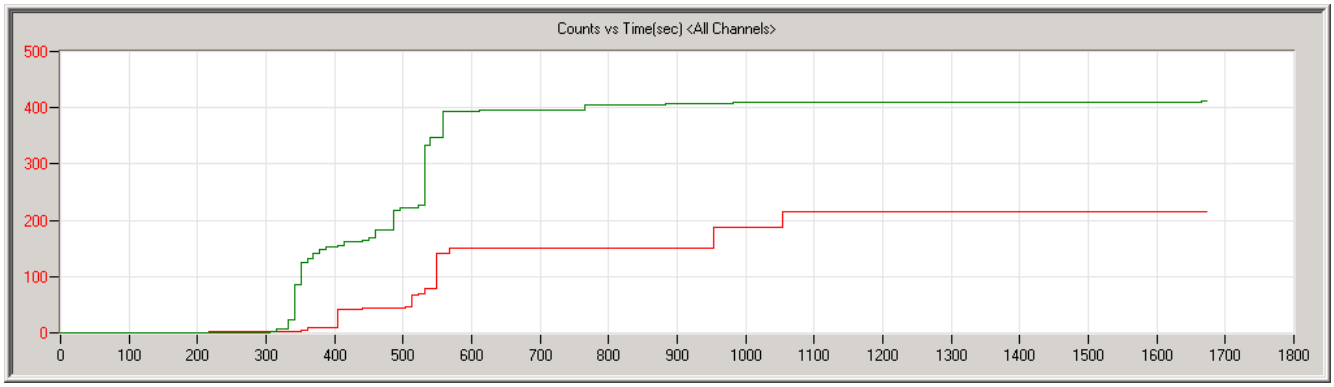

Cnts vs time (CUM) Ch1/4m – RED, Ch2/11m - GREEN

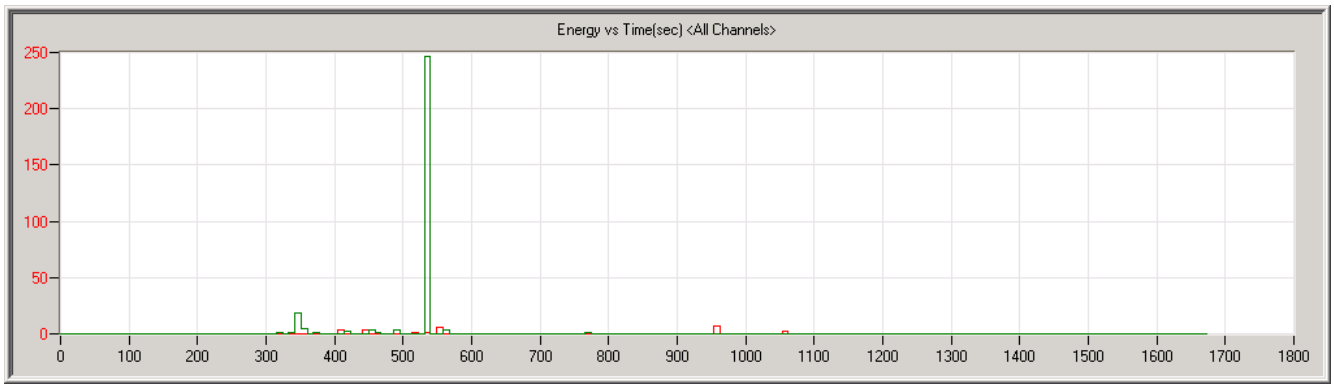

Energy vs time (Burst) Ch1/4m – RED, Ch2/11m - GREEN

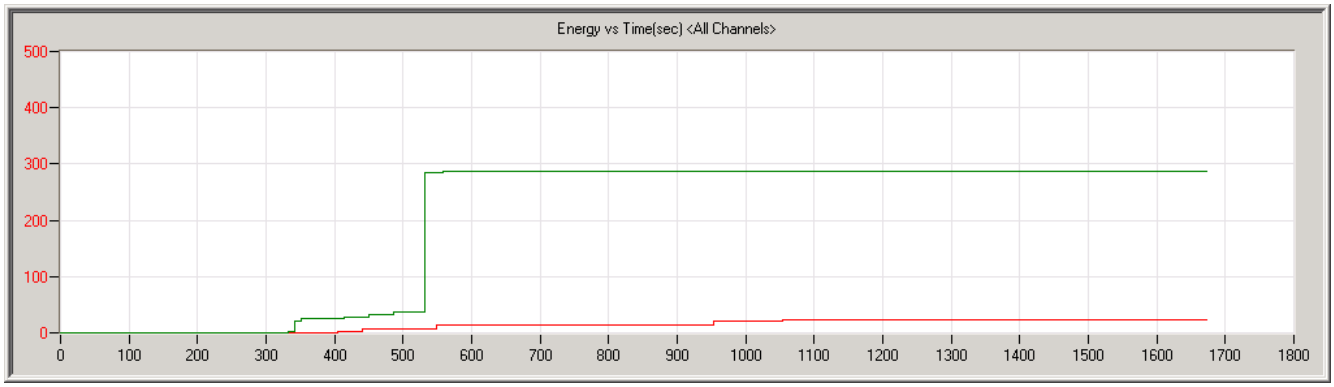

Energy vs time (CUM) Ch1/4m – RED, Ch2/11m - GREEN

Notes:

There is some activity from load level 35% on both sensors (mostly CH2, 10,5m) increasing up to the maximum load of 55%.

Only one event of significance occurs on CH2 (10,5m) at approximately 530s, when the blade is at maximum load (55%). The hit is AMP 78dB with an energy content of almost 250.

D Deformation of the sections

Deformationen af vingen for to snit 4 og 7 meter.

4 Meter

Test: Ecombined_020910 – 35% last.

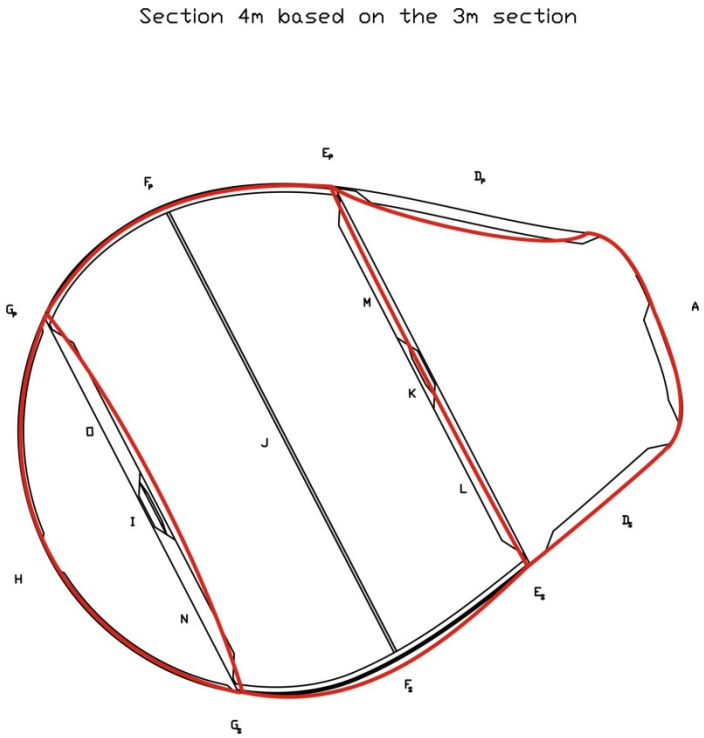

ASM resultater	[mm]
I-J	-2,9
K-J	-0,45
G_s-E_p	0
G_p-E_s	0
D_s-D_p	-3,9

	F_s	D_s	D_p	F_p
NT [mm]	1,5	0	-4,25	-0,4

7 meter

Test: ECombined_070910 – 55% last.

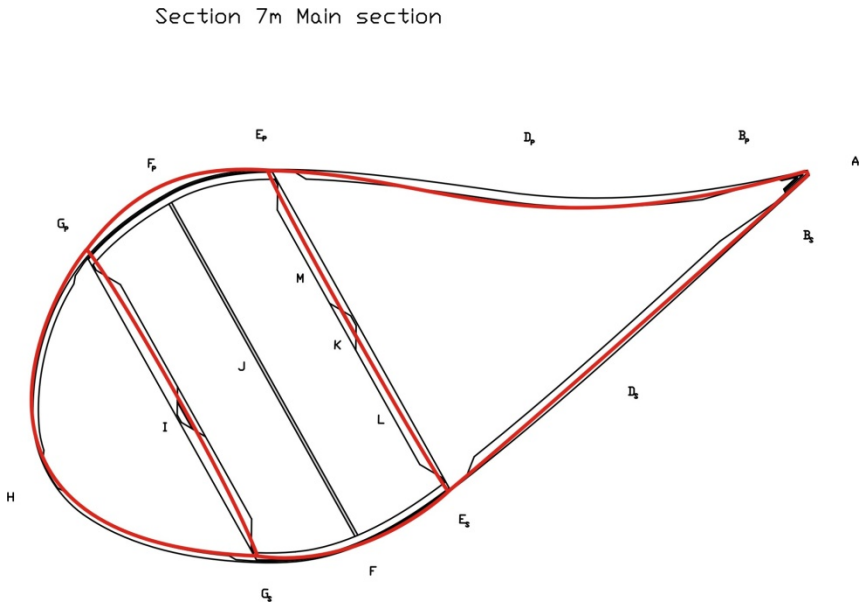

ASM resultater	[mm]
I-J	-1,2
K-J	-0,6
G_s-E_p	-1
G_p-E_s	1,5
D_s-D_p	-3,5

	F_s	D_s	D_p	F_p
NT [mm]	0,8	-1	-2	1,4

Test: Ecombined_070910

Deformationen af vingen for tre snit, 10, 16 og 22 meter.

10m section

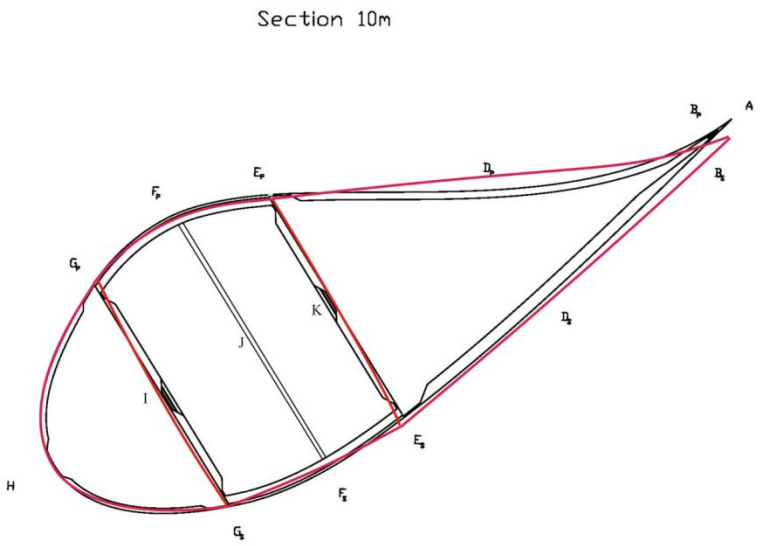

ASM målninger	[mm]
I-J	0,1
K-J	0,1
G_s-E_p	0,35
G_p-E_s	-0,15
D_s-D_p	0,3

	G_s – E_s	G_s – A	E_s - A
Global udbøjning [mm]	-1,07	-2,21	-1,14

	F_s	D_s	D_p	F_p
NT [mm]	-1,4	-0,75	3	-0,4

16m section

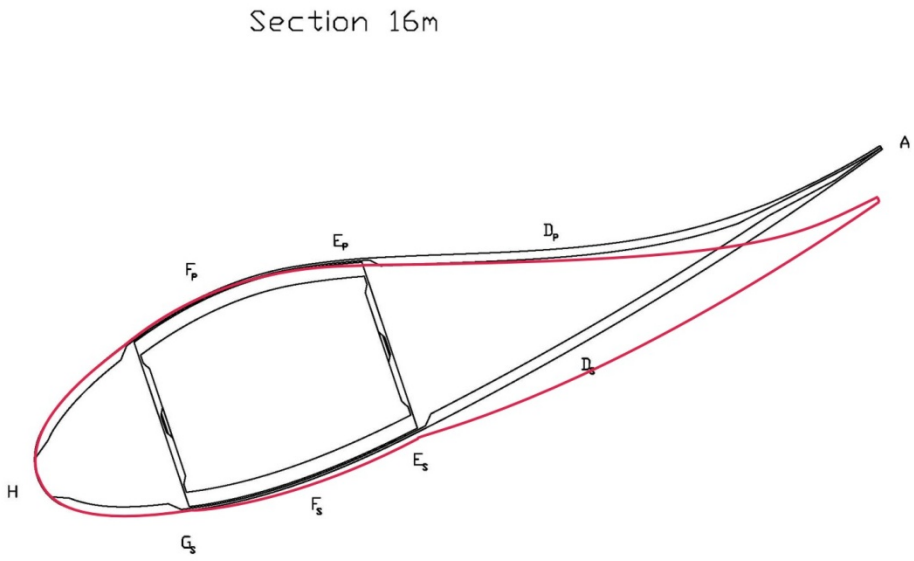

	$G_s - E_s$	$G_s - A$	E_s - A
Global udbøjning [mm]	-1,82	-13,4	-11,6

	F_s	D_s	D_p	F_p
NT [mm]	0	-0,5	-0,3	N/A

22m section

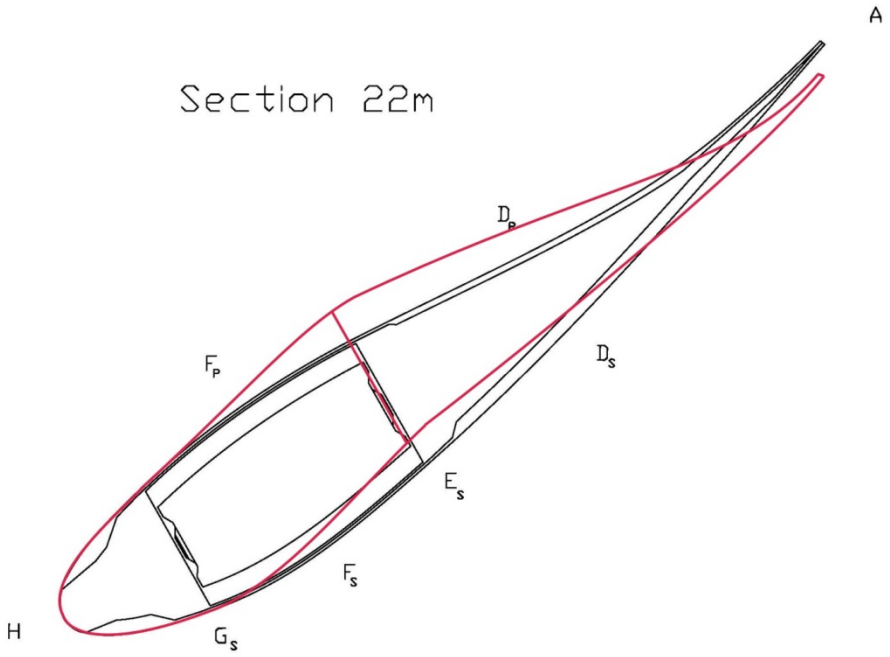

	$G_S - E_S$	$G_S - A$	E_S - A
Global udbøjning [mm]	21,9	-16,5	-38,4

E Calculation of the global horizontal deflection.

Vingens bevægelse er ned mod gulvet og den samlede flytning af vingen denne vej er ca. 1 m. Det er derfor nødvendigt at korrigere målingen for denne bevægelse når man vil bestemme vingens vandrette bevægelse.

Nedenfor at angivet de nødvendige mål der er taget i hallen for at bestemme den vandrette bevægelse.

Vandret på gulv.	Fra væg til f	a-e	E g
	4,95	0,68	0,36
Lodret fra gulv	til a	til e	Til g
	4,60m	3,95m	3,60m

22m

vandret	Fra væg til f	a-e	e-g
	4,10	1,08	0,46
Lodret fra gulv	til a	til e	Til g
	4,20	3,35	3,10

16m

vandret	Fra væg til f	a-e	e-g
	3,75	1,13	0,64
Lodret fra gulv	til a	til e	Til g
	3,60	2,80	2,53

Overslag over vandret bevægelse i 22m.

Nedenfor er vist fremgangsmåden og resultatet af beregningen af den vandrette bevægelse samt størrelsen af den vandrette bevægelses indflydelse på den lodrette bevægelse.

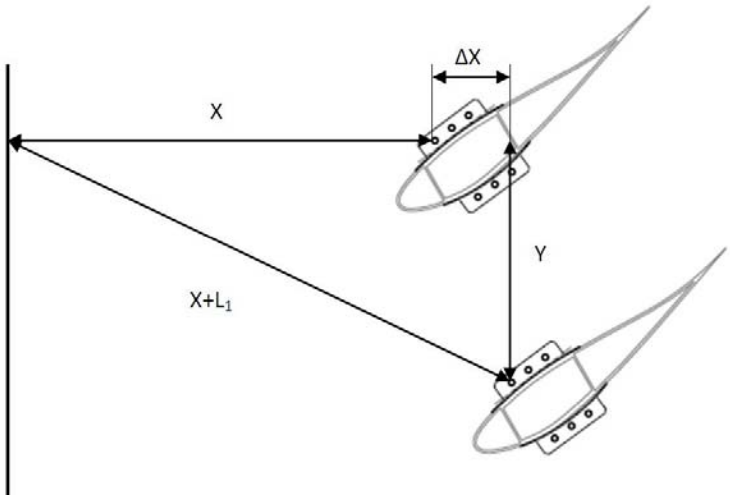

Billedet viser sammenhængen mellem de registrerede længdeændringer af ASM-målingerne Y og L_1 samt den deraf følgende sidevers forskydning ΔX.

$$\Delta X = \sqrt{(X + L_1)^2 - Y^2} - X$$

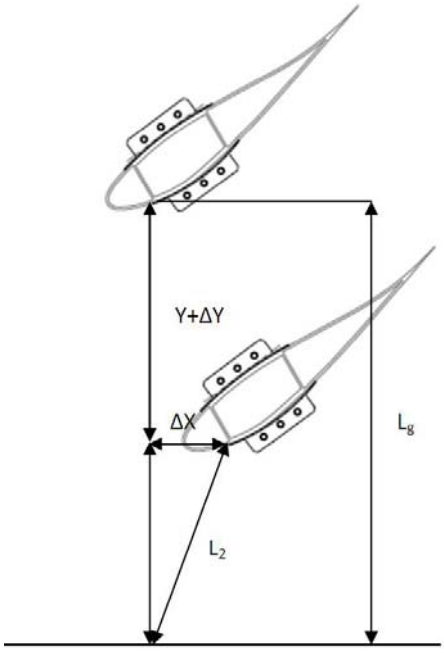

Billedet viser det sideværts forskydning, og den betydning denne har på målingen af vingens lodrette bevægelse. L_2 er differensen mellem afstanden til vingen i ubelastede tilstand L_g og den registrerede

længdeændring af ASM-målingen Y. Den vandrette bevægelses indflydelse på den lodrette bevægelse findes som ΔY, hvor ΔY er forskellen mellem den registrerede måling og den lodrette bevægelse.

Værdierne i for L1 og Y i tabellen er resultater fra Pull Ecombined070910

$$\Delta Y = L_g - \sqrt{(L_g - Y)^2 - \Delta X^2} - Y$$

Section	**22m**	**16m**	**10m**
X	4950	4100	3750
Lg	3600	3100	2350
L1	158,5	19,4	-25
Y	1150	512	167,5
vandret forskydning			
ΔX	27,4	-12,5	-28,8
korrektion for lodret udbøjning som følge af ΔX			
ΔY	0,153	0,030	0,190

Tabellen viser sammenhængen mellem den sideværts forskydning og den lodrette udbøjning. Det ses tydeligt at den sideværts forskydning har negligerbar betydning for den lodrette udbøjning.

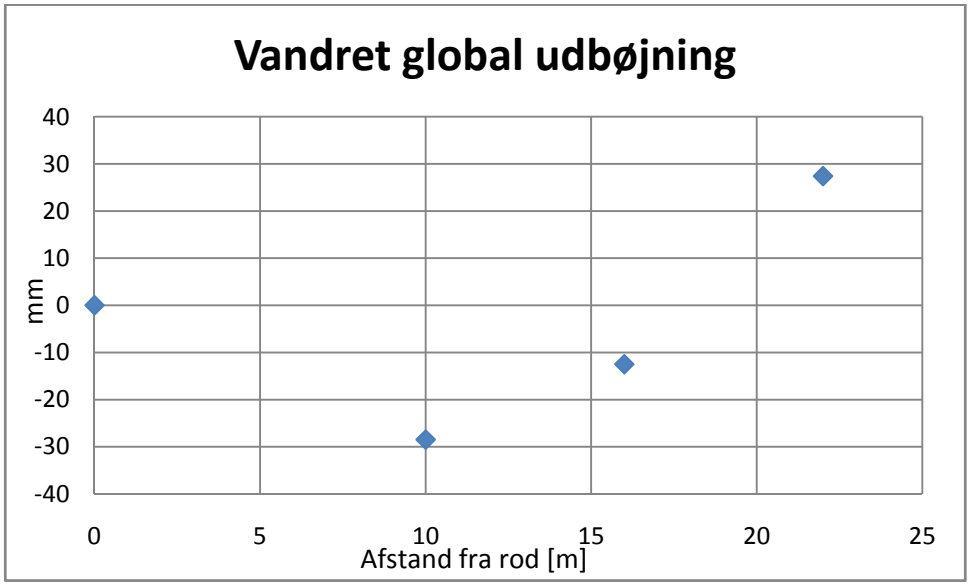

F Repeated deflection measurement graphs.

Results of deflection measurements from pull Ecombined_300810, Ecombined_010910, Ecombined_020910 put together.

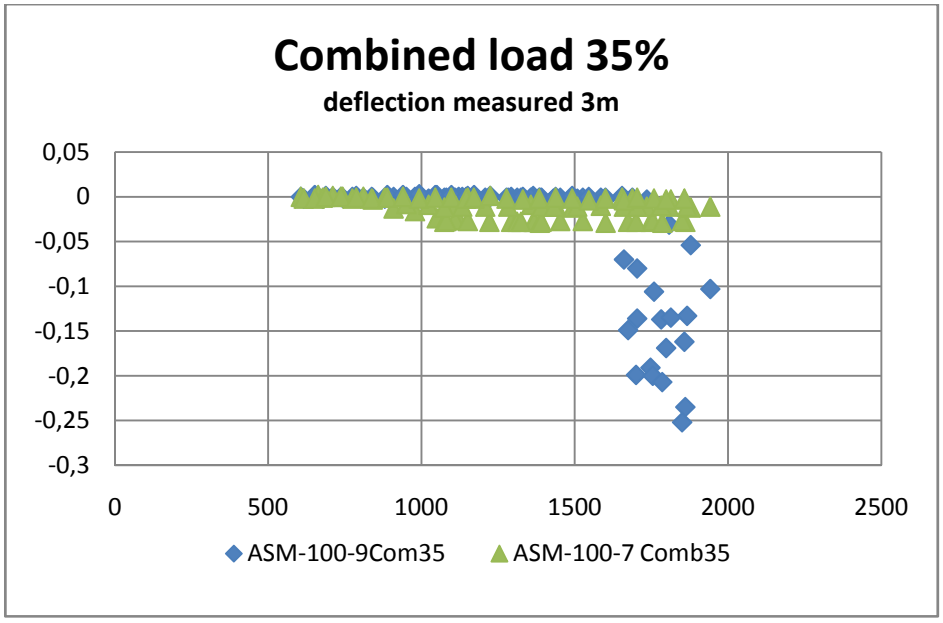

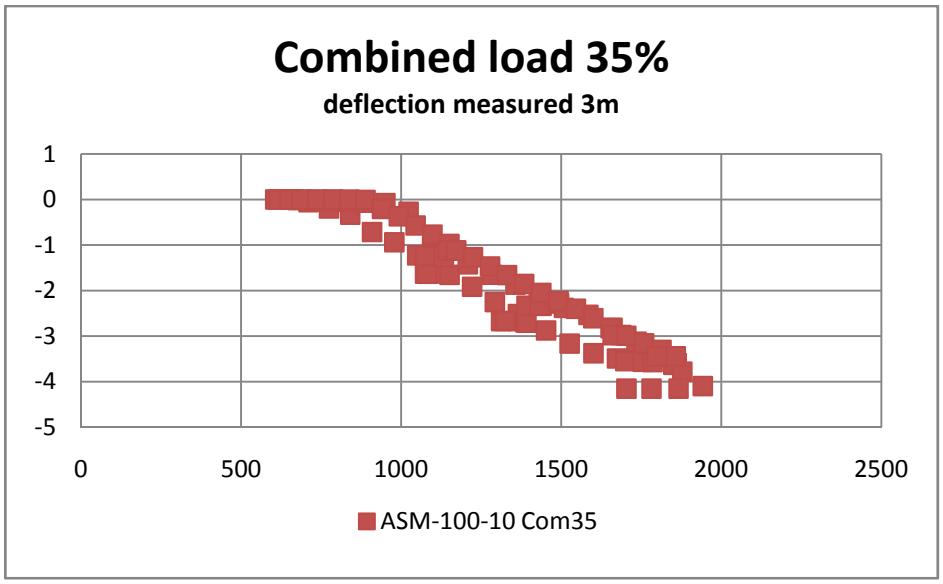

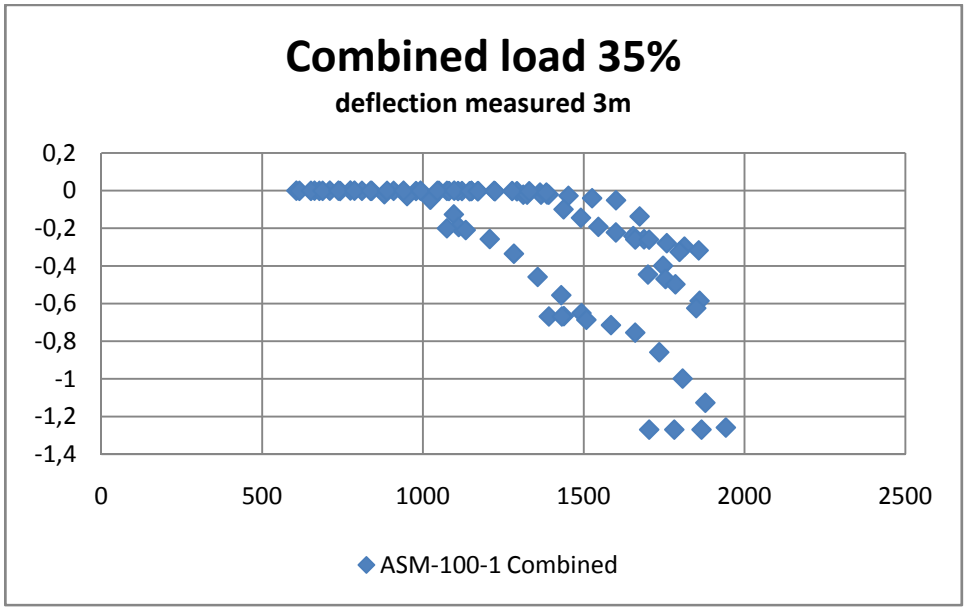
Combined load 35%
deflection measured 3m
0,2
0
-0,2
-0,4
-0,6
-0,8
-1
-1,2
-1,4
0
500
1000
1500
2000
2500
ASM-100-1 Combined

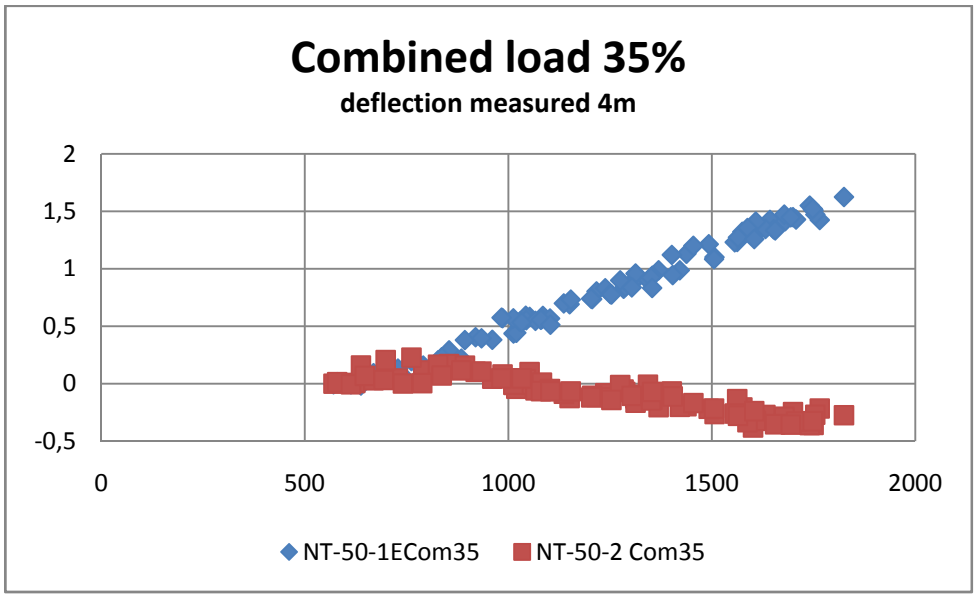
Combined load 35%
deflection measured 4m
2
1,5
1
0,5
0
-0,5
0
500
1000
1500
2000
NT-50-1ECom35
NT-50-2 Com35

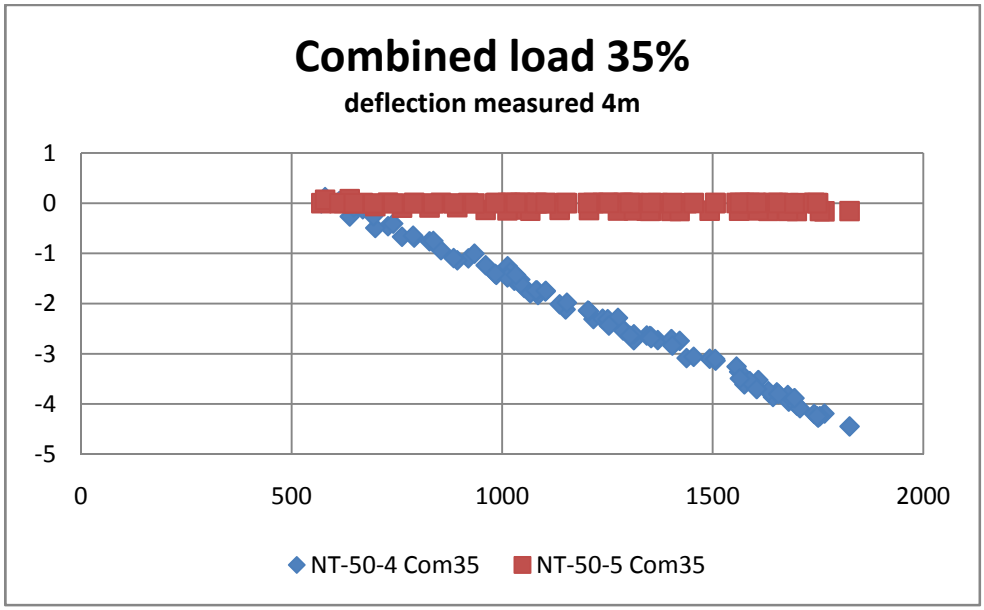
Combined load 35%
deflection measured 4m
1
0
-1
-2
-3
-4
-5
0
500
1000
1500
2000
NT-50-4 Com35
NT-50-5 Com35

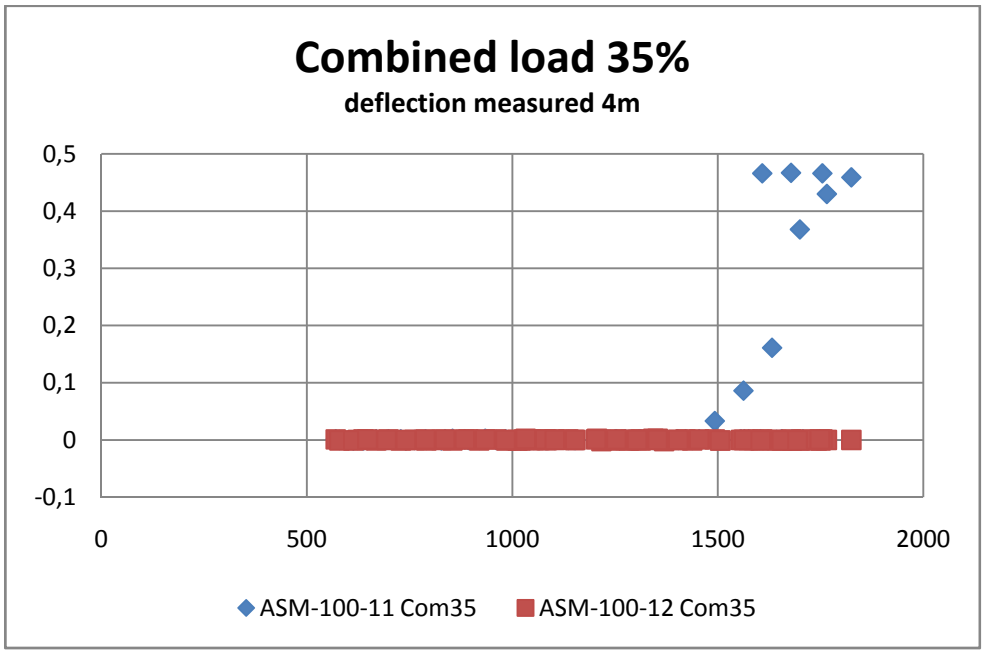
Combined load 35%
deflection measured 4m
0,5
0,4
0,3
0,2
0,1
0
-0,1
0
500
1000
1500
2000
ASM-100-11 Com35
ASM-100-12 Com35

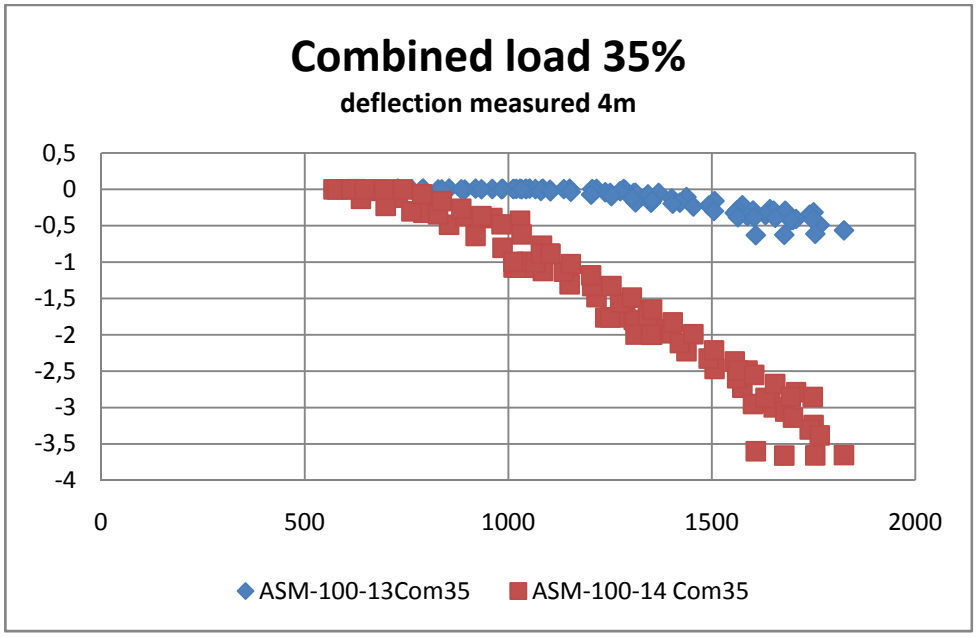
Combined load 35%
deflection measured 4m
0,5
0
-0,5
-1
-1,5
-2
-2,5
-3
-3,5
-4
0
500
1000
1500
2000
ASM-100-13Com35
ASM-100-14 Com35

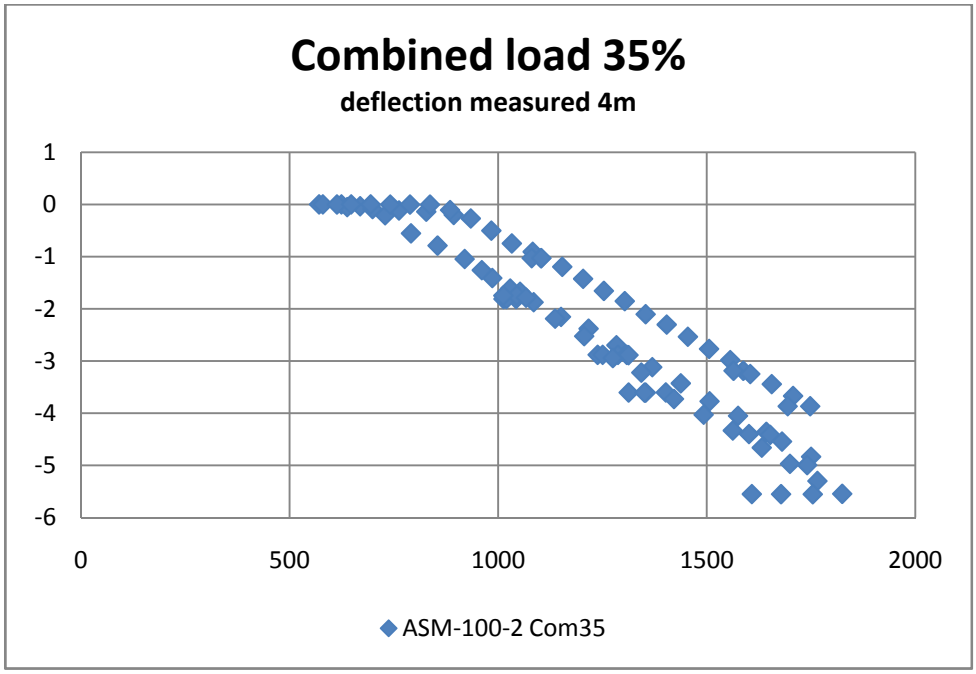
Combined load 35%
deflection measured 4m
1
0
-1
-2
-3
-4
-5
-6
0
500
1000
1500
2000
ASM-100-2 Com35

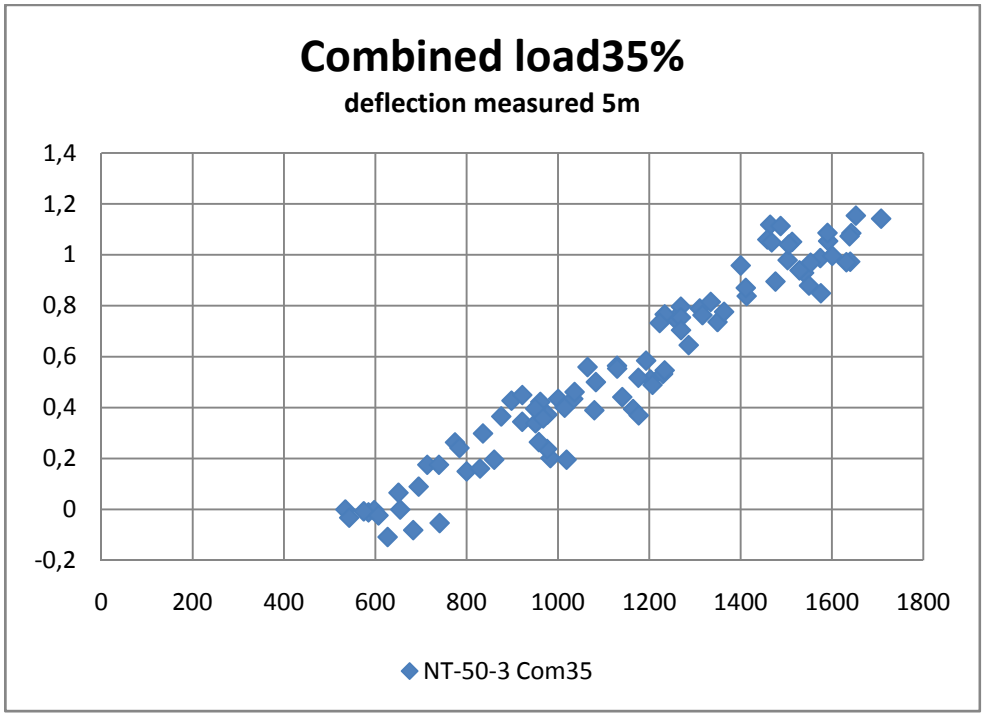
Combined load35%
deflection measured 5m
1,4
1,2
1
0,8
0,6
0,4
0,2
0
-0,2
0
200
400
600
800
1000
1200
1400
1600
1800
NT-50-3 Com35

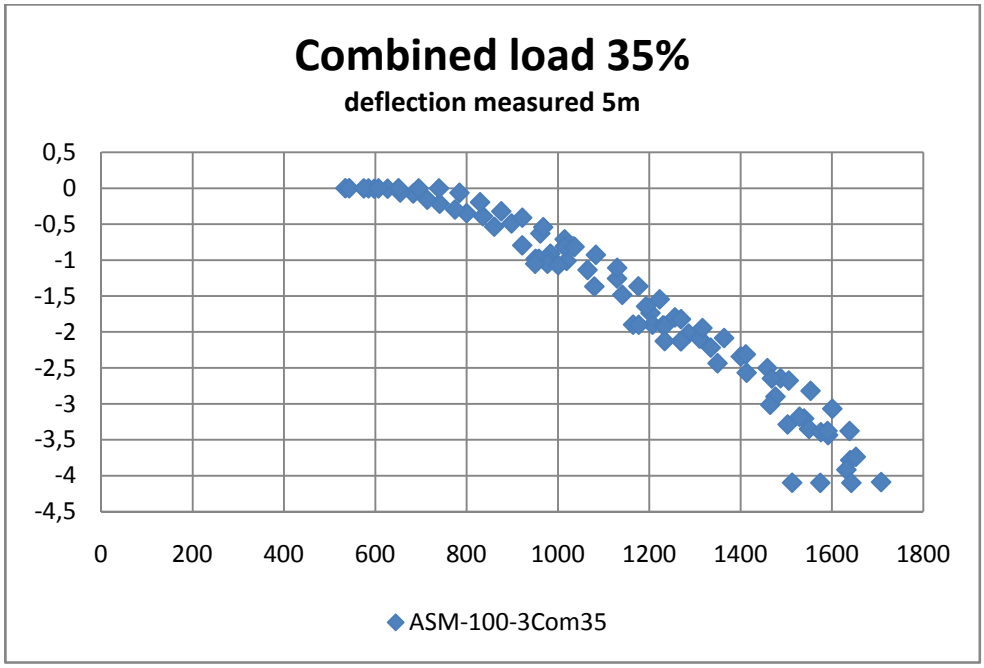
Combined load 35%
deflection measured 5m
0,5
0
-0,5
-1
-1,5
-2
-2,5
-3
-3,5
-4
-4,5
0
200
400
600
800
1000
1200
1400
1600
1800
ASM-100-3Com35

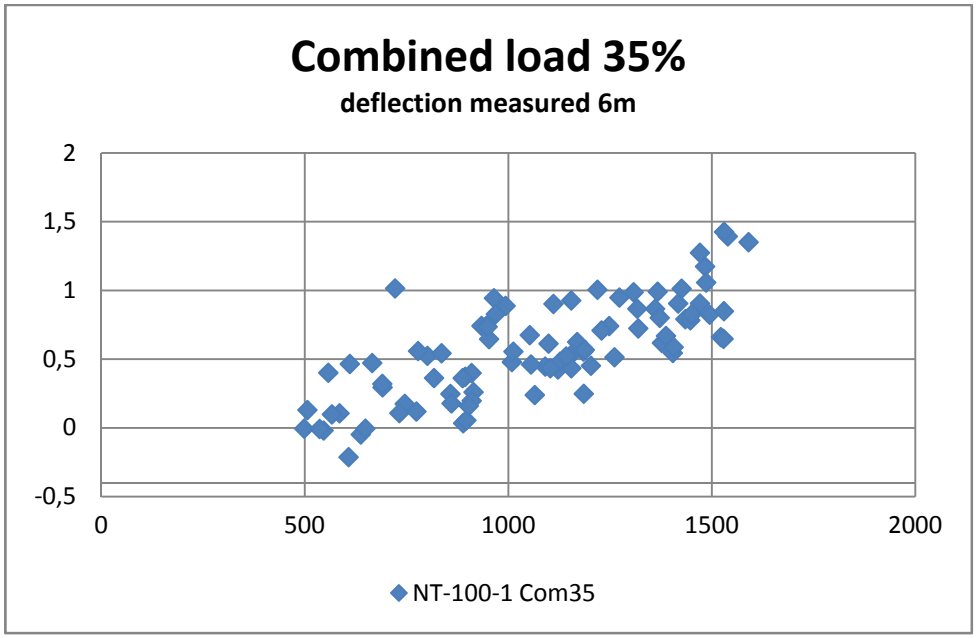
Combined load 35%
deflection measured 6m
2
1,5
1
0,5
0
-0,5
0
500
1000
1500
2000
NT-100-1 Com35

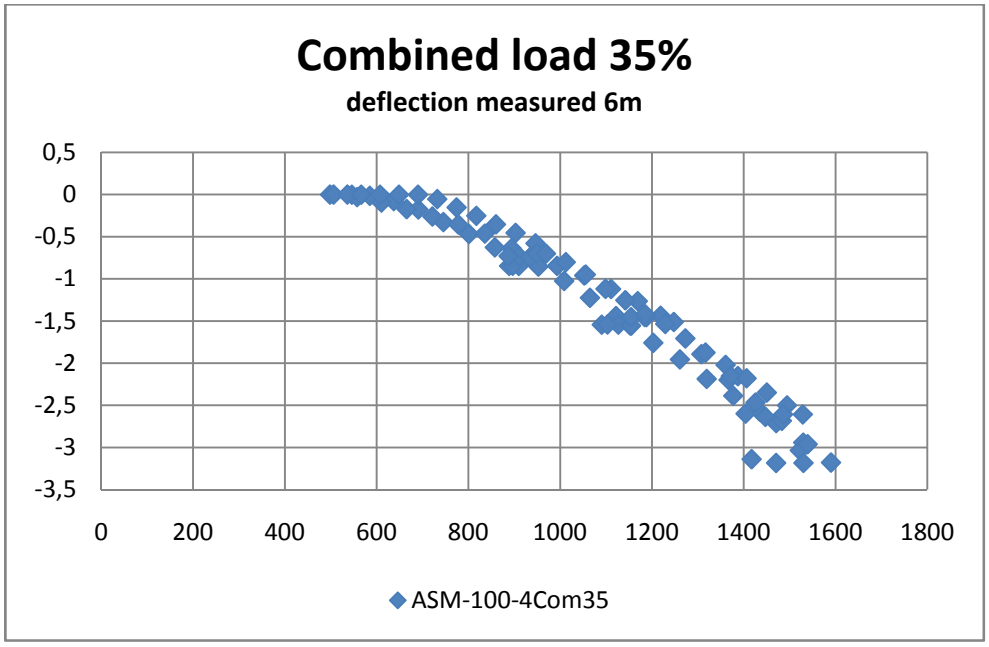
Combined load 35%
deflection measured 6m
0,5
0
-0,5
-1
-1,5
-2
-2,5
-3
-3,5
0
200
400
600
800
1000
1200
1400
1600
1800
ASM-100-4Com35

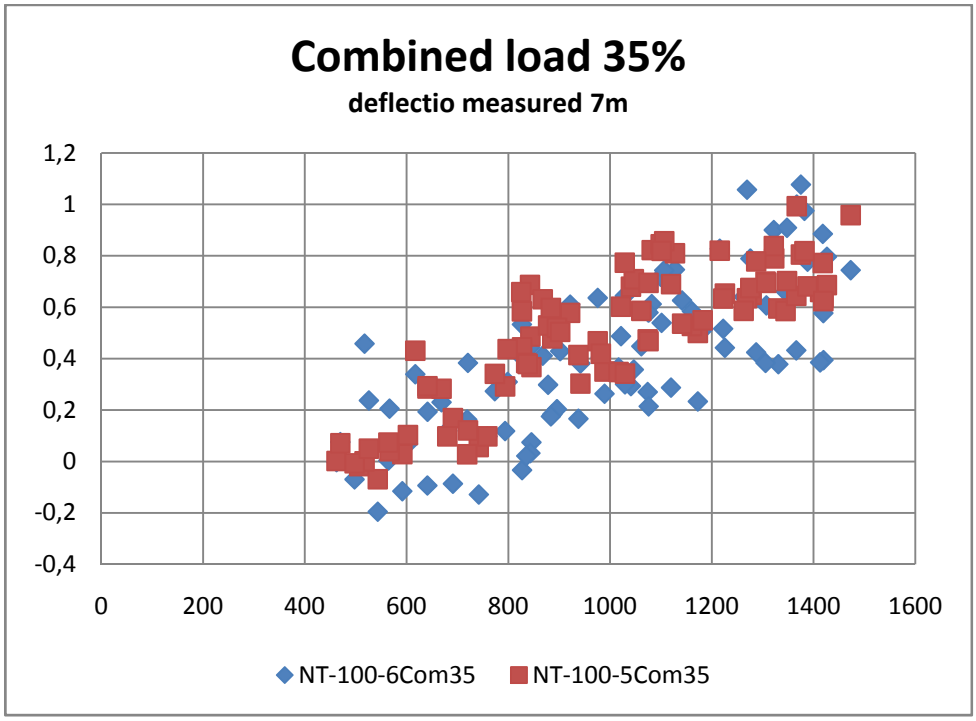
Combined load 35%
deflectio measured 7m
1,2
1
0,8
0,6
0,4
0,2
0
-0,2
-0,4
0
200
400
600
800
1000
1200
1400
1600
NT-100-6Com35
NT-100-5Com35

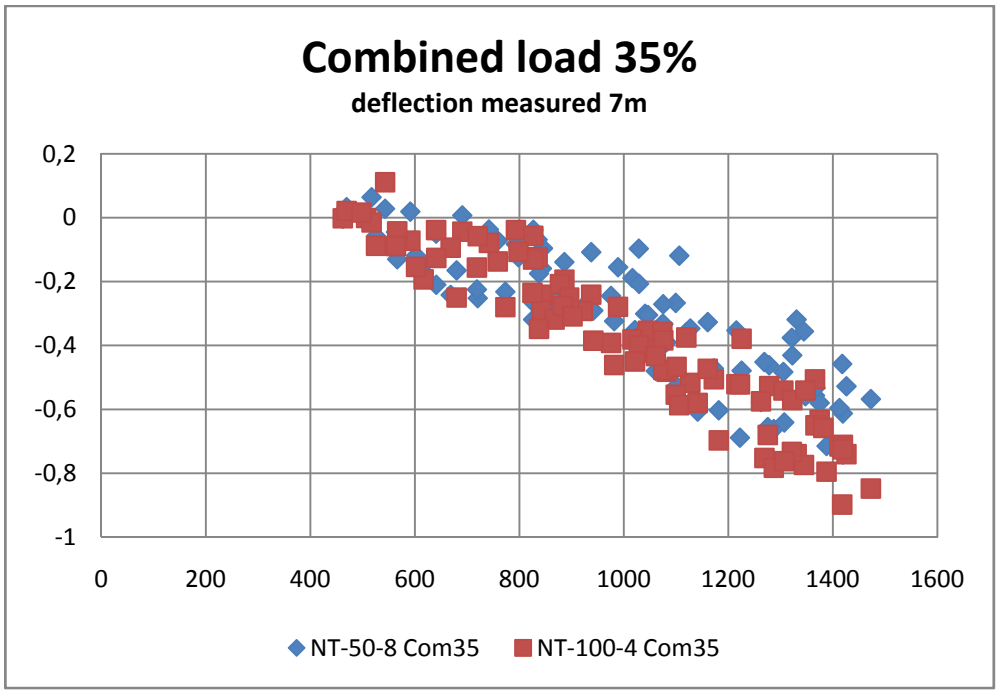
Combined load 35%
deflection measured 7m
0,2
0
-0,2
-0,4
-0,6
-0,8
-1
0
200
400
600
800
1000
1200
1400
1600
NT-50-8 Com35
NT-100-4 Com35

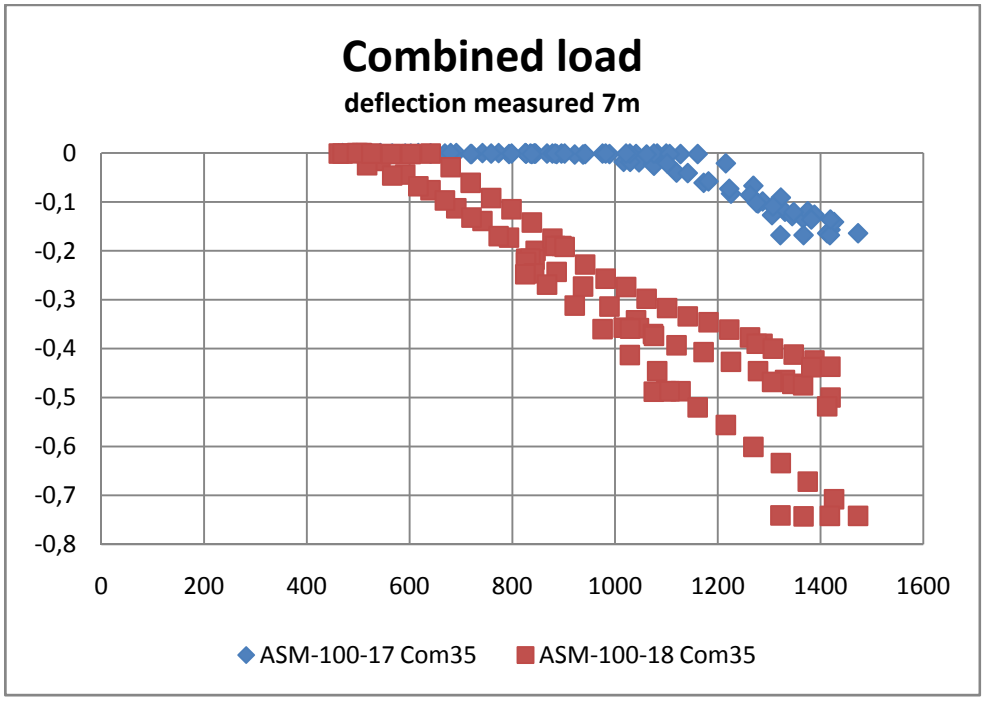
Combined load
deflection measured 7m
0
-0,1
-0,2
-0,3
-0,4
-0,5
-0,6
-0,7
-0,8
0
200
400
600
800
1000
1200
1400
1600
ASM-100-17 Com35
ASM-100-18 Com35

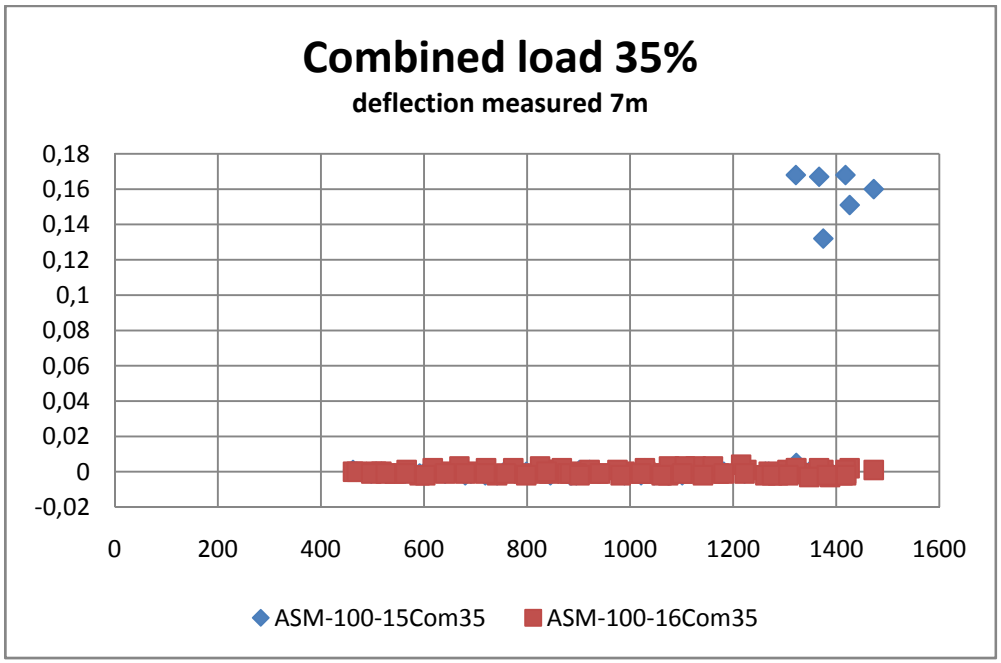
Combined load 35%
deflection measured 7m
0,18
0,16
0,14
0,12
0,1
0,08
0,06
0,04
0,02
0
-0,02
0
200
400
600
800
1000
1200
1400
1600
ASM-100-15Com35
ASM-100-16Com35

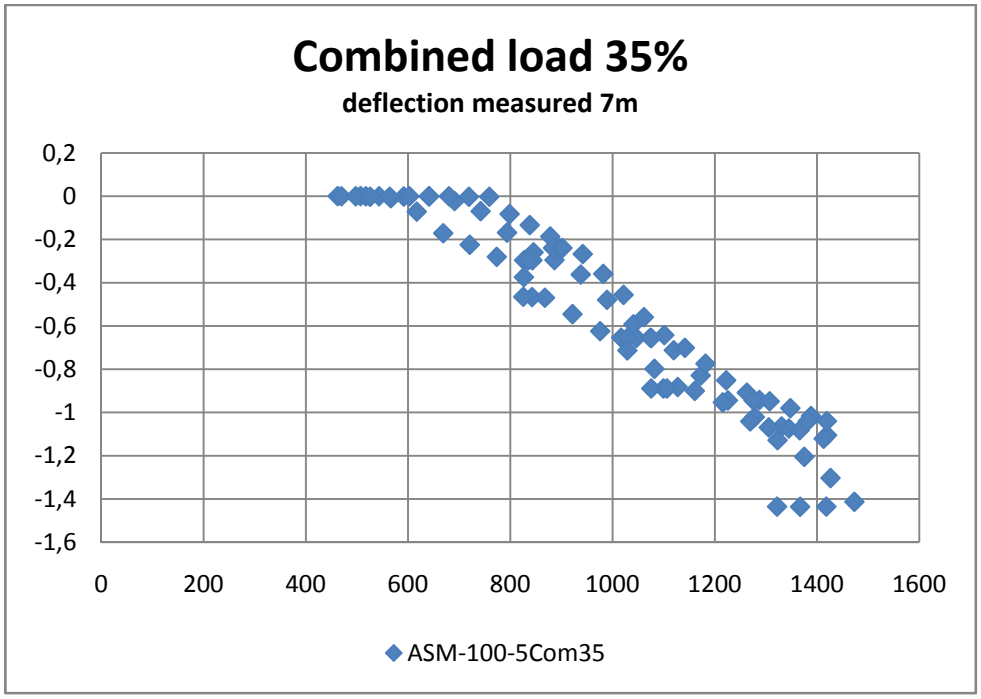
Combined load 35%
deflection measured 7m
0,2
0
-0,2
-0,4
-0,6
-0,8
-1
-1,2
-1,4
-1,6
0
200
400
600
800
1000
1200
1400
1600
ASM-100-5Com35

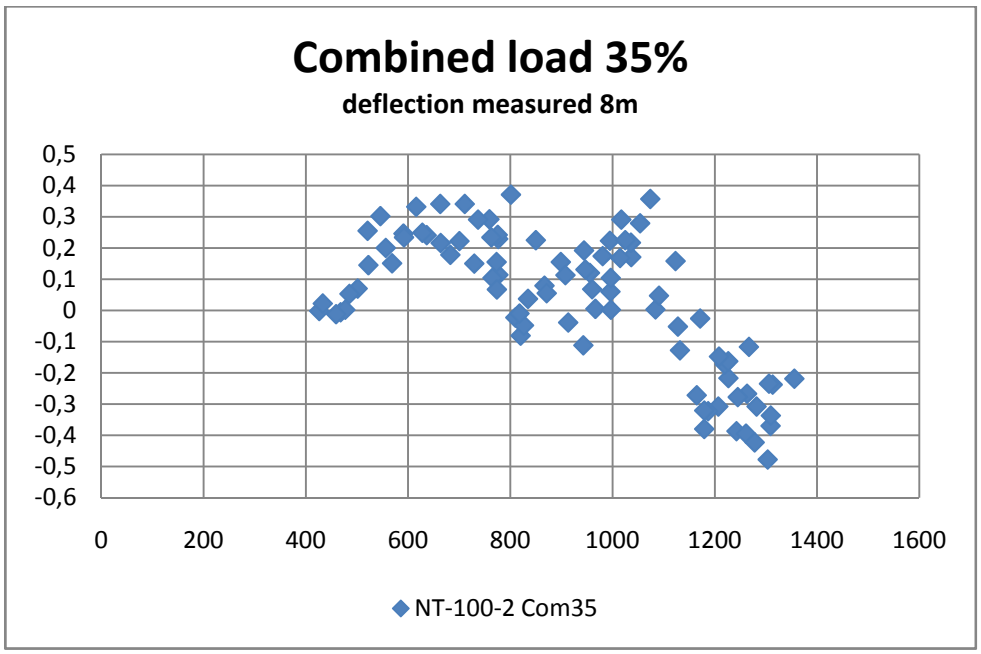
Combined load 35%
deflection measured 8m
0,5
0,4
0,3
0,2
0,1
0
-0,1
-0,2
-0,3
-0,4
-0,5
-0,6
0
200
400
600
800
1000
1200
1400
1600
NT-100-2 Com35

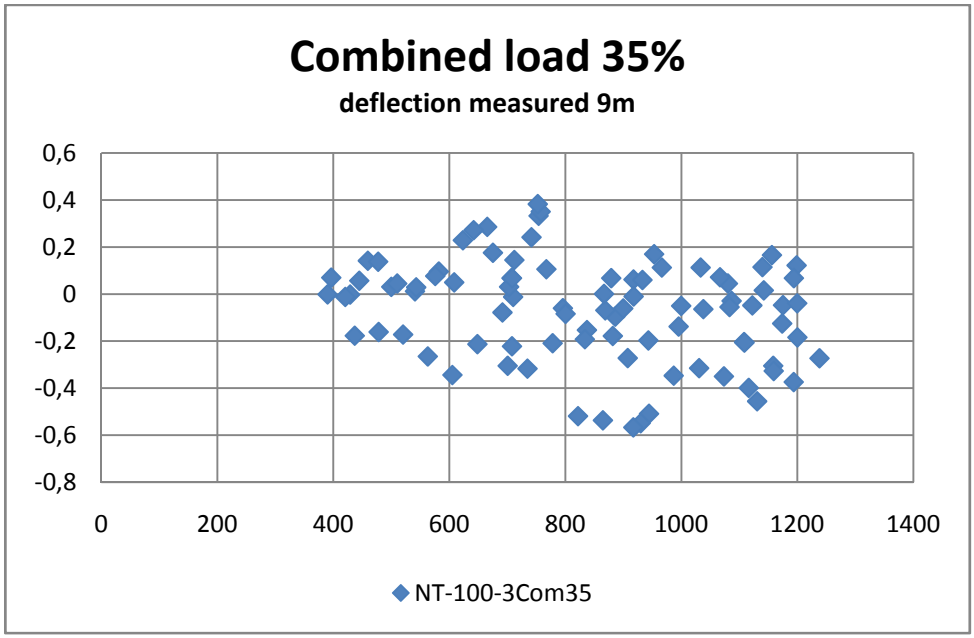
Combined load 35%
deflection measured 9m
0,6
0,4
0,2
0
-0,2
-0,4
-0,6
-0,8
0
200
400
600
800
1000
1200
1400
NT-100-3Com35

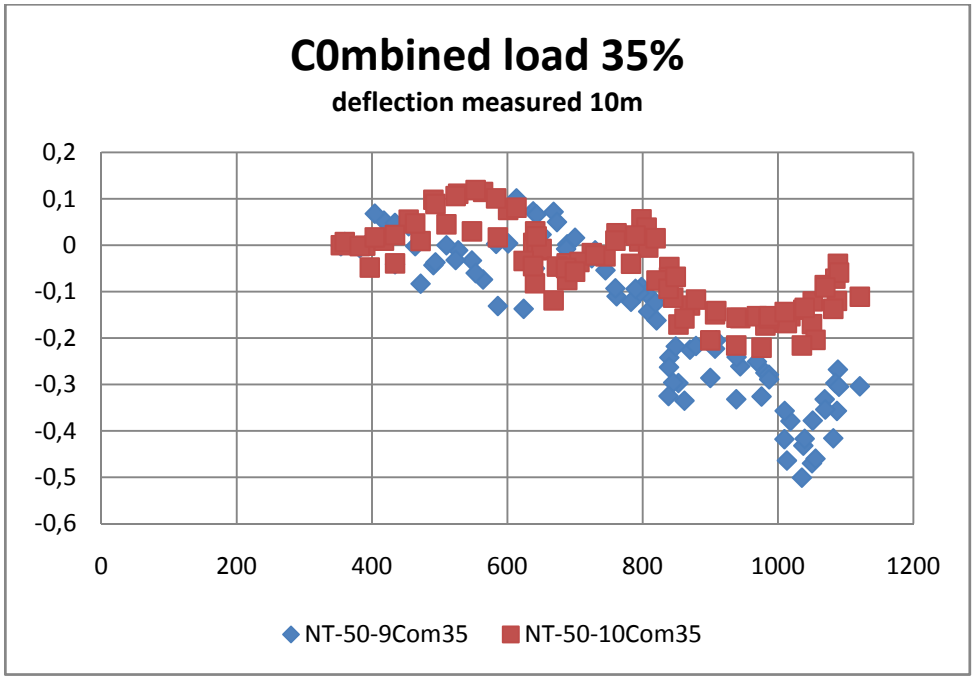
C0mbined load 35%
deflection measured 10m
0,2
0,1
0
-0,1
-0,2
-0,3
-0,4
-0,5
-0,6
0
200
400
600
800
1000
1200
NT-50-9Com35
NT-50-10Com35

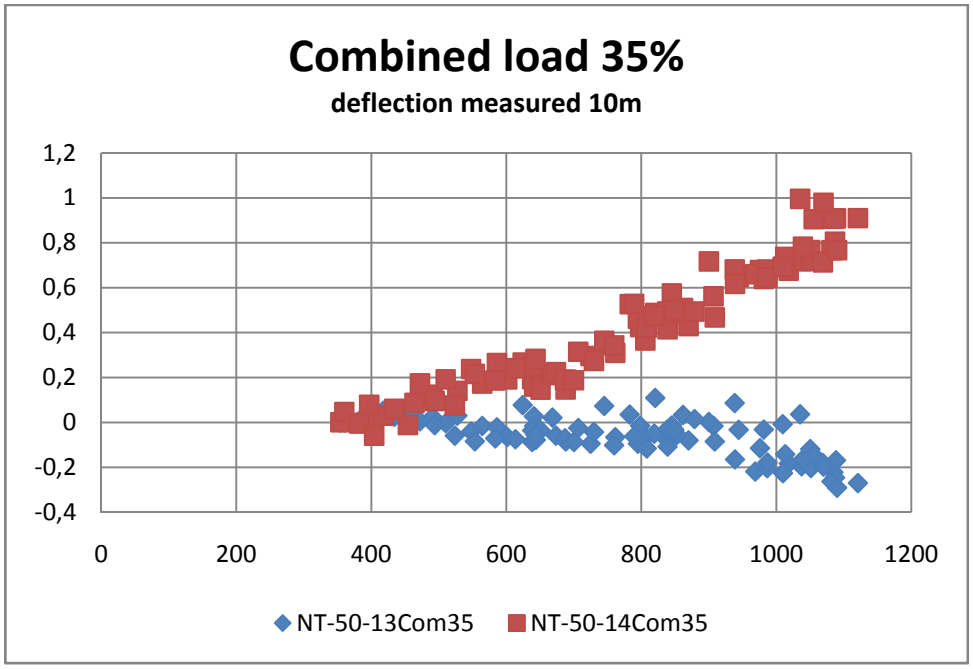
Combined load 35%
deflection measured 10m
1,2
1
0,8
0,6
0,4
0,2
0
-0,2
-0,4
0
200
400
600
800
1000
1200
NT-50-13Com35
NT-50-14Com35

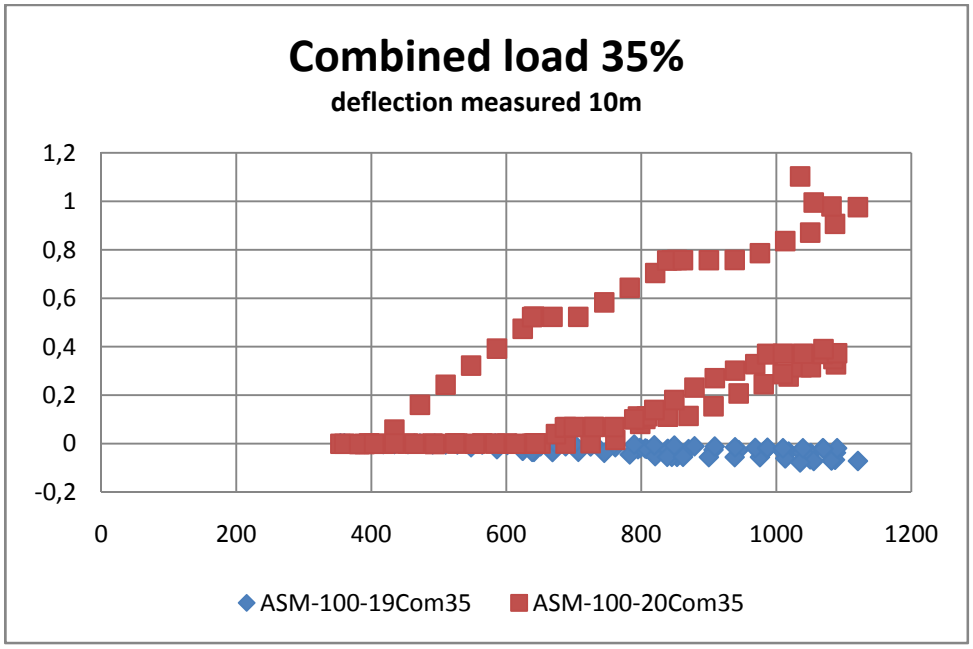
Combined load 35%
deflection measured 10m
1,2
1
0,8
0,6
0,4
0,2
0
-0,2
0
200
400
600
800
1000
1200
ASM-100-19Com35
ASM-100-20Com35

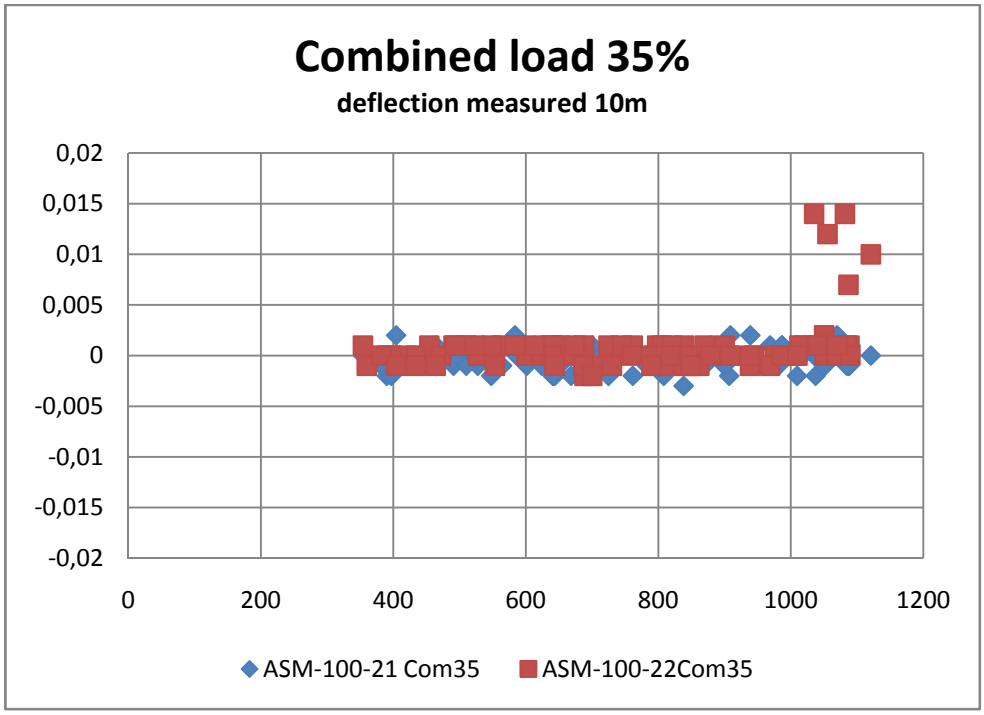
Combined load 35%
deflection measured 10m
0,02
0,015
0,01
0,005
0
-0,005
-0,01
-0,015
-0,02
0
200
400
600
800
1000
1200
ASM-100-21 Com35
ASM-100-22Com35

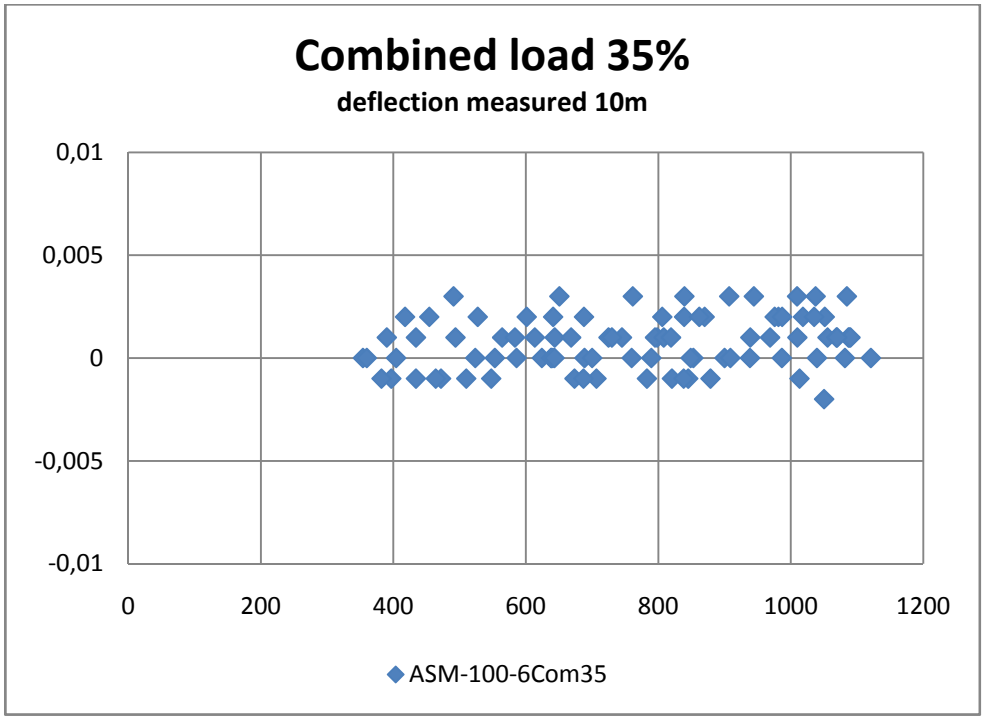
Combined load 35%
deflection measured 10m
0,01
0,005
0
-0,005
-0,01
0
200
400
600
800
1000
1200
ASM-100-6Com35

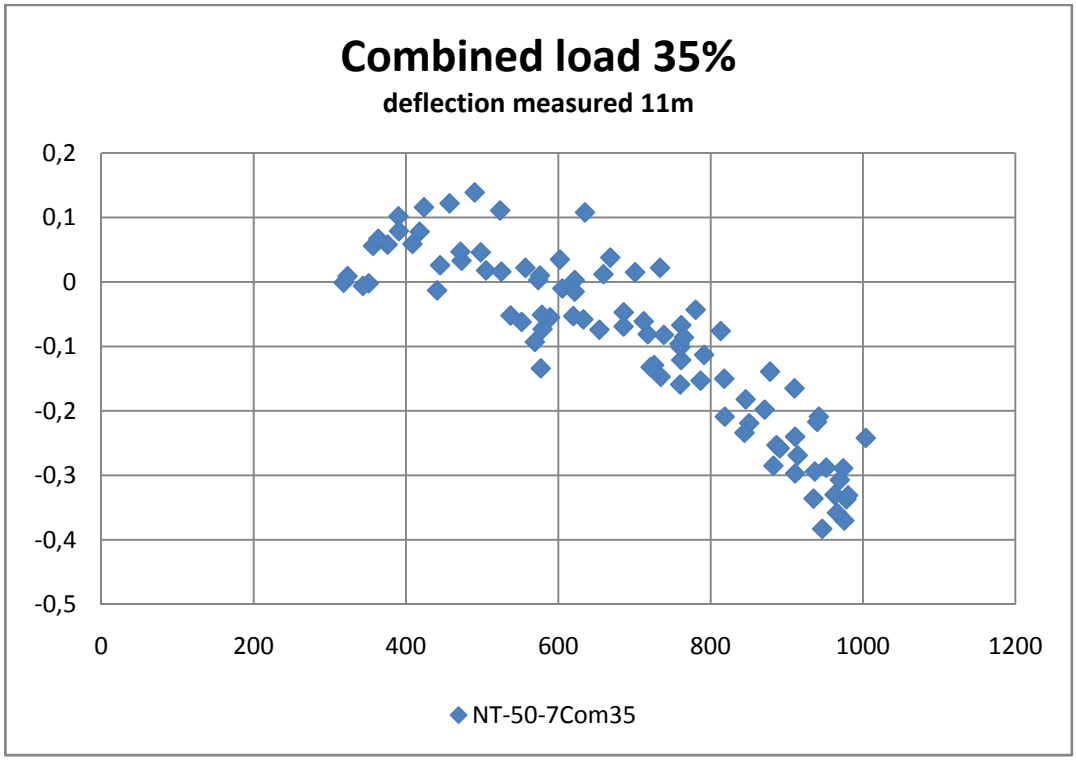
Combined load 35%
deflection measured 11m
0,2
0,1
0
-0,1
-0,2
-0,3
-0,4
-0,5
0
200
400
600
800
1000
1200
NT-50-7Com35

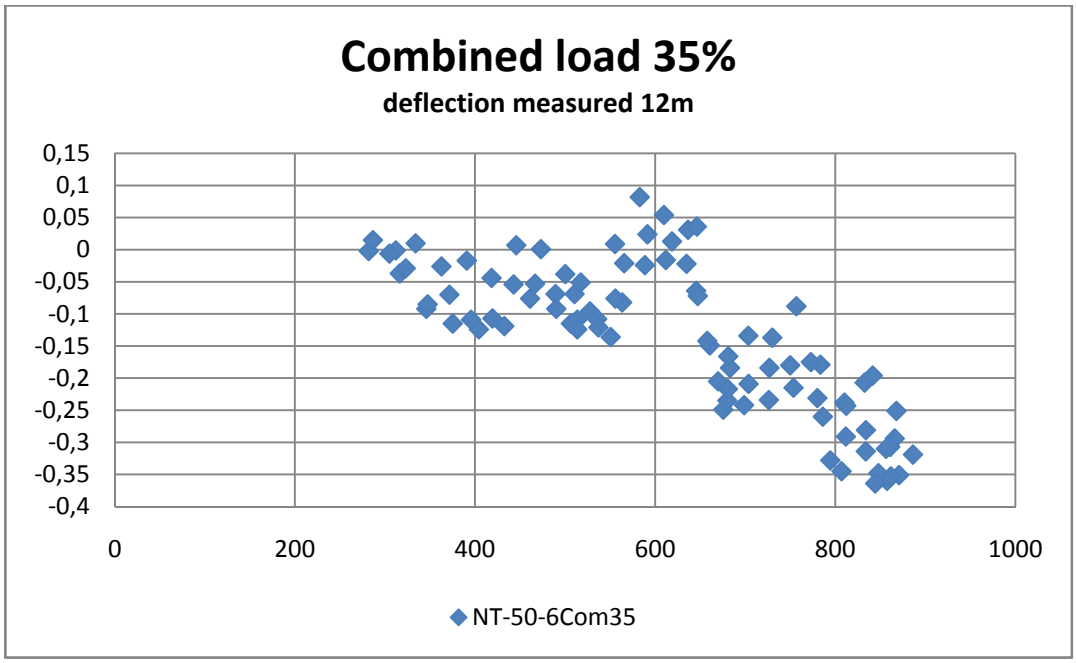
Combined load 35%
deflection measured 12m
0,15
0,1
0,05
0
-0,05
-0,1
-0,15
-0,2
-0,25
-0,3
-0,35
-0,4
0
200
400
600
800
1000
NT-50-6Com35

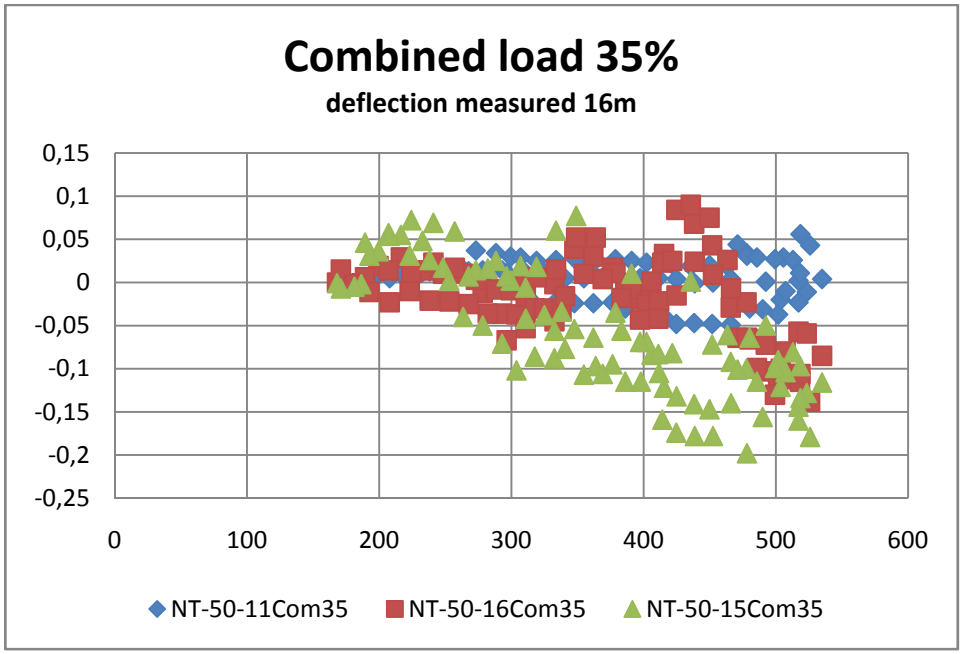
Combined load 35%
deflection measured 16m
0,15
0,1
0,05
0
-0,05
-0,1
-0,15
-0,2
-0,25
0
100
200
300
400
500
600
NT-50-11Com35
NT-50-16Com35
NT-50-15Com35

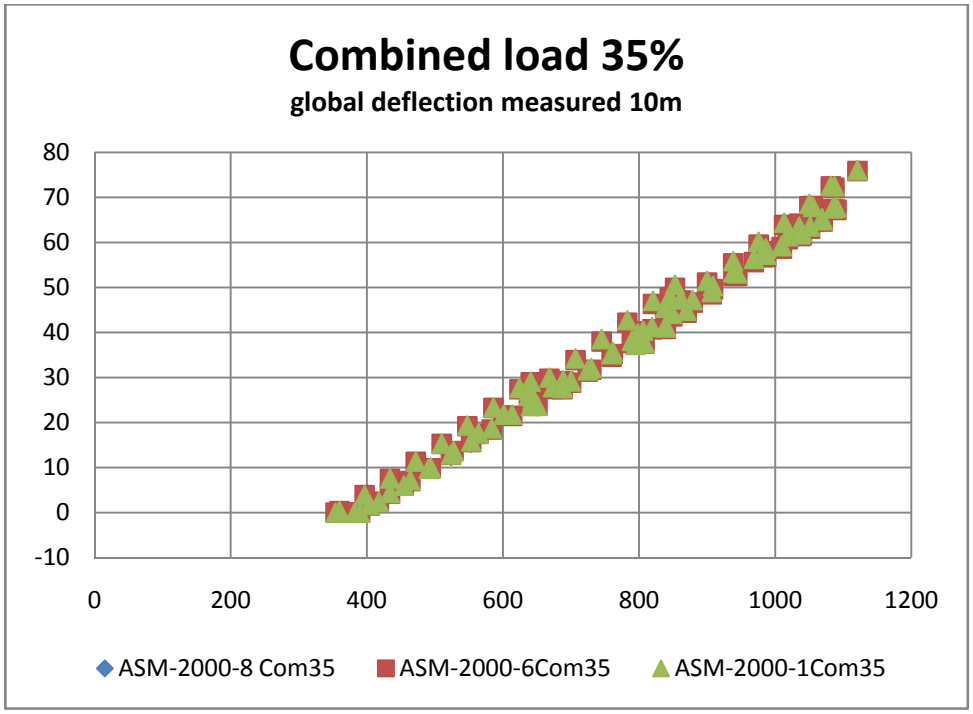
Combined load 35%
global deflection measured 10m
80
70
60
50
40
30
20
10
0
-10
0
200
400
600
800
1000
1200
ASM-2000-8 Com35
ASM-2000-6Com35
ASM-2000-1Com35

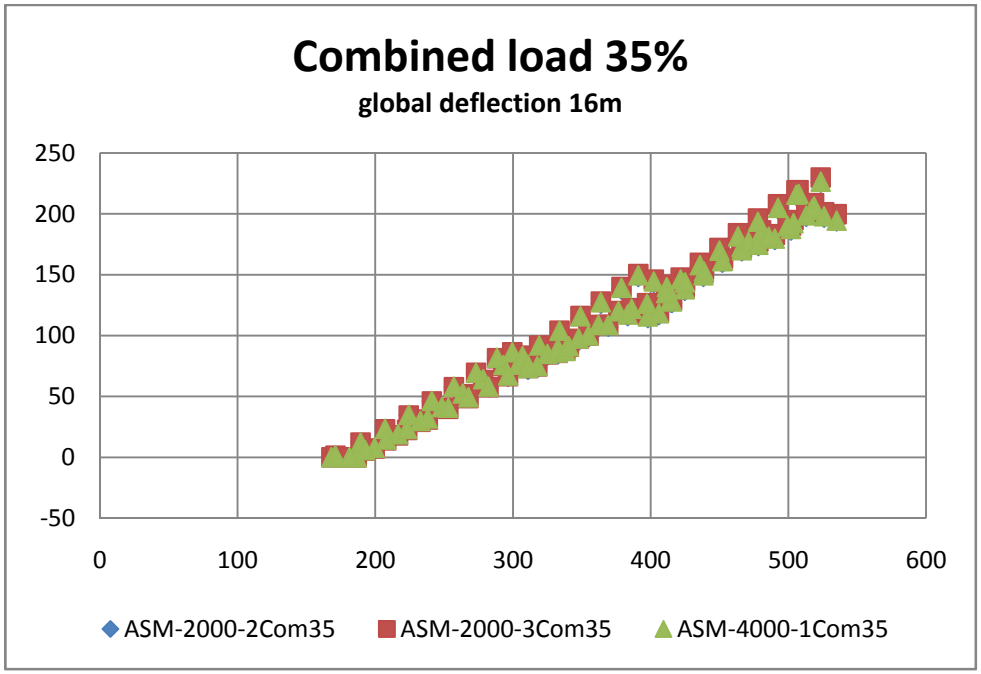
Combined load 35%
global deflection 16m
250
200
150
100
50
0
-50
0
100
200
300
400
500
600
ASM-2000-2Com35
ASM-2000-3Com35
ASM-4000-1Com35

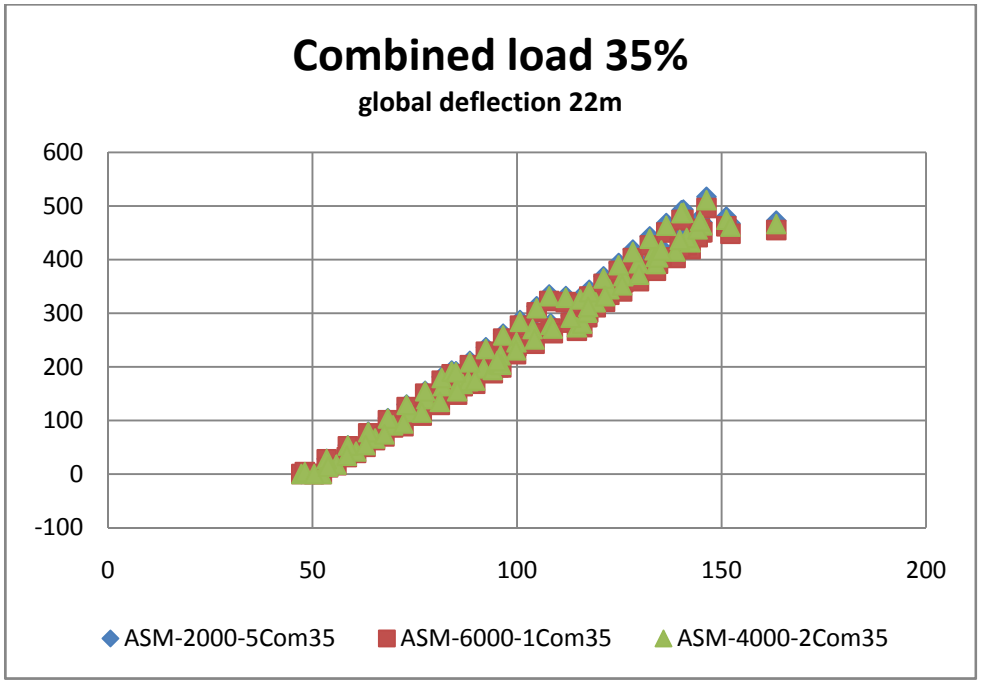
Combined load 35%
global deflection 22m
600
500
400
300
200
100
0
-100
0
50
100
150
200
ASM-2000-5Com35
ASM-6000-1Com35
ASM-4000-2Com35

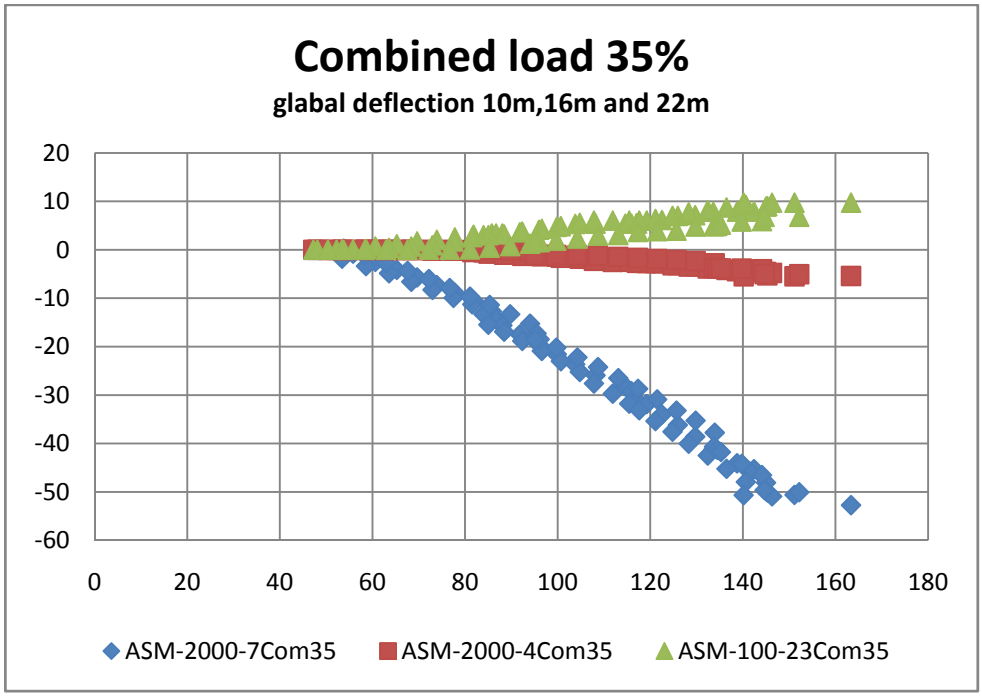
Combined load 35%
glabal deflection 10m,16m and 22m
20
10
0
-10
-20
-30
-40
-50
-60
0
20
40
60
80
100
120
140
160
180
ASM-2000-7Com35
ASM-2000-4Com35
ASM-100-23Com35

G FEM analysis of combined load

10MPC, Tøjninger-X
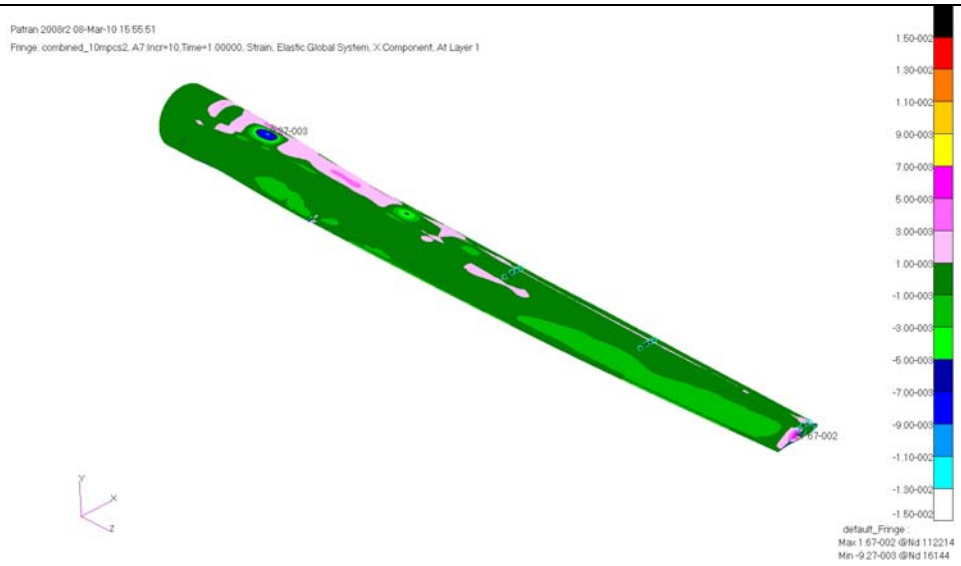
Figuren viser tvær tøjningerne, og som det se at figuren er der tildens til buling i radius 3.5, 9 og 11.5m.
Aag, Tøjninger-X
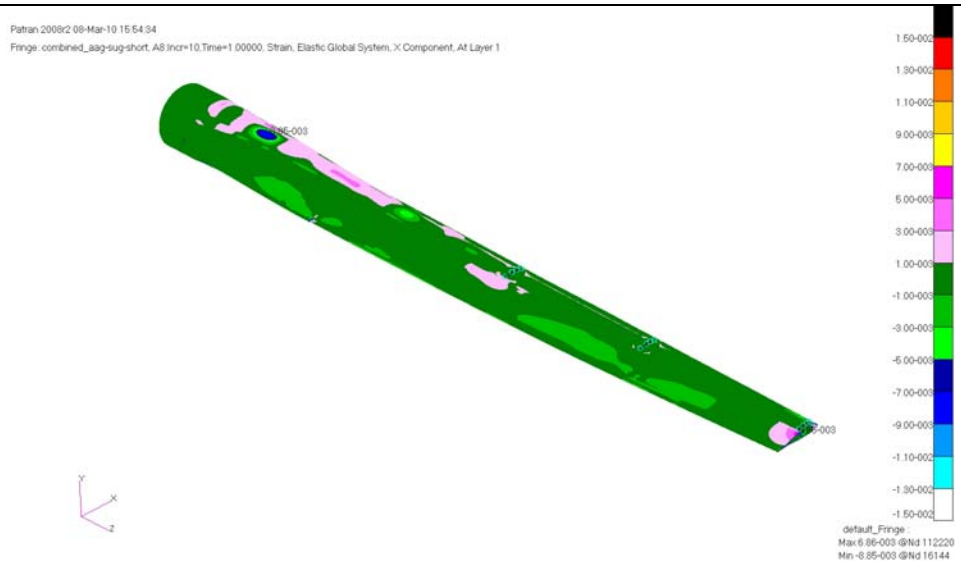
Figuren viser tvær tøjningerne, og som det se at figuren er der tildens til buling i radius 3.5, 9m.

10MPC, Tøjninger-X

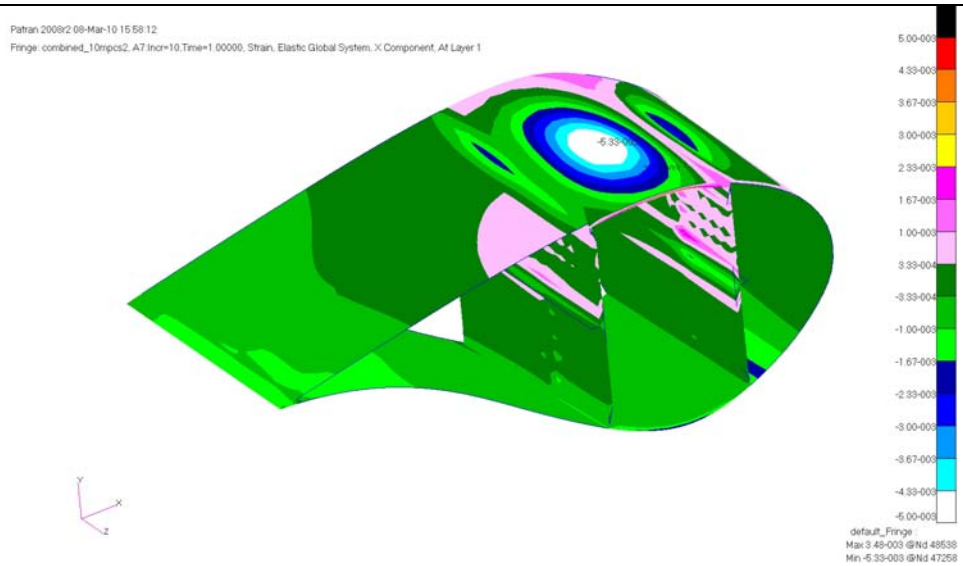

Figuren viser tvær tøjningerne, for vinge udsnittet mellem 8.5 og 9.5m. Tøjningerne viser tegn på buling.

Aag, Tøjninger-X

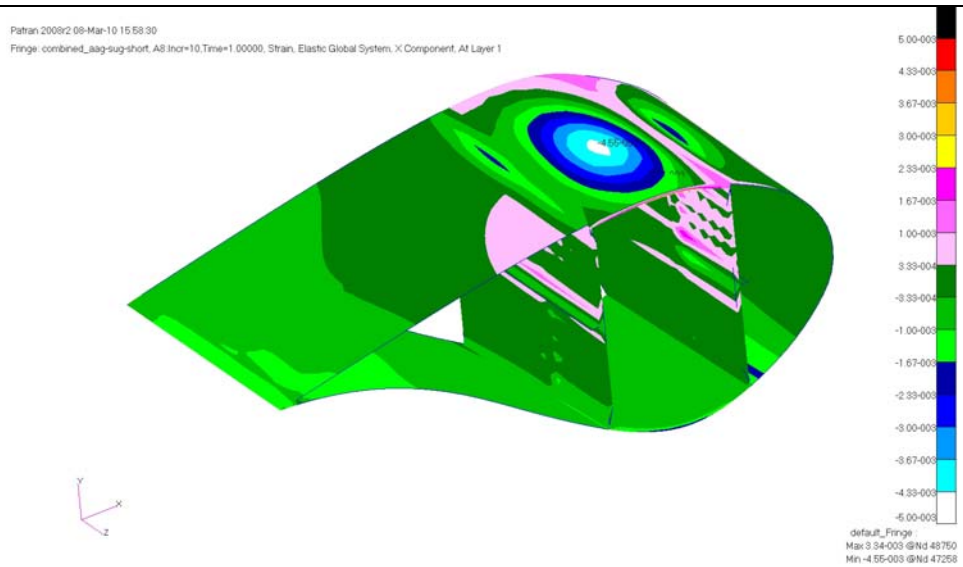

Figuren viser tvær tøjningerne, for vinge udsnittet mellem 8.5 og 9.5m. Tøjningerne viser tegn på buling.

10MPC, Relative deformationer-X
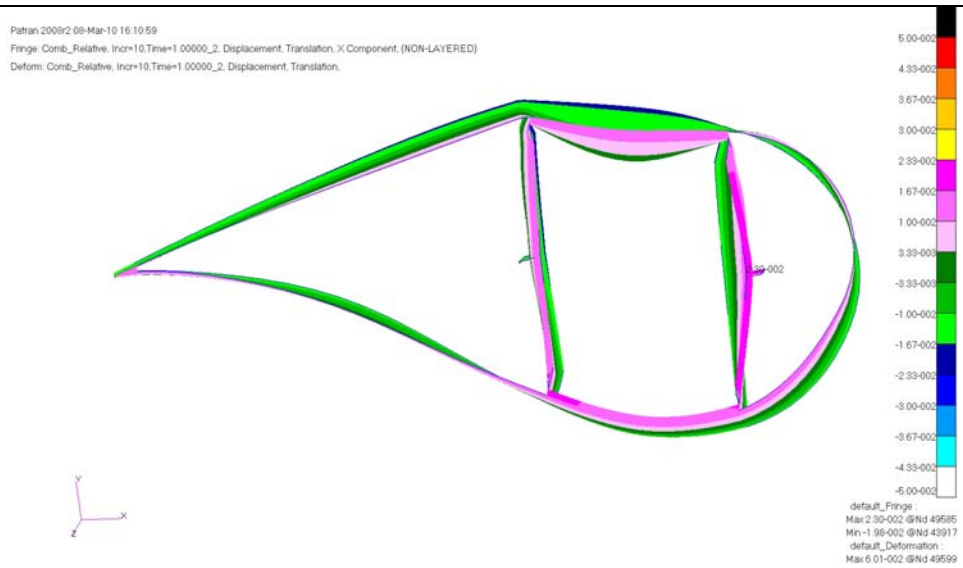
Figuren viser de relative kant deformationer, for vinge udsnittet mellem 8.5 og 9.5m. Deformationerne viser tegn på buling. Deformationerne er skaleret med en faktor 10.

Aag, Relative deformationer-X
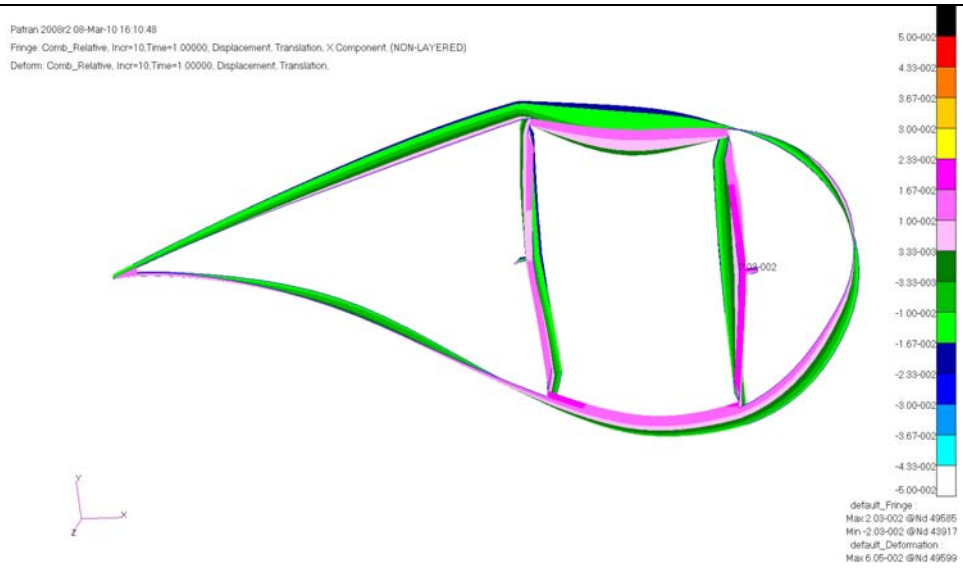
Figuren viser de relative kant deformationer, for vinge udsnittet mellem 8.5 og 9.5m. Deformationerne viser tegn på buling. Deformationerne er skaleret med en faktor 10.

10MPC, Relative deformationer-Y
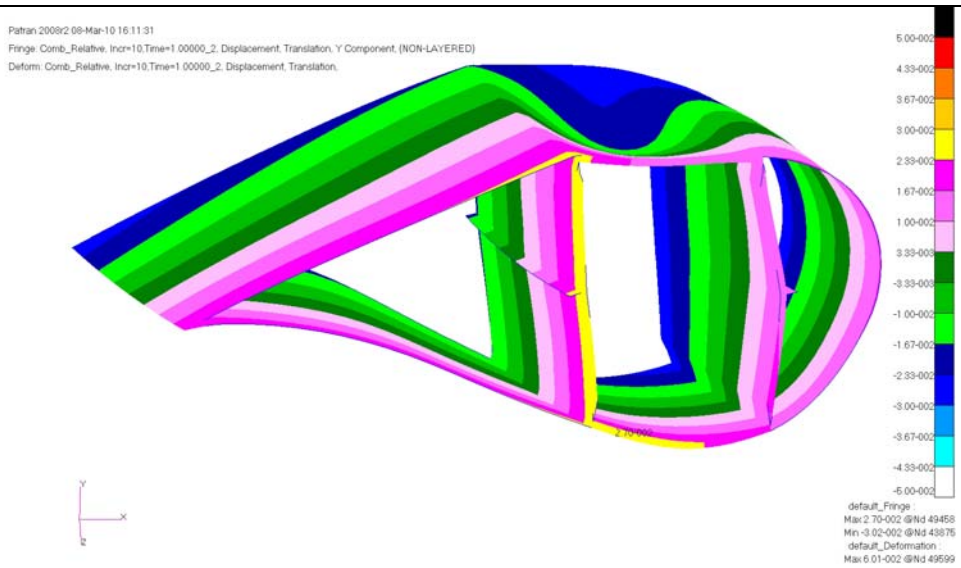
Figuren viser de relative flapvis deformationer, for vinge udsnittet mellem 8.5 og 9.5m. Deformationerne viser tegn på buling. Deformationerne er skaleret med en faktor 10.

Aag, Relative deformationer-Y
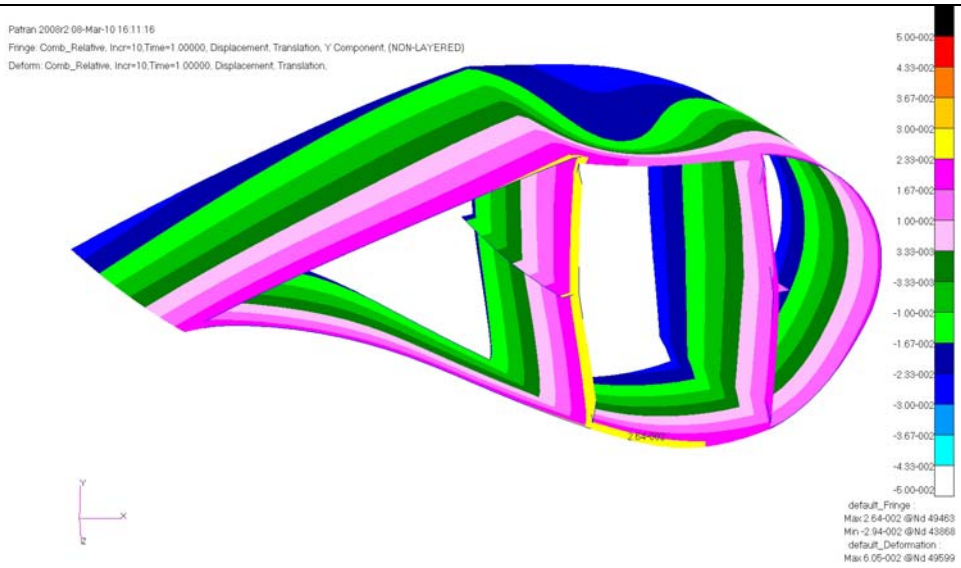
Figuren viser de relative flapvis deformationer, for vinge udsnittet mellem 8.5 og 9.5m. Deformationerne viser tegn på buling. Deformationerne er skaleret med en faktor 10.

10MPC, Relative deformationer-X
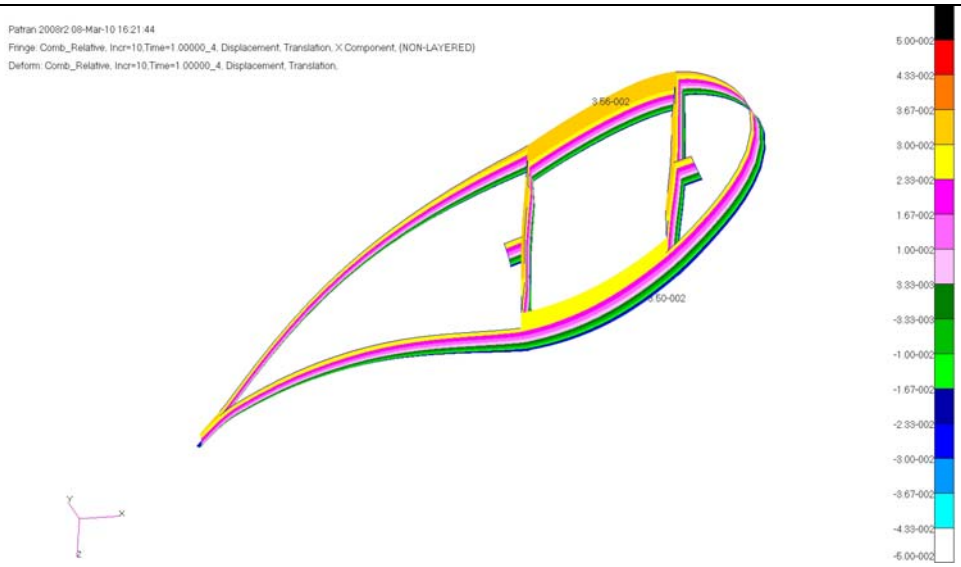
Figuren viser de relative kant deformationer, for vinge udsnittet mellem 18 og 19m. Deformationerne er skaleret med en faktor 10.

Aag, Relative deformationer-X

Figuren viser de relative kant deformationer, for vinge udsnittet mellem 18 og 19m. Deformationerne er skaleret med en faktor 10.

10MPC, Tøjninger-X
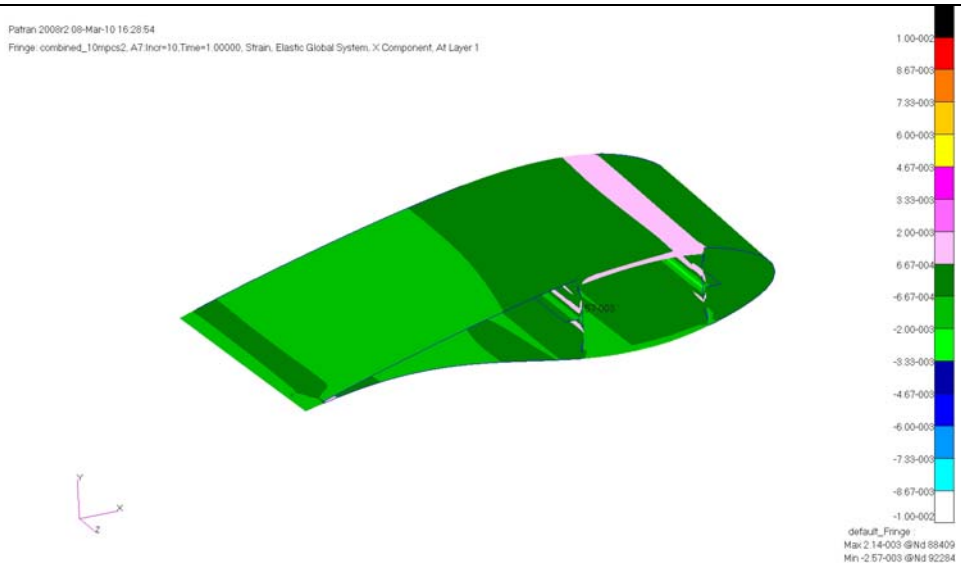
Figuren viser tvær tøjningerne, for vinge udsnittet mellem 18 og 19m.

Aag, Tøjninger-X
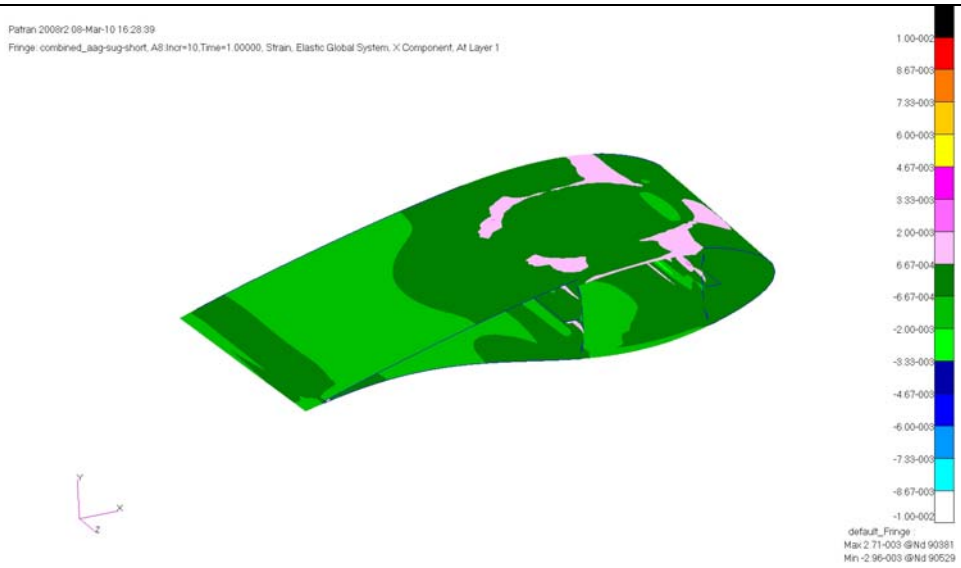
Figuren viser tvær tøjningerne, for vinge udsnittet mellem 18 og 19m hvor aaget er placeret i 18.6m.

10MPC, Tøjninger-Y

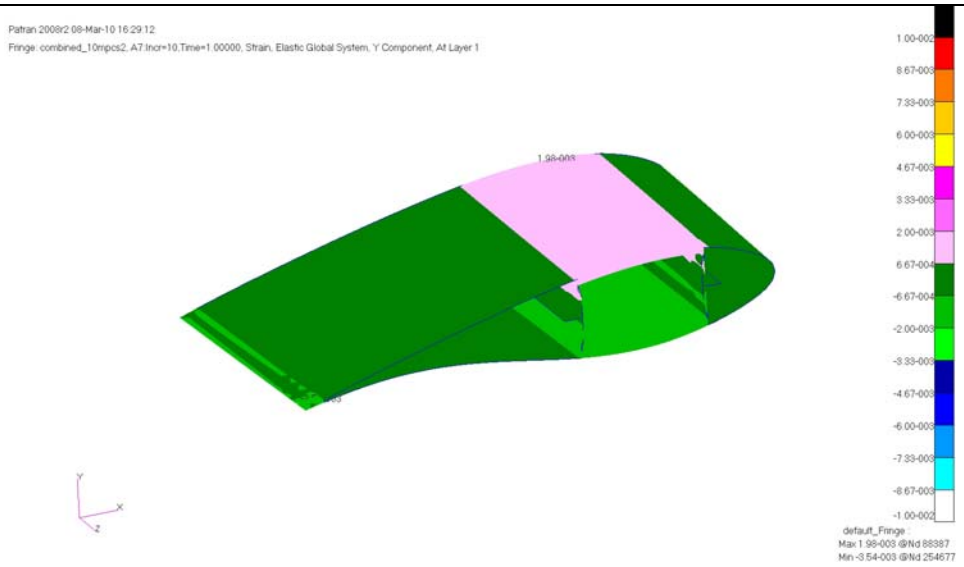

Figuren viser ”ud af planet” tøjningerne, for vinge udsnittet mellem 18 og 19m.

Aag, Tøjninger-Y

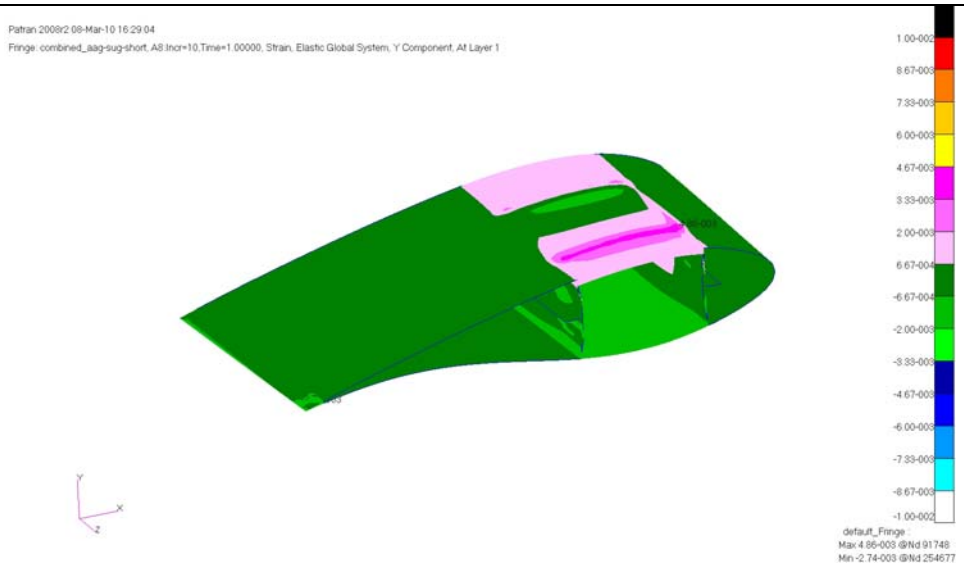

Figuren viser ”ud af planet” tøjningerne, for vinge udsnittet mellem 18 og 19m hvor aaget er placeret i 18.6m.

10MPC, Tøjninger-Z

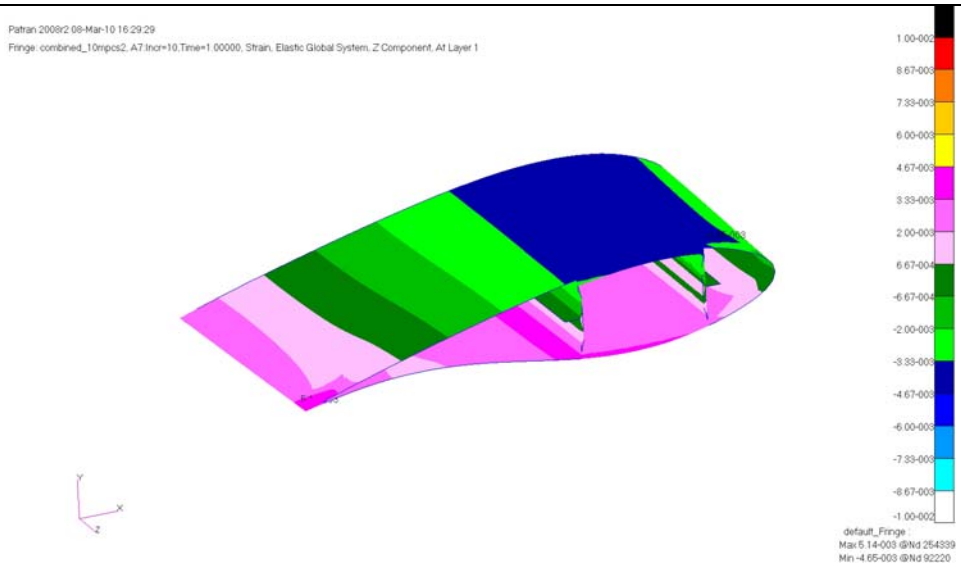

Figuren viser langsgående tøjningerne, for vinge udsnittet mellem 18 og 19m.

Aag, Tøjninger-Z

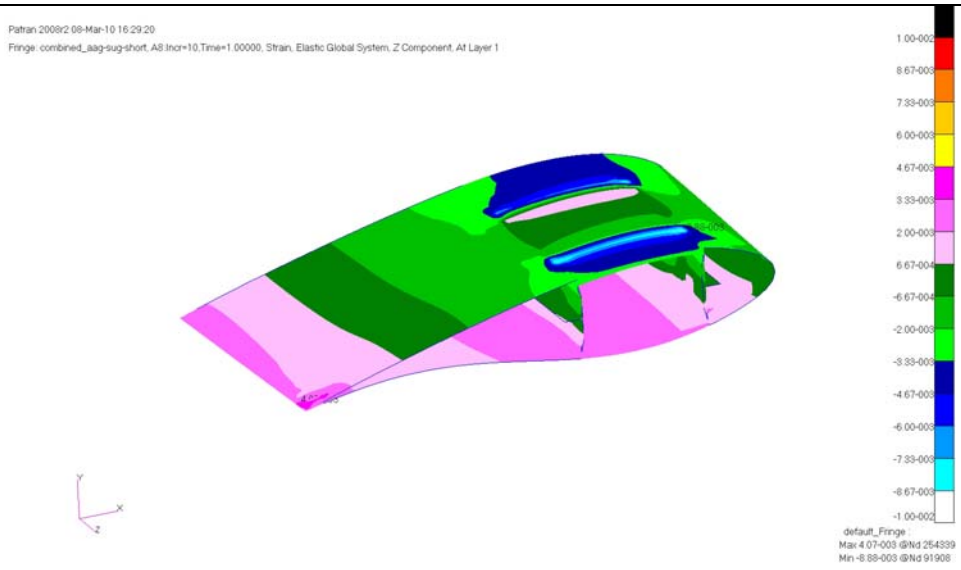

Figuren viser tvær langsgående, for vinge udsnittet mellem 18 og 19m hvor aaget er placeret i 18.6m.

10MPC, Min Principal Tøjning

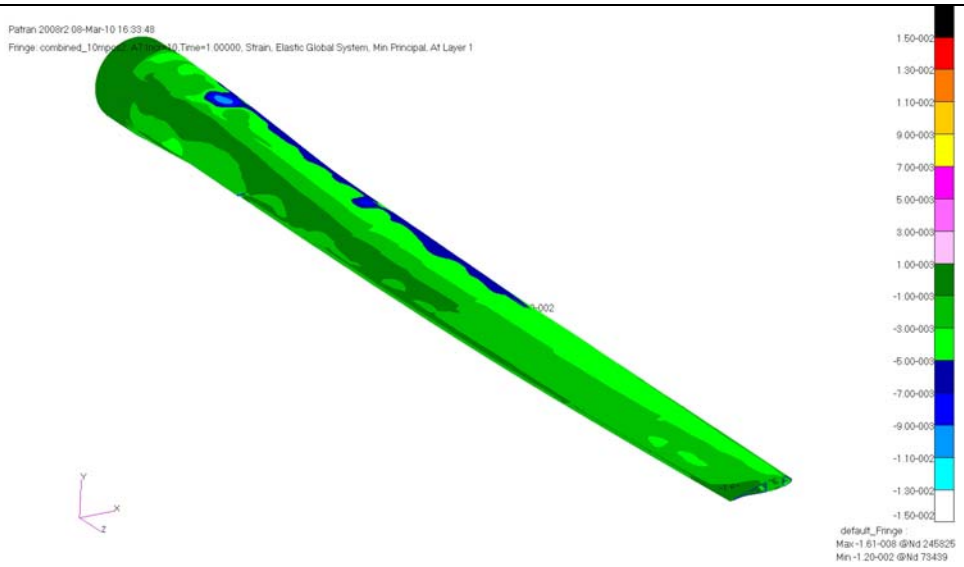

Figuren viser minimum principal tøjningerne set fra sugsiden af vingen.

Aag, Min Principal Tøjning

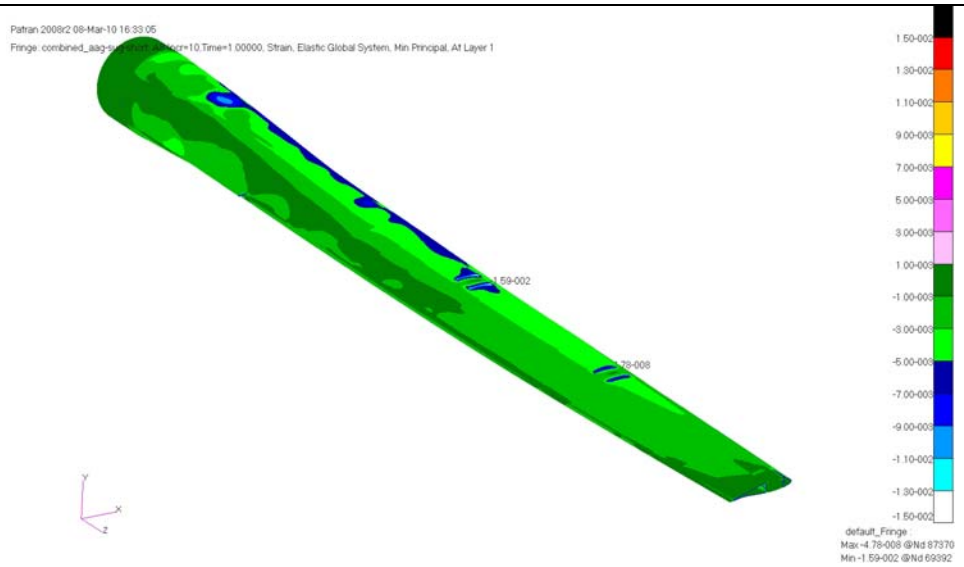

Figuren viser minimum principal tøjningerne set fra sugsiden af vingen.

10MPC, Max Principal Tøjning

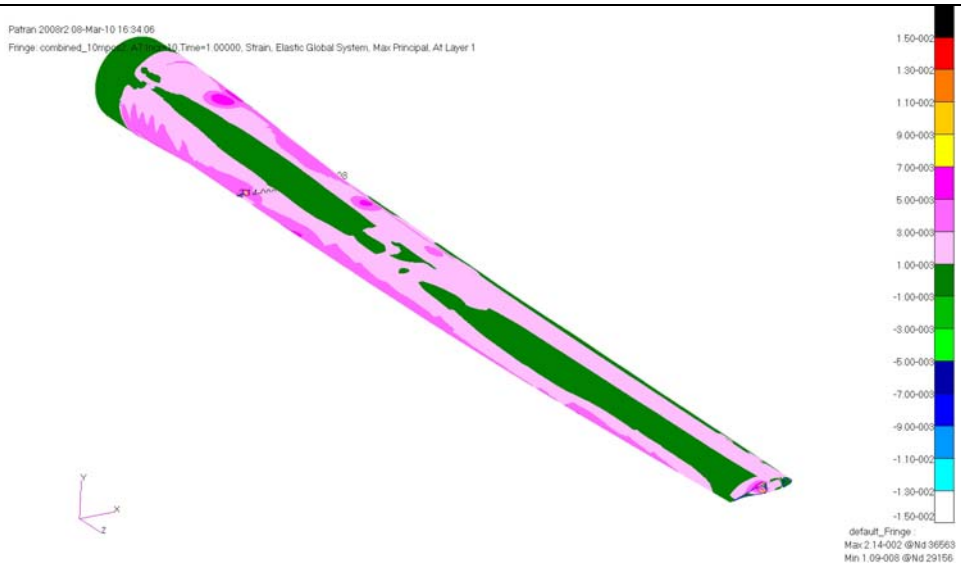

Figuren viser maksimum principal tøjningerne set fra sugsiden af vingen.

Aag, Max Principal Tøjning

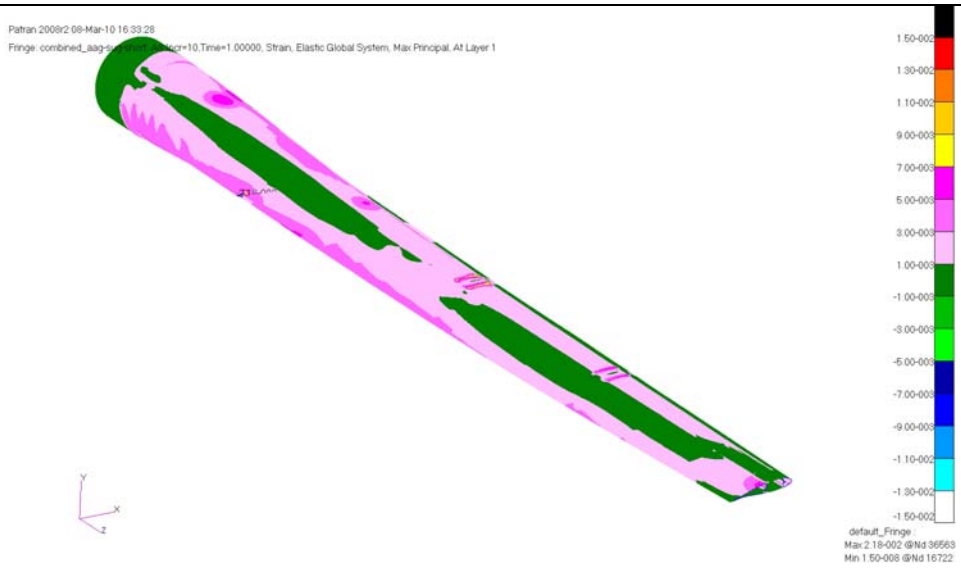

Figuren viser maksimum principal tøjningerne set fra sugsiden af vingen.

10MPC

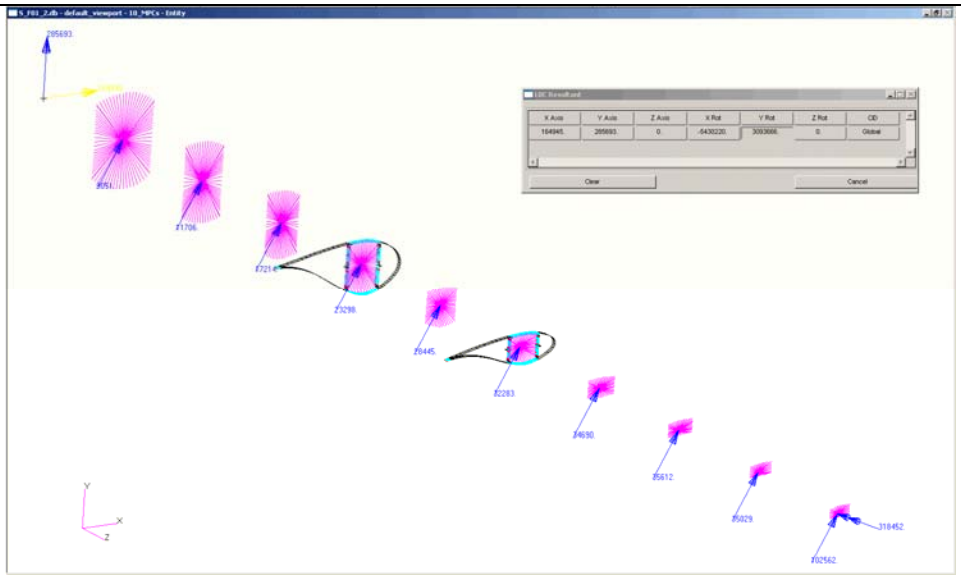

Figuren viser placering af MPC'er (RBE 3) samt resulterende rod-kræfter og momenter.

Aag

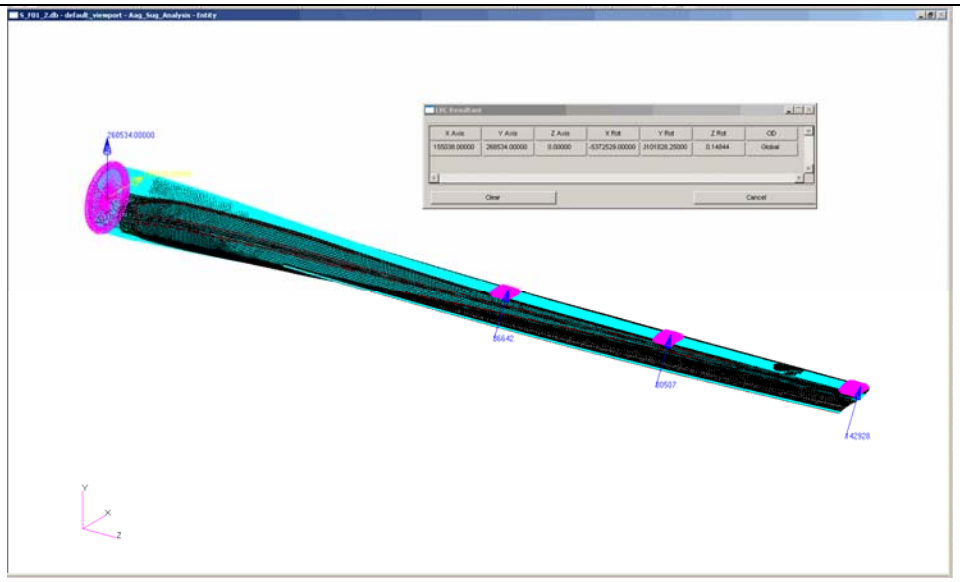

Figuren viser placering af MPC'er/åg (RBE 2) samt resulterende rod-kræfter og momenter.

Aag, 13.21m

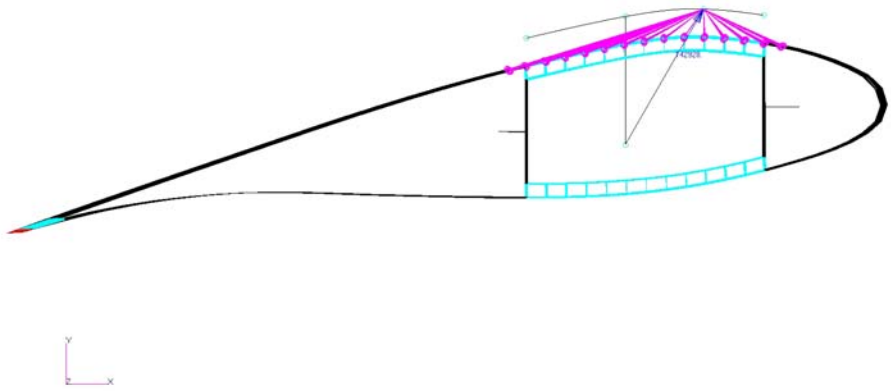

Figuren viser placering af inderste MPC/åg og placering af træk punkt således at kraften går gennem [0,0,0]. Trækpunktet er placeret 50mm over vingeskindet.

Aag, Relative deformationer-Y

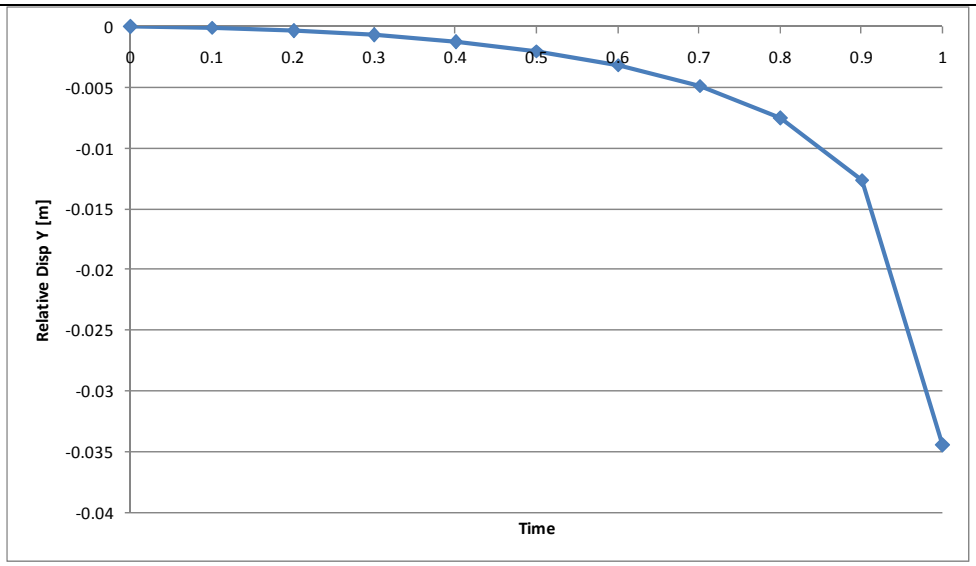

Figuren viser den relative deformation i flapvis retning i 3.5m, grafen viser forskellen mellem center deformationer af sug siden minus den gennemsnitlige deformation af hjørne punkterne.

Aag, Relative deformationer-Y

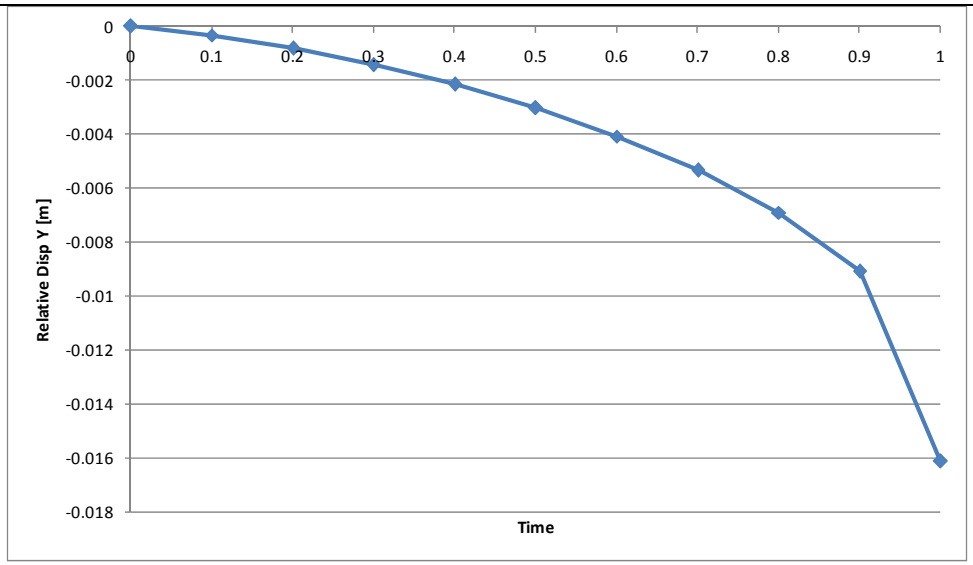

Figuren viser den relative deformation i flapvis retning i 9m, grafen viser forskellen mellem center deformationer af sug siden minus den gennemsnitlige deformation af hjørne punkterne.

Risø DTU is the National Laboratory for Sustainable Energy. Our research focuses on development of energy technologies and systems with minimal effect on climate, and contributes to innovation, education and policy. Risø DTU has large experimental facilities and interdisciplinary research environments, and includes the national centre for nuclear technologies.

Risø DTU
National Laboratory for Sustainable Energy
Technical University of Denmark

Frederiksborgvej 399
PO Box 49
DK-4000 Roskilde
Denmark
Phone +45 4677 4677
Fax +45 4677 5688

www.risoe.dtu.dk